Lactose and Lactic acid Biosensor Development for Dairy Sample Analysis

A thesis submitted by

Grace Halpin B.Sc (Hons)

to the

National University of Ireland, Maynooth

For the degree of Masters of Science

Volume 1 of 1

Based on research carried out in the

Department of Chemistry, Faculty of Science and Engineering,

National University of Ireland, Maynooth

under the supervision and direction of

Dr. Eithne Dempsey

Head of Department – Dr. Jennifer McManus

2019

Abstract

Rapid and selective monitoring of small molecules is important in relation to fermentation process control where optimisation and scale up relies on accurate measurement of species such as lactose and lactic acid. Currently, chromatographic approaches such as HPLC are the most commonly used methods for such analysis but can be both costly and time consuming. Here, development of an enzymatic biosensor for rapid quantitation of key analytes in dairy samples (whey permeate, milk protein concentrates and fermentation samples) is presented. This involved 1st and 2nd generation biosensor fabrication using Chitosan/Enzyme(s)/Chitosan/GA or PEGDE configuration utilising the enzymes GOx, β-gal and LOx. Due to the complex matrix of dairy samples, solution phase mediation at carbon transducers was used to lower the operating potential (E_{app} = 0.3 V vs. Ag/AgCl), improving sensitivity and eliminating any contribution from endogenous background electroactive species. Following sensor design and development, CV and CC realised analytical data for the lactose sensor with linear range 5.83 x 10^{-3} to 1.65 x 10^{-2} M, sensitivity 9.41 x10^{-4} C cm^{-2} mM^{-1} and LOD of 1.38 mM. In the case of the lactate biosensor, a linear range 9.9 x 10^{-4} to 5.66 x 10^{-3} M, sensitivity 1.44 x 10^{-3} C cm^{-2} mM^{-1} and LOD of 0.54 mM was realised. Further investigation into lactate sensing involved use of the heterocyclic quinoid species 1,10-phenanthroline-5,6-dione which acted as a proton and electron acceptor in relation to $FADH_2$ cofactor regeneration. Graphite ink was formulated and utilised as an underlying conductive layer for LOx enzyme immobilisation and enzymatic polymerisation of 1,10-phenanthroline-5,6-dione at a GC electrode, resulting in a linear range of 0.74 – 2.44 x 10^{-3} M, sensitivity of 4.11 x 10^{-4} C cm^{-2} mM^{-1} and LOD of 0.06 mM. On-site analytical performance was examined in diluted fermentation media, comparing well to the established HPLC-RI separation approach, with 93 -100 % correlation for lactose analysis and 72 – 96 % correlation for lactate analysis over the range of sampling time points investigated (lactose levels ranged 4 – 306 mM and lactate levels 69 – 805 mM). Data generated in this thesis provides evidence that the developed biosensors have enormous potential for on-site industry deployment with proven capability for accurate, reliable measurement of lactose and lactic acid levels in a range of dairy samples.

Declaration

This is to certify that the material presented within this thesis has not been submitted previously for a Degree to this or any other University. All material presented herein, except where acknowledged and cited appropriately, is the work of the author.

_____

Grace Halpin

National University of Ireland, Maynooth

2019

Acknowledgements

I would like to firstly express my deepest appreciation to my academic supervisor Dr. Eithne Dempsey, for giving me the opportunity to carry out this research. I am forever grateful for the invaluable guidance, support and words of wisdom! Thank you for the precious time and effort you provided to me as your first MU postgraduate student.

Secondly, I want to thank my amazing mother for her continued encouragement and support from the very beginning. I wouldn't be where I am, or who I am today without you. To my sisters Lisa, Roisin, Lily and my brother Barry, thanks for all the love, support and patience.

I would also like to take the opportunity to thank my funding body The Irish Research Council and my industry partner for believing in this project and making it possible. I would particularly like to thank Fergal Lawless for his support, helpful advice, suggestions and enthusiasm along the way. Many thanks to the R&D team for their helping hand and knowledge from the industry perspective.

To all the academic and technical staff in the Chemistry Department, thank you for all your hard work and help throughout the last two years. I really appreciate all you do for us postgrads by helping us get to the finish line. A special thanks to Karen Herdman for the SEM training and help with running my samples.

To the postgrads and postdocs, thank you for everything! The laughs, the tears and the cake. Good luck with the rest of your studies, you're all amazing. A huge thank you to my lab partner in crime Jessica for keeping me company and sane for the last year.

Last but not least, a special mention to my other half, Lee. Thank you for always being there for support and encouragement over the last few years.

Table of Contents **Page**

Figures **Page No.**

Schemes **Page no.**

Tables **Page no.**

Chapter 1 : Introduction

1.0 Introduction - Bioprocessing in the Dairy Industry

Ireland is one of the biggest dairy product exporters in the world. It relies greatly on the processing of raw milk which results in the production and export of consumer dairy products including various cheeses, yoghurts, butter and whey derived products. Various industrial processes are used in the production of high quality dairy products including pasteurisation, centrifugation, filtration, coagulation and chilling.[1] Generally, raw milk does not undergo rigorous processing and is limited to heat treatment and pasteurisation. This is implemented in order to decelerate the proliferation of microbes present in the milk, thus aiding stability and shelf-life of the product and avoids separation of fat components present in the milk.

Figure 1.1 gives an overview of a typical dairy industry process from the importation of raw milk into the manufacturing facility to processing of the raw milk using various techniques, and the final exportation of a wide range of dairy products. Along with the production and exportation of such products, at the final stage of processing, whey effluent is generated as a by-product. One of Europe's leading sources of industrial effluent is the dairy industry.[2] The majority of waste derived by dairy industries contains a wide variety of components. This waste is now being used as substrates and/or nutrients for a broad range of microbial or enzymatic processes which can result in the generation of products with added-value.[3] Such processes include the fermentation of lactose from whey protein which can produce high levels of lactic acid when e.g *Lactobacillus spp.* micro-organisms are introduced.[4] Lactic acid production generated from whey is a major side-stream of the dairy industry.[3] Industry fermentation such as this requires the study and analysis of lactose concentrations throughout the process. This is a key requirement in order to sustain quality control and efficiency during production. During the fermentation of whey, lactose is broken down by *Lactobacillus spp.* present in the nutrient media and lactic acid is produced as a result. Therefore, the analysis of various time points of the fermentation will show a decrease in lactose concentration and an increase in lactic acid over the course of time. Currently, such analysis relies on chromatographic techniques which require rigorous sample preparation and time-consuming testing.[4] Often, such analysis requires the use of external labs to carry out this testing and can take a number of weeks to obtain a result. This limits the ability to monitor the concentrations of key

components of the process and prevents early detection of any deviations that may occur.

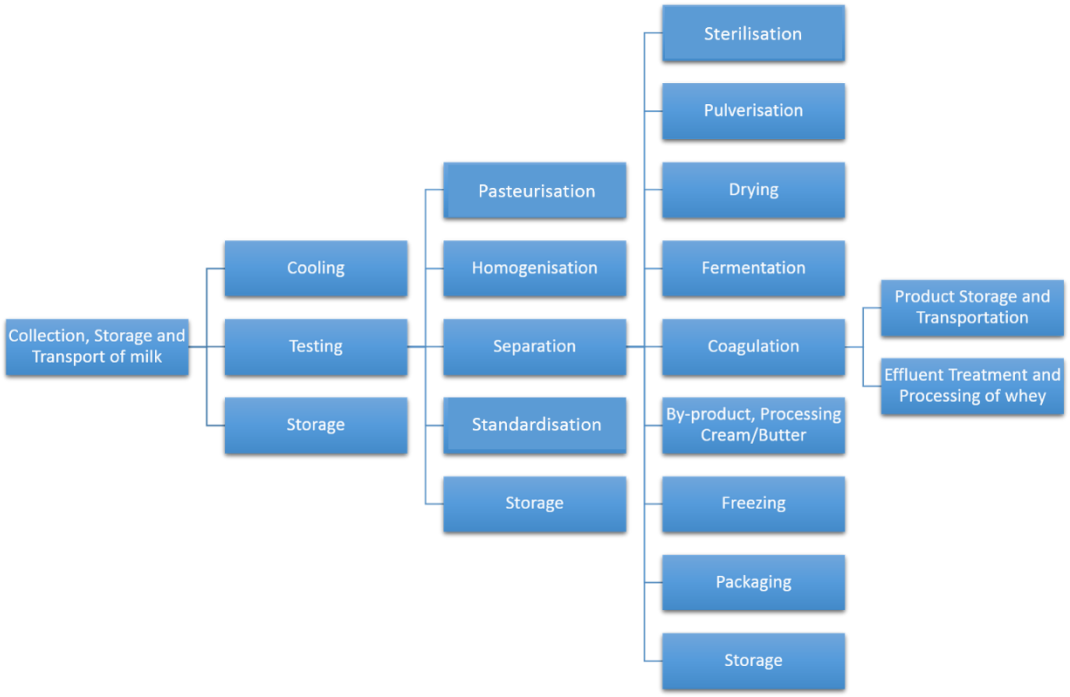

Figure 1.1: Flowchart of a typical dairy process [5]

There are copious analytical techniques available for the analysis of a variety of components within a dairy sample. Key components such as small and large molecules can be identified as indicators of milk quality. Analytical procedures include the use of enzymatic assays followed by spectrophotometry[6], colorimetric methods[7], enzyme micro-assay methods involving the use of microliter plate readings[8] and chromatographic methods via HPLC[6] and LC-MS/MS.[6] Although these methods have shown to give accurate and reliable results, they involve high levels of sample pre-treatment and are quite time consuming. Therefore, the attraction of bio-sensing methods has increased giving reliable, highly accurate and rapid analysis of key components involved in lactate production.

1.1 Lactose and its role in Lactic acid production in the Dairy Industry

Lactose is a disaccharide molecule which is derived from monosaccharides galactose and glucose with formation of β-1 →4 glycosidic linkage, shown in *Figure 1.2*. The systematic name for Lactose is β-D-galactopyranosyl- (1→4)-D-glucose. Glucose molecules can either be in the α-pyranose or the β-pyranose form while galactose only

forms a β-pyranose structure. Therefore, lactose can either be in α-lactose or β-lactose form. [9]

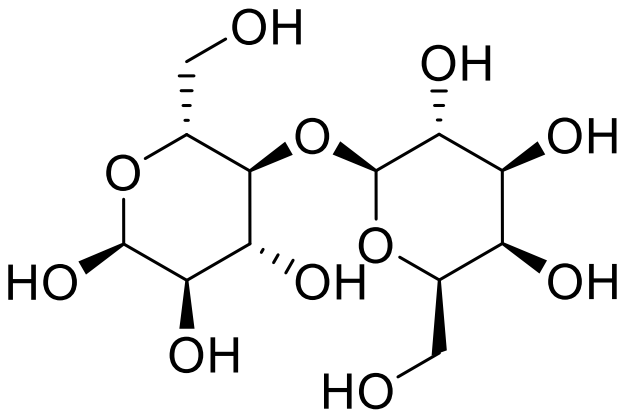

Figure 1.2: Chemical structure of Lactose

Lactose is abundant in milk but levels can vary depending on which mammal the milk is derived from. Lactose levels in the milk of humans can reach up to 8 % w/v [10] whereas in other mammals such as cows, goats or sheep, it may be present in levels as low as 4 % w/v.[11] The dairy industry uses lactose determination for evaluation of product quality as it is a good indicator of any abnormalities that may be present. Studies have shown that cows suffering from mastitis had a lower level of lactose in their milk than cows who were in a healthy state.[12] The determination of lactose levels in food products is also a cause for concern in public health for patients who suffer with lactose intolerance. People with this condition are unable to metabolise lactose and break down the sugar into glucose and galactose. This is due to a lack of the enzyme known as lactase or β-galactosidase in their digestive system. [13]

Here, we are interested in the importance of monitoring the concentration of lactose and its conversion to lactic acid in a typical dairy fermentation process. Production of lactic acid by biotechnological fermentation is more attractive than chemical syntheses of lactic acid due to the limited nature of petrochemical feedstock.[3] In addition, optically pure L (+) or D (-) lactic acid isomers can be obtained via inoculation of an appropriate microorganism in the fermentation process with fermentable carbohydrates such as lactose from whey protein. Generally, this method is preferred over chemical synthesis as both isomers, L (+) lactic acid and D (-) lactic acid, shown

in *Figure 1.3*, can be produced separately. A disadvantage of chemical synthesis would be that it produces a mix of both isomers.[3]

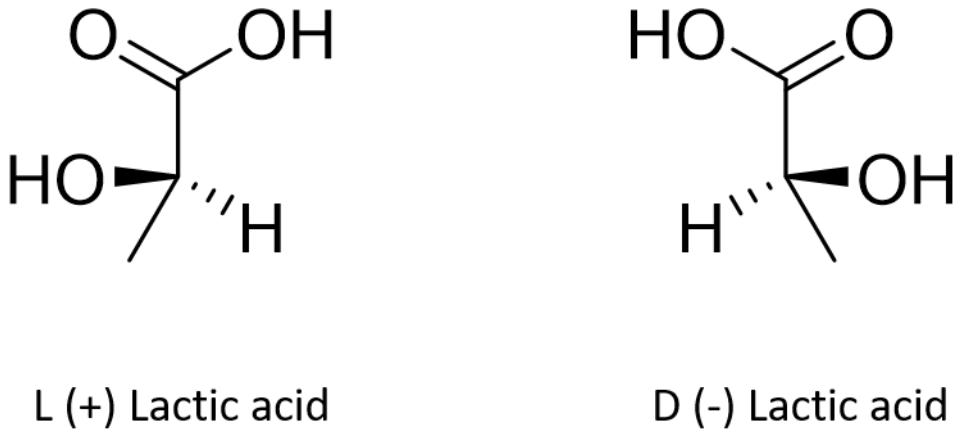

Figure 1.3: Lactic acid isomers

Whey permeate, a by-product of the dairy industry, was often thought of as waste. More recently, it is used in the conversion of lactose to lactic acid in the presence of lactic acid bacteria (LAB). Certain *Lactobacillus* species have the ability to proliferate in whey and aid in the production of lactic acid.[14] Other species have been shown to require more complex nutrients in order to grow. Therefore, yeast extract has been previously added to some whey permeate media in order to generate growth of LAB.[14]

Lactobacillus spp., are microorganisms commonly used in the bioprocessing of dairy products. LAB have shown great potential in the food industry due to their recognition of being "Generally Regarded as Safe" (GRAS). This family of bacteria have the ability to ferment dairy products and can contribute to the improvement of food safety. They also possess several health benefits and aid in the enrichment of nutritional value of products. [15] In particular, the fermentation process of these bacterial cells vastly contributes to the increased shelf-life and aids in the stabilisation of nutritional components within dairy products. Other advantages of LAB fermentation include the production of high quality products with increased existence of organoleptic characteristics. [15] Milk fermentation can be carried out by either spontaneous growth of naturally occurring bacteria already present in the raw milk or by inoculation of a starter culture [16] [17].

The "inoculation" technique is more advantageous due to its higher controlled environment in which a known concentration of bacteria is introduced to the process.

LAB are favourable for their use in the quality and stability of dairy products and are known as natural food preservatives. Often referred to as “probiotics”, they have shown to aid in the stimulation of the host's immune cells, with data providing evidence of a decrease in the risk of cancer [1819]. These microbes have the capability to inhibit the proliferation of other bacteria due to their ability to produce organic acids and bacteriocins. Bacteriocins are small peptides produced by bacterial cells that hold antimicrobial properties in order to influence the bacterial proliferation of other microbes in the same environment.

1.2 Bioplastics

Recently, the area of biopolymer production has been of interest as bioplastics, which can help alleviate the harmful effects of micro plastics and single use plastic waste in the environment. This domain has the potential to replace the use of fossil or “petrol-based” materials with bio-based plastics which are biodegradable in nature. Furthermore, the incineration of fossil-based plastics can also have tendencies to fabricate other toxic substances which can be harmful to the environment. [20] The process of incineration is difficult to replace with other forms of disposal e.g. recycling of plastics. Plastic recycling requires a certain level of purity in order to be implemented. Along with the high cost, recycling can cause a decrease in the quality of the material as it can weaken the structure and therefore has its own negative attributes. [20] Recycling of plastics can also accumulate a lot of microplastic granules, shown in *Figure 1.4*, which can affect marine environments as not all plastic is 100 % recyclable.

Figure 1.4: Microplastics. Image taken from https://technikjournal.de/2018/06/28/microplastics-in-the-water-an-invisible-threat/

This has been a huge cause of concern across the globe, with many people fighting for the depletion of such plastics completely from the manufacturing industry. However, the use of biopolymers, such as Poly-lactic acid (PLA) has not received real interest, mainly due to the high cost of lactic acid production which affects the ability to achieve high scale manufacturing of PLA. In order to overcome this issue, products that are derived from these biopolymers should be more desirable in terms of quality, cost of manufacture and economic stability. [21]

The high cost of raw materials, including glucose and specific proteins, have also hindered the success of replacing such materials with bioplastics. Therefore, researchers have studied different avenues in which the cost of supplies is less of a concern. Whey, a dairy industry side stream often thought of as waste, has the ability to produce "added-value" products, one of which includes PLA production.[3] Fermentation processes can be carried out in order to achieve huge turnover of lactic acid production. Both bacterial and yeast cells can be utilised in whey fermentations in order to obtain key compounds of interest or to generate unique consumer products in the dairy industry. Alternative processes include the use of enzymes. However, as enzymatic processes can be quite expensive, the use of microbial fermentations are

more favourable. By observing and controlling these fermentation processes, successful biopolymer production can be achieved.[3]

1.2.1 Lactic acid bacteria and their role in Bioplastic production

During the fermentation of dairy products, LAB produces lactic acid as a by-product. The production of lactic acid is dependent on what strain of *lactobacillus* species that is deployed in the fermentation. One species that has been shown to produce high concentrations of L (+) - lactic acid is *Lactobacillus paracasei subsp. Paracasei CHB2121*. It was shown to produce
192 g/L of lactic acid when fermentation media comprised 200 g/L of glucose.[22] An estimated value of 96.6 % optical purity of the lactic acid was achieved. This recently identified species of *Lactobacillus* could have great potential in the dairy industry for production of poly-lactic acid (PLA). [22]

Figure 1.5: Chemical structure of Poly (Lactic acid) and biodegradable plastic (Image taken from http://sustpkgg.blogspot.com/2009/07/pla-polylactide.html)

The generation of biodegradable polymers such as PLA, shown in *Figure 1.5*, are becoming more and more of interest due to their positive impact on the environment. These commodity plastics hold physical properties which allow them to be broken down in the environment by microbial degradation.[23] As a result, dairy industries are becoming keen to exploit their side stream processes in which polymerisable small molecules are produced from renewable sources e.g. whey protein. The optical purity of lactic acid achieved in the fermentation process will control the physical properties of the PLA end product, which in turn will affect the commercial uses of the biopolymer. The biotechnological production of lactic acid is a more appealing substitute to chemical synthesis as it attains a higher optical purity.[14] Therefore, the lactic acid can be subject to polymerisation and result in high molecular mass poly-

lactic acid by polycondensation, depolymerisation and ring-opening polymerisation. Due to the recent interest in PLA production, there is a demand for more interest into lactic acid production and fermentation.[23]

The production of L (+) or D (-) lactic acid can be achieved by the addition of a suitable microbe in the fermentation process that contains carbohydrates e.g. lactose from whey protein. During the process, lactose is broken down by lactic acid bacteria present which will promote the production of lactic acid, depicted in *Figure 1.6*. It also contains other components such as polypeptides, organic acids and minerals which all contribute to the final result of the process. Organic acids and mineral salts can affect the bacterial growth within the fermenter. Organic acids, such as iso-butyric and iso-valeric acids can also indicate interferences within the process.

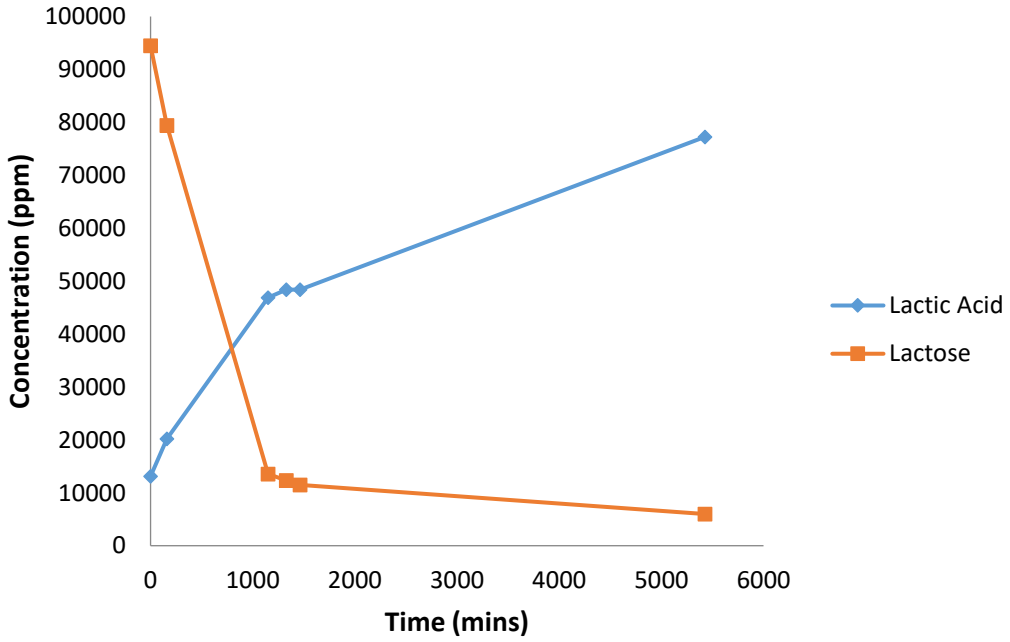

Figure 1.6: Typical whey fermentation curve with corresponding lactose and lactic acid concentration profiles, showing a decrease in lactose concentration and increase in lactic acid production as time increases.

All components of the process require constant monitoring to ensure the quality of the biotechnological process under controlled conditions. Temperature and pH are also factors which need to be monitored during fermentation as they have been shown to

influence the proliferation of bacteria and therefore interfere with the ability of microorganisms to carry out their function.

1.3 Biosensors

A biosensor is defined as an analytical device that incorporates the use of a biological element that is coupled to a transducer. Similar to other physical and chemical sensors, a biosensor responds to the presence of a particular analyte to determine its quality or quantity by means of an electrochemical signal. [25] Biosensors, shown in *Scheme 1.1*, are distinct in their own way due to the recognition element being biological in nature. The most widely used recognition element utilised in these devices are enzymes. The immobilisation of enzymes on the surface of the working electrode is depicted in *Figure 9*. [26] Other bio recognition elements used in biosensor development include nucleic acids, antibodies and protein receptors [16].

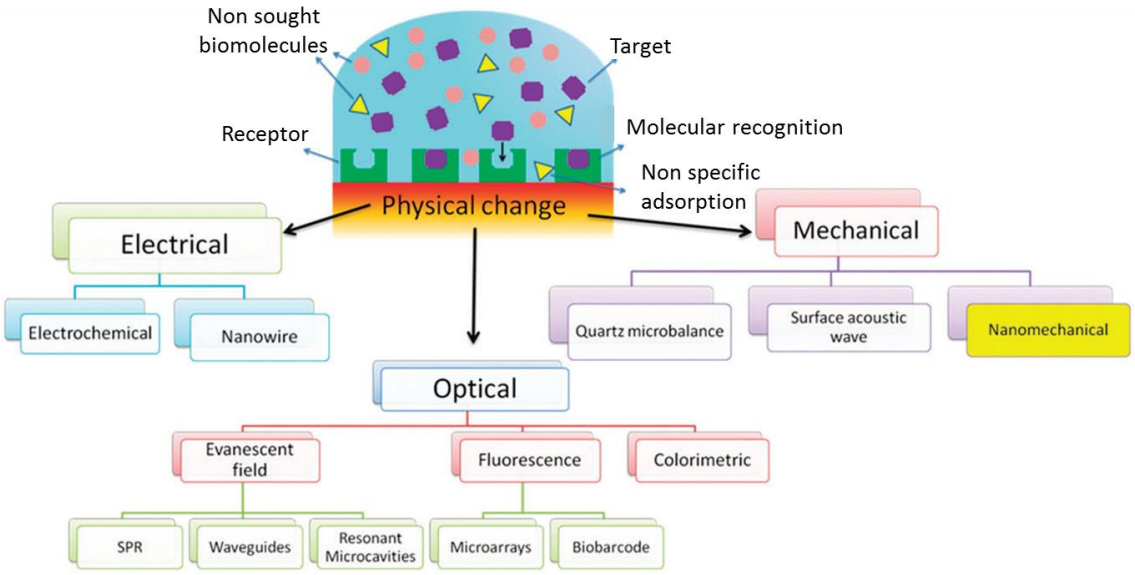

Scheme 1.1: Different types of biosensors [27]

1.3.1 Enzymes as bio-recognition elements

Enzymatic biosensors (*Scheme 1.2*) were first introduced in 1962 by Professor Leland C. Clark when he reported the use of "enzymatic transducers as membrane-closed sandwiches" in order to improve the intelligence of electrochemical sensors.[26] Here, he described the incorporation of the enzyme, glucose oxidase, in a "Clark oxygen electrode" which measures the decreasing concentration level of oxygen as a

proportional measurement of glucose concentration.[28] Many commercial biosensors are still manufactured using this style of biosensor development. More recently, the measurement of hydrogen peroxide has been favoured and was used in the development of amperometric glucose biosensors by Yellow Springs Instrument Company in 1975. [6]

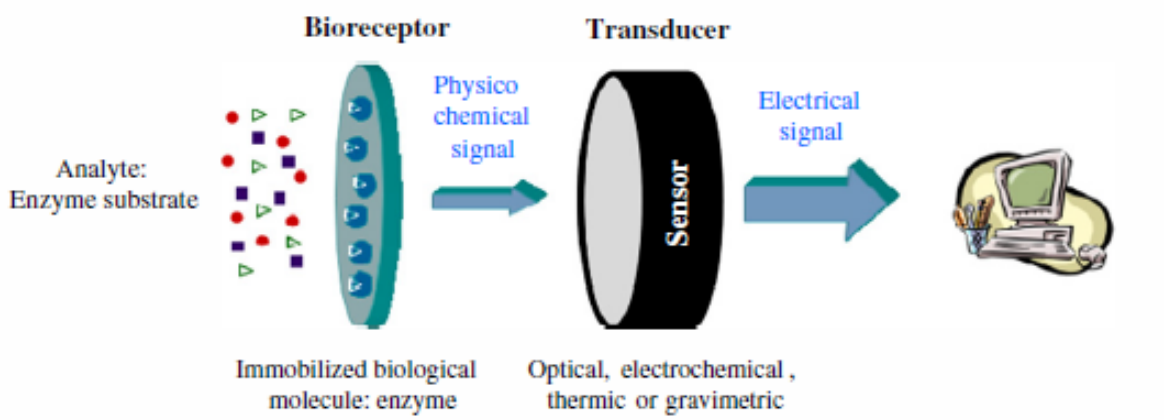

Scheme 1.2: Enzymatic biosensor [26]

1.3.1.1 Enzyme kinetics

Enzymes are large, complex protein catalysts that consist of polymers of α-amino acids. Each specific enzyme has its own genetically differentiated primary sequence which folds back on itself in a distinct position. The primary structure of a protein is made up of amino acids that have a particular sequence and are held together by peptide bonds.[29] The most important feature of an enzyme, particularly in the case of their use in biosensors, is their mode of action. Many enzymes involve oxidation and reduction reactions and therefore can be electrochemically analysed.[30] An example of a simple enzyme catalysis mechanism is shown below in *1.1*.

$$E + S \underset{k_2}{\overset{k_1}{\leftrightarrow}} ES \xrightarrow{k_{CAT}} E + P \quad \text{..... (1.1)}$$

Where; E = Enzyme

S = Substrate

ES = Enzyme/ Substrate complex

P = Product

k_{CAT} is the turnover number of substrate molecules converted to product per enzyme molecule per sec and maximum rate $V_{max} = k_{CAT}[E_o]$, where $[E_o]$ is the initial concentration of enzyme.

An enzyme catalysed reaction is dependent on the concentration of substrate present. Therefore, as the concentration of substrate increases, the rate of reaction will increase. As the concentration of substrate reduces due to the accumulation of product, the rate of reaction will cease and if the reaction is reversible, a state of equilibrium will occur. [31] If the initial velocity of the reaction is measured and determined, a graph representing velocity *vs*. substrate concentration can be constructed which shows that a state of maximum velocity occurs at a certain level of substrate concentration. Therefore, the velocity of the reaction will no longer increase when the substrate increases, (V_{max}). This can be explained by examining the enzyme-substrate complex concentration which is proportional to the rate of reaction or product formation. At higher concentrations of substrate, the enzyme present will be held in the enzyme/substrate complex. Enzyme kinetics can be described by the Michaelis-Menten equation, depicted in *equation 1.2* below;

$$V = \frac{V_{max}\,[S]}{[S] + K_m} \quad \text{.....(1.2)}$$

Where, V = Rate of reaction

V_{max} = Maximum rate of reaction

S = Substrate concentration

K_m = Michaelis-Menten constant

The units for V_{max} are moles of product per unit of time. It is constant at a certain concentration of enzyme. Hence, if the concentration of enzyme is altered, the V_{max} will increase or decrease in value. K_m can be described as the substrate concentration at half the V_{max} (*Figure 1.7)*. When the rate of the reaction is equal to K_m, the enzyme is equally distributed between enzyme/substrate complex structure and as "free-enzyme". [31] The 1st order rate of reaction depends on [S], 2nd order rate depends on both [E] and [S] and zero order is independent of the concentrations of substrate and enzyme.

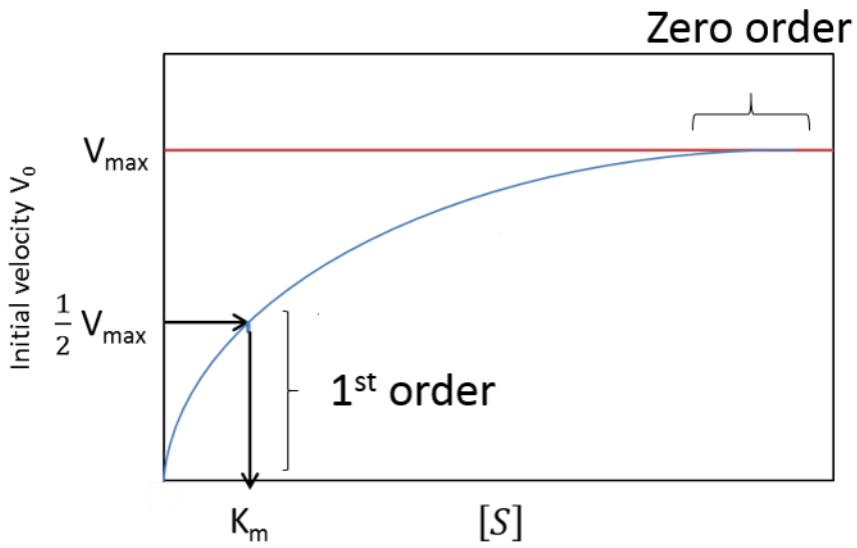

Figure 1.7: Michaelis-Menten plot.

The Lineweaver-Burk plot, shown in *Figure 1.8*, also known as the double-reciprocol plot is constructed from the inverse initial velocity $\left(\frac{1}{V}\right)$ and the inverse of substrate concentration $\left(\frac{1}{[S]}\right)$ (*Equation 1.3*).

V_{max} and K_m can be obtained from examining the slope of the line which is $\frac{K_m}{V_{max}}$ as the x-intercept is - $\frac{1}{K_m}$ and the y-intercept is $\frac{1}{V_{max}}$

$$\frac{1}{V} = \frac{K_m}{V_{max}} . \frac{1}{[S]} + \frac{1}{V_{max}} \quad \text{.....(1.3)}$$

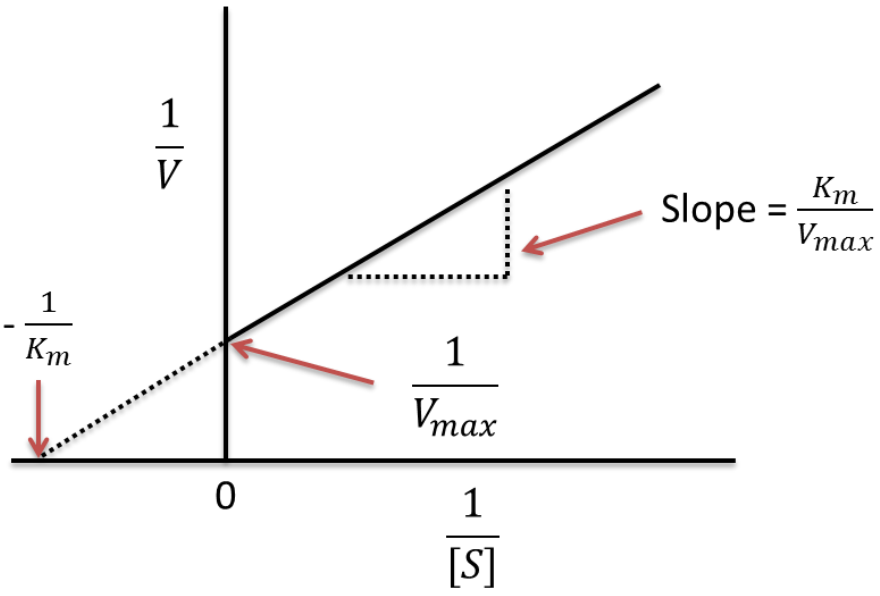

Figure 1.8: Lineweaver-Burk plot.

1.3.2 Electrochemical Biosensors

A wide range of biosensors have been developed over the years. Different transduction modes have been developed including amperometric, potentiometric and conductivity detection.[30] Amperometric biosensors involve measurement of current following a potential step. This results in a diffusion controlled signal which is proportional to the analyte concentration. Amperometric sensors are more advantageous compared to potentiometric and conductive sensors due to their low cost, high sensitivity, rapid turnaround times and their disposability.

1.3.2.1 First Generation

First generation sensors shown in *Scheme 1.3*, also known as the "Oxygen Electrode" were first developed in 1953. The most commonly known is the original glucose enzymatic electrode which involved the use of molecular oxygen as the oxidising agent.

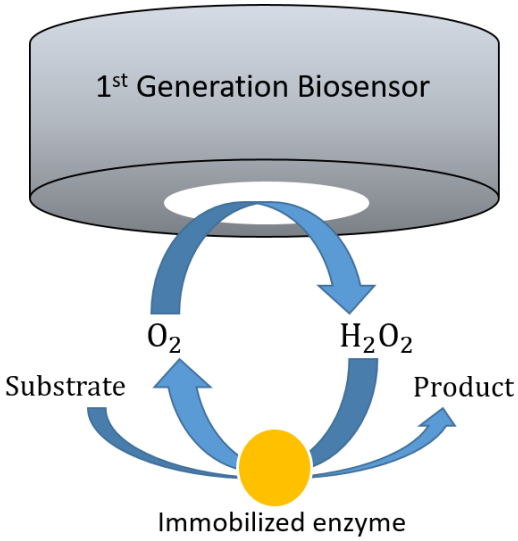

Scheme 1.3: First Generation biosensor [32]

The reaction monitored is the fluctuation in the concentration of oxygen using a Clark Oxygen electrode. The current measured is directly proportional to the glucose concentration. This method involved the enzyme, Glucose oxidase (GOx) immobilised in a polyacrylamide gel on a gas permeable membrane on the surface of the electrode which also holds a silver anode and a platinum cathode. The catalytic reaction involves the flavin (FAD) group in the enzyme reduced to $FADH_2$ in the presence of glucose *(equation 1.4)*. This is followed by the re-oxidation of the $FADH_2$ by molecular oxygen to regenerate FAD and produce hydrogen peroxide *(equation 1.5)*. This system is used regularly in the medical field and can be used as a model system during the development of newly designed biosensors. [30]

GOx (FAD) + glucose → GOx ($FADH_2$) + gluconolactone…….... (1.4)

GOx ($FADH_2$) + O_2 → GOx (FAD) + H_2O_2 ..... (1.5)

Since then, biosensors have been developed with the use of other oxidases including Lactate oxidase[33], Alcohol oxidase[34] and NADH oxidase[35]. One of the disadvantages associated with first generation enzyme electrodes included the high level of controlled atmospheric oxygen required. As these devices measured oxygen to determine of glucose concentration, the ambient oxygen must be kept constant or the electrode response would not give accurate measurements of glucose concentration.

In order to overcome such issues, second generation enzyme electrodes were developed.[28]

1.3.2.2 Mediated enzyme electrodes

Second generation sensors, shown in *Scheme 1.4*, involve the use of oxidising agents that act as electron acceptors, with the advantages of reversibility and better suited oxidation potentials. The electron transfer agents are known as "mediators". Favourable mediators have specific properties that include their ability to rapidly react with the chosen enzyme in the system. They should not be reactive with oxygen and have good stability.[28] The most well-known mediators are iron salts such as potassium ferricyanide ($K_3Fe(CN)_6$) and ferrocene. [36] Oxidation of glucose is controlled by FAD prosthetic group in the protein molecule. FAD is converted to $FADH_2$, as shown in *equation 1.6*. Ferrocene then re-oxidises the latter to FAD, followed by its re-oxidisation at the surface of the electrode, as depicted in *equation 1.7*. Glucose concentration is then measured by an amperometric current response.

$$\text{Glucose} + \text{GOx(FAD)} \rightarrow \text{gluconic acid} + \text{GOx}(FADH_2) \quad (1.6)$$

$$\text{GOx}(FADH_2) + 2\text{M(ox)} \rightarrow \text{GOx(FAD)} + 2\text{M(red)} + 2H^+ \quad (1.7)$$

$$2\text{M(red)} \rightarrow 2\text{M(ox)} + 2e^- \quad (1.8)$$

Where,

GOx(FAD) = Oxidised Glucose Oxidase

$GOx(FADH_2)$ = Reduced Glucose Oxidase

M(ox) = Oxidised mediator

M(red) = Reduced mediator

An example of a novel biosensor includes an amperometric biosensor developed for glucose detection which utilises potassium ferricyanide as a mediator. The sensor configuration involves glucose oxidase entrapped in a polyaniline-polyvinylsulfonate-potassium ferricyanide film. [37] Other complexes have been reviewed and shown their capability to act as redox mediators include osmium complexes and organic dyes.[38] [39]

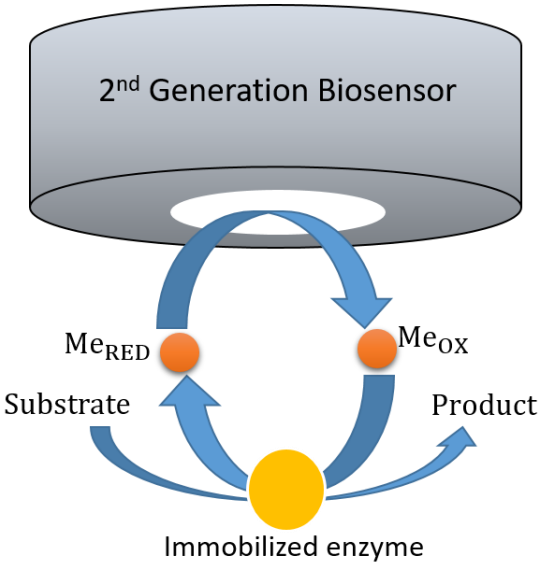

Scheme 1.4: Second Generation biosensor[32]

1.3.2.3 Third generation enzyme electrodes

Third generation sensors (*Scheme 1.5*) involve the direct coupling of a particular enzyme to the electrode. Various techniques have been developed in order to "wire" the enzyme directly to an electrode. This allows the transfer of electrons to occur quite rapidly resulting in high current densities. Generally, third generation biosensors involve the use of a redox polymer *in situ*.

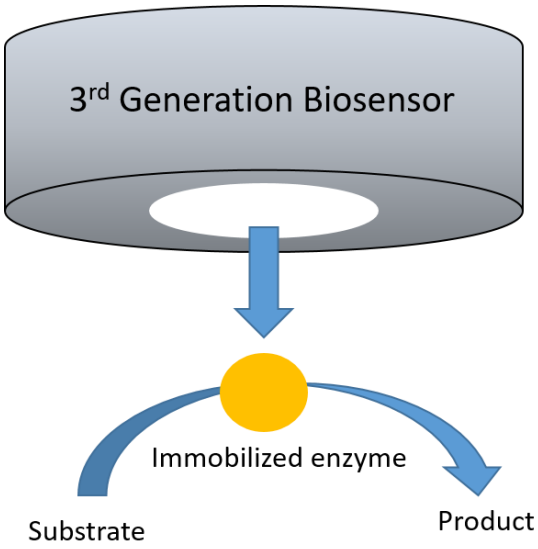

Scheme 1.5: Third Generation biosensor[32]

An example of a third generation biosensor is a glucose dehydrogenase sensor with pyrroloquinolinequinone (PQQ) acting as the "redox centre" for the system[30]. This was then wired to a glassy carbon electrode through poly(vinylpyridine), a redox polymer which was partially nitrogen-complexed with osmium bis(bipyridine) chloride^{2+}. This was followed by quarternisation with bromoethylamine, (POs-EA) and cross-linking via poly (ethylene glycol diglycidyl ether) (PEGDE), resulting in a high current density of 1.8 mA cm^{-2} for a 70 mM glucose sample. These results showed the third generation sensor was three times more sensitive than a glucose oxidase first generation sensor. The glucose dehydrogenase enzyme had a half-life of 5 days when stored in solution. However, following continuous use the current showed baseline decay after 8 h. [30]

More recent work has involved the investigation of faradaic electrochemical impedance spectroscopy (faradaic EIS) for glucose biosensor development. Here, enzymes such as flavin adenine dinucleotide (FAD) dependant glucose dehydrogenase (GDH) complex, were used based on the principle of faradaic EIS in the development of a impedimetric immunosensor. The sensor showed its ability to detect glucose being related to the change in charge transfer resistance, showing a higher sensitivity at lower concentrations of glucose with a narrow linear range of 0.02 – 0.2 mM. [40]

1.4 Biosensors in the Dairy Industry

The use of electrochemical biosensors for analysis of milk samples at various stages of processing are highly attractive and potentially very beneficial to the dairy industry. On-site, handheld and easy to use sensors would replace the use of conventional time-consuming analytical methods.

1.4.1 Sample preparation methods for electroanalysis

While there are many positive attributes to the use of biosensors for dairy sample analysis, sample matrix issues can be a challenge. One of the limitations to the use of biosensors is the interference issues between the components of the sample. [41] Many of the components within such a complex matrix may be electroactive and therefore cause inaccuracies in the measurement of the target species. Here, we will discuss different types of sample pre-treatment that may be implemented prior to the use of biosensors.

A simple pre-treatment method to overcome the issue with sample matrix is sample dilution. This involves dilution with the appropriate electrolyte for the electrochemical system. The degree of dilution depends on the type of sample analysed and can vary from matrix to matrix. Many studies have shown the successful use of diluting samples in order to accurately assess target analytes. [42] [43] [44] Studies have shown that different types of samples require different dilution pre-treatment steps, most likely depending on the sample matrix. When a study was carried out on dairy milk samples, raw full cream milk and ultra-high temperature processed milk, a dilution ratio of 1/4 was required. Other samples, such as skimmed ultra-high temperature milk and semi-skimmed milk did not require any dilution pre-treatment steps. [45] Studies have also shown that due to the complexity of dairy sample matrices, dilution of the sample sometimes does not always eliminate matrix effects. This includes a study carried out by Chemburu *et al*. in which milk samples that were spiked with bacterial cells were diluted 1/10 and still showed signs of interferences from the matrix. [46]

Centrifugation of dairy samples can be used in order to minimise background activity and interferences.[47] [48] [49] This is often implemented to remove the fat components of the dairy sample. In some cases, centrifugation only has shown to successfully decrease interferences within the sample without any further pre-treatment. [50]

1.4.2 Lactose Biosensing

Quantitation of lactose in milk is essential in the dairy industry.[41] Therefore, it is routinely carried out in order to ensure both quality control and efficiency during production. The determination of lactose in food samples can be carried out in a number of ways. Standard methods for quantitation of lactose in food samples include HPLC[51] and Raman Spectroscopy.[52] Below are examples of reports on lactose biosensors and their use in various dairy samples.

1.4.2.1 Optical Lactose Biosensing

Co-immobilisation of Glucose oxidase (GOx) and β-galactosidase (β-gal) has been utilised in the analysis of lactose via an optical-based biosensor. [53] Allyl glycidyl ether (AGE) – ethylene glycol dimethacrylate (EGDM) copolymer was coated with Bovine Serum Albumin (BSA) with 25 % crosslink density and a pH value of 8.0. BSA has naturally occurring functional groups including amino, thiol and carboxylic acids.

Following immobilisation, the BSA coated surface was treated with glutaraldehyde to activate the amino groups, disuccinimidyl carbonate (DSC) to activate the thiol groups and 1-ethyl-3-(3- dimethylaminopropyl) carbodiimide EDC to activate the carboxylic acid groups. Functional groups were then used to covalently attach GOx and β-gal via surface amino groups, with ≤ 10 % loss of enzyme activity and high stability. Lactose determination was then carried out by incubating the immobilised enzyme along with the milk sample for 1.5 hrs, extracting the supernatant and measuring the absorbance at 560 nm, which was proportional to lactose concentration. This method showed the ability of these enzymes to accurately determine the level of lactose in a milk sample using simple colorimetric methods.[53] The understanding of this pathway is that the first enzyme, β-gal hydrolyses β-lactose to form glucose and galactose, as illustrated in *equation 1.9*. GOx can then be used to oxidise glucose which will result in hydrogen peroxide (*equation 1.10)*. Therefore, using these enzymes in the development of an electrochemical amperometric biosensor would be ideal. An alternative to using glucose oxidase in this method is be the use of galactose dehydrogenase (GDH), which hydrolyses galactose by the reduction of NAD^+ to NADH.

β-Lactose + β-galactosidase → Glucose + Galactose……...…… (1.9)

Glucose + GOx → Gluconic acid + H_2O_2 ……...….. (1.10)

1.4.2.2 Electrochemical Biosensing of Lactose

1.4.2.2.1 The use of β-gal and GOx for the fabrication of lactose biosensors

Studies in which a dual-enzyme system consisting of glucose oxidase and β-galactosidase were carried out by Ammam *et al.* (2010). [9] This study involved the construction of a lactose sensor via alternating current electrophoretic deposition (AC-EPD). The sensor was modified with the enzymes by immersing the electrode in an enzyme solution which consisted of 10 mg of glucose oxidase and 90 mg of β-galactosidase in 1 mL of ultrapure water. This system permitted the electrophoretic deposition of a homogenous dual-enzyme layer on the working electrode. The overall aim of this experiment was to show that this dual-enzyme system could be simultaneously deposited via AC-EPD in order to develop a lactose sensor with good response. The results of the study showed that the alteration of AC signal, pH, temperature, enzyme activity, frequency and amplitude can affect the response of the

sensor in the presence of lactose. Following the determination of the optimum deposition parameters and testing conditions, the sensor was shown to have a sensitivity of up to 111 $nAmM^{-1}cm^{-2}$. The enzyme activities were 9 units/mg for β-gal and 5.6 units/mg for GOx.[9]

The hydrogen peroxide oxidised at the electrode was measured at 0.65 V vs. Ag/AgCl resulting in an amperometric signal which was proportional to the concentration of β-lactose present in the sample. Accuracy and performance studies of the sensor to detect and quantify β-lactose were carried out on various milk samples. It was noted that if electroactive species including uric acid and ascorbic acid were present in the sample, it may generate a false positive in current response as polarisation of the Pt electrode was at 0.65 V vs. Ag/AgCl. Therefore, a bare Pt electrode was used prior to examine the milk samples and detect any background current response. Results showed that electroactive species were present in the milk samples as the current signal increased by 1-2 nA at 0.65 V. [9] Additional studies were carried out by Ammam *et al.* (2010), to detect free glucose present. As the sensor configuration contains glucose oxidase, background glucose levels will result in false positives. Therefore, another sensor containing only one enzyme, glucose oxidase, was used to analyse each sample, and the signal subtraction can be used to determine more accurate lactose measurements. After analysis of possible interferences in the samples, lactose determination was carried out via the dual-enzyme lactose sensor. Results showed that there was a higher presence of lactose in extra-concentrated whole milk compared to whole, skimmed and semi-skimmed milk samples. This indicates that the sensor was a reliable and accurate source for the determination of lactose in a variety of milk samples. The sensor showed a wide linear range up to 14 mM lactose and very high reproducibility of ~85 %. It had a rapid response time of around 8 s and showed relativity good stability. It is also noted it was quite cheap to manufacture due to the use of low enzymatic activities giving it an advantage over other sensors for lactose quantitation.[9]

Glucose oxidase and β-galactosidase were used in the development of an amperometric biosensor by immobilization in gelatin by Loğoğlu *et al* (2006). [54] Gelatin is formed during partial hydrolysis of collagen. It is a hydrophilic protein that has the ability to form "reversible elastic gels" at low temperature. This study involved

the use of gelatin as the enzyme carrier and glutaraldehyde as the hardener or cross-linker. The electrodes were prepared by drop-casting the gel containing the two enzymes, onto the surface of the electrodes which were allowed to rest for 48 hours at 25 ^{o}C. The electrodes were stored in 0.1 M phosphate buffer at 4 ^{o}C while not in use.

The study was based on hydrogen peroxide detection at 0.7 V via amperometry. Various parameters were studied in order to determine the optimal conditions for enzyme immobilisation. The effect of glutaraldehyde concentration was investigated by mixing a 7.5 % gel containing the enzymes with different concentrations of glutaraldehyde solutions ranging from 0.004-0.015 M. The electrode with the highest response was found to be the electrode with 12 mM glutaraldehyde solution. A higher level of glutaraldehyde showed a decrease in activity which may be as a result of deactivation of the enzymes and increasing diffusion barrier. The effect of pH on the sensor was investigated by analysing the performance of the sensor with 20 mM lactose with a pH range of 3.5-9.6. The results showed the optimum pH for the sensor was 8.0. At pH 7.0, the sensor retained 87 % of that recorded for the sensor at pH 8.0. All measurements for further studies were carried out at pH 7.0. Temperature variations between 8-75 ^{o}C were carried out on the sensor. Stability studies were achieved by taking measurements every three days. This was carried out in order to determine the effects of re-usability and investigate shelf life of the biosensor. Ten measurements were taken over a 30-day cycle with the exact same conditions and parameters. Results showed very little or no loss of activity of the sensor after 30 days. The sensor was also analysed for its reusability by taking measurements of the biosensor in standard lactose solutions of 20 mM and also in milk samples every 30 minutes. Results for this study showed low loss of activity from the biosensor even after its 10th measurement in samples. Therefore, this sensor has shown its high performance and strong stability for use in determination of lactose in milk samples. The development of this sensor could be used in both the medical and dairy industry for accurate lactose determination.[54]

Modification of lactose biosensors with polymers have shown to enhance the signal of an unmodified electrode surface. A study carried out by Nguyen *et al* (2016)[55], used a polymer known as 1, 5 – diaminonaphthalene shown in *Figure 1.9*, p(1,5–DAN), to increase the signal of a lactose microsensor.

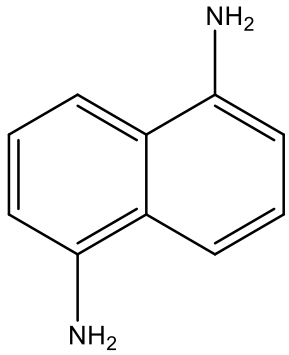

Figure 1.9: Chemical structure of 1,5-diaminonaphthalene

p(1,5-DAN), a known conductive polymer, has favourable characteristics including electro-activity, electroconductivity and electrocatalysis. The functional amino groups present on the chemical structure are responsible for the reactivity of the compound due to chelating and reduction properties.[56] Research into the possible use of p(1,5-DAN) for the development of biological sensors has been of interest as it has the ability to bind biomolecules or to decrease the space between the surface of the electrode and the active sites of the enzymes. [57]

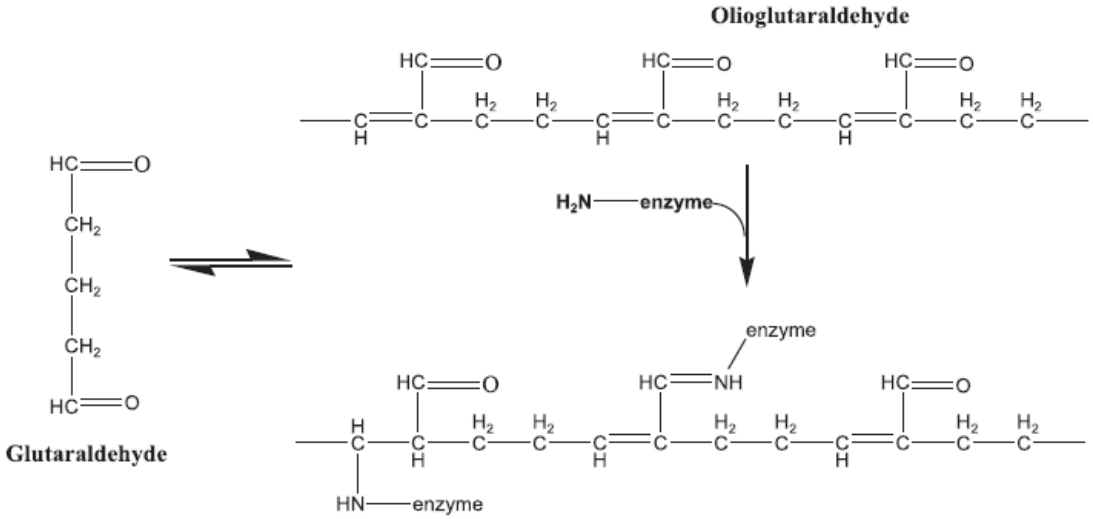

Scheme 1.6: Schematic co-immobilization of β-galactosidase and glucose oxidase on modified Pt/graphene/P(1,5-DAN) electrode using glutaraldehyde [55]

The sensor was developed using co-immobilisation of glucose oxidase and β-galactosidase on a pre-modified platinum electrode, as depicted in *Scheme 1.6*. 80 IU of β-galactosidase and 22131 IU of glucose oxidase were drop cast onto the surface of the modified working electrode. Following enzyme deposition, the electrode was allowed dry overnight at 4^{o}C. Results show that the modification of the Pt electrode

with p(1,5–DAN) gave a higher current intensity than that at an unmodified surface. The electrode was tested for lactose response over the range 0-60 µg/mL. The results showed a good linear relationship between current response and lactose concentration with a correlation co-efficient R^2 value of 0.995 with a limit of detection of 1.3 µg/mL. The sensitivity of the electrode was determined to be 1.33 $\mu A \mu g m L^{-1}$. [55]

1.4.2.2.2 The use of Cellobiose Dehydrogenase in the fabrication of 3rd generation lactose biosensors

Third generation lactose sensors have been developed based on Cellobiose Dehydrogenase (CDH).[58] This work, carried out by Stoica *et al.* was based on the direct electron transfer between two recently discovered Cellulose Dehydrogenases, isolated from fungi species *Phanerochaete sordida* and *Trametes villosa*. The overall aim of this work was to develop a third generation biosensor via direct electron communication between the CDH enzyme and a solid-supported graphite electrode surface. CDH is made up of two domains, one flavodomain of FAD and one heme domain of the cytochrome b type which in their resting state, are both fully oxidised. The role of FAD is to oxidise the sugar substrate cellobiose or lactose. The oxidation reaction of lactose involves 2 e^- being transferred to the FAD component which causes electrons to pass to the heme co-factor, as shown in *Scheme 1.7*. This is known as an internal electron transfer (IET) system. Due to the close proximity of the heme domain and the surface protein, electrons can be passed to the graphite electrode via direct electron transfer (DET). The signal response at the enzyme-modified sensor is directly proportional to low lactose concentrations. Therefore, the current response is not dependent on diffusion barriers unlike previously developed lactose biosensors.

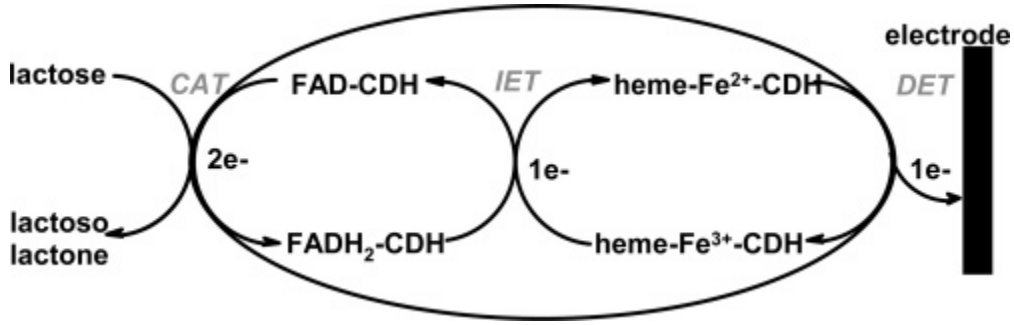

Scheme 1.7:Diagram of reactions occurring at the enzyme-electrode interface [58]

The advantage of this third generation biosensor is that cellobiose dehydrogenase is not present in milk, unlike β-galactosidase which can be added to low lactose milk in order to breakdown β-lactose into glucose and galactose for consumption by lactose intolerant consumers. Therefore, it will not interfere with the accuracy of the sensor. One of the key points of this sensor is that it is highly suitable for trace detection of lactose due to its very low linear detection range of 1- 100 µM. Therefore, it could detect lactose in low lactose or lactose-free samples that require a range of <0.01 % (w/w). [59] This is far less than any other commercial lactose sensors available. Therefore, it can be advantageous in the use of low-lactose or "lactose free" products specially designed for lactose intolerant individuals. Overall, results based on these CDH biosensors show that the *P. sordida* CDH-modified lactose sensor was found to be the more reliable sensor. Analysis of the ability of the sensor to detect lactose in samples such as low-lactose milk, pasteurised milk and buttermilk were carried out via the standard addition method. Analytical performance included LOD of 1 µM, a sensitivity of 1100 μAmM^{-1}, a rapid response time of 4 s and a linear range of 1-100 µM lactose with a R^2 value of 0.998.

CDH has also been employed elsewhere, for the development of a novel amperometric lactose biosensor based on an immobilised enzymatic system for the determination of lactose in milk.[43] CDH, derived from *Phanerochaete chrysoporium*, was immobilised in an enzyme reactor using aminopropyl-silanised controlled pore glass beads and crosslinking with glutaraldehyde solution. p-benzoquinone, was used as the electron acceptor in the oxidation of lactose in samples. The sensor utilised two measurement systems, a thermometric detection involving the analysis of heat production during the enzyme catalytic reaction of lactose and the reduction of p-benzoquinone. The other measurement system was the electrochemical re-oxidation of the reduced p-benzoquinone, which acts here as a mediator. The sensor showed a linear range of 0.05 – 30 mM with a RSD < 10%. The sensor was used to determine the lactose concentration of a number of dairy milk samples including 1.5 % and 3 % fat milk along with a lactose-free milk sample. [43]

1.4.3 Lactic acid Biosensing

Lactate fermentation is a key process in the dairy industry. Lactic acid biosensors have been of interest to the food industry for rapid quantitation of lactate in samples for quality determination, and here we give an account of lactate biosensors in food monitoring with emphasis on the dairy industry. Lactate biosensors can be classified based on their detection methods - electrochemical, electrochemiluminescence, fluorescence, microband and reagentless lactate biosensors. Electrochemical based devices utilise potentiometric, amperometric or conductivity measurements. Amperometric lactate biosensors have shown a high level of deployment in the food control sector due to their simplicity, ease of use, portable nature and simple integration into various devices. Biosensors that are reagent-less and require very little sample preparation are of interest and are more likely to be made of single-use, disposable material.[60]

Both L-lactate oxidase (LOx) and Lactate Dehydrogenase (LDH) have been widely exploited for L-lactate detection. LOx is a preferred enzyme due to its simple configuration. It is a globular flavoprotein most commonly derived from a variety of microorganisms, including *Pediococcus* species and *Aerococcus viridians*. [60] LOx is also more commonly used due to the enzyme reaction involving production of H_2O_2 which can be detected amperometrically, (see *equations 1.11-13*).

$$L\text{-}lactate \xrightarrow{LOx} pyruvate + LOx_{red} \quad \text{(1.11)}$$

$$LOx_{red} + O_2 \rightarrow LOx_{ox} + H_2O_2 \quad \text{(1.12)}$$

$$H_2O_2 \rightarrow O_2 + 2H^+ + 2e^- \quad \text{(1.13)}$$

The enzyme can then be re-oxidised in the presence of dissolved oxygen, releasing hydrogen peroxide. When the hydrogen peroxide is then oxidised at the surface, the initial oxygen concentration is regained and the measure of current is proportional to the amount of lactate present in the sample matrix. [61] Due to the oxidation of peroxide requiring a high over-potential, mediators e.g ruthenium or polymers e.g poly(diaminonaphthalene) can be used in order to overcome this issue. [60] Transducer surfaces utilised for Lactate oxidase based biosensors include screen-printed

electrodes (SPE), microporous gold electrodes, glassy carbon electrodes, ITO plate based electrodes, carbon, platinum and gold electrodes.

Development of a lactate reagent-less biosensor has been carried out recently by Bravo *et al.* (2017) for determination of lactate in food samples.[60] Here, LOx was immobilised onto carbon screen-printed electrodes that had been previously treated with N,N'-Bis(3,4-dihydroxybenzylidene)-1,2-diaminobenzene Schiff base tetradentate ligand-modified gold nanoparticles (3,4DHS-AuNPs). These sensors were able to detect and quantify lactate concentrations by measuring the increase of peroxide production. By using this co-immobilisation technique, Bravo *et al.* expressed their ability to simplify the development of a lactate biosensor in the determination of lactate in point-of-care analysis. Once the lactate sensor was optimised, its response to lactate concentrations was analysed via chronoamperometry by applying a step potential of 0.3 V vs. Ag/AgCl. Calibration studies were carried out and the biosensor showed good reproducibility and stability. A calibration curve was constructed by plotting lactate concentration vs. current response, which followed a Michaelis-Menten type kinetics, as depicted in *Figure 1.10* below.

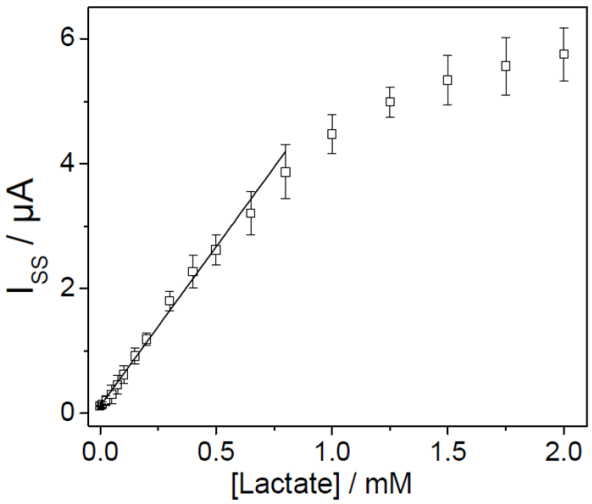

Figure 1.10: Calibration curve obtained showing current response via chronoamperometry for LOx/3,4DHS-AuNP/SPCE in 0.1 M PBS (pH 7.0) [60]

Investigations into the development of a bi-enzyme amperometric graphite biosensor for the determination of lactic acid was carried out by Herrero *et al*. (2004).[62] This was achieved by immobilisation of Horseradish Peroxidase (HRP), Lactate Oxidase (LOx) and ferrocene onto a Graphite-Teflon sensor. The use of graphite and Teflon

composites in the development of biosensors can improve the stability and robustness of the sensors in order to achieve commercialisation. The objective of the work carried out by Herrero *et al*., was to use the biosensor to determine lactate quantity in yoghurt products. Results were compared to those obtained from standard colorimetric methods. The samples analysed were yoghurts made from cow's milk, goat's milk and goat's milk containing added whey protein concentrate. Therefore, a comparison in both the physical and biological characteristics of each product could be made. The samples were all diluted with phosphate buffer at physiological pH (7.4) prior to analysis by the standard addition method, as shown in *Figure 1.11*.

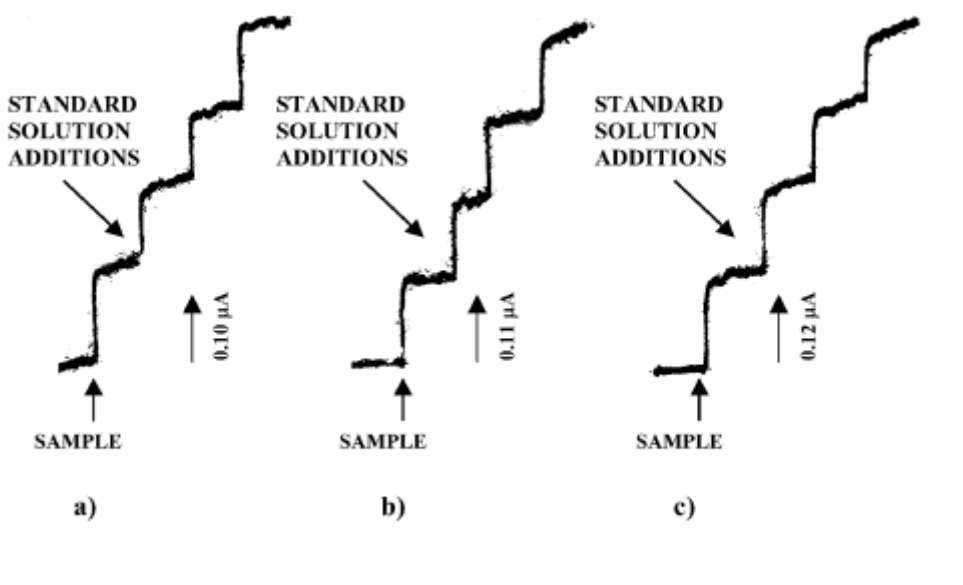

Figure 1.11: Current-Time response for a graphite/Teflon/LOx/HRP/ferrocene biosensor of a) cow's milk yoghurt b) goat's milk yoghurt and c) goat's milk yoghurt containing whey permeate concentrate and 25 µL additions of 0.01 mM L-lactate standard. E_{app} = 0.0 V.[62].

Lactic acid determination by LDH is an alternative technique that involves an enzymatic reaction of lactic acid in the presence of co-factor nicotinamide adenine dinucleotide (NAD^+), depicted in *Scheme 1.8*. The catalytic reaction for lactate dehydrogenase is as follows (*equation 1.14*).

$$L\text{-}lactate + NAD^+ \xrightarrow{LDH} pyruvate + NADH + H^+ \quad (1.14)$$

Where, the H^+ ions produced alter the potential of the surface of the electrode which relate to lactate concentration, or alternatively the re-oxidation of NADH is monitored

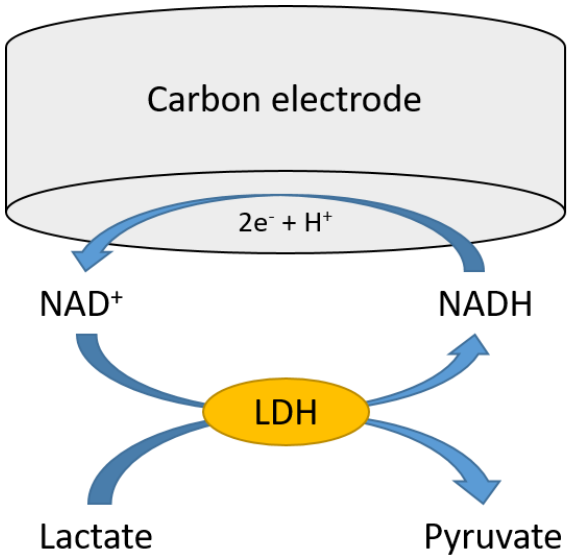

Scheme 1.8: Scheme of LDH at Carbon electrode [63]

Although this technique is currently used in a widespread of laboratories, there are some slight disadvantages to the use of LDH over LOx. LDH requires the addition of co-factor NAD^+ which can cross-react with other endogenous components in serum or plasma samples which can affect the accuracy of results. [64]

Studies performed by Lupu *et al.* (2007) have shown how nanostructured surfaces improve the limit of detection and the signal to noise ratio in lactic acid biosensors.[65] A nanostructured Si_4N_3 surface potentiometric sensor was reported, which employed an electrolyte-membrane-insulator-semiconductor (EMIS). Modification of the electrode surface was carried out using a polyacrylic acid layer, deposited by plasma enhanced chemical vapour deposition (PECVD). PECVD was covalently linked to amine (NH_2) groups on the surface of the LDH enzyme. The Si_4N_3 nanosurface was then applied to the electrode surface by colloidal lithography. The results showed the limit of detection for lactate to be 2×10^{-7} M with a linear range up to 10^{-5} M. The inter- and intra- electrode standard deviations were 2.4 % and 11 % respectively. [65]

An amperometric lactate biosensor was developed via immobilisation of the enzyme LDH on the surface of a grapheme oxide nanoparticles-modified pencil graphite electrode. During each step of modification, the surface of the electrode was analysed by Scanning Electron Microscopy (SEM), Fourier Transform-Infrared Spectroscopy (FTIR) and Cyclic Voltammetry (CV). The biosensor resulted in a limit of detection of 0.1 µM (5 s response time) and a linear range of 5-50 mM at pH 7.3. The biosensor was used to determine the lactate concentration in dairy products including milk, yoghurt and curd. [66]

1.5 Experimental Techniques

1.5.1 Electrochemical methods

Electrochemistry involves the study of redox reactions present in an electrolyte solution by monitoring parameters such as current, charge or potential.[30] Molecules which have the ability to accept or donate electrons to a source are termed electroactive species. Therefore, oxidation or reduction reactions can occur by transfer of electrons to the working electrode in an electrochemical cell. During these redox reactions, changes occur in the parameters, mentioned above, which can be detected and measured.[67] Various techniques can be used in order to measure specific electrical properties of a sample of interest. Here, we discuss the various types of electrochemical techniques used widely in the development and utilisation of biosensors.

There are two main types of current produced during an electrochemical redox reaction, Faradaic and non-Faradaic or capacitive current.[68] Electron transfer between the analyte in the electrolyte and the working electrode results in Faradaic current as described by Faraday's Law, which states that the amount of electricity that passes through an electrolyte solution during an electrochemical reaction, is proportional to the amount of chemical change.[68]

$Q = nFN$……..(1.15)

Where Q = Charge (C)

n = number of electrons

F = Faraday's constant (96,485) C mol^{-1}

N = number of moles of substance converted

Non-faradaic current, also known as capacitive current, is created by an array of both polar and charged species that are present at the interface between the electrode surface and the solution. This interface area is known as the electrical double layer, as shown below in *Figure 1.12.*

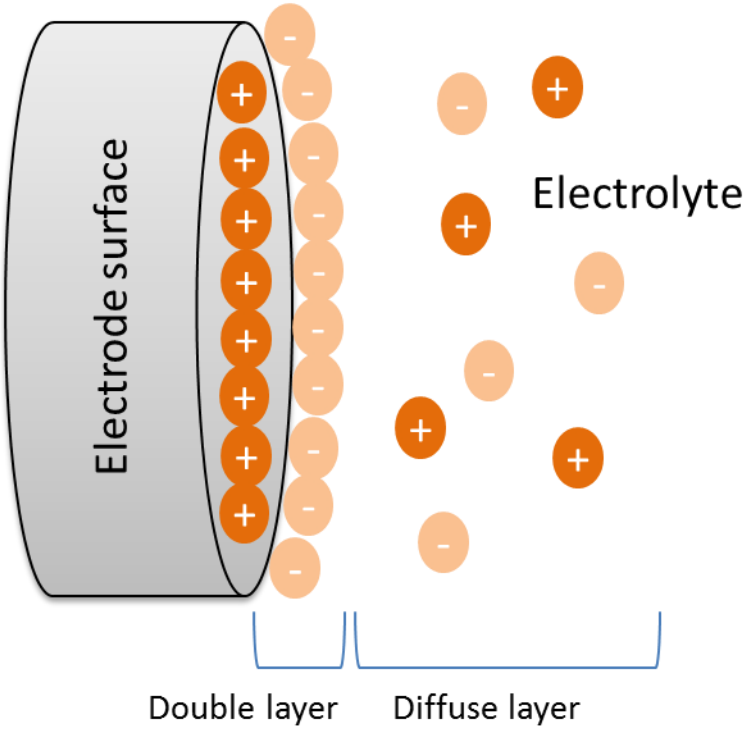

Figure 1.12: Electrical double layer and diffusion layer interface at electrode surface

If the electrode holds a negative charge, positively charged ions in the area of the electrode surface will arrange themselves next to the negatively charged surface. If the electrode possesses a positively charged surface, negatively charged ions will align themselves at the electrode surface. This double layer can act as a capacitor which can impede the flow of current. Therefore, this capacitive current must be evaluated in the determination of faradaic current values.

1.5.1.1 Mass Transport

There are three processes involved in the passing of electrochemical current through an electrolyte solution in an electrochemical cell known as migration, convection and diffusion.[30]

Migration involves the movement of ions across a potential gradient created by two electrodes that hold different potentials. It can be observed by the use of impedance studies or conductivity measurements. The effects of migration can be eradicated with the use of a high concentration electrolyte.[30] The role of the supporting electrolyte is to maintain a constant ionic conducting environment while remaining inert to electrochemical analysis. Convection involves the movement of the whole solution, transporting the ions across the solution. This can be executed by stirring the solution or by rotating the electrode. In techniques such as Cyclic Voltammetry, convection is avoided by maintaining a convection free environment within the cell.[30]

Diffusion involves the movement of ion species across a concentration gradient from an area of high concentration to an area of low concentration. Therefore, if the analyte is oxidised or reduced due to the potential applied to the electrode, the concentration of the analyte at the electrode surface will decrease which will cause an increase the movement of analyte across from the solution to the electrode surface.[30] Fick's law of diffusion describes an amount of material, M, that flows through a unit cross section, S, in any given unit of time, t, known as the flux, J, being proportional to the concentration gradient, dc/dx. [67]

$$J = \frac{dM}{S.dt} \quad \text{.....(1.16)}$$

$$J = -D\frac{dC}{dx} \quad \text{.....(1.17)}$$

Where,

J = flux (gcm^2s^{-1})

M = mass (g)

S = cross section area (cm^2)

t = time (s)

D = diffusion co-efficient (cm^2s^{-1})

dC/dx = concentration gradient

C = concentration (gcm^{-3})

x = distance of movement perpendicular to the barrier surface (cm)

1.5.2 Cyclic Voltammetry

CV is the most widely utilised electrochemical technique for initial evaluation of the redox activity of a sample of interest and can be used to determine the electrode potential at which a species of interest undergoes oxidation or reduction.[30] It involves the application of a potential scan to a WE (immersed in an unstirred solution), over a relevant range and measurement of resultant faradaic and capacitive current. The output signal is a cyclic voltammogram which shows Current (A) vs. Potential (V), including peaks (I_p) which are proportional to concentration [69].

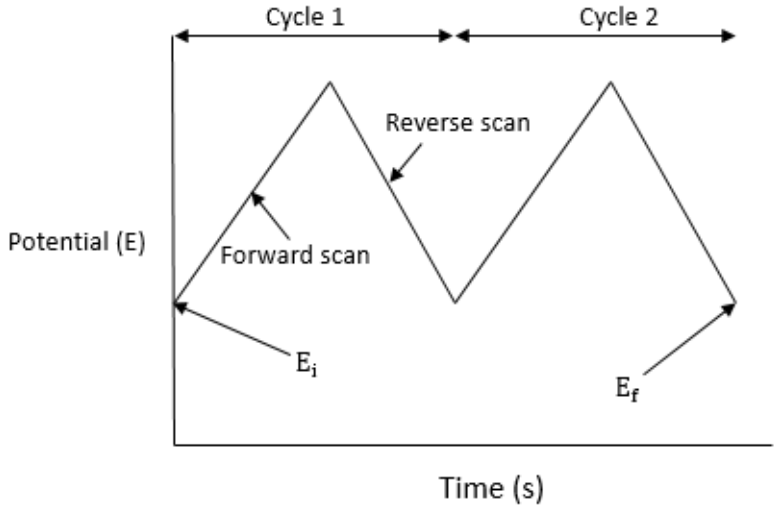

Figure 1.13: Triangular potential waveform for Cyclic Voltammetry

The controlling potential can be also described as an "excitation signal" and in the case of CV, is a linear potential scan expressing a triangular waveform, shown in *Figure 1.13*.

The excitation signal causes potential sweeping of the electrode between two determined values, also known as switching potentials. The forward and reverse scans can be represented for oxidation and reduction taking place. However, single or multiple cycles can be used in any experimental setup. The rate of change in potential is termed scan rate (ν) and is measured in Vs^{-1}. Scan rate is an important parameter to control as it can affect the resultant voltammogram in terms of peak current and peak potential. Instrumentation software allows for variation of potential scans and scan rates.

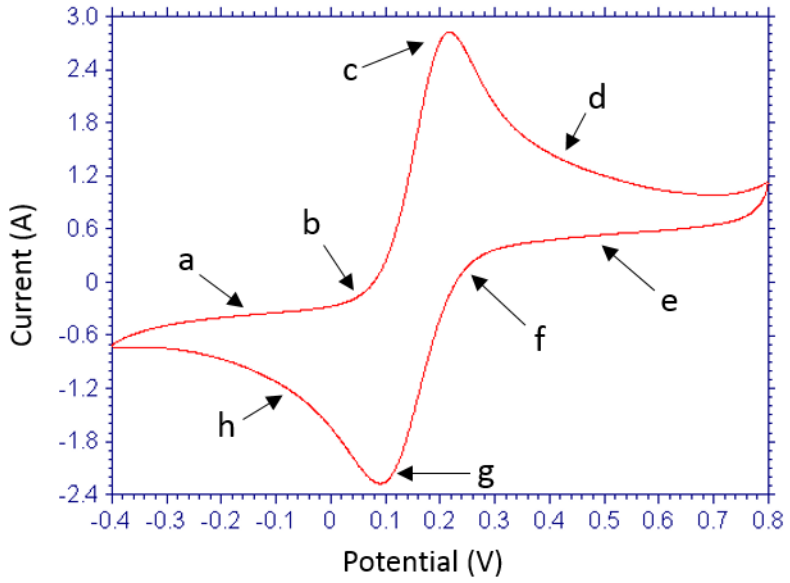

Figure 1.14: Cyclic Voltammetry of 5 mM $K_3Fe(CN)_6$ in 0.1 M KCl at a gold electrode with scan rate of 0.1 V/s vs. Ag/AgCl

Figure 1.14 above shows a typical cyclic voltammogram of a 5 mM $K_3Fe(CN)_6$ solution representing a reversible redox reaction. Cyclic voltammetry was used to analyse the redox potential of the 5 mM $K_3Fe(CN)_6$ in a 0.1 M KCl, which acts as the supporting electrolyte. Here, we observe the oxidation and reduction of Fe^{2+} to Fe^{3+} at a gold macroelectrode between a potential range of -0.4 V to 0.8 V at a scan rate of 100 mVs^{-1}. Point (a) represents the point in which no redox behaviour of the species is observed. Point (b), a potential of 0.05 V, the current begins to increase indicating

the oxidation of Fe^{2+} to Fe^{3+}. Analysis of this region can be carried out in order to investigate the kinetics of the reaction, providing information on the electron transfer rate of the analyte. Point (c) represents the maximum anodic peak current ($I_{p(a)}$). Past point (c), there is decay in current with respect to $t^{-1/2}$ as the concentration of Fe^{2+} surrounding the electrode surface is depleted due to an increasing diffusion layer, as shown previously in *Figure 1.12*. This is due to its electrolytic conversion to Fe^{3+} at the electrode surface. The direction of the potential scan is then switched negatively to produce a reverse scan, shown in point (e). During the reverse scan, the Fe^{3+} produced during the anodic oxidation reaction, will be reduced back to form Fe^{2+}. This results in an acceleration of current, evident in point (f). Point (g) shows the maximum cathodic peak current ($I_{p(c)}$). The redox kinetics can be determined by analysis of the region between point (f) and (g). The current then begins to decay as the Fe^{3+} concentration surrounding the electrode decreases and the current value returns to baseline and the scan returns to the initial potential of -0.4 V.

1.5.3 Chronoamperometry and Chronocoulometry

CA and CC are techniques that involve a controlled potential step applied to the working electrode. These electrochemical techniques use a single or multiple step system where the potential is switched from an initial potential (E_1) to a determined controlled potential (E_2) that has been previously determined by CV, as shown in *Figure 1.15*.[30]

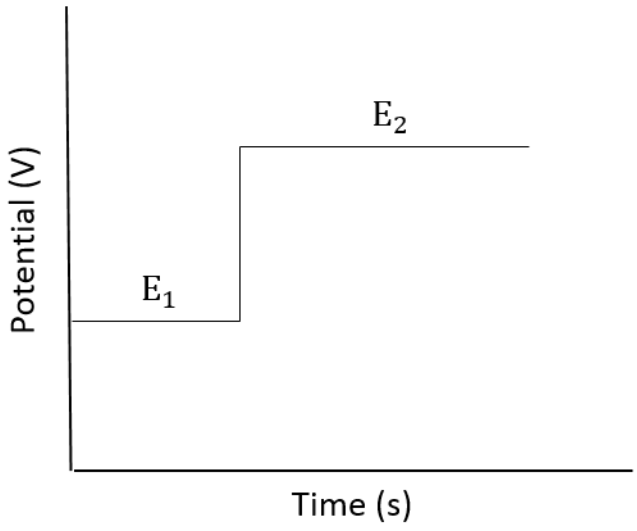

Figure 1.15: Potential step function for CA and CC

The electrode is immersed in an electrolyte solution containing the redox species. A flow of electrical current is caused by a change in the composition of electrolyte at the interface, where the concentration of the redox species will vary. The depletion of the electroactive species at the surface of the working electrode causes signal decay, according to *equation 1.18.* [70]

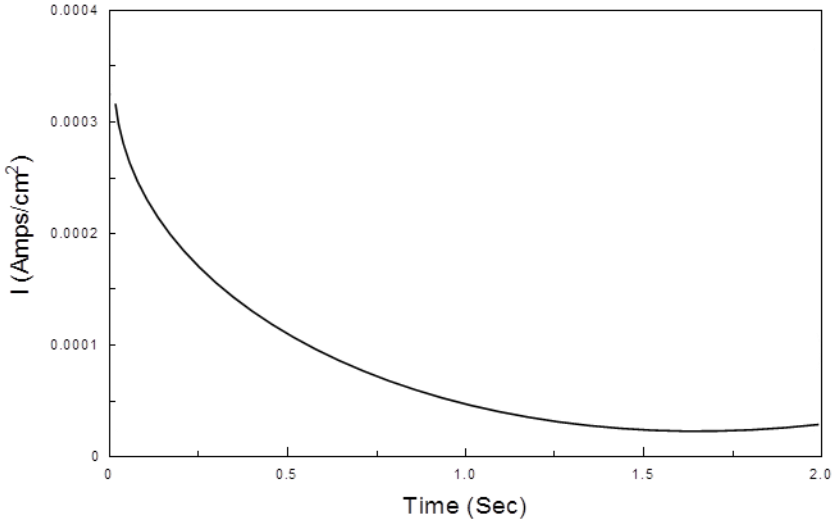

Figure 1.16: Current density vs. Time response for 5 mM $K_3Fe(CN)_6$ at Au electrode

Figure 1.16 above shows the relationship between current and time via Chronoamperometry which is explained by the Cottrell equation.[30]

$$i_d = \frac{nFADC}{\pi^{1/2}t^{1/2}} \quad \text{(1.18)}$$

Where n = number of electrons

F = Faraday's constant (96,485 C/equivalent)

A = Area of electrode (cm^2)

D =diffusion constant for electroactive species (cm^2s^{-1})

C =concentration of electroactive species ($molcm^{-3}$)

t = Time (s)

The decay in current signal is the result of a diffusion layer at the surface of the electrode. This diffusion layer increases over time as the concentration of the species depletes at the electrode surface. Due to the expansion of this layer, diffusion limits

the current signal. The linear relationship between current and the inverse of $t^{1/2}$ can be described as a diffusion limited process and is described in *Figure 1.17*.[30]

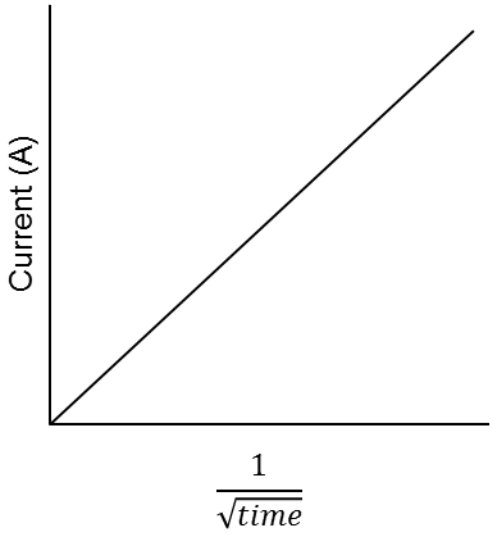

Figure 1.17: Cottrell plot showing current vs. $1/\sqrt{time}$

Chronocoulometry is an electrochemical technique, similar to Chronoamperometry, but measures the charge expressed during a redox reaction, depicted in *Figure 1.18*.

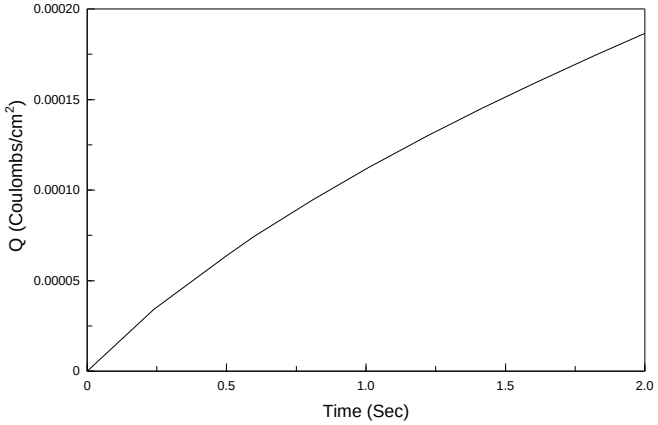

Figure 1.18: Charge vs. Time response for 5 mM $K_3Fe(CN)_6$ at Au electrode with E_{app} = 0.25 V vs. Ag/AgCl for 2 s.

As the potential of the working electrode is set at a fixed value, meaning the redox reaction proceeds at a rate limited by diffusion alone, the charge taken up by the

reaction can be described by the integrated form of the *Cottrell equation (equation 1.19)*:

$$Q = \frac{2.n.F.\sqrt{D}.c_o\ .A\ .\sqrt{t}}{\sqrt{\pi}} \quad \text{.....(1.19)}$$

Where Q = Charge

n = number of electrons

F = Faraday's constant (96,485 C/ equivalent)

D = Diffusion constant for electroactive species (cm^2/s)

c_o = Concentration of electroactive species (mol/cm^3)

A = area of electrode surface (cm^2)

t = time (s)

1.5.4 Thin Film Voltammetry

Electrochemical techniques such as CV and CC can be used for characterisation of redox polymer films. In order to study the redox behaviour of a thin-layer film on an electrode, slower scan rates are usually performed (5 – 10 mVs^{-1}). A typical thin-film voltammogram with a one electron reaction is shown in *Figure 1.19*. Here, we can demonstrate that both the oxidation and reduction peak are symmetrical, in contrast to a typical quasi-reversible voltammogram. The symmetrical nature of the two peaks will only be seen in a fully reversible electrode reaction. The symmetry of both the oxidation and reduction peaks can be affected by the heterogeneous rate constant and when this value is low, they can lose their symmetrical shape.

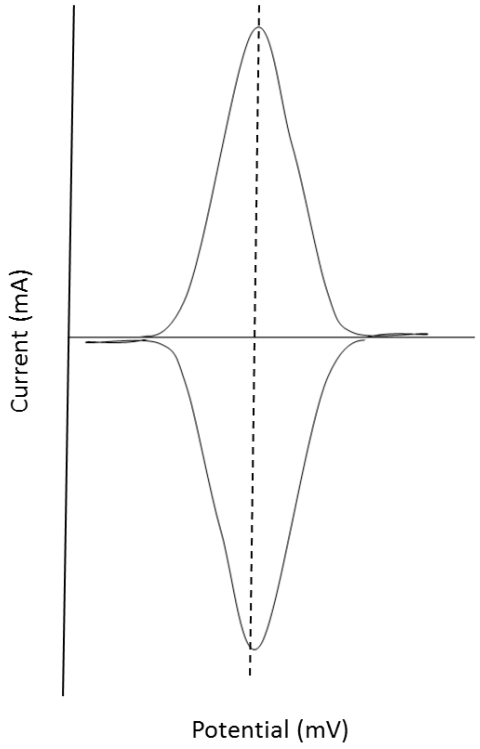

Figure 1.19: Typical reversible thin-film voltammogram

In thin-film voltammograms, peak current can be expressed as;

$$\dot{\imath} = \frac{n^2F^2\Gamma A\nu}{4RT} \quad \text{.....(1.20)}$$

An ideal thin film voltammogram would illustrate two symmetrical peaks with a peak potential separation (ΔE) = 0 and a half-peak width (FWHPM) = $\frac{90.6\ mV}{n}$. However, this is not always the case in thin-film voltammetry and therefore other thin-layer theories are used to model kinetic and electrochemical behaviour of films.[68] The kinetic response of thin-film polymer electrodes is often examined using the Temkin isotherm due to electron transfer interactions that are carried out between redox centres. Therefore, Faraday's Laws of electrolysis are used for the determination of the charge storage capability of the redox film.

$$Q = nF\Gamma A \quad \text{.....(1.21)}$$

Where, Q = Charge

F = Faraday's constant

Γ = surface concentration of redox centres (moles cm^{-2})

A = Area

Figure 1.20(a) shows the linear relationship of both anodic and cathodic peak currents and scan rate at a thin-film electrode, indicating diffusion controlled redox process at the electrode surface. Laviron's approach *(Figure 1.20(b))* is often applied to help better understand the electron transfer kinetics of the redox process with a thin-film layer such as the determination of electron transfer coefficient (α) and charge-transfer rate constant (k_s) for the electroactive species.[71] Here, the electroactive material on the surface is electrolysed rapidly when applied potential changed. Therefore, peak positions can be expressed by the following equations;

$$E_{pc} = E^o - \frac{RT}{\alpha nF} \ln \nu \quad \text{.....(1.22)}$$

$$E_{pa} = E^o + \frac{RT}{(1-\alpha)nF} \ln \nu \quad \text{.....(1.23)}$$

Furthermore, plots of E_p vs. In ν should result in two straight lines, as shown below in *Figure 1.20(b)*. Determination of α and k_s values can then be performed using the following equations, where s_a and s_c are the slope of the lines.

$$\alpha = \frac{s_a}{s_a - s_c} \quad \text{.....(1.24)}$$

$$k_s = \frac{\alpha nF \nu_c}{RT} \text{ or } \frac{(1-\alpha nF)\nu_a}{RT} \quad \text{.....(1.25)}$$

Where ν_c and ν_a = cathodic and anodic sweep rates at $E_p = E^o$.

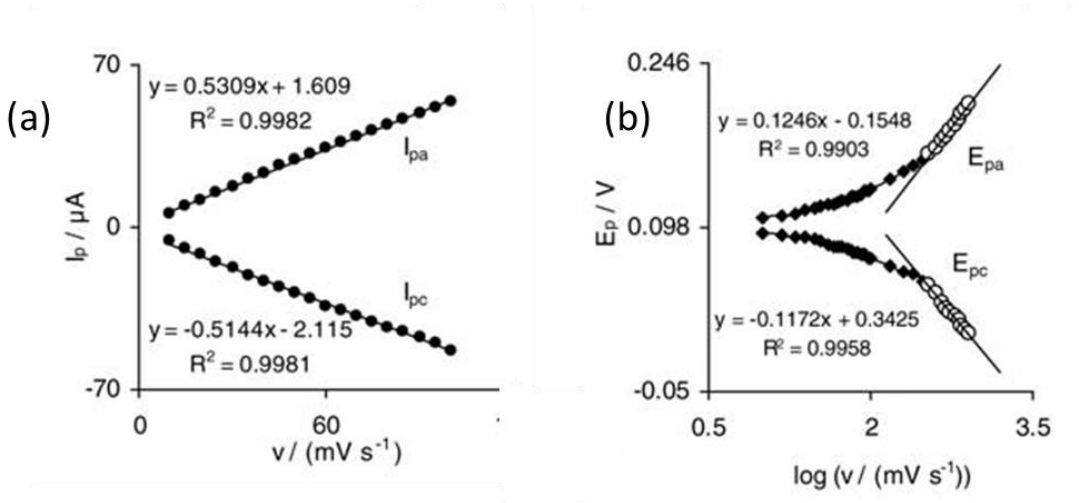

Figure 1.20: (a) Data plot of scan rate vs. peak current for thin-film electrode (b) E_p vs. logν [71]

For scenarios where $\Delta E_p = E_{pa} - E_{pc} > 200/n$ mV, the following equation can be applied;

$$\text{Log } k_s = \alpha\log(1-\alpha) + (1-\alpha)\log\alpha - \log\frac{RT}{nF\nu} - \frac{\alpha nF\Delta E_p(1-\alpha)}{2.3\,RT} \quad \ldots\ldots\ldots\ldots\ldots\ldots\ldots\ldots(1.26)$$

Where, k_s = apparent charge-transfer rate constant for electron transfer between the electrode surface and the surface of the thin-film.

1.6 Surface analysis techniques

1.6.1 Scanning Electron Microscope

The scanning electron microscope is a versatile instrument and was originally developed for an improvement to the conventional light microscope. It allows the analysis and imaging of a wide variety of different samples both chemical and biological. Samples can range from large proteins to small scale nanomaterials. A schematic diagram, shown in *Figure 1.21*, of an SEM illustrates the basic components that make up the instrument.

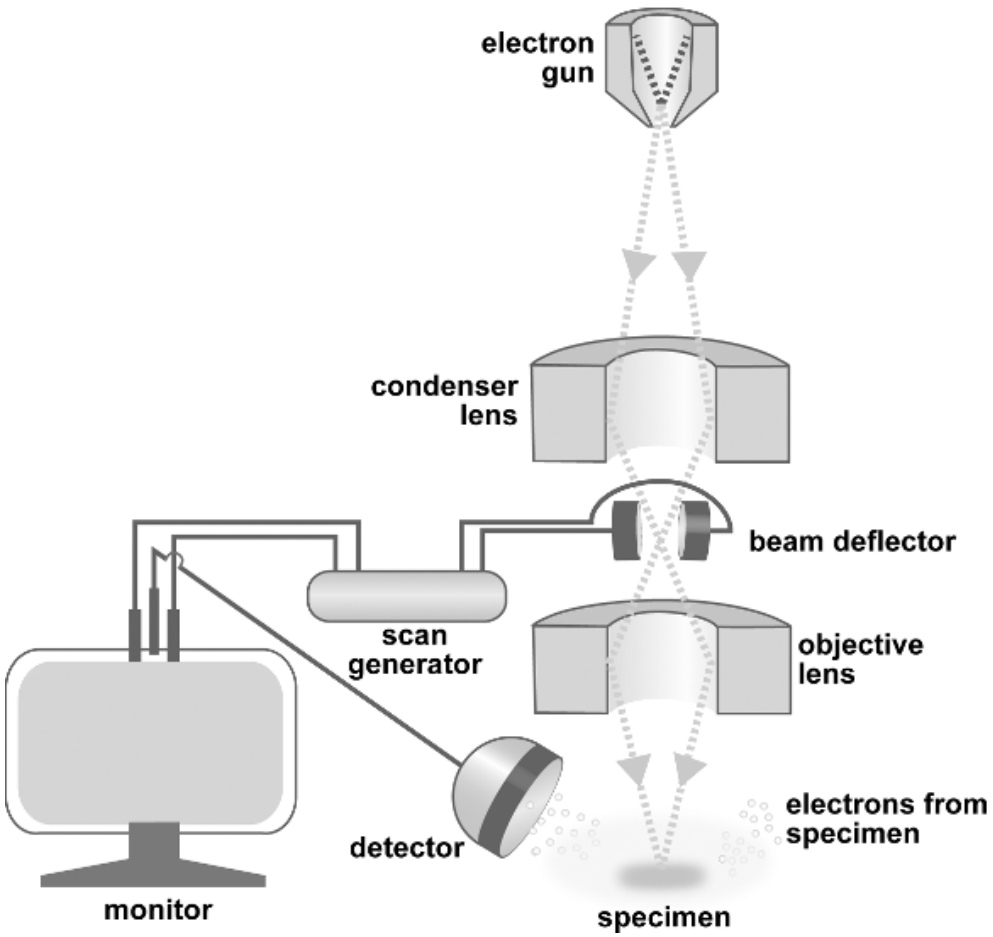

Figure 1.21: Basic components of a scanning electron microscope [72]

The principle of this technique involves the scanning of the sample of interest with a high-energy electron beam that interacts with the surface of the sample which causes the production of emitted electrons that are detected. This provides information on the surface topography of the sample and allows for surface characterisation to be performed. The electron beam involved in the imaging process originates from the heated tungsten filament. Due to the high temperature of the electron source, it causes the excitation of electrons with energy between 1 – 30 keV. The high energy electrons can then escape the cathode, a process known as thermionic emission. The velocity of the moving electrons can alter depending on the accelerated voltage applied. The electron beam flowing to the sample of interest is passed through a Wehnelt cylinder that causes it to flow with a diameter between 10-50 μm. In order to prevent the electrons from dispersing, a vacuum system is required in the chamber of the instrument. The diameter of the electron beam is maintained by two condenser lenses which demagnify the flow of electrons and reduces it to about 2-10 nm. The electron beam then passes through the scanning coils that are positioned along the axis of the beam and causes the aligning of the beam to a focal point. Alternating the current that passes through the scanning coils can affect the electromagnetic strength. The electron beam is finally passed through a second magnifying lens known as the objective lens where it comes into contact with the sample of interest.

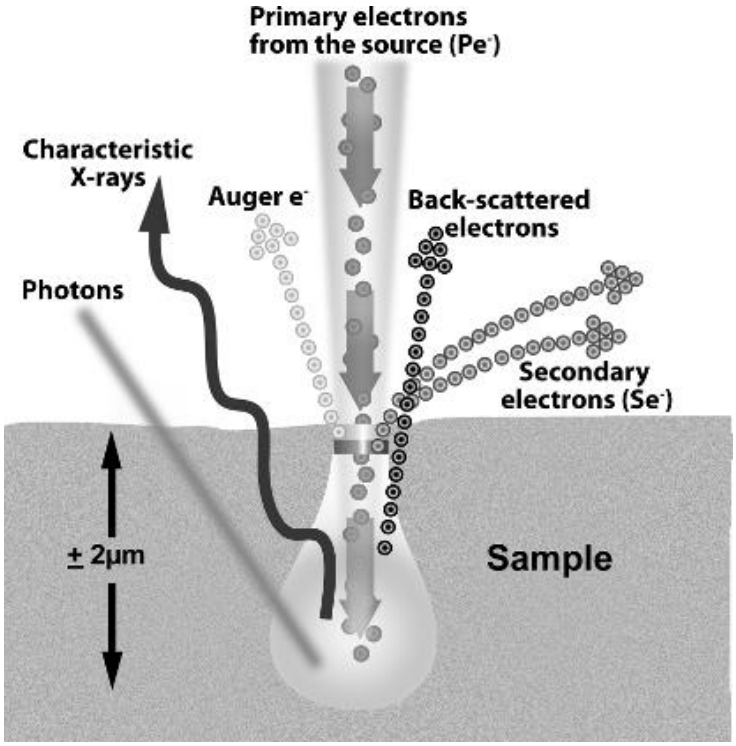

Figure 1.22: Schematic diagram of sample interactions via scanning electron microscope [72]

As the electron beam hits the sample of interest, two different signals are produced made up of photon and electron signals, as shown in *Figure 1.22*. Although all interactions presented in the scheme occur, not all of them are analysed or detected with SEM. The secondary and backscattered electrons are the most commonly used signals. Generally, SEM instruments have various different signals including secondary, backscattered electrons and x-ray signals. The electrons that have been scattered from the sample surface are known as secondary electrons and tend to possess a low energy. [73] [72]

1.6.2 Scanning Electrochemical Microscopy

Scanning electrochemical microscopy (SECM) is an electrochemical tool that is used to probe surfaces and analyse surface reactions by using a scanning probe technique. SECM was firstly described and developed in the 1980's by Bard laboratories and since then has been continuously improved and used for a wide range of applications.[74] The basis of SECM involves the use of an ultramicroelectrode (UME) tip which has been described as an electrode with a radius usually 25 μm in size. SECM measures the current that passes through the ultramicroelectrode while it is held stationary or moving through an electrolyte solution surrounding the substrate. The substrate presence causes an electrochemical response at the tip of the ultramicroelectrode which provides the ability to obtain information regarding the properties of the substrate at the micrometer and nanometer scale. The substrate can be both a solid support such as metals, polymers, glass and biosensors to liquid materials including mercury and immiscible oils. [74] A typical SECM setup, including all major components, is shown in *Figure 1.23.*

SECM utilises the electrochemical behaviour of a substance and combines it with piezoelectric elements to control the ultramicroelectrode tip in an x, y and z position. Therefore, an SECM setup requires a bipotentiostat, used to control the potential of the tip and the substrate, and piezocontrollers, used to manage the movement of the tip over the substrate. The main applications of SECM are to analyse both heterogenous and homogenous electrochemical reactions, use it as an imaging tool to analyse the topography of different material surfaces and examine at its use in microfabrication. [75]

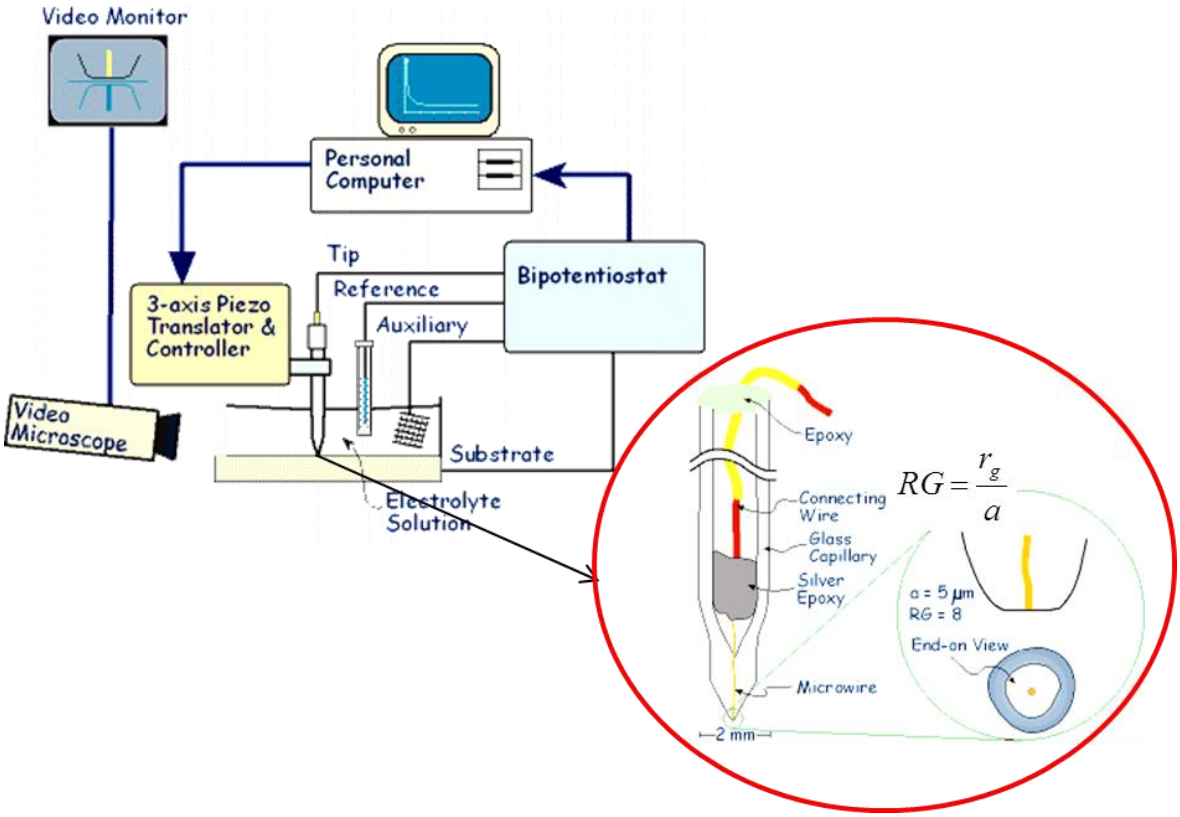

Figure 1.23: Schematic diagram of scanning electrochemical microscopy setup and ultra microelectrode

There are various different types of operation of SECM that are continuously used. These modes of operation include feedback and generation/collection modes.[76] As these two applications are of most interest due to their ability to be used for enzymatic systems, we will discuss both of these in further detail. Feedback mode is a form of SECM operation that only monitors the current at the tip and was first described in 1989. The measured current is perturbed by the substrate present a distance, d, away from the tip which may be either conducting or insulating. This can result in negative feedback, where the diffusion of the species across the solution to the tip can be obstructed, or positive feedback in which the regeneration of the species occurs. Therefore, both positive and negative feedback can allow for the study of different substrate surfaces for their insulating and conductive properties, enabling imaging of the surfaces to be carried out. An SECM experiment involves the substrate being held in a solid inert support stage and surrounded by an electrolyte solution containing an electroactive species. The tip is then immersed in the solution directly above the substrate. As the tip approaches the substrate, positive or negative feedback can occur, as shown in *Figure 1.24*.

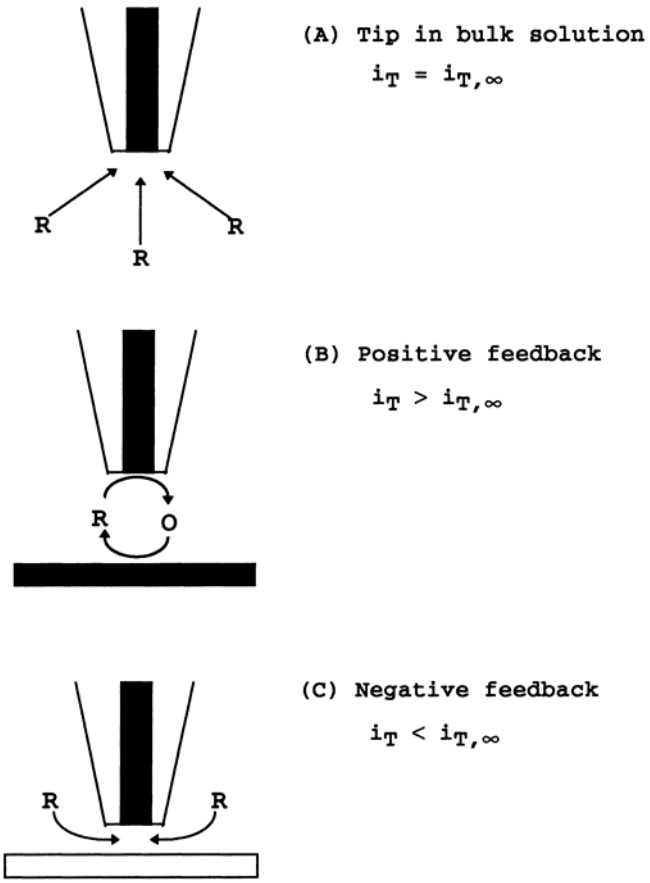

Figure 1.24: Feedback mode of scanning electrochemical microscopy

Figure 1.25 shows two different scenarios that can occur during an SECM approach curve experiment, where i_T is known as the ratio of the tip current at normalized distance, $L = d/a$, where d is the infinite distance from the substrate ($i_{T\infty}$) and a is the radius of the ultramicroelectrode tip. If the tip is held over an insulating surface, the tip current ratio will decrease as there is no regeneration of the electroactive species. If the tip approaches the substrate surface that has conducting properties, the measured current will increase. An approach curve experiment can help in the determination of the distance from the measured i_T and greater understanding with respect to the position of the tip over the substrate. The RG is the radius of the insulating sheath surrounding the conducting surface of the ultramicroelectrode ($RG = r_g/a$) and can affect the approach curve for an insulator.

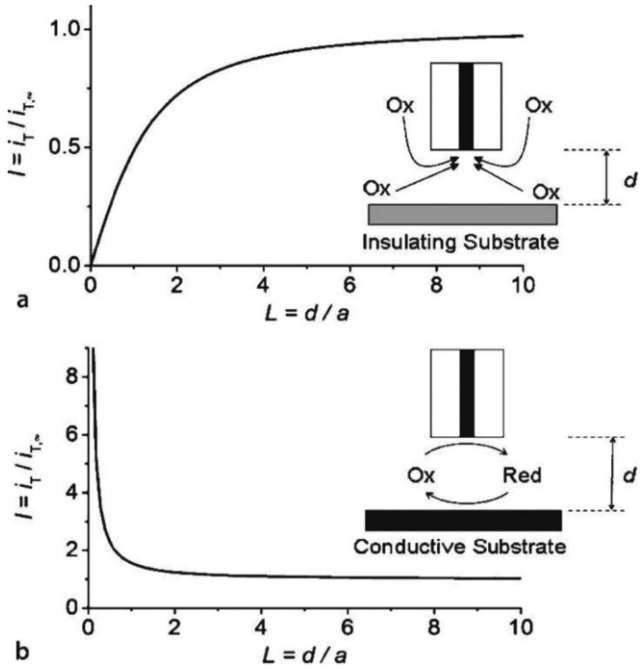

Figure 1.25: Scanning electrochemical microscopy approach curves on (a) insulating substrates i.e. negative feedback and (b) conducting substrates i.e. positive feedback.

Generally, the generation/collection mode will involve monitoring the current of both the ultramicroelectrode tip and the substrate. The tip is usually placed at a ten tip radii or less distance away from the substrate surface. There are two types of generation/collection modes, known as the tip generation/substrate collection (TG/SC) mode and the substrate generation/tip collection (SG/TC) mode.

In the TG/SC mode, shown in *Figure 1.26*, the tip is held at a constant potential which gives rise to a reactant that is then measured at the substrate electrode surface held at a different potential, where the product reactant is detected. When the product reacts as it moves from the tip to the substrate, the collection efficiency decreases. The rate constant of the reaction can be determined by examining the product reactivity and its separation distance. [76]

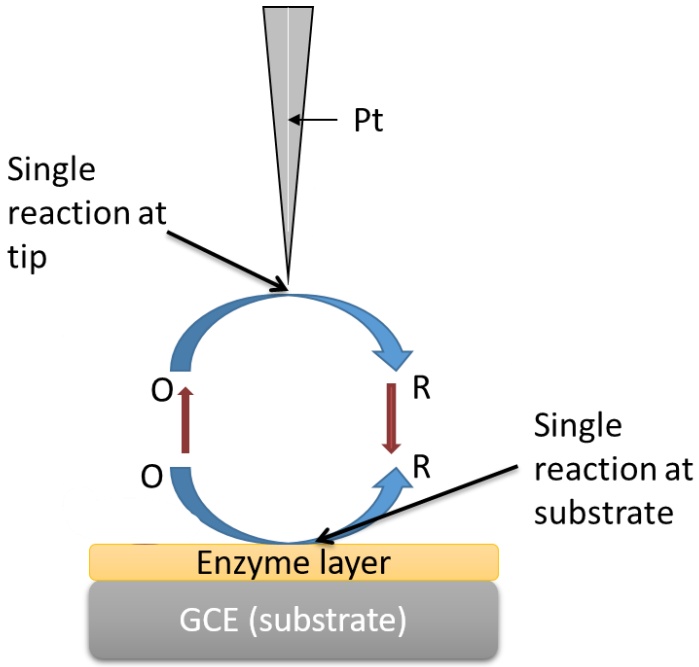

Figure 1.26: Tip generation/substrate collection mode of scanning electrochemical microscopy

The SG/TC mode involves the detection of the analyte species at the tip after it has been formed at the substrate. Therefore, the tip can be used to scan over the surface of the substrate and determine a concentration profile and can show regions of higher activity. For example, a tip can scan over an enzyme modified surface electrode, the substrate, and determine the level of activity of the enzyme across the working surface. Therefore, it can show the coverage performance of the modification layer across the surface of the electrode.

Redox competition mode (RC-SECM), shown in *Scheme 1.9*, was developed by Schuhmann's group and described by Morkvenaite-Vilkonciene *et al.* for its use in evaluation of enzyme kinetics in GOx immobilised electrodes.[77] It involves the UME and the sample competing for the same analyte in the bulk solution.[78] The current for oxygen reduction is generally held constant throughout the experiment unless the UME is within the area of oxygen consumption which can be measured at a bipotentiostatic mode involving the UME and the substrate electrode held at the potential for oxygen reduction. [79]

It is often used to investigate local catalytic activity of immobilised enzymes on the surface of electrodes by evaluation of oxygen reduction reactions. This is performed

by both the immobilised enzyme and the UME competing for dissolved O_2. When higher concentrations of glucose are present, the concentration of oxygen at the surface of the enzyme modified surface decreases as it is used up in the enzymatic reaction. Along with horizontal scanning methods, RC-SECM can be used for the analysis of enzyme electrode substrates and the redox mediator can be involved into two simultaneous processes including the electron uptake with the enzyme and recycling of the mediator to its oxidation state at the conducting surface.

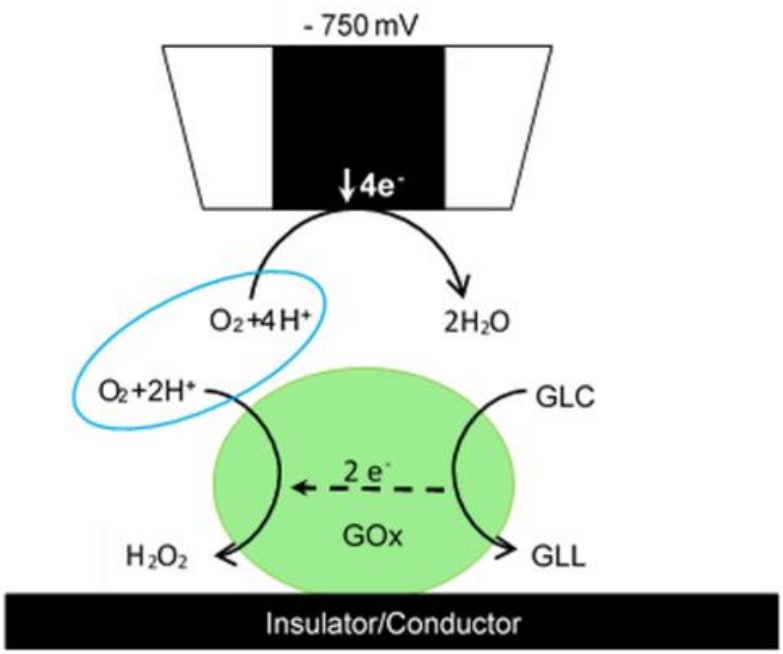

Scheme 1.9: Redox competition mode [77]

1.7 Overall goal of this research

Development of bespoke sensors to realise rapid testing would be ideal for industrial processes, such that if deviations were to occur, there could be steps taken to return to optimum conditions. Although there have been numerous publications on the commercial use of biosensors in diabetes and human health, there is little evidence of commercially successful biosensors deployed in the dairy industry.

The research question for this thesis is whether it is possible to develop a bio-sensing tool for rapid determination and monitoring of glucose, lactose and lactic acid concentrations during a fermentation process.

The specific objectives of this project are:

(A) To develop Glucose and Lactose biosensor for dairy sample analysis and process monitoring.

- Optimisation of analytical performance of first and second generation biosensors;
- Verify operation and analytical performance of glucose and lactose sensors for fermentation process monitoring.

(B) To develop a Lactate biosensor for use in rapid monitoring of lactate production in a fermentation process.

- Develop and calibrate first and second generation biosensors for lactate;
- Enzymatic polymerisation of 1,10-Phenanthroline-5,6-dione as a redox active film for lactate biosensing;
- Deploy lactate biosensor in fermentation media to monitor lactate production during a fermentation process.

Bibliography

1. Rivas J, Prazeres AR, Carvalho F, Beltrán F. Treatment of cheese whey wastewater: Combined Coagulation - Flocculation and aerobic biodegradation. *J Agric Food Chem*. 2010;58(13):7871-7877. doi:10.1021/jf100602j
2. Demirel B, Yenigun O, Onay TT. Anaerobic treatment of dairy wastewaters: A review. *Process Biochem*. 2005;40(8):2583-2595. doi:10.1016/j.procbio.2004.12.015
3. Pescuma M, de Valdez GF, Mozzi F. Whey-derived valuable products obtained by microbial fermentation. *Appl Microbiol Biotechnol*. 2015;99(15):6183-6196. doi:10.1007/s00253-015-6766-z
4. Pundir CS, Narwal V, Batra B. Determination of lactic acid with special emphasis on biosensing methods: A review. *Biosens Bioelectron*. 2016;86:777-790. doi:10.1016/j.bios.2016.07.076
5. https://cbecl.wordpress.com/products/milk-processing-plants/.
6. Dias LG, Veloso ACA, Correia DM, Rocha O, Torres D, Rocha I, Rodrigues L, Peres A. UV spectrophotometry method for the monitoring of galacto-oligosaccharides production. *Food Chem*. 2009;113(1):246-252. doi:10.1016/j.foodchem.2008.06.072
7. Yang L, Huo D, Jiang Y, Hou C, Zhang S. Monitoring the adulteration of milk with melamine: a visualised sensor array approach. *Food Addit Contam - Part A Chem Anal Control Expo Risk Assess*. 2013;30(5):786-795. doi:10.1080/19440049.2013.793457
8. Blais BW, Vailhen C. A novel enzymatic microassay for the determination of lactose in grated parmesan cheese. *Food Control*. 1995;6(4):215-217. doi:10.1016/0956-7135(95)00023-K
9. Ammam M, Fransaer J. Two-enzyme lactose biosensor based on β-galactosidase and glucose oxidase deposited by AC-electrophoresis: Characteristics and performance for lactose determination in milk. *Sensors Actuators, B Chem*. 2010;148(2):583-589. doi:10.1016/j.snb.2010.05.027
10. Nommsen, C.A. Lovelady, M.J. Heinig, B. Lonnerdal KGD. Determinants of energy, protein, lipid, and lactose concentrations in human milk during the first 12mo of lactation: the DARLING Study. *Am J Clin Nutr*.

1991;53(2):457-465.

11. Jiang, X.P; Liu, G.Q; Wang, C; Mao, Y.J; Xiong Y. Milk trait heritability and correlation with heterozygosity in yak. *J Appl Genet*. 2004;45(2):215-224.
12. Jäger A, Bilitewski U. Screen-printed enzyme electrode for the determination of lactose. *Analyst*. 1994;119(6):1251-1255. doi:10.1039/AN9941901251
13. Paige, DM; Bayless, TM; Huang, SS; Wexler R. LACTOSE-INTOLERANCE AND LACTOSE HYDROLYZED MILK. *ACS Symp Ser*. 1975;(15):191-206.
14. Abdel-Rahman MA, Tashiro Y, Sonomoto K. Recent advances in lactic acid production by microbial fermentation processes. *Biotechnol Adv*. 2013;31(6):877-902. doi:10.1016/j.biotechadv.2013.04.002
15. Panesar PS. Fermented Dairy Products: Starter Cultures and Potential Nutritional Benefits. *Food Nutr Sci*. 2011;02(01):47-51. doi:10.4236/fns.2011.21006
16. Delavenne E, Mounier J, Déniel F, Barbier G, Le Blay G. Biodiversity of antifungal lactic acid bacteria isolated from raw milk samples from cow, ewe and goat over one-year period. *Int J Food Microbiol*. 2012;155(3):185-190. doi:10.1016/j.ijfoodmicro.2012.02.003
17. Wouters JTM, Ayad EHE, Hugenholtz J, Smit G. Microbes from raw milk for fermented dairy products. *Int Dairy J*. 2002;12(2-3):91-109. doi:10.1016/S0958-6946(01)00151-0
18. Castellano P, González C, Carduza F, Vignolo G. Protective action of Lactobacillus curvatus CRL705 on vacuum-packaged raw beef. Effect on sensory and structural characteristics. *Meat Sci*. 2010;85(3):394-401. doi:10.1016/j.meatsci.2010.02.007
19. Mohd Adnan AF, Tan IKP. Isolation of lactic acid bacteria from Malaysian foods and assessment of the isolates for industrial potential. *Bioresour Technol*. 2007;98(7):1380-1385. doi:10.1016/j.biortech.2006.05.034
20. Braunegg, G; Bona, R; Koller M. Sustainable polymer production. *Polym - Plast Technol Eng*. 2004;43(6):1779-1793.
21. Van Dam JEG, De Klerk-Engels B, Struik PC, Rabbinge R. Securing renewable resource supplies for changing market demands in a bio-based economy. *Ind Crops Prod*. 2005;21(1):129-144. doi:10.1016/j.indcrop.2004.02.003

22. Moon SK, Wee YJ, Choi GW. A novel lactic acid bacterium for the production of high purity l-lactic acid, Lactobacillus paracasei subsp. paracasei CHB2121. *J Biosci Bioeng*. 2012;114(2):155-159. doi:10.1016/j.jbiosc.2012.03.016
23. Datta R, Tsai S, Bonsignore P, Moon S, Frank JR. Technological and economic potential of poly(lactic acid) and Lactic Acid Derivatives. 1995;16:221-231.
24. Trujillo-de Santiago G, Sáenz-Collins CP, Rojas-de Gante C. Elaboration of a probiotic oblea from whey fermented using Lactobacillus acidophilus or Bifidobacterium infantis. *J Dairy Sci*. 2012;95(12):6897-6904. doi:10.3168/jds.2012-5418
25. Krejcova L, Michalek P, Rodrigo M, Heger Z, Krizkova S, Vaculovicova M, Hynek D, Adam V, Kizek R. Nanoscale virus biosensors: state of the art. *Nanobiosensors Dis Diagnosis*. 2015:47. doi:10.2147/NDD.S56771
26. Sassolas A, Blum LJ, Leca-Bouvier BD. Immobilization strategies to develop enzymatic biosensors. *Biotechnol Adv*. 2012;30(3):489-511. doi:10.1016/j.biotechadv.2011.09.003
27. Tamayo J, Kosaka PM, Ruz JJ, San Paulo Á, Calleja M. Biosensors based on nanomechanical systems. *Chem Soc Rev*. 2013;42(3):1287-1311. doi:10.1039/c2cs35293a
28. Wang J. Electrochemical glucose biosensors. *Electrochem Sensors, Biosens their Biomed Appl*. 2008:57-69. doi:10.1016/B978-012373738-0.50005-2
29. Leskovac V. *Comprehensive Enzyme Kinetics*. Kluwer Academic Publishers; 2003.
30. Eggins, Brian R. *Chemical Sensors and Biosensors.* Chichester: Wiley, 2006.
31. E. B. Roche. *Textbook of Biochemistry with Clinical Correlations*. Devlin TM, ed.; 2005.
32. Rocchitta G, Spanu A, Babudieri S, Latte G, Madeddu G, Galleri G, Nuvoli S, Bagella P, Demartis MI, Fiore V, Manetti R, Serra PA. Enzyme biosensors for biomedical applications: Strategies for safeguarding analytical performances in biological fluids. *Sensors (Switzerland)*. 2016;16(6). doi:10.3390/s16060780
33. Cunha-Silva H, Arcos-Martinez MJ. Dual range lactate oxidase-based screen printed amperometric biosensor for analysis of lactate in diversified samples.

Talanta. 2018;188(March):779-787. doi:10.1016/j.talanta.2018.06.054

34. Azevedo AM, Prazeres DMF, Cabral JMS, Fonseca LP. Ethanol biosensors based on alcohol oxidase. *Biosens Bioelectron*. 2005;21(2):235-247. doi:10.1016/j.bios.2004.09.030
35. Creanga C, El Murr N. Development of new disposable NADH biosensors based on NADH oxidase. *J Electroanal Chem*. 2011;656(1-2):179-184. doi:10.1016/j.jelechem.2010.11.030
36. Sun R, Wang L, Yu H, Abdin Z, Yongsheng C. Molecular recognition and sensing based on ferrocene derivatives and ferrocene-based polymers. *Organometallics*. 2014;33(18):4560-4573. doi:10.1021/om5000453
37. Arslan F, Beskan U. An amperometric biosensor for glucose detection from glucose oxidase immobilized in polyaniline-polyvinylsulfonate-potassium ferricyanide film. *Artif Cells, Nanomedicine Biotechnol*. 2014;42(4):284-288. doi:10.3109/21691401.2013.812650
38. Hedenmo M, Narváez A, Domínguez E, Katakis I. Reagentless amperometric glucose dehydrogenase biosensor based on electrocatalytic oxidation of NADH by osmium phenanthrolinedione mediator. *Analyst*. 1996;121(12):1891-1895. doi:10.1039/an9962101891
39. Yao H, Li N, Xu S, Xu JZ, Zhu JJ, Chen HY. Electrochemical study of a new methylene blue/silicon oxide nanocomposition mediator and its application for stable biosensor of hydrogen peroxide. *Biosens Bioelectron*. 2005;21(2):372-377. doi:10.1016/j.bios.2004.08.051
40. Ito Y, Okuda-Shimazaki J, Tsugawa W, Loew N, Shitanda I, Lin C, La Belle J, Sode K. Third generation impedimetric sensor employing direct electron transfer type glucose dehydrogenase. *Biosens Bioelectron*. 2019;129(January):189-197. doi:10.1016/j.bios.2019.01.018
41. Booth, Marsilea. A. ; Karaosmanoglu, Hande ; Wu, Yinqiu ; Partridge A. Biosensor Platforms for Detecting Target Species in Milk Samples. *Food Chem Funct Anal*. 2017:71-103.
42. Gillis, Els H; Traynor, Imelda; Gosling, James P; Kane M. Improvements to a surface plasmon resonance-based immunoassay for the steroid hormone progesterone. *J AOAC Int*. 2006;89(3):838-842.
43. Yakovleva M, Buzas O, Matsumura H, Samejima M, Igarashi K, Larsson P, Gorton L, Danielsson B. A novel combined thermometric and amperometric

biosensor for lactose determination based on immobilised cellobiose dehydrogenase. *Biosens Bioelectron*. 2012;31(1):251-256. doi:10.1016/j.bios.2011.10.027

44. Conzuelo F, Gamella M, Campuzano S, Reviejo AJ, Pingarrón JM. Disposable amperometric magneto-immunosensor for direct detection of tetracyclines antibiotics residues in milk. *Anal Chim Acta*. 2012;737:29-36. doi:10.1016/j.aca.2012.05.051
45. Zacco E, Adrian J, Galve R, Marco MP, Alegret S, Pividori MI. Electrochemical magneto immunosensing of antibiotic residues in milk. *Biosens Bioelectron*. 2007;22(9-10):2184-2191. doi:10.1016/j.bios.2006.10.014
46. Chemburu S, Wilkins E, Abdel-Hamid I. Detection of pathogenic bacteria in food samples using highly-dispersed carbon particles. *Biosens Bioelectron*. 2005;21(3):491-499. doi:10.1016/j.bios.2004.11.025
47. Sternesjö Å, Mellgren C, Björck L. Determination of sulfamethazine residues in milk by a surface plasmon resonance-based biosensor assay. *Anal Biochem*. 1995;226(1):175-181. doi:10.1006/abio.1995.1206
48. Cacciatore G, Petz M, Rachid S, Hakenbeck R, Bergwerff AA. Development of an optical biosensor assay for detection of β-lactam antibiotics in milk using the penicillin-binding protein 2x*. *Anal Chim Acta*. 2004;520(1-2):105-115. doi:10.1016/j.aca.2004.06.060
49. Wang Y, Dostálek J, Knoll W. Long range surface plasmon-enhanced fluorescence spectroscopy for the detection of aflatoxin M1 in milk. *Biosens Bioelectron*. 2009;24(7):2264-2267. doi:10.1016/j.bios.2008.10.029
50. Micheli L, Grecco R, Badea M, Moscone D, Palleschi G. An electrochemical immunosensor for aflatoxin M1 determination in milk using screen-printed electrodes. *Biosens Bioelectron*. 2005;21(4):588-596. doi:10.1016/j.bios.2004.12.017
51. Trani A, Gambacorta G, Loizzo P, Cassone A, Fasciano C, Zambrini A.V, Faccia M. Comparison of HPLC-RI, LC/MS-MS and enzymatic assays for the analysis of residual lactose in lactose-free milk. *Food Chem*. 2017;233:385-390. doi:10.1016/j.foodchem.2017.04.134
52. Li M, Chen J, Xu J, Fu S, Gong H. Determination of Lactose in Milk by Raman Spectroscopy. *Anal Lett*. 2015;48(8):1333-1340.

doi:10.1080/00032719.2014.979358

53. Jasti LS, Dola SR, Fadnavis NW, Addepally U, Daniels S, Ponrathnam S. Co-immobilized glucose oxidase and β-galactosidase on bovine serum albumin coated allyl glycidyl ether (AGE)-ethylene glycol dimethacrylate (EGDM) copolymer as a biosensor for lactose determination in milk. *Enzyme Microb Technol*. 2014;64-65:67-73. doi:10.1016/j.enzmictec.2014.07.005
54. Loğoğlu E, Sungur S, Yildiz Y. Development of lactose biosensor based on β-galactosidase and glucose oxidase immobilized into gelatin. *J Macromol Sci - Pure Appl Chem*. 2006;43(3):525-533. doi:10.1080/10601320600575256
55. Nguyen BH, Nguyen BT, Van Vu H, Nguyen CV, Nguyen DT, Nguyen LT, Vu TT, Tran LD. Development of label-free electrochemical lactose biosensor based on graphene/poly(1,5-diaminonaphthalene) film. *Curr Appl Phys*. 2016;16(2):135-140. doi:10.1016/j.cap.2015.11.004
56. Nguyen DT, Tran LD, Le Nguyen H, Nguyen BH, Van Hieu N. Modified interdigitated arrays by novel poly(1,8-diaminonaphthalene)/carbon nanotubes composite for selective detection of mercury(II). *Talanta*. 2011;85(5):2445-2450. doi:10.1016/j.talanta.2011.07.094
57. Zhang J, Yang S, Wang H, Wang S. Enhanced sensitivity for biosensors: Functionalized P1,5- diaminonaphthalene-multiwall carbon nanotube composite film-modified electrode. *Electrochim Acta*. 2012;85:467-474. doi:10.1016/j.electacta.2012.08.089
58. Stoica L, Ludwig R, Haltrich D, Gorton L. Third-generation biosensor for lactose based on newly discovered cellobiose dehydrogenase. *Anal Chem*. 2006;78(2):393-398. doi:10.1021/ac050327o
59. Churakova E, Peri K, Vis JS, Smith DW, Beam J M, Vijverberg M P, Stor M C, Winter R T. Accurate analysis of residual lactose in low-lactose milk: Comparing a variety of analytical techniques. *Int Dairy J*. 2019;96:126-131. doi:10.1016/j.idairyj.2019.02.020
60. Bravo I, Revenga-Parra M, Pariente F, Lorenzo E. Reagent-less and robust biosensor for direct determination of lactate in food samples. *Sensors (Switzerland)*. 2017;17(1):1-11. doi:10.3390/s17010144
61. Taurino I, Reiss R, Richter M, Fairhead M, Thony-Meyer L, De Micheli G, Carrara S. Comparative study of three lactate oxidases from Aerococcus viridans for biosensing applications. *Electrochim Acta*. 2013;93:72-79.

doi:10.1016/j.electacta.2013.01.080

62. Herrero AM, Requena T, Reviejo AJ, Pingarrón JM. Determination of L-lactic acid in yoghurt by a bienzyme amperometric graphite-Teflon composite biosensor. *Eur Food Res Technol*. 2004;219(5):556-559. doi:10.1007/s00217-004-0973-7
63. Rosati G, Gherardi G, Grigoletto D, Marcolin G, Cancellara P, Mammucari C, Scaramuzza M, De Toni A, Reggiana C, Rizzuto R, Paccagnella A. Lactate Dehydrogenase and Glutamate Pyruvate Transaminase biosensing strategies for lactate detection on screen-printed sensors. Catalysis efficiency and interference analysis in complex matrices: from cell cultures to sport medicine. *Sens Bio-Sensing Res*. 2018;21(June):54-64. doi:10.1016/j.sbsr.2018.10.004
64. Brandt, R.B., Brandt, R.B., Siegel, S.A., Siegel, S.A., Waters, M.G., Waters, M.G., Bloch, M.H. & Bloch MH. Spectrophotometric assay for D-(-)-lactate in plasma. *Anal Biochem*. 1980;102(1):39-46.
65. Lupu A, Valsesia A, Bretagnol F, Colpo P, Rossi F. Development of a potentiometric biosensor based on nanostructured surface for lactate determination. *Sensors Actuators, B Chem*. 2007;127(2):606-612. doi:10.1016/j.snb.2007.05.020
66. Batra B, Narwal V, Pundir CS. An amperometric lactate biosensor based on lactate dehydrogenase immobilized onto graphene oxide nanoparticles-modified pencil graphite electrode. *Eng Life Sci*. 2016;16(8):786-794. doi:10.1002/elsc.201600082
67. Horwood E. *Instrumental Methods in Electrochemistry*. (Kemp TJ, ed.). Ellis Horwood Limited; 1985.
68. Dekker M. *Laboratory Techniques in Electroanalytical Chemistry*. (Kissinger, Peter. T. Heineman WR, ed.).; 1996.
69. Evans DH, O'Connell KM, Petersen RA, Kelly MJ. Cyclic voltammetry. *J Chem Educ*. 1983;60(4):290. doi:10.1021/ed060p290
70. Bagotsky, Vladimir S. ; Mueller K. *Fundamentals of Electrochemistry*. (Bagotsky VS, ed.). John Wiley & Sons, Incorporated; 2005.
71. Zare HR, Chatraei F, Nasirizadeh N. Differential pulse voltammetric determination of hydroxylamine at an indenedione derivative electrodeposited on a multi-wall carbon nanotube modified glassy carbon

electrode. *J Braz Chem Soc*. 2010;21(10):1977-1985. doi:10.1590/S0103-50532010001000025

72. Schatten H. The role of scanning electron microscopy in cell and molecular biology: Sem basics, past accomplishments, and new frontiers. *Scanning Electron Microsc Life Sci*. 2010;9780521195(September):1-15. doi:10.1017/CBO9781139018173.002
73. Goodhew P, Humphreys J, Beanland R. *Electron Microscopy and Analysis*. CRC Press LLc. 2000.
74. Zoski CG. Review—Advances in Scanning Electrochemical Microscopy (SECM). *J Electrochem Soc*. 2016;163(4):H3088-H3100. doi:10.1149/2.0141604jes
75. M. Mirkin BH. Electroanalytical measurements using the scanning electrochemical microscope. 2000;406:119-146.
76. Zoski CG. *Handbook of Electrochemistry*. (Zoski CG, ed.). Elsevier Science & Technology; 2006.
77. Morkvenaite-Vilkonciene I, Ramanaviciene A, Genys P, Ramanavicius A. Evaluation of Enzymatic Kinetics of GOx-based Electrodes by Scanning Electrochemical Microscopy at Redox Competition Mode. *Electroanalysis*. 2017;29(6):1532-1542. doi:10.1002/elan.201700022
78. Morkvenaite-Vilkonciene I, Ramanaviciene A, Ramanavicius A. Redox competition and generation-collection modes based scanning electrochemical microscopy for the evaluation of immobilised glucose oxidase-catalysed reactions. *RSC Adv*. 2014;4(91):50064-50069. doi:10.1039/c4ra08697j
79. Okunola AO, Nagaiah TC, Chen X, Eckhard K, Schuhmann W, Bron M. Visualization of local electrocatalytic activity of metalloporphyrins towards oxygen reduction by means of redox competition scanning electrochemical microscopy (RC-SECM). *Electrochim Acta*. 2009;54(22):4971-4978. doi:10.1016/j.electacta.2009.02.047

Chapter 2 : Development of both direct and mediated glucose and lactose biosensors

2.1 Introduction

The development of biosensors for use in dairy side stream monitoring relies on the use of sensitive and selective biomolecules that act as recognition elements, allowing miniaturisation of analytical methods to provide on-site testing and continuous monitoring of key analytes.[1] Enzymes are widely utilised due to their specificity, sensitivity and low-cost.[2] A wide range of immobilisation techniques are utilised in the deposition of enzymes onto transducer surfaces, including either physical or chemical methods. Generally, physical methods include the absorption or entrapment of the proteins onto the active surface whereas chemical methods can involve covalent bonding between functional groups present on the enzyme surface and a polymeric support that may be pre-treated to activate carboxylic or amino groups present.[3]

Cross-linking agents are compounds that promote chemical binding between biomolecules and are used in sensor development due to their simplicity, low-cost and ease of use. However, such methods can cause distortion of protein structures and inhibit active sites. Therefore, the concentration of cross-linking agents utilised is an important factor in the optimisation of enzyme immobilisation. Glutaraldehyde (GA), shown in *Figure 2.1*, is a widely used cross-linking agent and is often thought of as a reference method for simple and reproducible enzyme immobilisation. Poly(ethylene glycol) diglycidal ether (PEGDE) (*Figure 2.1*) has been used in the cross-linking of polymers that contained amine, carboxyl and hydroxyl groups on the surface.[4] It was often thought of as an essential component in redox hydrogels but was rarely as a sole method of immobilisation of enzymes on electrode surfaces. PEGDE contains two epoxy groups that can react with amine functional groups present on the surface of a protein which causes a matrix to form allowing enzyme immobilisation on a transducer surface. [4]

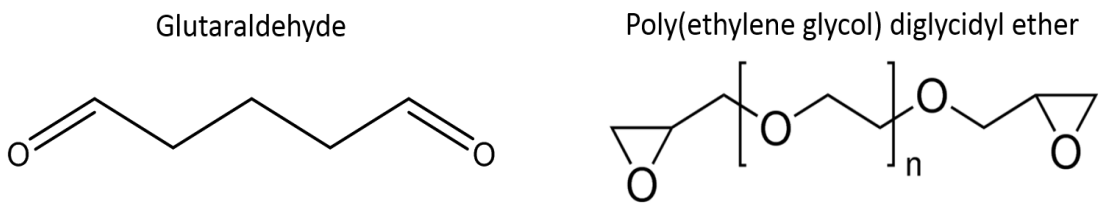

Figure 2.1: Chemical structures of crosslinking agents glutaraldehyde and poly(ethylene glycol) diglycidyl ether.

The use of PEGDE for enzyme immobilisation of GOx on a microsensor was studied by Vasylieva *et al.* in 2011. [4] PEGDE (4 – 100 mg/mL) was examined to determine the optimum concentration for enzyme immobilisation which was found to be 20 mg/mL. Results showed that only 36.4 % of biosensors exhibited stable enzyme immobilisation at lower concentrations of PEGDE and higher concentrations caused limited sensitivity. This suggests that at higher concentrations, over cross-linking of the enzyme can inhibit the enzyme activity. PEGDE was utilised in the fabrication of a lactose biosensor via GOx, β-gal and Horse-radish peroxidase (HRP).[5] Crosslinking of the enzymes was achieved by addition of an enzyme/PEGDE mixture on the surface of the electrode. Results showed that the presence of PEGDE improved the stability of the biosensor and stabilised the signal to achieve a linear range of $1 \times 10^{-7} – 1 \times 10^{-4}$ mol dm^{-3}. The sensor was used to detect lactose in milk samples using ferrocene as a redox mediator. Results were compared with GC/MS which showed the biosensor detected 4.9 ± 1.9 g while GC/MS determined 5.5 ± 0.1 g in the sample.

Another cross-linker mentioned here is GA, which has been used in the development of a mediated glucose biosensor by Miao *et al.* that involved a sandwich configuration of a chitosan-ferrocene: GOx: chitosan on a carbon paste electrode, with GA.[6] Enzyme immobilisation methods vary depending on the type of biosensor under fabrication but should not influence the efficacy of the enzyme, change its conformity or hinder its ability to function. Various techniques include entrapment, adsorption, covalent bonding, crosslinking and affinity of enzyme to the transducer surface. Therefore, it is important to choose an immobilisation method that will maintain good stability of the biosensor during optimal storage conditions. The use of chitosan in this method is to further enhance the immobilisation process of GOx. Chitosan is an oligosaccharide which is commonly used in the development of biosensors for immobilisation of biological elements. It is derived from the deacetylation of chitin, shown in *Scheme 2.1*, which is naturally found in crustaceans.[7]

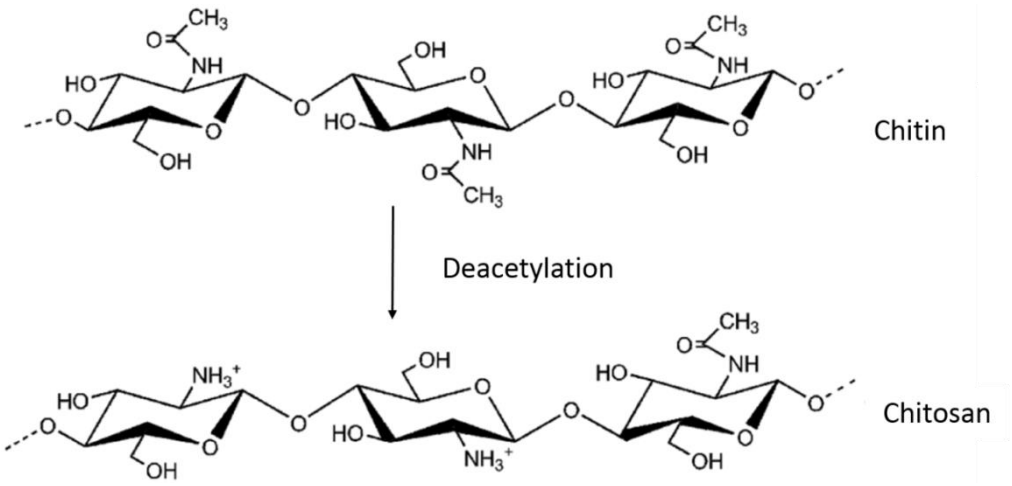

Scheme 2.1: Deacetylation of chitin to form chitosan [8]

There are many advantages to the use of chitosan including its low cost, inert properties, high mechanical strength, hydrophilicity and low toxicity. The incorporation of both chitosan and GA in sensor fabrication promotes a very stable surface for the enzyme to be embedded in. This allows for high enzyme loadings due to the cross-linking reaction involved between the chitosan amino groups and the aldehyde groups in GA (*Scheme 2.2)*. [6]

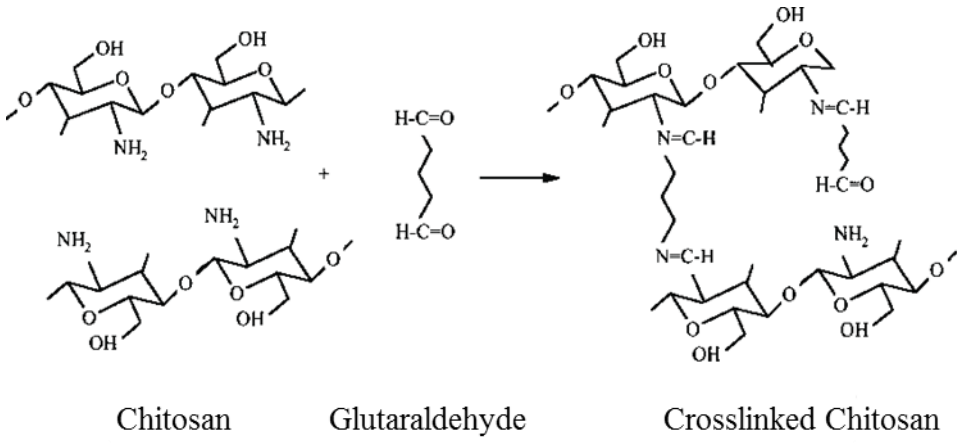

Scheme 2.2: Crosslinking between chitosan and GA functional groups. [9]

The combination of both chitosan and GA is a very popular approach in enzyme immobilisation and has previously been utilised in the development of a H_2O_2 sensor modified with HRP. Fabrication of the sensor consisted of drop casting of the enzyme layer onto the electrode surface, followed by a 1 % chitosan solution and finally 0.025

% GA with set drying times between each layer. Investigation studies were carried out on the chitosan film thickness (0.25- 1 %) and the highest response was observed by the sensor with 1 % chitosan and 0.025 % GA. It was suggested this was due to less enzyme leakage of the electrode at higher concentrations of chitosan. [10]

Mediated systems are an attractive approach in the development of biosensors for use in samples that contain a complex matrix. The accurate measurement of analytes in such samples can be difficult when using a direct detection approach. The use of redox mediators can help eliminate interferences caused by electroactive species present by lowering the operating potential.[11] A good mediator should have rapid reactivity with the enzyme involved, be pH independent, highly stable in both its oxidised and reduced form, hold reversible electron transfer kinetics with low over-potential for oxidation at the electrode surface and should not react with free oxygen atoms.[12] Mediators, such as iron salts, are often incorporated in biosensor fabrication as they enhance electron transfer between the analyte and the electrode surface during the electrochemical response in the presence of an analyte. [13]

Potassium ferricyanide ($K_3Fe(CN)_6$) is a widely used mediator in commercial sensor research and development due to its ideal chemical and physical properties. $K_3Fe(CN)_6$ in its oxidised and reduced form, is very easily accessible, soluble in aqueous liquids and highly stable when kept in dry and light restricted storage conditions. Often used as a standard probe for the characterisation of electrochemical surfaces, the redox couple of ferro/ferricyanide can demonstrate reversible electron transfer kinetics of an electrode. Previous studies have shown the use of ($K_3Fe(CN)_6$) as a model mediator in the development of an amperometric glucose biosensor where GOx was immobilised in a polyaniline-polyvinylsulfonate-potassium ferricyanide film.[14] Amperometric measurements were performed with a fixed potential of 0.3 V vs. Ag/AgCl and the sensor showed a linear range of 5×10^{-6} to 1×10^{-3} M ($R^2 = 0.962$) at pH 7.5.[14]

2.2 Chapter aims

The overall goal of this chapter was to develop two enzymatic biosensors for further use as on-site testing methods for dairy process monitoring. Glucose and lactose detection will be performed by both direct and solution mediated approach methods using Pt, carbon SPE and GCE. Key objectives are outlined below.

- Development of 1st generation glucose and lactose biosensors for direct H_2O_2 detection at Pt electrodes;
- Fabrication of 2nd generation glucose and lactose biosensors via solution mediated biosensing using $K_3Fe(CN)_6$;
- Perform surface characterisation of modified surfaces via SECM.

2.3 Experimental

2.3.1 Materials

MetaDi Monocrystalline Diamond suspension (1 μm) was purchased from Akasel. Glucose Oxidase from *Aspergillus niger* (Type VII, lyophilized powder 10 KU), β-galactosidase from *Aspergillus oryzae* (25 KU), Chitosan (from Shrimp shells, practical grade), D-(+)-Glucose (≥99.5% (GC)), Bovine Serum Albumin (lyophilized powder, ≥ 96 % (agarose gel electrophoresis)), Poly(ethylene glycol) diglycidyl ether and Potassium phosphate dibasic trihydrate (ReagentPlus ≥99.0%) were all obtained from Sigma Aldrich. D (+)-Lactose 1-hydrate BioChemica, Glutaraldehyde solution 25 % for synthesis, Acetic acid (100%) and Potassium di-Hydrogen Phosphate for Analysis, ACS were purchased from ITW reagents.

2.3.2 Instrumentation

All electrochemical techniques including Cyclic Voltammetry (CV), Chronoamperometry (CA) and Chronocoulometry (CC) were carried out on a Solartron 1285 Potentiostat, shown in *Figure 2.2(a)*, which was connected to a computer with general purpose electrochemical software CorrWare and electrochemical data analyser CView. A three electrochemical cell set up was used that contained a platinum wire for the counter electrode, an Ag/AgCl reference electrode (stored in 3 M KCl) along with either Pt or GCE as WE *(Figure 2.2(b))*.

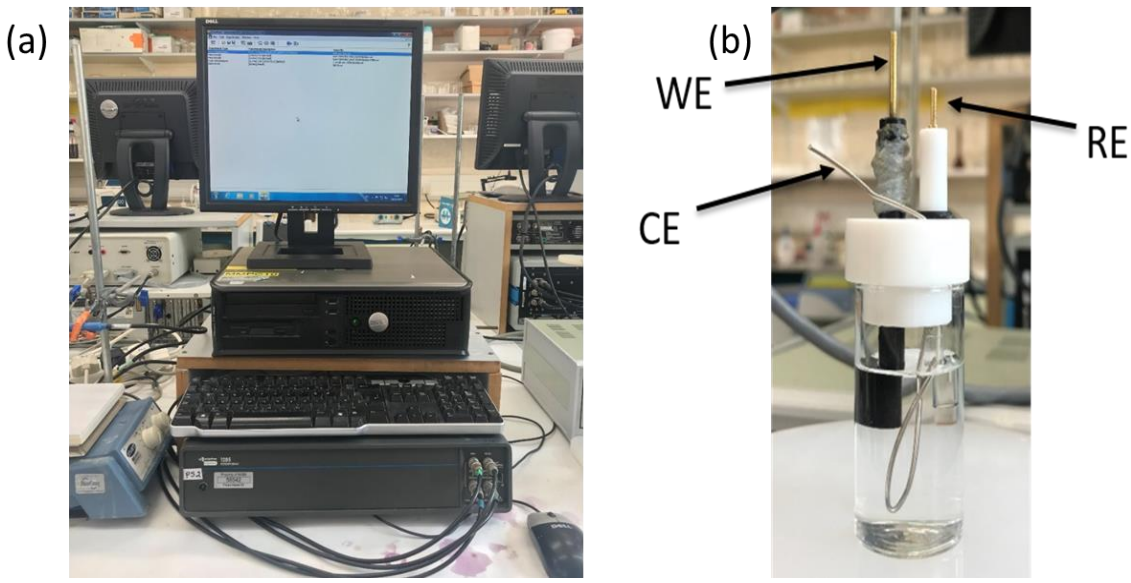

Figure 2.2: (a) Solartron 1285 potentiostat (b) Three electrode cell for electrochemical analysis showing working electrode (WE), reference electrode (RE) and counter electrode (CE).

Prior to modification, all Pt and GC electrodes were prepared by polishing with 1 µm MetaDi Monocrystalline Diamond Suspension, followed by rinsing in deionised water, sonication for 1 min and drying at room temperature.

2.4 Procedures

2.4.1 Fabrication of enzyme electrode

In the case of all biosensors, electrode preparation was adapted from the method described by Miao *et al.* (2000) for GOx immoblisation, as shown in *Scheme 2.3*. 1st generation sensors were fabricated using Pt electrodes and 2nd generation sensors involved modification of GC or commercial carbon SPE. Enzymes were aliquoted into 0.02 M PB containing 0.5 mg/mL BSA and stored at -20 ^{o}C.

Enzyme immobilisation was achieved by a four-layer sandwich consisting of (a) 5 µL of a 0.5 % chitosan in 0.8 % acetic acid, (b) 5 µL of enzyme mixture 50 U GOx for glucose or 50 U GOx and 22.25 U β-gal for lactose detection, (c) Repeat step (a), (d) 5 µL of 0.05 % GA or 1.5 % PEGDE. Each layer was allowed to dry at room temperature between modification steps. Electrodes are referred to as Pt/Chit/GOx/Chit/GA, Pt/Chit/GOx/Chit/PEGDE, Pt/Chit/GOxβ-gal/Chit/GA, GC/Chit/GOx/Chit/GA and GC/Chit/GOxβ-gal/Chit/GA as shown in *Table 2.1*. Once fabricated, the electrodes were allowed to air dry for 1 hour at room temperature and

rinsed with deionised water before use to remove any excess modification layers. Electrodes were stored in 0.1 M PB, pH 6.0 at 4 ºC when not in use.

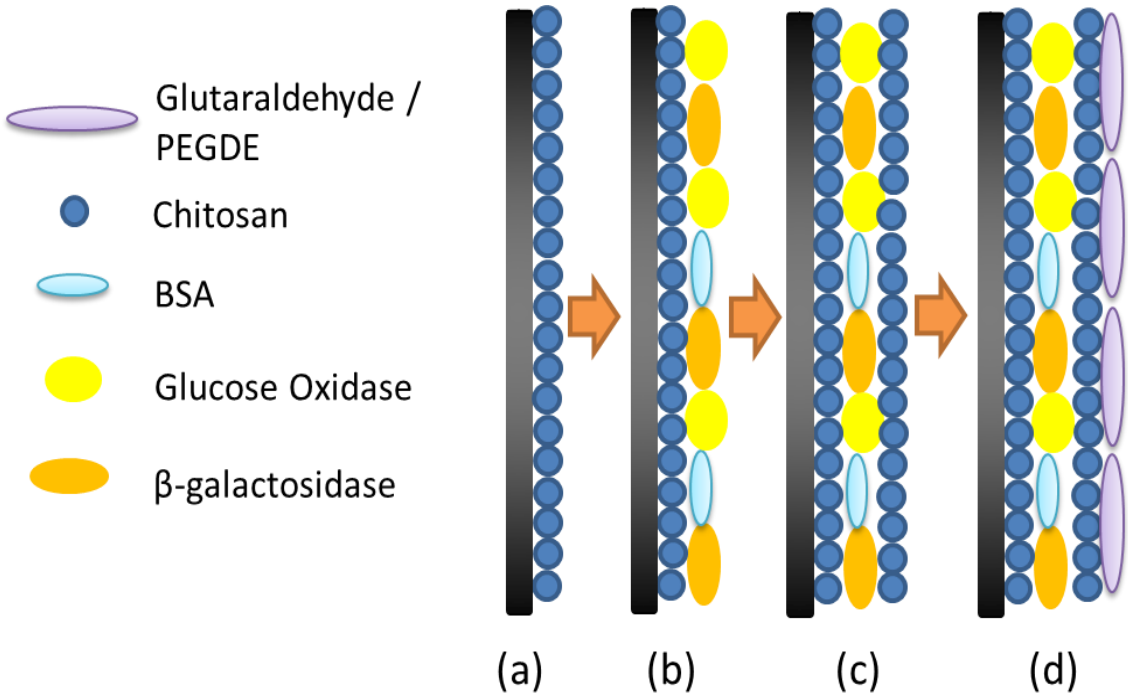

Scheme 2.3: Development of biosensor with (a) 5 µL of 0.5 % chitosan (made up in 0.8 % acetic acid), (b) enzyme layer: 5 µL of GOx (50 U) for glucose detection or 5 µL of GOx (50 U) and 5 µL of β-gal (22.25 U) for lactose detection (made up in 0.02 M phosphate buffer containing 0.5 mg/mL) (c) 5 µL of 0.5 % chitosan and (d) 5 µL of 0.05 % GA or 1.5 % PEGDE.

Table 2.1: Electrode configuration of glucose and lactose biosensors for 1st and 2nd generation fabrication.

Biosensor Type	**Enzyme Activity units**	**Electrode configuration**	
		1st generation	2nd generation
Glucose	GOx = 50 U	Pt/Chit/GOx/Chit/GA / Pt/Chit/GOx/Chit/PEGDE	GC/Chit/GOx/Chit/GA
Lactose	GOx = 50 U β-gal = 22.25 U	Pt/Chit/GOxβ-gal/Chit/GA	GC/Chit/GOxβ-gal/Chit/GA

2.4.2 Direct detection of glucose and lactose at Pt electrode via H_2O_2 detection

The response to 0-7 mM gluose was measured via CV at 100 mVs^{-1} over a potential range -0.2 to 1.0 V vs. Ag/AgCl. CA and CC measurements of 0-7 mM glucose were performed at a fixed potential of 0.8 V vs. Ag/AgCl.

Detection of lactose (0-4 mM) was performed via CV over the range -0.1 V - 1.0 V vs.

Ag/AgCl at 100 mVs^{-1}. A fixed potential study (0.65 - 0.8 V) was carried out to establish the appropriate applied potential for CC analysis of 0-100 mM lactose. Based on the optimum applied potential, further CC analysis was performed with E_{app} = 0.65 V vs. Ag/AgCl to calibrate the lactose biosensor over two different analyte ranges (0-40 mM and 40-60 mM).

2.4.3 Solution mediated glucose and lactose biosensing

Chronocoulometric analysis was carried out on two glucose biosensors (GC/Chit/GOx/Chit/PEGDE) and (GC/Chit/GOx/Chit/GA) to determine the influence of cross linkers (1.5 % PEGDE and 0.05 % GA) on the glucose response. CC was performed over the range 0-47 mM with E_{app} of 0.35 V vs. Ag/AgCl for 5 s.

Scan rate studies were performed on two glucose biosensors fabricated using the two reagents (GA or PEGDE). Detection of glucose was performed over the range 0-7 mM using CV (-0.5 – 1.0 V vs. Ag/AgCl) at scan rates 20-100 mVs^{-1}.

Detection of lactose (1 mM in 5 mM $K_3Fe(CN)_6$) was carried out using CV over the range -0.5 to 0.8 V vs. Ag/AgCl at 100 mVs^{-1}. A background charge signal was first measured in 0.1 M phosphate buffer (pH 6.0) and 5 mM $K_3Fe(CN)_6$. Calibration of lactose (0-18 mM) was achieved via CC analysis at E_{app} = 0.3 V vs. Ag/AgCl for 5 s.

2.4.4 Negative control studies

Two modified electrodes were prepared for glucose positive (GC/Chit/GOx/Chit/GA) and negative (GC/Chit/Chit/GA) control studies. CC analysis was carried out with E_{app} = 0.35 V vs. Ag/AgCl for 5 s. Charge measurements were recorded for 0.1 M phosphate buffer, 5 mM $K_3Fe(CN)_6$ and 10 mM glucose.

Two electrodes were prepared for lactose positive (Pt/Chit/GOxβgal/Chit/GA) and negative (Pt/Chit/Chit/GA) control studies. CV was employed to detect lactose (1.98 mM) at the surface of both modified electrode surfaces. 0.1 M phosphate buffer was analysed with potential range of -0.1 V to 1.0 V vs. Ag/AgCl at 100 mVs^{-1} to determine background signal prior to lactose detection.

(GC/Chit/GOxβ-gal/Chit/GA) and (GC/Chit/Chit/GA) electrodes were used as positive and negative controls for lactose via CC analysis. Charge was measured at 0.3 V vs. Ag/AgCl for 5 s for 0.1 M phosphate buffer (pH 6.0), 5 mM $K_3Fe(CN)_6$ and lactose standards (3.92, 7.69 and 11.32 mM).

Four electrodes were fabricated as follows; negative control i.e. no enzymes (GC/Chit/Chit/GA), GOx only (GC/Chit/GOx/Chit/GA), β-gal only (GC/Chit/β-gal/Chit/GA) and positive control (GC/Chit/GOxβ-gal/Chit/GA) for their response to 0.1 M phosphate buffer (pH 6.0), 5 mM $K_3Fe(CN)_6$ and lactose (1.98 mM in 5 mM $K_3Fe(CN)_6$). CV was performed with a potential range -0.3 to 0.5 V vs. Ag/AgCl at 100 mVs^{-1}.

2.4.5 Surface characterisation of glucose and lactose biosensors using scanning electrochemical microscopy

Approach curves were carried out for each biosensor in 5 mM $K_3Fe(CN)_6$ using a Pt microelectrode tip with the tip potential (E_T) held at -0.4 V vs. Ag/AgCl (E_{sub} = OFF). The movement of the tip to the surface of the substrate (enzyme modified GC electrode) was monitored and stopped prior to contact. Redox competition mode[15] was utilised (*Scheme 2.4*) – where both sample and tip compete for Fe^{3+}. High local electroactivity was indicated by low currents monitored at SECM tip as enzyme modified surface was approached.

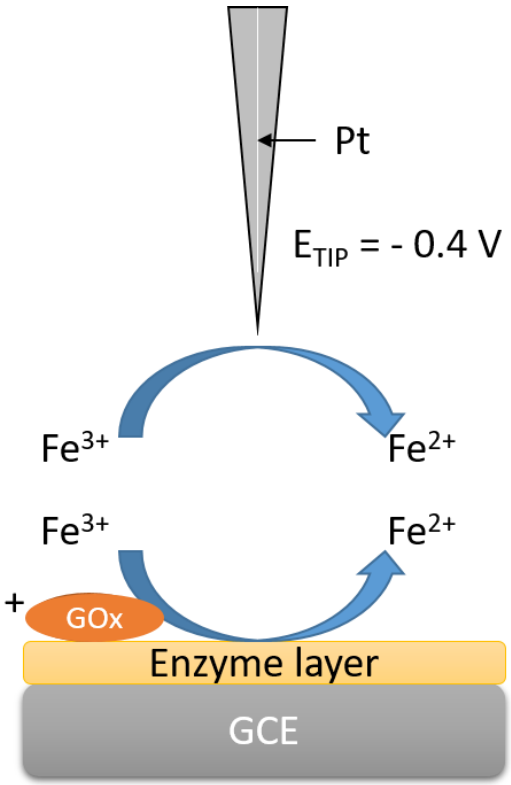

Scheme 2.4: Redox competition mode for Fe^{3+} using scanning electrochemical microscopy at GOx modified GCE (E_T = -0.4 V vs. Ag/AgCl) E_{sub} = OFF, 20 mm Pt UME (RG = 23.8).

Line scans were carried out by measuring the current at -0.4 V vs. Ag/AgCl as it scanned across the electrode surface (0 - 8000 mm) in 5 mM $K_3Fe(CN)_6$ and in the presence of glucose (20 and 40 mM).

Imaging of the enzyme layer was achieved via area scans of the modified substrate electrode to examine the area of enzyme activity with (E_T = -0.4 V vs. Ag/AgCl E_{sub} = OFF) 5000 x 8000 mm^2 (glucose biosensor) and 5000 x 5500 mm^2 (lactose biosensor) with 100 mm^2 per point. Scans were carried out in 5 mM $K_3Fe(CN)_6$ with 0 and 20 mM substrate (glucose or lactose).

2.5 Results and Discussion

1st and 2nd generation glucose and lactose biosensors were developed and tested for their potential use in the detection and quantitation of key analytes in dairy sample monitoring (subject of chapter 4). Here, we will examine the outcome of the studies carried out on the sensors via electrochemical analysis and SECM studies. The results will be discussed by dividing into two sections as follows;

(A) Direct detection sensing at Pt transducers
(B) Solution mediated biosensing using GCE

As the biosensors were designed for deployment in a dairy sample or fermentation media, all experiments were carried out in an environment typical of a fermentation sample. This included the use of a phosphate buffer electrolyte solution to maintain the pH and mimic a typical fermentation sample which generally has a pH of ~ 6.0. All experiments were carried out at room temperature as it would vary during a fermentation process. Therefore, the effect of temperature was not studied in this work.

2.5.1 Direct detection at Pt transducers

1st generation glucose and lactose biosensors were prepared based on the procedure described earlier in section 2.4.1 *(Scheme 2.3).* Following preparation, electrodes were subjected to electrochemical analysis studies using CV, CA and/or CC to obtain analytical data - linear range, sensitivity, limit of detection (LOD) and limit of quantitation (LOQ).

2.5.1.1 Detection of glucose at Pt modified electrode

Calibration studies were carried out on the glucose biosensor (50 U GOx) in 0.1 M phosphate buffer (pH 6.0). CV was initially performed to determine the optimum

detection potential for H_2O_2 generated (*Equation 2.1*) and to assess glucose detection at the Pt/Chit/GOx/Chit/GA electrode.

$$\text{Glucose} + O_2 \xrightarrow{GOx} \text{Gluconic acid} + H_2O_2 \quad \text{(2.1)}$$

Figure 2.3 shows a CV of buffer followed by glucose additions (0 – 7 mM) demonstrating the biosensor successfully detected glucose at a potential of ~0.6 V. Measured current increased as the concentration of glucose increased in the cell due to more H_2O_2 generated by GOx substrate turnover. A calibration curve, depicted in *Figure 2.4*, shows the linear relationship between glucose concentration and the current measured at 0.8 V vs. Ag/AgCl, resulting in a linear range of 0-7 mM and sensitivity of 1.33 x 10^{-6} A $cm^{-2}mM^{-1}$. This allowed for further electrochemical analysis via CA at E_{app} = 0.8 V over the same range.

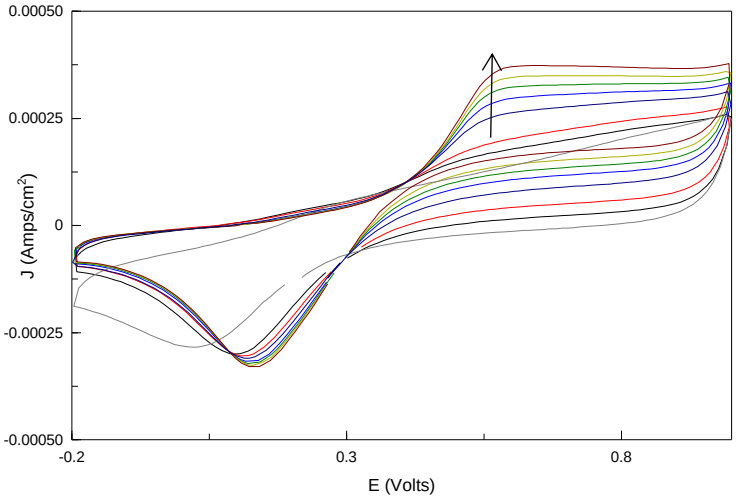

Figure 2.3: Overlay of CV data for 0-7 mM Glucose in 0.1 M phosphate buffer with a potential range of -0.2 V to 1.0 V vs. Ag/AgCl, scan rate of 0.1 V/s.

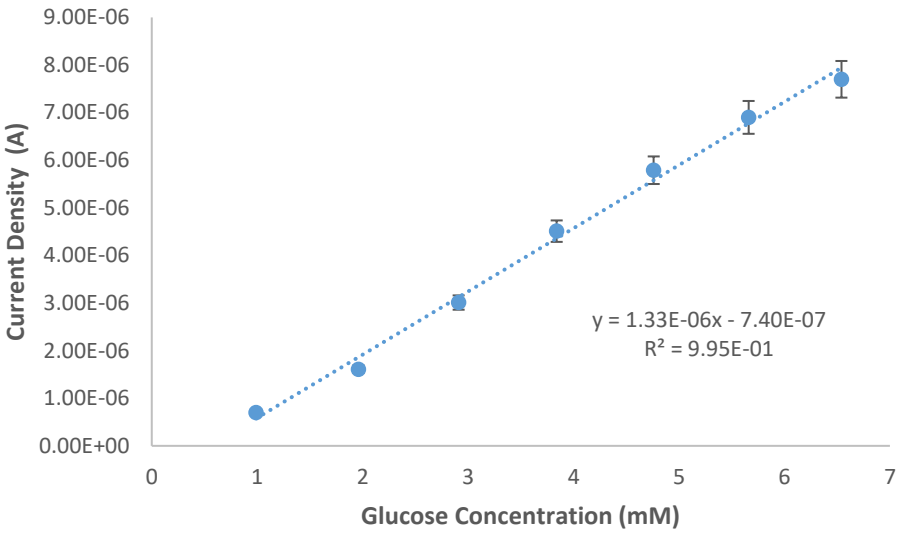

Figure 2.4: Calibration Curve showing direct relationship between current density measured at 0.8 V vs. Ag/AgCl and glucose concentration (mM) (n=3).

Figure 2.5 shows a chronoamperometric response showing an increase in current as the concentration of glucose increased, with linear range 0-7 mM glucose (*Figure 2.6*) with a sensitivity of 1.62 x 10^{-6} A $cm^{-2}mM^{-1}$. CC followed (*Figure 2.7*) under the same conditions.

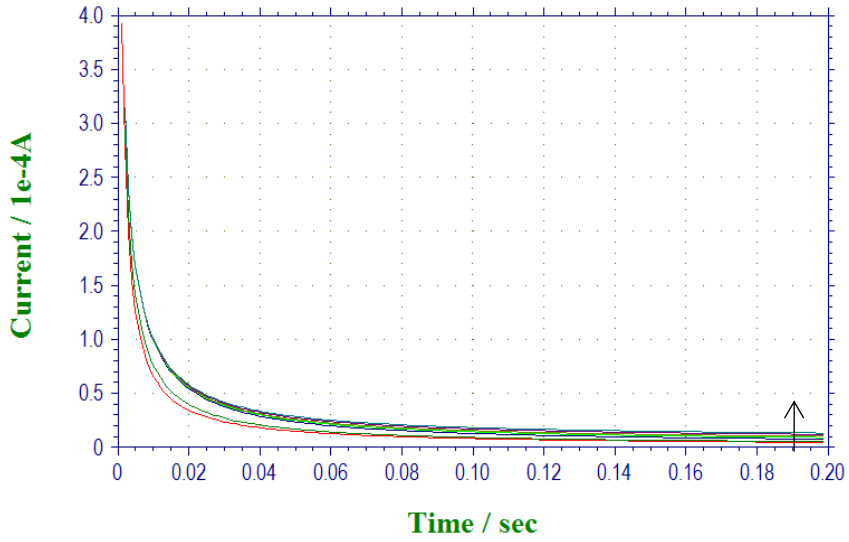

Figure 2.5: Overlay of glucose concentrations 0-7 mM in 0.1 M PB (pH 6.0) via CA with E_{app} = 0.8 V vs. Ag/AgCl, pulse width is 0.2 s.

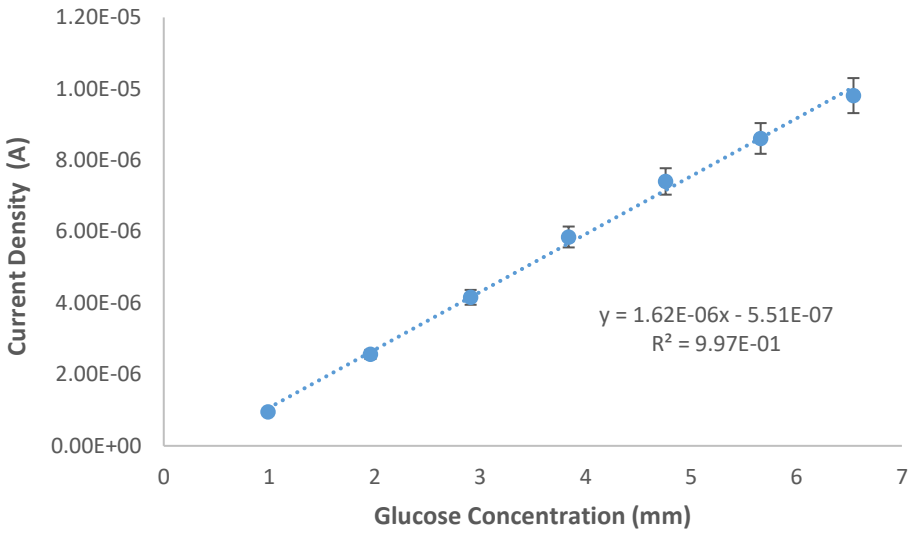

Figure 2.6: Calibration curve of current density (A) vs. glucose concentration (mM) ranging from 1-6.5 mM (n=3).

An overlay of the data, shown in *Figure 2.7*, illustrates how charge is directly proportional to concentration, resulting in linear range of 0-7 mM and sensitivity of 3.25 x 10^{-6} C $cm^{-2}mM^{-1}$ (*Figure 2.8*). CC data resulted in two-fold greater sensitivity relative to previous techniques CV and CA, and is a technique which is routinely used for the rapid detection of analytes via biosensor devices.[16] The LOD and LOQ were calculated from the CC data to be 0.51 mM and 1.70 mM respectively. These results can be compared to results obtained from Zhao *et al.* where a direct electron transfer glucose biosensor modified with GOx resulted in a linear range 0 – 0.64 mM, LOD of 1.07 x 10^{-3} mM and sensitivity 6.1 x 10^{-6} AmM^{-1}. Another biosensor developed by Miao *et al.* utilising HRP for H_2O_2 detection with similar enzyme immobilisation methods showed sensitivity of 1.87 x 10^{-5} AmM^{-1} and linear range of 0.047 – 2 mM. [10] Here, we can observe that the glucose biosensor developed in this work has a lower sensitivity and greater linear range relative to these reports.

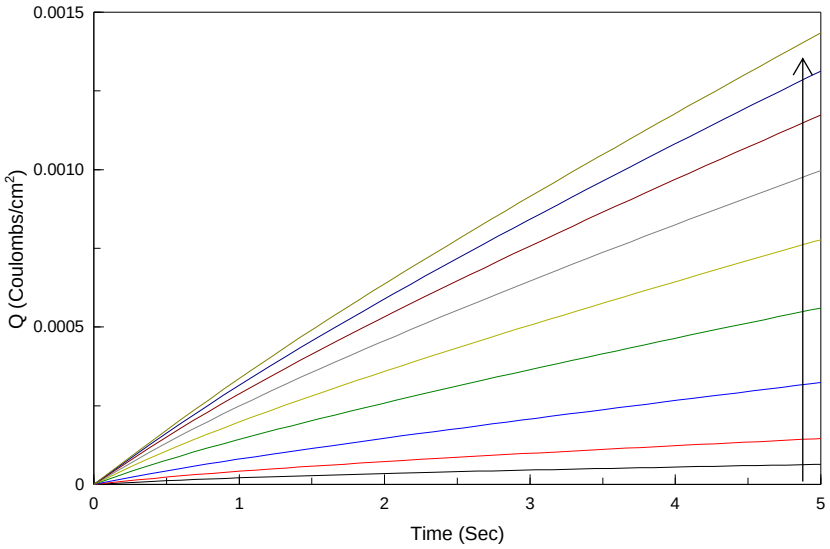

Figure 2.7: Overlay of CC data for glucose 0.99 - 6.54 mM additions in 0.1 M PB with E_{app} = 0.8 V vs. Ag/AgCl for 5 s.

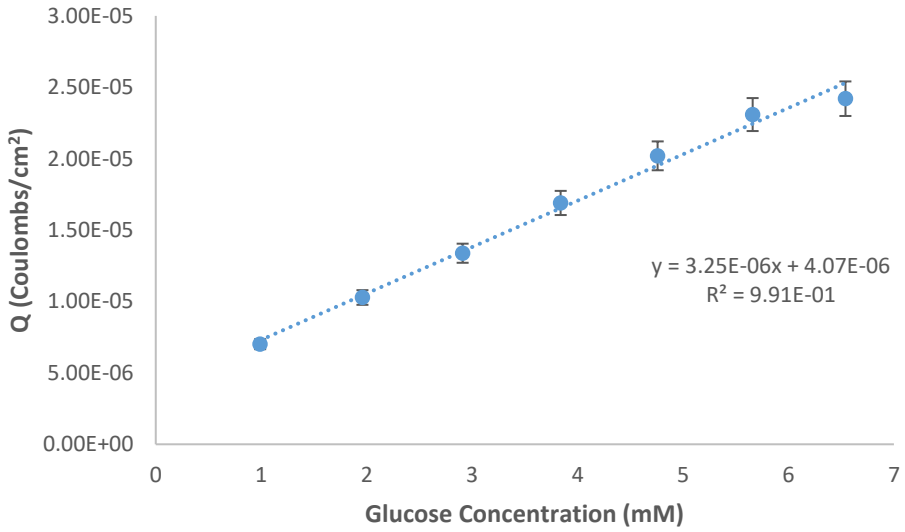

Figure 2.8: Calibration curve showing charge vs. glucose concentration over the range 0.99 - 6.54 mM (n=3).

2.5.1.2 Evaluation of enzyme kinetics for glucose sensor

A Lineweaver-Burk double reciprocal plot (*Figure 2.9*) was constructed using the above CC data resulting in K_m and V_{max} values which were determined using the reciprocal Lineweaver-Burk plot. The K_m value represents the concentration of glucose required for the reaction to reach half the V_{max}. A low K_m value will indicate a higher affinity of the enzyme to the substrate as a lower glucose concentration would be required for the reaction to approach half of V_{max}. A graph of 1/[S] vs. 1/V resulted in a K_m value of 4.25 mM and V_{max} of 3.57 x 10^{-5} mM.min^{-1}.

$$\frac{1}{V_o} = \frac{K_m}{V_{max}[S]} + \frac{1}{V_{max}} \quad \text{.....(2.2)}$$

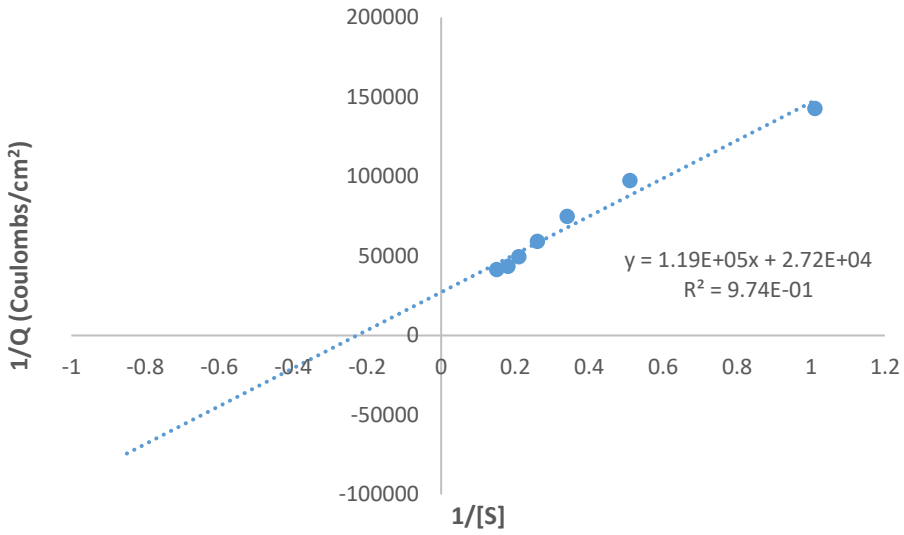

Figure 2.9: Lineweaver Burk plot from CC data, conditions of experiment per *Figure 2.8.*

2.5.1.3 Detection of lactose at Pt modified electrodes

Figure 2.7 shows a CV recorded at Pt/Chit/GOxβ-gal/Chit/GA electrode with additions of 0 to 4 mM lactose resulting in an increased H_2O_2 oxidation current at 0.55 V vs. Ag/AgCl.

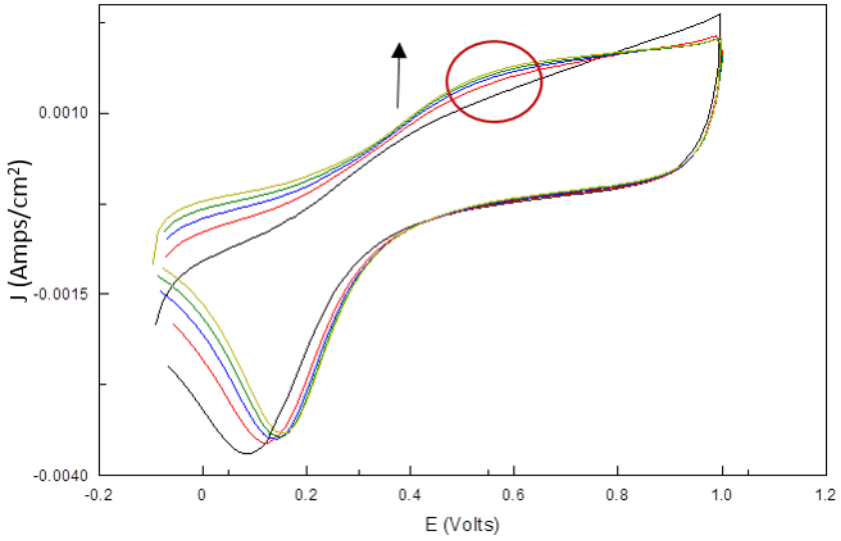

Figure 2.10: CV of Pt/Chit/GOxβ-gal/Chit/GA lactose sensor showing lactose response to 0-4 mM lactose additions, potential range -0.1 V to 1.0 V vs. Ag/AgCl, scan rate 0.1 V/s.

2.5.1.4 Optimisation of operating potential for lactose detection by CC

A series of applied potentials (0.65 V, 0.7 V, 0.75 V and 0.8 V vs. Ag/AgCl) were examined using CC analysis at the Pt/Chit/GOxβ-gal/Chit/GA. The relationship between lactose concentration and charge at each applied potential is shown in *Figure 2.11*, each of which resulted in a sigmoidal relationship between charge and concentration.

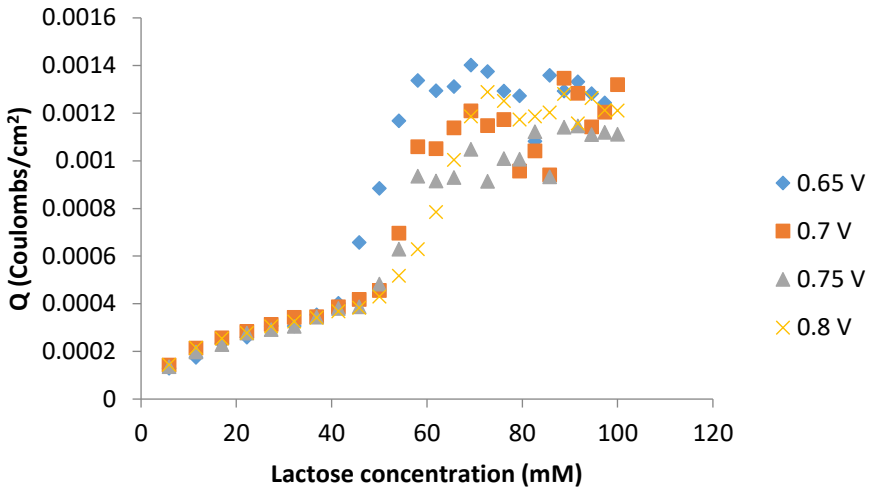

Figure 2.11: Overlay of CC data for charge, E_{app} = 0.65 V, 0.7 V, 0.75 V and 0.8 V vs. Ag/AgCl and 5.88 - 100 mM lactose additions in 0.1 M phosphate buffer at Pt/Chit/GOxβ-gal/Chit/GA.

Sigmoidal concentration profiles are common in dual-enzyme biosensors where two enzymes are used for the determination of a particular analyte. Sigmoidal kinetic profiles are the result of enzymes that hold positive cooperative binding characteristics. Allosteric enzymes have multiple active sites and do not obey the Michaelis-Menten kinetics. Such a response involves the substrate binding at one active site affecting the affinity of the substrate at other active sites.[17] Further CC analysis was carried out to determine the analytical data for each of the two linear ranges at E_{app} = 0.65 V vs. Ag/AgCl. Two different linear ranges of 0-40 mM (*Figure 2.12a*) and 40-60 mM (*Figure 2.12b*) lactose were realised.

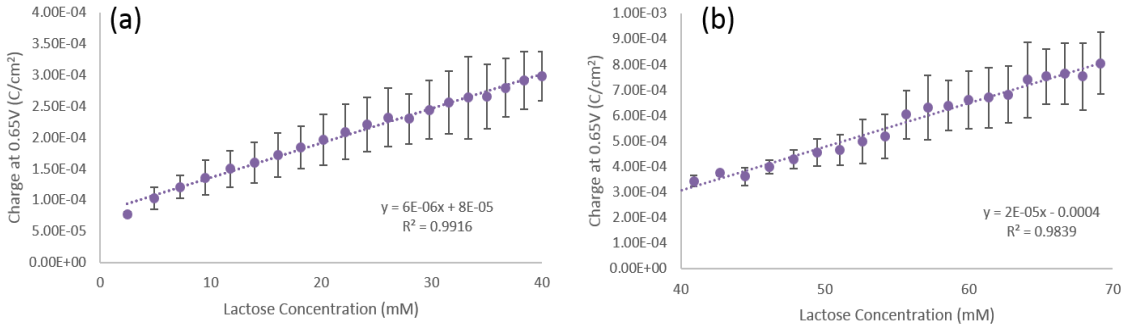

Figure 2.12: (a) Calibration curve of CC data showing relationship between charge (C/cm^2) (E_{app} = 0.65 V vs. Ag/AgCl) and lactose concentration (a) 2.47 - 40 mM (b) 39.08 – 69.16 mM. (n=3)

The lactose biosensor showed two linear ranges for lactose detection. The lower linear range of 2.47 – 4 x 10^{-2} M, shown in *Figure 2.12(a)*, had a sensitivity of 6 x 10^{-6} C cm^{-2}mM^{-1} with a limit of detection of 1.29 mM and a limit of quantitation of 4.29 mM. The higher linear range of 3.91 – 6.92 x 10^{-2} M, shown in *Figure 2.12(b)*, had a sensitivity of 2 x 10^{-5} C cm^{-2}mM^{-1} with a limit of detection of 4.29 mM and a limit of quantitation of 4.72 mM. These results can be compared to analytical data obtained by Tkáč *et al.* for a lactose biosensor developed using galactose oxidase, HRP and β-gal. This resulted in a linear range of 9 x 10^{-5} – 3.6 x 10^{-3} M, sensitivity of 4.4 x 10^{-7} A mM^{-1} and a limit of detection of 4.4 x 10^{-2} mM.[21] The greater sensitivity and lower detection limit may be due to the different enzymes employed which can affect the overall performance of the biosensor.

2.5.1.5 Positive and negative control studies via CV

A negative control analysis was carried out on the lactose biosensor via CV. 0.1 M PB and 1.98 mM lactose were analysed at modified electrodes with and without the presence of the two enzymes, GOx and β-gal. Positive electrodes are referred to as Pt/CHIT/GOx-β-gal/CHIT/GA and negative electrodes as Pt/Chit/Chit/GA.

Figure 2.13(a) shows the CV response for background PB plus addition of 1.98 mM lactose at Pt/Chit/Chit/GA, resulting in no significant increase in current relative to the background. *Figure 2.13(b)* shows the CV response for background PB and addition of 1.98 mM lactose at Pt/CHIT/GOx-β-gal/CHIT/GA. Here, an increase in the oxidation peak was evident at 0.65 V showing the detection of lactose, providing evidence that the dual enzyme system does catalyse the lactose and glucose reactions

and no significant background effect was observed.

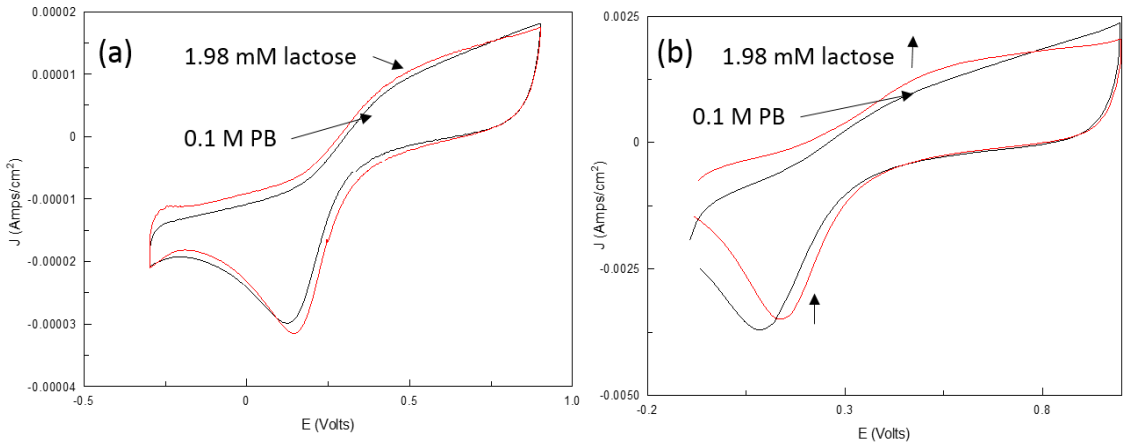

Figure 2.13: (a) CV of PB solution (pH 6.0) and 1.98 mM lactose at (a) Pt/Chit/Chit/GA and (b) Pt/Chit/GOxβ-gal/Chit/GA, potential range -0.1 V to 1.0 V vs. Ag/AgCl at 100 mVs^{-1}.

Figure 2.14 shows the quantitative difference between the electrode responses relative to background. This confirms the presence of the two enzymes is required in order to detect lactose by the catalytic breakdown to H_2O_2.

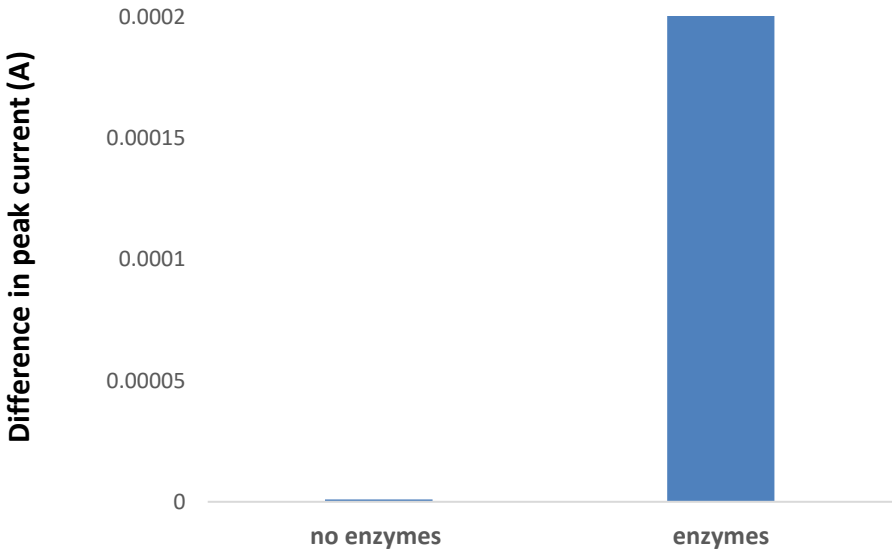

Figure 2.14: Relative difference in peak current for 0.1 M PB and lactose (1.98 mM) at Pt/Chit/Chit/GA (absence of enzymes) and Pt/Chit/GOxβ-gal/Chit/GA (presence of enzymes).

Table 2.2 shows a summary of the analytical data obtained for direct glucose and lactose sensing including – linear range, sensitivity and LOD for sensors developed in this work and biosensors found in literature.

Table 2.2: Summary table for analytical data achieved in the case of direct glucose and lactose sensing

Analytical Data	**Comparison of 1st generation Glucose Biosensors**		
	REST-FM sensor	**Ziao *et al.***	**Miao *et al.***
Linear Range (M)	$0 – 7 \times 10^{-3}$	$0 – 6.4 \times 10^{-4}$	$0 – 2 \times 10^{-3}$
Sensitivity (C cm^{-2} mM^{-1})	3.25×10^{-6}	6.1×10^{-6}	1.87×10^{-5}
LOD (mM)	0.51	1.07×10^{-3}	
Analytical Data	**Comparison of 1st generation Lactose Biosensor**		
	REST-FM sensor		**Tkáč *et al.***
Linear Range (M)	2.47×10^{-3} - 4.00×10^{-2}	3.91×10^{-2} - 6.92×10^{-2}	9×10^{-5} – 3.6×10^{-3}
Sensitivity (C $cm^{-2}mM^{-1}$)	6×10^{-6}	2×10^{-5}	4.4×10^{-7}*
LOD (mM)	1.29	1.42	4.4×10^{-2}

*units are A mM^{-1}

2.5.2 Solution mediated biosensing using GCE

Mediated glucose and lactose biosensors were developed using glassy carbon macroelectrodes in the presence of $K_3Fe(CN)_6$ (5 mM) in solution. Initial studies involved an investigation into the use of two different cross-linking agents for use in enzyme immobilisation of GOx (*see section 2.4.3*). The effect on linearity and response characteristics was performed in each case. The two crosslinking agents investigated were 1.5 % PEGDE solution and a 0.05 % GA solution. Electrodes are referred to as GC/CHIT/GOx/CHIT/GA and GC/CHIT/GOx/CHIT/PEGDE.

2.5.2.1 Scan rate study at GOx modified GCE

To investigate the effects of 1.5 % PEGDE and 0.5 % GA as GOx enzyme immobilisation cross-linking agents, a scan rate study was performed over the range 20-100 mVs^{-1} at different concentrations of the substrate, glucose (0-7 mM) in 5 mM $K_3Fe(CN)_6$. Increased Fe^{2+} reoxidation signals resulted in enhanced current as Fe^{3+} is required to oxidise the $FADH_2$ enzyme prosthetic group FAD, as described in *Equations 2.2 – 2.4.*[11]

$$\text{Glucose} + \text{GOx(FAD)} \rightarrow \text{gluconic acid} + \text{GOx}(FADH_2) \quad (2.2)$$

$$\text{GOx}(FADH_2) + 2M(ox) \rightarrow \text{GOx(FAD)} + 2M(red) + 2H^+ \quad (2.3)$$

$$2M(red) \rightarrow 2M(ox) + 2e^- \quad (2.4)$$

Data plots of glucose concentration and peak current were constructed in order to highlight the effect of scan rate on the catalytic response at a GC/Chit/GOx/Chit/PEGDE (*Figure 2.15*). It was evident that scan rate influenced the linearity of the biosensor as the linear range for 100 mVs^{-1}, 50 mVs^{-1} and 20 mVs^{-1} was 0–1.96 mM, 0-2.91 mM and 0 – 4.76 mM respectively. Furthermore, there was greater change between measurements in the oxidation and reduction current at 20 mVs^{-1}, with an increase in oxidation peak and decrease in the reduction peak not observed at 50 or 100 mVs^{-1}. This was apparent at both modified GC/Chit/GOx/Chit/PEGDE and GC/Chit/GOx/GA electrodes. Therefore, slower scan rates resulted in better observation of mediated response at modified electrodes.

Further CV analysis was carried out at 20 mVs^{-1} over a wider concentration range, with calibration curve shown in *Figure 2.16*. Using these voltammetric conditions, the glucose biosensor resulted a linear range of 5.96 – 29.13 mM with sensitivity of 4.65×10^{-5} A $cm^{-2}mM^{-1}$ ($R^2 = 0.98$) (n=2).

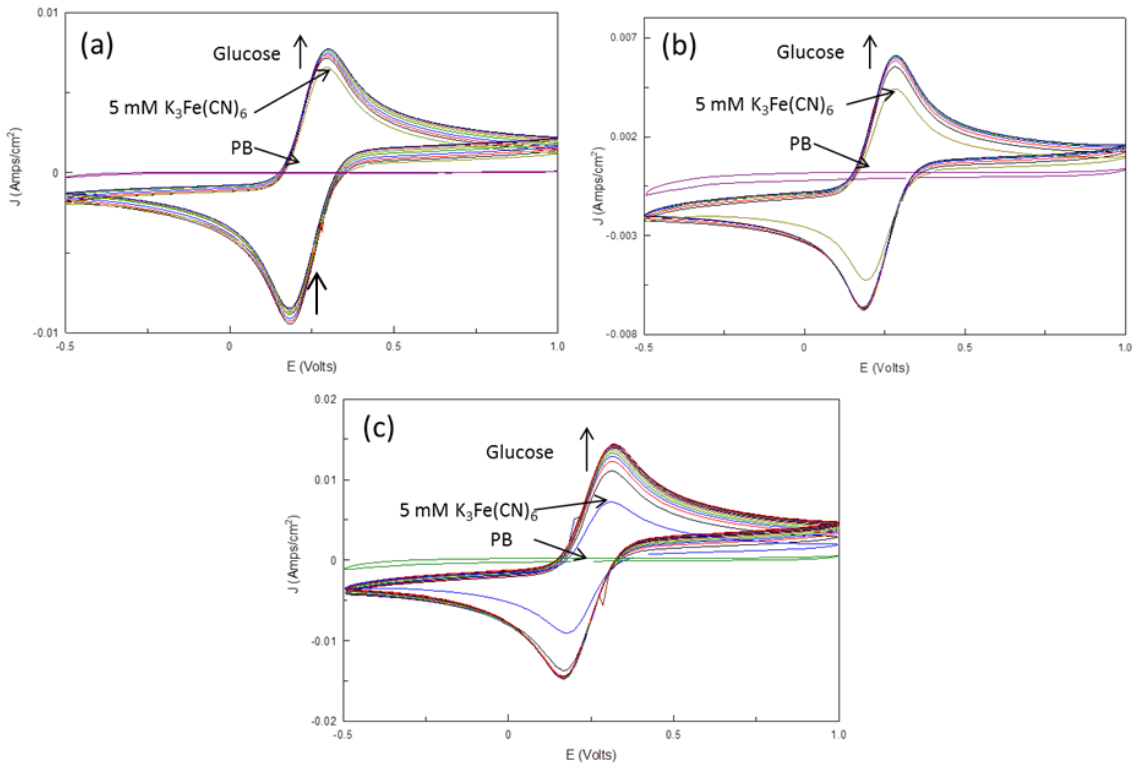

Figure 2.15: CV of GC/CHIT/GOx/CHIT/PEGDE in 5 mM $K_3Fe(CN)_6$ with additions of 0-7 mM glucose. Potential range -0.5 V – 1.0 V with scan rates (a) 20 mVs^{-1} (b) 50 mVs^{-1} and (c) 100 mVs^{-1} vs. Ag/AgCl.

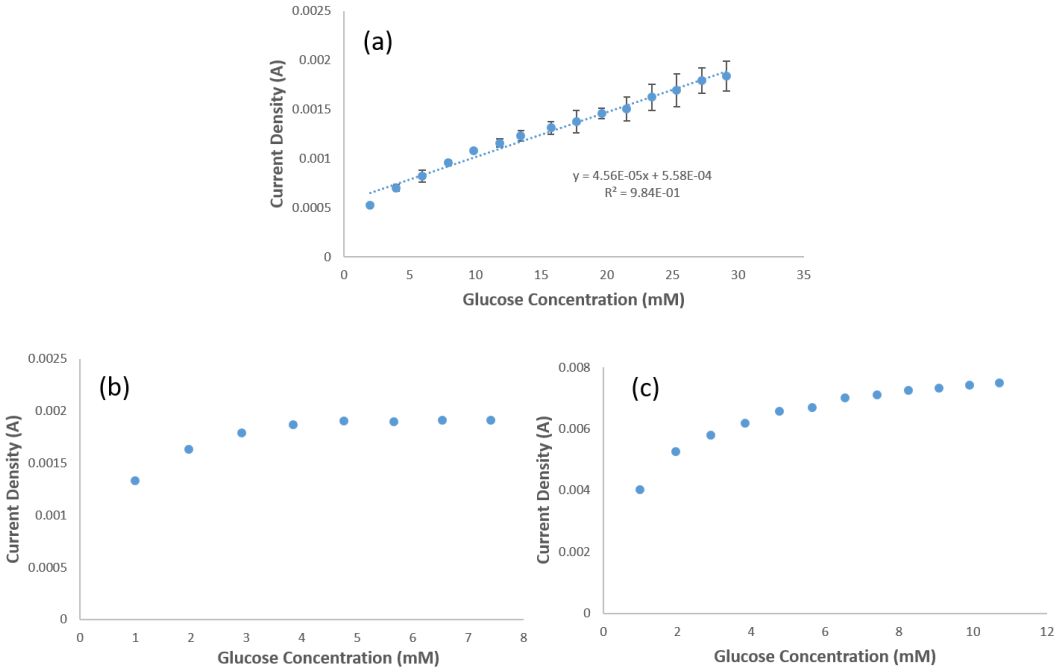

Figure 2.16: Calibration curve of current density vs. glucose concentration for corresponding CV data at GC/Chit/GOx/Chit/PEGDE at (a) 20 (b) 50 and (c) 100 mVs^{-1} (n=2) (Other conditions as per *Figure 2.12*)

Using GA as crosslinker, the effect of scan rate is shown in *Figure 2.17* at GC/Chit/GOx/Chit/GA. It was evident that at a slower scan rate, 20 mVs^{-1} with R^2 = 0.98, the relationship between concentration and peak current obtained a more linear response relative to 50 and 100 mVs^{-1}. Corresponding calibration curve resulted in linear range of 0-2.91 mM, 0-4.76 mM and 0-6.54 mM for 100, 50 and 20 mVs^{-1}. Therefore, the slower the scan rate of the potential sweeping can influence the biosensor linear range for the enzyme-substrate reaction, resulting in an increase in the oxidation current and a decrease in the reduction current as indicated earlier in the case of the GC/Chit/GOx/Chit/PEGDE, and according to the mechanism in *Equations 2.2 – 2.4*.

Calibration studies followed at scan rate 20 mVs^{-1}. *Figure 2.18* shows a calibration curve for the data obtained using CV, resulting in linear range of 1.99-17.68 mM with a sensitivity of 1.88 x 10^{-4} A $cm^{-2}mM^{-1}$ (R^2 = 0.98) (n=2). Results showed that the PEGDE electrode was four times less sensitive than the GA sensor. It was also evident that the PEGDE sensor resulted in a wider linear range relative to the GA electrode, possibly due to PEGDE forming a thicker layer on the transducer surface relative to GA which can enable controlled diffusion of the substrate.

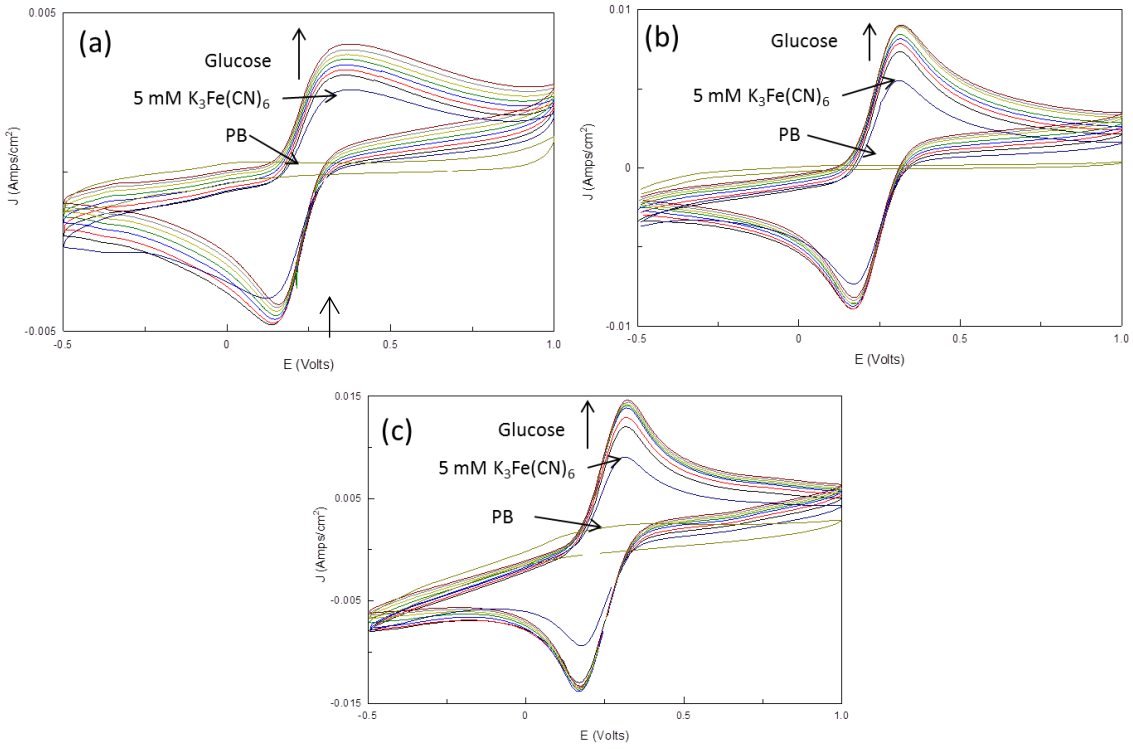

Figure 2.17: CV of GC/Chit/GOx/Chit/GA in 5 mM $K_3Fe(CN)_6$ with additions of 0-7 mM glucose. Potential range -0.5 V - 1.0 V with scan rates (a) 20 mVs^{-1} (b) 50 mVs^{-1} and (c) 100 mVs^{-1} vs. Ag/AgCl.

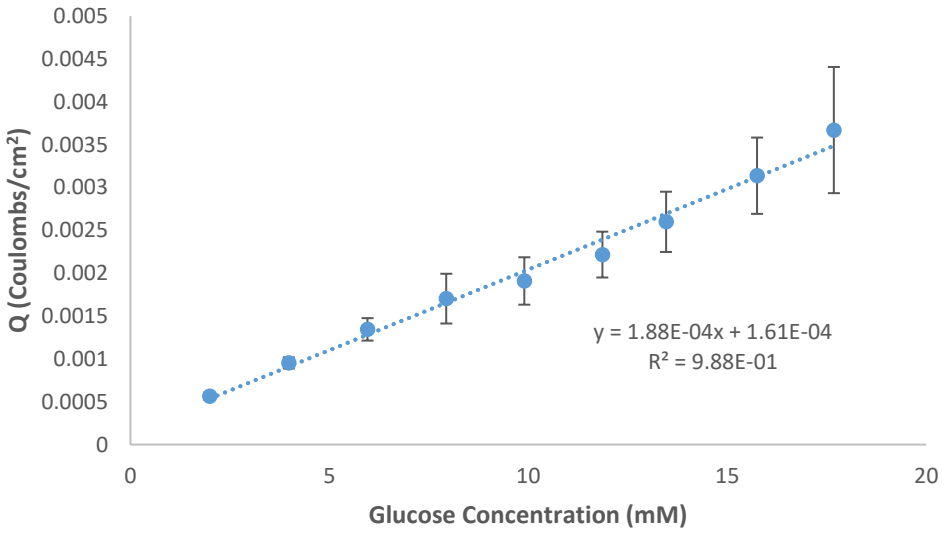

Figure 2.18: Calibration curve of CV data showing current density (A) vs. glucose concentration (mM) at GC/Chit/GOx/Chit/GA at 20 mVs^{-1} (n = 2).

The catalytic regeneration mechanism (ECAT) describes the initial electroactive species being regenerated by a homogenous reaction (see *equations 2.5* and *2.6*).[18]

$O + ne^- \leftrightarrow R$ ……..……...…..(2.5)

$R + X \xrightarrow{k} O + Y$ ……..…..……..(2.6)

In the case of the mediated enzyme electrode developed in this work;

E: $Fe^{2+} \leftrightarrow Fe^{3+} + e$ ……..……...…….(2.7)

CAT: $Fe^{3+} + FADH_2 \rightarrow Fe^{2+} + FAD$ ……..…..……(2.8)

In order to confirm the catalytic reactions, plots of $I_p/\sqrt{v}$ vs. v were performed in the absence and presence of the substrate, where $I_p/\sqrt{v}$ decreased with increasing scan rate, according to this mechanism.[19] *Figure 2.19* shows the relationship between scan rate and $I_p/\sqrt{v}$ in the absence and presence of 7 mM glucose at GC/Chit/GOx/Chit/GA electrode, confirming the mechanism as an electrochemical step followed by catalysis.

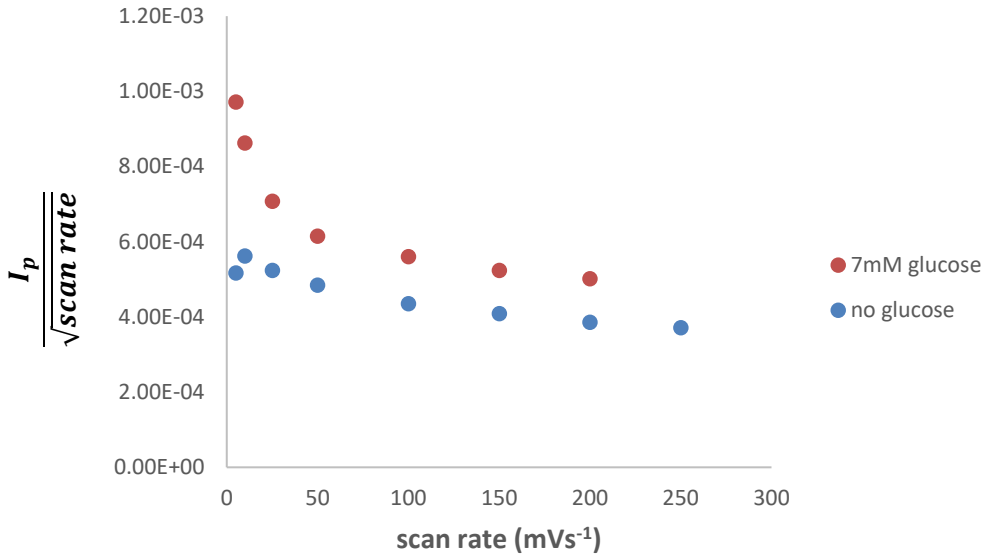

Figure 2.19: Data plot showing $I_p/\sqrt{v}$ vs. v of 5 mM $K_3Fe(CN)_6$ in the absence and presence of 7 mM glucose at GC/Chit/GOx/Chit/GA.

Chronocoulometric analysis (E_{app} = 0.35 V vs. Ag/AgCl for 5 s) was performed at both GOx electrodes GC/Chit/GOx/Chit/PEGDE and GC/Chit/GOx/Chit/GA with corresponding data - charge vs. co□centration plots shown in *Figure 2.20*.

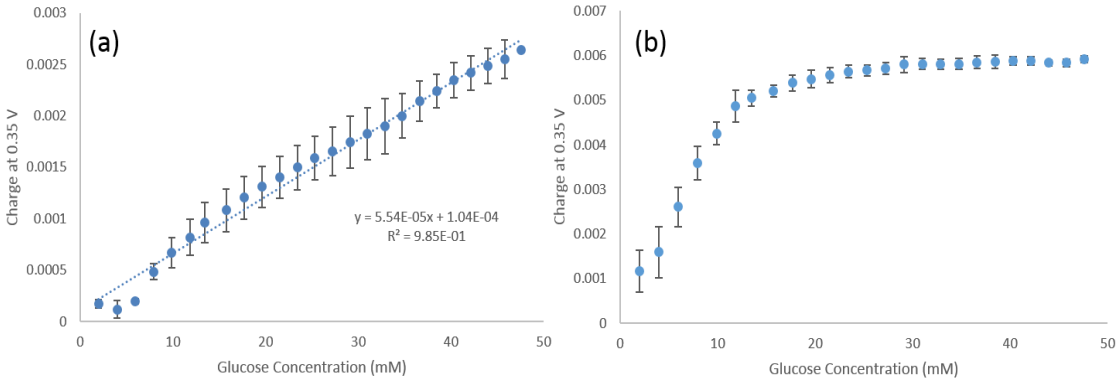

Figure 2.20: CC data for (a) GC/Chit/GOx/Chit/PEGDE and (b) GC/Chit/GOx/Chit/GA response to glucose concentration (0- 47.61 mM) vs. charge (E_{app} = 0.35 V vs. Ag/AgCl for 5 s) (n=3).

It was apparent that different cross-linking agents can influence the linear range, with GC/Chit/GOx/Chit/PEGDE electrode showing a wider linear range between 7.94-47.61 mM relative to the GC/Chit/GOx/Chit/GA electrode (linear range of 1.99- 11.86 mM).

Due to the desire to progress the work in relation to process monitoring at portable sensors, the GA cross-linker was employed going forward in relation to transfer to SPE as the PEGDE cross-linker was found to be unsuitable on the portable transducer surface. It was discovered that the PEGDE caused the printed carbon of the electrode to lift from the surface affecting the stability of the electrode. However, similar issues were not found to be reported in literature.

2.5.2.2 Solution phase mediation of lactose at GCE

A 2nd generation lactose biosensor was developed at a GCE using GA as crosslinker, as per procedure in section 2.4.1 and operated in the presence of 5 mM $K_3Fe(CN)_6$ in PB (pH 6.0). *Figure 2.21* shows a CV of 5 mM $K_3Fe(CN)_6$ solution and addition of 1 mM lactose at GC/GOxβ-gal/Chit/GA. An increase in the oxidation peak current was evident at 0.3 V, indicating the lactose response.

CC analysis followed at E_{app} = 0.3 V vs. Ag/AgCl (*Figure 2.22 and 2.23*). As discussed earlier for direct lactose detection at Pt/Chit/GOxβ-gal/Chit/GA electrode, results showed a sigmoidal relationship between charge and 0-18 mM concentration for solution mediated lactose detection.

The sensor resulted in a linear range of 5.83 x 10^{-3} – 1.65 x 10^{-2} M with sensitivity of 9.41 x 10^{-4} C $cm^{-2}mM^{-1}$, LOD of 1.38 mM and LOQ of 4.59 mM. The results showed an initial lag in sensor response from 0 – 5.83 mM which may be due oxygen interference. Results can be compared to literature values of bi-enzyme lactose biosensors, developed by Ammam *et al.* with linear range of 0-14 mM lactose and a lower sensitivity of 1.11 x 10^{-7} AmM^{-1}. [20] It can be suggested that the difference in sensitivity could be as a result of very different development methods. Fabrication of the lactose biosensor by Ammam *et al.* did not involve any immobilisation or cross-linking agents which could contribute to lower sensitivity of the biosensor. Immobilisation of enzymes on electrode surfaces using cross-linking agents can hinder the ability of enzymes to work efficiently. Therefore, it is important to not use high concentrations of cross-linking agents during enzyme fabrication. Without the use of immobilisation, enzyme electrodes tend to have low shelf life and stability issues. It must also be noted Ammam *et al.* also uses amperometry to measure the current response of the electrode whereas we have opted to use chronocoulometry as the electrochemical interrogation method.

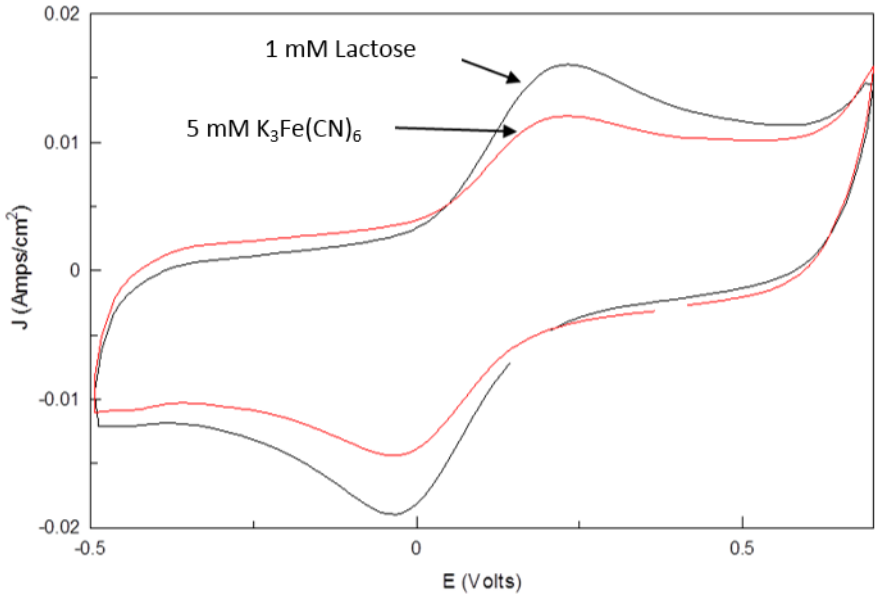

Figure 2.21: CV response to 1 mM lactose addition in 5 mM $K_3Fe(CN)_6$ at GC/Chit/GOxβ-gal/Chit/GA over the range -0.5 V to 0.8 V at a scan rate of 0.1 V/s vs. Ag/AgCl.

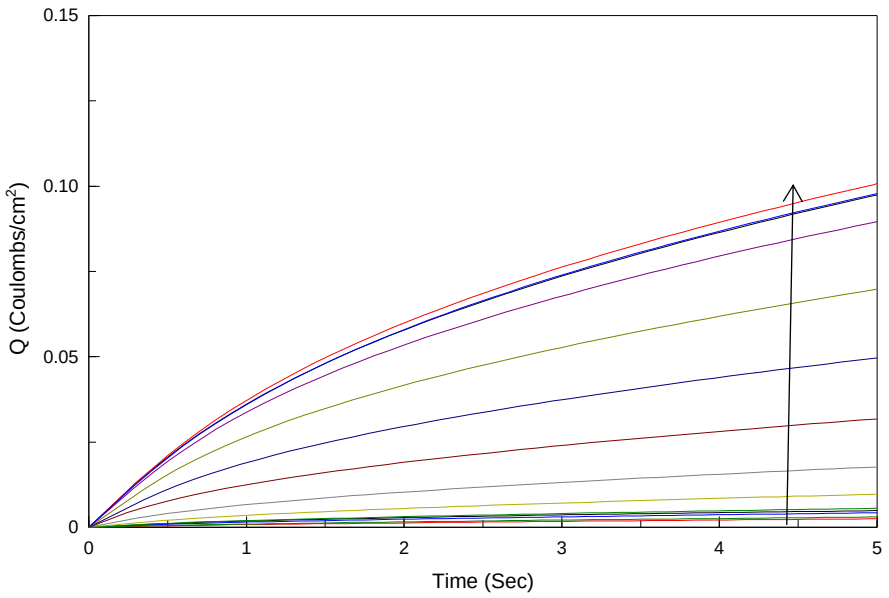

Figure 2.22: Overlay of CC response for 0-18 mM lactose in the presence of 5 mM $K_3Fe(CN)_6$ at GC/Chit/GOxβ-gal/Chit/GA, E_{app} = 0.3 V with charge taken at 5 s.

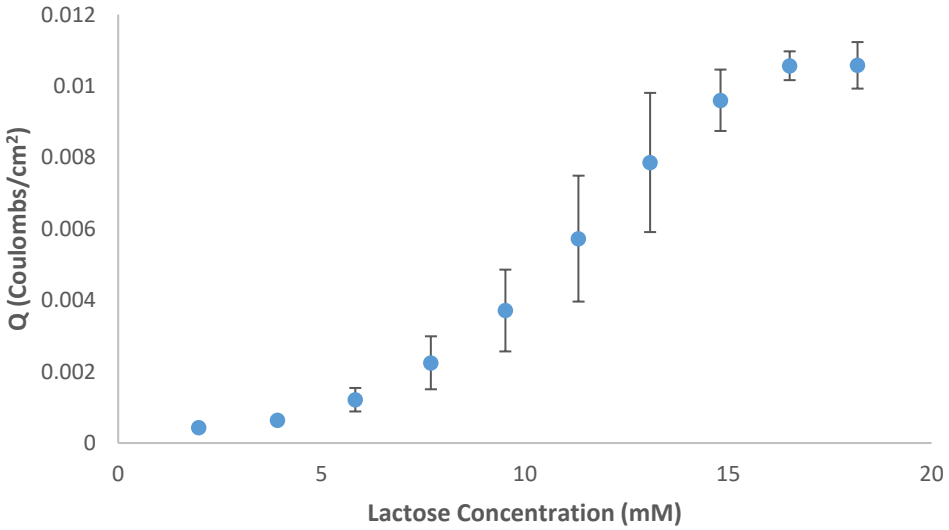

Figure 2.23: Corresponding calibration curve of charge vs. lactose concentration over the range 0-18.18 mM (CC analysis) (n=3).

Figure 2.24 illustrates the relationship between scan rate and $I_p/\sqrt{v}$ at the GC/Chit/GOxβ-gal/Chit/GA electrode, thus confirming the mediation electrochemical (E) followed by catalytic (CAT) mechanism as per glucose biosensor.

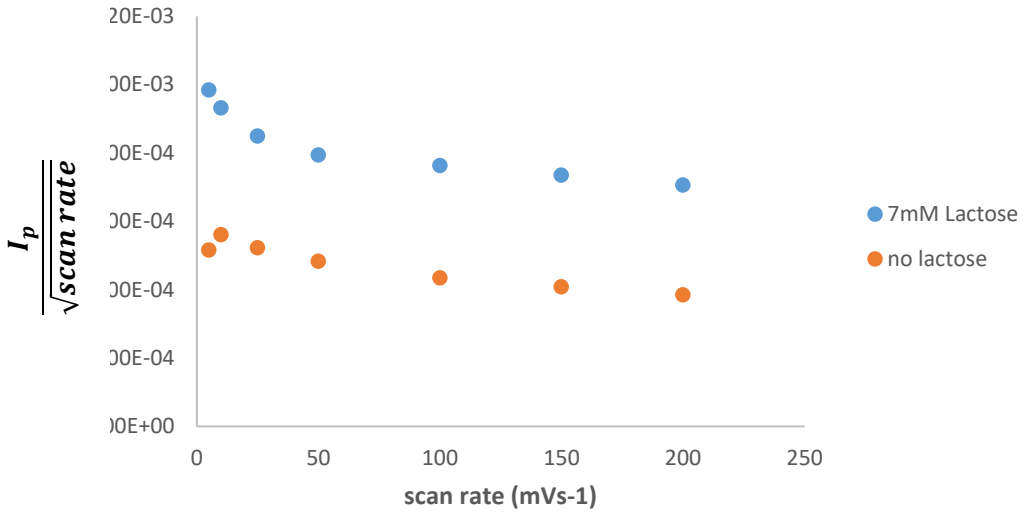

Figure 2.24: Data plot showing $I_p/\sqrt{v}$ vs. v in 5 mM $K_3Fe(CN)_6$ in the presence and absence of 7 mM lactose at GC/Chit/GOxβ-gal/Chit/GA.

2.5.2.3 Control studies for mediated glucose and lactose biosensors

A negative control study was carried out in order to ensure that any electrochemical signal obtained from CV or CC at the glucose biosensor was in response to the glucose substrate. *Figure 2.25(a)* shows a voltammogram of 0.1 M PB, 5 mM $K_3Fe(CN)_6$ and 10 mM glucose at a GOx modified electrode (GC/Chit/GOx/Chit/GA) and an electrode modified with chitosan and GA, without enzyme (GC/Chit/Chit/GA). The results of the negative control showed that when the enzyme was absent, there was the expected lack of response to glucose relative to the active electrode.

A negative lactose control sensor was also fabricated and data shown in *Figure 2.25(b)* shows the CC response with E_{app} = 0.3 V vs. Ag/AgCl for 5 s. The response to (11.32 mM lactose) was compared for two biosensors, one with the two specific enzymes present on the surface (GOx/β-gal), referred to as GC/Chit/GOx/β-gal/Chit/GA and a control electrode modified with chitosan and GA in the absence of enzymes (GC/Chit/Chit/GA).

The results of the negative control analysis showed that there was a large difference in charge values recorded for lactose addition at the active electrode relative to control electrode as expected, as shown in *Figure 2.25*.

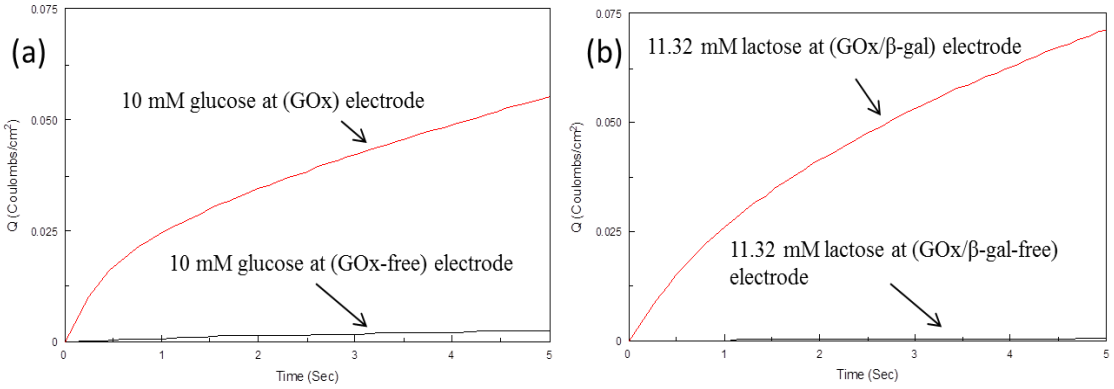

Figure 2.25: (a) CC data of PB, 5 mM $K_3Fe(CN)_6$ and 10 mM glucose at a GOx modified electrode and a control electrode. Charge measured at 0.35 V vs. Ag/AgCl for 5 s. (b) CC data showing 11.32 mM lactose at GC/CHIT/GOx-βgal/CHIT/GA and GC/CHIT/CHIT/GA; Charge taken at 0.3 V vs. Ag/AgCl at 5 s.

2.5.2.4 Investigation into the effect of each reagent layer on lactose response

Further lactose sensor control studies followed and *Table 2.3* shows the configurations (a – d) involved. Each were monitored for their respective response to addition of 14.81 mM lactose (in presence of 5 mM $K_3Fe(CN)_6$).

Figure 2.26 shows the voltammetric response to each electrode format (*Table 2.3*) and corresponding differential data is shown in *Figure 2.27*, thus confirming the maximum lactose response present at the GC/Chit/GOxβ-gal/Chit/GA. *Figure 2.27* shows that there was a background current signal at all control electrodes. However, the greatest current signal was evident at the electrode with GOx and β-gal present. The CV for lactose response at GC/CHIT/GOx-β-gal/CHIT/GA (d), provides evidence that there was a greater linear range (0 – 14.81 mM) for lactose as the concentration increases relative to other electrodes (a), (b) and (c) that show no linear increase in lactose response after 1.98 mM. It was evident that no further increase in lactose response was observed after the initial deviation which may be due to non-specific interactions between lactose and crosslinking agents. It can be suggested that the initial signal response of electrode (a-c) could be due to the solution breakdown of lactose to glucose. A false positive response could also be due to substrate interactions with individual reagents within the bienzyme layer.

Table 2.3: Description of electrode configuration used for the investigation into response of various layers on lactose.

Label	Sensor	Configuration
(a)	No enzymes (Negative control)	GC/CHIT/CHIT/GA
(b)	GOx only	GC/CHIT/GOx/CHIT/GA
(c)	B-gal only	GC/CHIT/β-gal/CHIT/GA
(d)	Dual enzyme lactose biosensor (Positive control)	GC/CHIT/GOx-β-gal/CHIT/GA

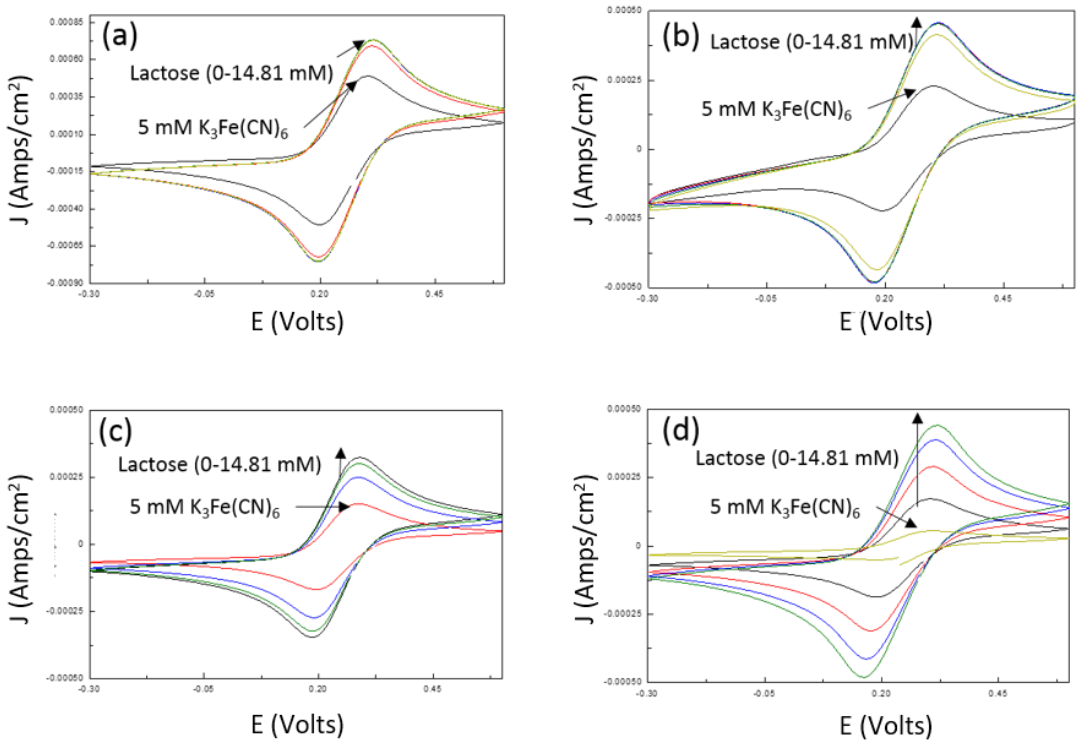

Figure 2.26: (a) CV of 0.1 M PB, 5 mM $K_3Fe(CN)_6$ followed by 0–14.81 mM lactose at (a) chitosan and GA modified GC electrode, (b) chitosan and GA modified GC electrode (with GOx), (c) chitosan and GA modified GC electrode (β-gal only), (d) modified GC electrode (with β-gal and GOx) potential range -0.3 V to 0.5 V vs. Ag/AgCl at 100 mVs^{-1}.

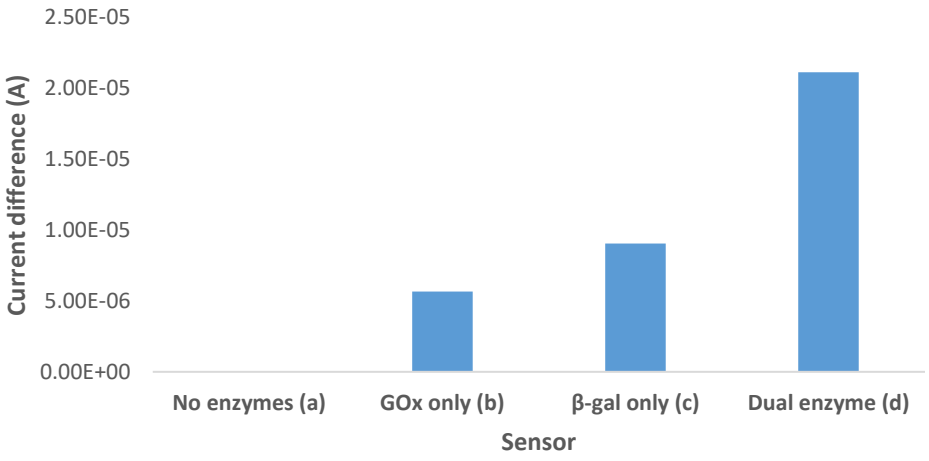

Figure 2.27: Difference between current signal for background and corrected lactose (14.81 mM) addition at the various control electrode formats (a-d).

A summary of the analytical data obtained for solution mediated biosensors for lactose detection is shown in *Table 2.4*.

Table 2.4: Summary of analytical data for lactose biosensors via CC analysis.

Analytical Data for 2nd generation Lactose Biosensor			
Linear Range (M)	**Sensitivity (C cm^{-2}mM^{-1})**	**LOD* (mM)**	**LOQ (mM)**
5.83 x 10^{-3} – 1.65 x 10^{-2}	9.41 x 10^{-4}	1.38	4.59

$* \frac{3\ x\ standard\ deviation\ (blank)}{slope\ (Ccm^{-2}mM^{-1})}$

2.5.3 Scanning Electrochemical Microscopy characterisation of glucose and lactose biosensors

The use of scanning electron microscopy and scanning electrochemical microscopy (SECM redox competition mode) provided surface topographical and imaging/enzyme reactivity information respectively. SECM was carried out on both glucose (GC/Chit/GOx/Chit/GA) and lactose (GC/Chit/GOxβ-gal/Chit/GA) biosensors. Surface imaging was performed at the enzyme modified substrate electrode (GCE) in the presence of mediator (5 mM $K_3Fe(CN)_6$) holding the potential of the Pt UME tip (E_T)= -0.4 V vs. Ag/AgCl, at the reduction potential of Fe^{3+} (see *Figure 2.28*).

Figure 2.28 and *Figure 2.29* shows CV of 5 mM $K_3Fe(CN)_6$ at a Pt UME and the GCE

substrate. Here, the Fe^{3+} was in solution as the enzyme required it to re-oxidise $FADH_2$ to FAD. When reduction occurred at the UME tip, there was less Fe^{3+} available to reoxidise GOx($FADH_2$) back to GOx(FAD). At E_{app} = -0.4 V, Fe^{3+} is reduced to Fe^{2+} and therefore, this potential will be utilised in further SECM analysis.

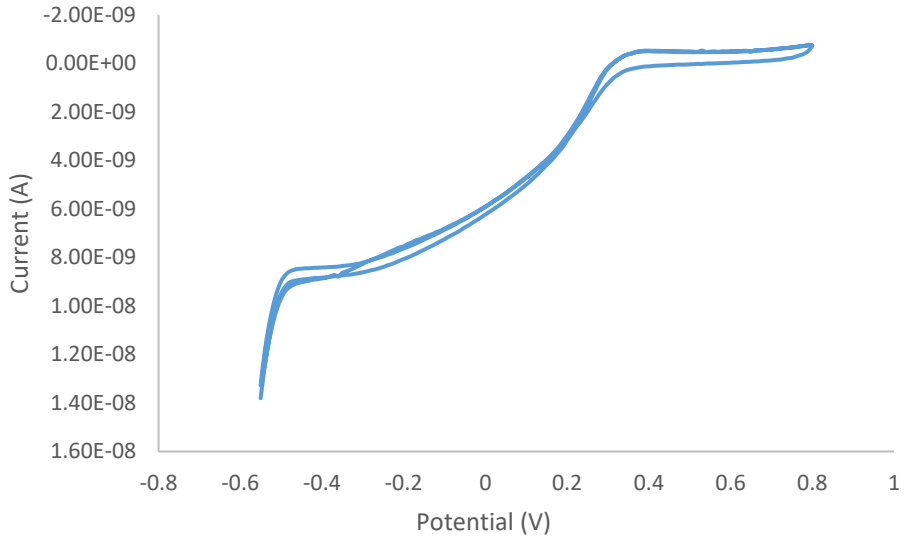

Figure 2.28: CV of 5 mM $K_3Fe(CN)_6$ at 20 µm Pt UME tip (RG = 23.8) over the range -0.5 to 0.8 V vs. Ag/AgCl at 50 mVs^{-1}.

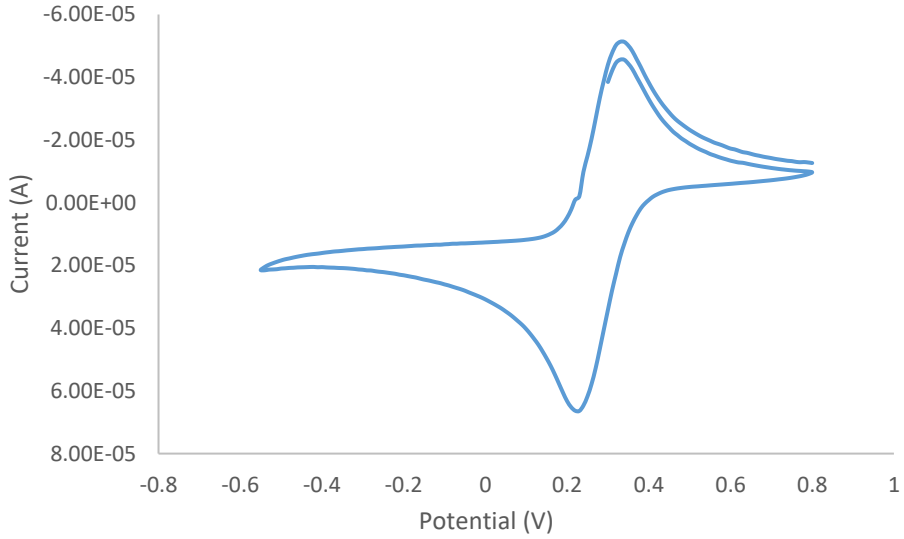

Figure 2.29: CV of 5 mM $K_3Fe(CN)_6$ at GCE substrate (0.0707 cm^2), potential range -0.5 to 0.8 V vs. Ag/AgCl at 50 mVs^{-1}.

Figure 2.30 illustrates approach curves showing an increase in the tip current ratio as the UME approaches a conducting surface (GCE substrate) and a decrease in current on approach to the insulating surround, where normalised current is I_{TIP}/I_{Inf} and I_{Inf} is the steady state current at infinite distance (taken from *Figure 2.28*). A decrease in current at the insulating surface occurred as no regeneration of Fe^{3+} was produced, whereas the presence of the enzyme at the conducting surface caused regeneration of the electroactive species incurring an increase in tip current ratio.

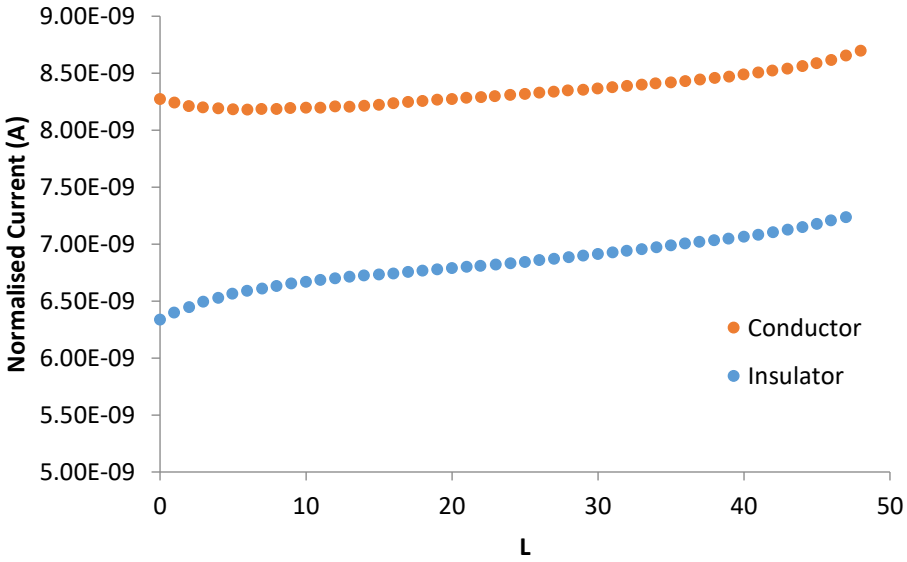

Figure 2.30: Normalised current (I_{TIP}/I_{Inf}) vs. distance (L) where L = d/a and d = distance from tip Pt ultramicroelectrode (UME) to substrate, a = tip radius 10 nm, RG = 23.8. Curves recorded above the insulating and conducting surface (Chit/GA-GOx film), by translating the UME vertically (z approach curve). E_T = -0.4 V vs. Ag/AgCl, E_{sub} = OFF, 5 mM $K_3Fe(CN)_6$ in PB pH 6.0.

Figure 2.31 and *Figure 2.32* shows approach curves towards the enzymatic glucose and lactose biosensor substrates (E_T) = -0.4 V vs. Ag/AgCl. As the tip approached the modified surface the current decreased causing a negative feedback response. When a sharp decrease in current was measured, the experiment was stopped and the distance required to achieve a suitable position for the tip was determined prior to line scan or area scan analysis. Redox competition mode was utilised where both sample and tip competed for the oxidised form Fe^{3+}. Low currents monitored at SECM tip as enzyme modified surface is approached indicated high local electroactivity.

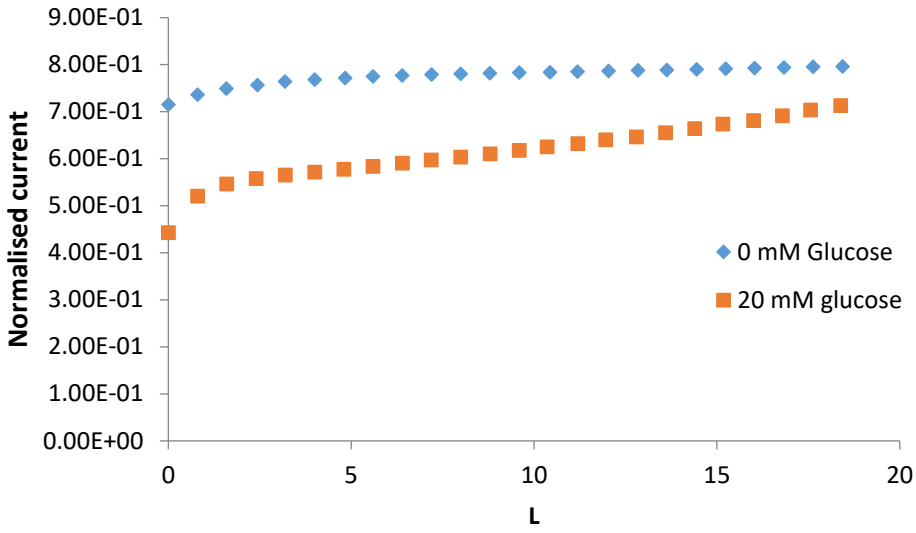

Figure 2.31: Normalised current (I_{TIP}/I_{Inf}) vs. distance (L) where L = d/a and d = distance from tip Pt ultramicroelectrode (UME) to substrate, a = tip radius 10 nm, RG = 23.8. Curves recorded above the Chit/GA-GOx film, by translating the UME vertically (z approach curve). E_T = -0.4 V vs. Ag/AgCl, E_{sub} = OFF, 5 mM $K_3Fe(CN)_6$ in PB pH 6.0.

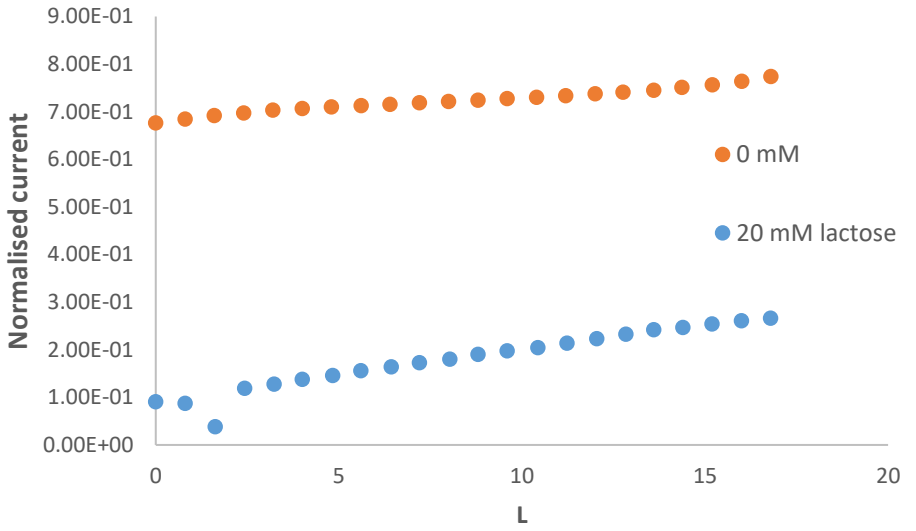

Figure 2.32: Normalised current (I_{TIP}/I_{Inf}) vs. distance (L) where L = d/a and d = distance from tip Pt ultramicroelectrode (UME) to substrate, a = tip radius 10 nm, RG = 23.8. Curves recorded above the Chit/GA-GOx+β-gal film, by translating the UME vertically (z approach curve). E_T = -0.4 V *vs.* Ag/AgCl, E_{sub} = OFF, 5 mM $K_3Fe(CN)_6$ in PB pH 6.0.

Line scan studies were performed on the glucose biosensor at different glucose concentrations (0, 20, 40 mM) in mediator (5 mM $K_3Fe(CN)_6$) to show that current detected is responsive to concentration of substrate. *Figure 2.33* shows the change in current value across the distance of the electrode (0-8000 µM). Results showed that at 0 mM glucose, no change in current was detected across the surface of the electrode as no regeneration of electroactive species occurs in the absence of substrate and the tip competes for Fe^{3+} reduction. When 20 mM glucose was added into the solution, there was a fluctuation in current as the tip crossed the enzyme modified electrode surface and increased again when the tip approached the unmodified surrounding substrate platform. There is also a difference in current value between the 20 and 40 mM glucose, indicating the higher substrate turnover.

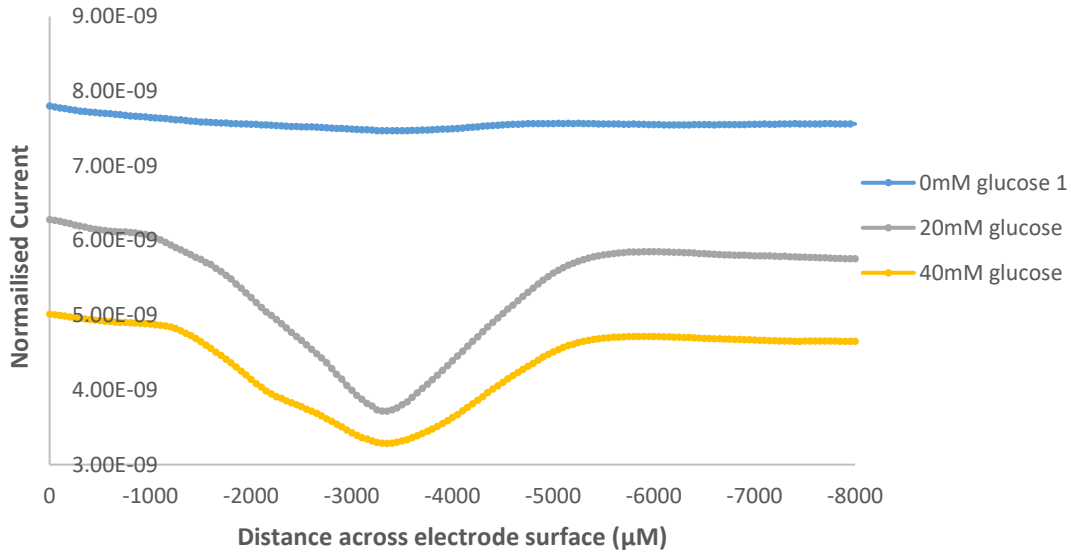

Figure 2.33: Normalised current (I_{TIP}/I_{Inf}) vs. distance (L) where L = d/a and d = distance from tip Pt ultramicroelectrode (UME) to substrate, a = tip radius 10 nm, RG = 23.8. Curves recorded above the Chit/GA-GOx film, by translating the UME vertically (z approach curve). E_T = -0.4 V *vs.* Ag/AgCl, E_{sub} = OFF, 5 mM $K_3Fe(CN)_6$ in PB pH 6.0.

Figure 2.34 shows area scan experiments at a GC/Chit/GOx/Chit/GA in the presence of 0 mM glucose (a and b) and 20 mM glucose (c and d) in 5 mM $K_3Fe(CN)_6$. The images show that in the presence of the glucose substrate, there was a decrease in current over the area where the surface is modified with GOx and the active region of the enzyme can be detected by observation of a dark blue circular feature in (c) and (d). The green and red regions show areas of relatively lower enzyme activity. The UME tip was held at a reduction potential (E_{app} = -0.4 V vs. Ag/AgCl) to reduce Fe^{3+} to Fe^{2+}. Therefore, we can highlight the region where GOx is catalytically regenerating the production of the electroactive species and the tip competes for Fe^{3+} reduction.

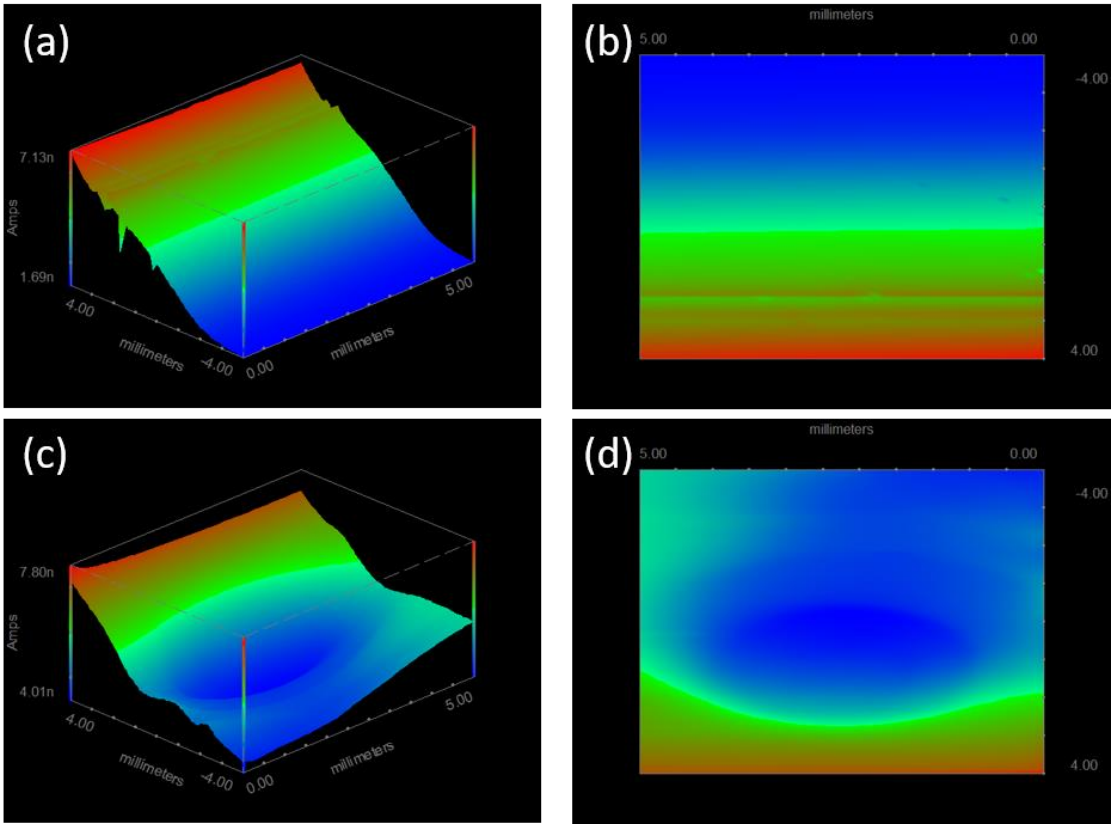

Figure 2.34: Area scan SECM experiment at E_T = -0.4 V vs.. Ag/AgCl E_{sub} = OFF, 20 mm Pt 5000 x 8000 mm^2 100 mm per point at GOx modified GCE substrate in 0 mM (a and b) 20 mM (c and d) glucose in the presence of 5 mM $K_3Fe(CN)_6$.

Figure 2.35 shows the same area scan experiment with a GC/Chit/GOxβ-gal/Chit/GA in the presence of 0 mM lactose (a and b) and 20 mM lactose (c and d) in 5 mM $K_3Fe(CN)_6$. The UME tip (E_{app} = -0.4 V vs. Ag/AgCl) competes for Fe^{3+} reduction. The surface images show that in the presence of lactose (20 mM), there was a decrease in current signal (blue) and an active area can be detected as the tip scans over the enzyme modified GCE substrate. This is due to the dual-enzyme system (GOx and β-gal) causing a regeneration and detection of Fe^{2+} as the UME tip competes for Fe^{3+} reduction.

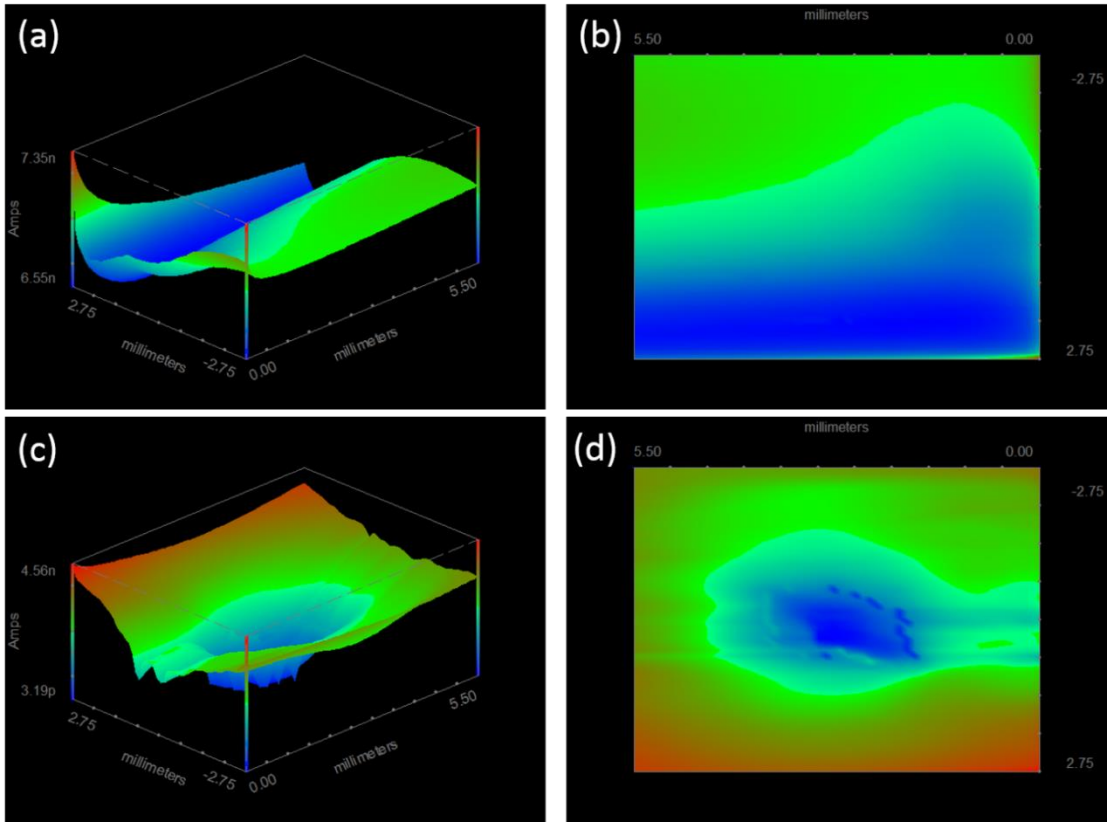

Figure 2.35: Area scan SECM experiment at E_T = -0.4 V vs.. Ag/AgCl E_{sub} = OFF, 20 mm Pt 5000 x 5500 mm^2 100 mm per point at GOx/β-gal modified GCE substrate in 0 mM (a and b) 20 mM (c and d) lactose in the presence of 5 mM $K_3Fe(CN)_6$.

2.6 Conclusion

Glucose and Lactose biosensors were fabricated using a sandwich method with Chitosan/Enzyme(s)/Chitosan/GA or PEGDE configuration. Initially, 1st generation biosensors were fabricated to assess enzyme activity in the industry required conditions i.e. room temperature at pH 6.0. Electrochemical studies were performed on the sensors to determine their suitability in detection and quantitation of glucose and lactose via CV and CC techniques. The glucose sensor modified with GA showed a linear range of 0 – 7 x 10^{-3} M with sensitivity of 3.25 x 10^{-6} C $cm^{-2}mM^{-1}$, LOD of 0.51 mM and LOQ of 1.70 mM. The lactose sensor resulted in two linear ranges of 2.47 x 10^{-3} to 4.00 x 10^{-2} M with sensitivity of 6 x 10^{-6} C $cm^{-2}mM^{-1}$ and 3.91 x 10^{-2} to 6.92 x 10^{-2} M with sensitivity of 2 x 10^{-5} C $cm^{-2}mM^{-1}$.

As the sensors were designed to assess concentration levels of analytes in samples with complex matrices, 2nd generation sensors were developed using solution phase mediation. A model mediator $K_3Fe(CN)_6$ was used to lower the operating potential (E_{app} = 0.3 V vs. Ag/AgCl) of the signal which improved sensitivity and helps eliminate issues with dairy samples that may have electroactive species present. Two enzyme cross-linking agents were investigated using the glucose biosensor in which PEGDE showed a greater linear range relative to GA. However, GA was employed going forward in relation to transfer to SPE as PEGDE was found to be unsuitable for SPE modification. CV and CC was conducted to obtain analytical data for the lactose sensor resulting in a linear range of 5.83 x 10^{-3} to 1.65 x 10^{-2} M with a sensitivity of 9.41 x10^{-4} C $cm^{-2}mM^{-1}$, LOD of 1.38 mM and LOQ of 4.59 mM.

The use of scanning electrochemical microscopy (SECM redox competition mode) provided surface topographical and imaging/enzyme reactivity information respectively. Approach curves and line scans confirmed the enzymatic catalytic response in the presence and absence of substrate using $K_3Fe(CN)_6$. Area scans were used to identify the enzyme active region of glucose and lactose biosensors in the absence and presence of substrate.

2.7 Bibliography

1. Mukhopadhyay SC, Gooneratne CP, Sen Gupta G, Demidenko SN. A low-cost sensing system for quality monitoring of dairy products. *IEEE Trans Instrum Meas*. 2006;55(4):1331-1338. doi:10.1109/TIM.2006.876541
2. Karunakaran C, Madasamy T, Sethy NK. Enzymatic Biosensors. *Biosens Bioelectron*. 2015;32:133204. doi:10.1016/B978-0-12-803100-1.00003-7
3. Sassolas A, Blum LJ, Leca-Bouvier BD. Immobilization strategies to develop enzymatic biosensors. *Biotechnol Adv*. 2012;30(3):489-511. doi:10.1016/j.biotechadv.2011.09.003
4. Vasylieva N, Barnych B, Meiller A, Maucler C, Pollegioni L, Lin JS, Barbier D, Marinesco S. Covalent enzyme immobilization by poly(ethylene glycol) diglycidyl ether (PEGDE) for microelectrode biosensor preparation. *Biosens Bioelectron*. 2011;26(10):3993-4000. doi:10.1016/j.bios.2011.03.012
5. Kučerová P, Komenská P, Tomková H, Skopalová J, Barták P. Determination of lactose in milk products: a comparison of three-enzyme amperometric biosensor and gas chromatography/tandem mass spectrometry. *Monatshefte fur Chemie*. 2017;148(3):517-524. doi:10.1007/s00706-016-1903-7
6. Hui Y, Nan L, Jing-Zhong X, Jun-Jie Z. A Glucose Biosensor Based on Immobilization of Glucose Oxidase in Chitosan Network Matrix. *Chinese J Chem*. 2000;23(3):275-279. doi:10.1002/cjoc.200590275
7. Uwimbabazi E, Mukasekuru MR, Sun X. Glucose Biosensor Based on a Glassy Carbon Electrode Modified with Multi-Walled Carbon Nanotubes-Chitosan for the Determination of Beef Freshness. *Food Anal Methods*. 2017;10(8):2667-2676. doi:10.1007/s12161-017-0793-6
8. Andreas Öchsner, Lucas F. M. da Silva HA. *Design and Analysis of Materials and Engineering Structures*.; 2013. doi:10.1007/978-3-642-20940-6
9. Ã-ztop HN, Saraydin D, Cetinus Ş. pH-sensitive chitosan films for baker's yeast immobilization. *Appl Biochem Biotechnol - Part A Enzym Eng Biotechnol*. 2002;101(3):239-249. doi:10.1385/ABAB:101:3:239
10. Miao Y, Tan SN. Amperometric hydrogen peroxide biosensor based on immobilization of peroxidase in chitosan matrix crosslinked with glutaraldehyde. *Analyst*. 2000;125(9):1591-1594. doi:10.1039/b003483p

11. Wang J. Electrochemical glucose biosensors. *Electrochem Sensors, Biosens their Biomed Appl*. 2008:57-69. doi:10.1016/B978-012373738-0.50005-2
12. Loew N, Tsugawa W, Nagae D, Kojima K, Sode K. Mediator preference of two different FAD-dependent glucose dehydrogenases employed in disposable enzyme glucose sensors. *Sensors (Switzerland)*. 2017;17(11). doi:10.3390/s17112636
13. Sun R, Wang L, Yu H, Abdin Z, Yongsheng C, Jin H, Rongbai T. Molecular recognition and sensing based on ferrocene derivatives and ferrocene-based polymers. *Organometallics*. 2014;33(18):4560-4573. doi:10.1021/om5000453
14. Arslan F, Beskan U. An amperometric biosensor for glucose detection from glucose oxidase immobilized in polyaniline-polyvinylsulfonate-potassium ferricyanide film. *Artif Cells, Nanomedicine Biotechnol*. 2014;42(4):284-288. doi:10.3109/21691401.2013.812650
15. Morkvenaite-Vilkonciene I, Ramanaviciene A, Genys P, Ramanavicius A. Evaluation of Enzymatic Kinetics of GOx-based Electrodes by Scanning Electrochemical Microscopy at Redox Competition Mode. *Electroanalysis*. 2017;29(6):1532-1542. doi:10.1002/elan.201700022
16. Eggins, Brian R. *Chemical Sensors and Biosensors.* Chichester: Wiley, 2006.
17. E. B. Roche. *Textbook of Biochemistry with Clinical Correlations*. Devlin TM, ed., 2005.
18. Dekker M. *Laboratory Techniques in Electroanalytical Chemistry*. Kissinger, Peter. T. ; Heineman WR, ed.; 1996.
19. Horwood E. *Instrumental Methods in Electrochemistry*. (Kemp TJ, ed.). Ellis Horwood Limited; 1985.
20. Ammam M, Fransaer J. Two-enzyme lactose biosensor based on β-galactosidase and glucose oxidase deposited by AC-electrophoresis: Characteristics and performance for lactose determination in milk. *Sensors Actuators, B Chem*. 2010;148(2):583-589. doi:10.1016/j.snb.2010.05.027
21. Tkáč, J., Šturdík, E. and Gemeiner, P. (2000). Novel glucose non-interference biosensor for lactose detection based on galactose oxidase–peroxidase with and without co-immobilised β-galactosidase. *The Analyst*, 125(7), pp.1285-1289.

Chapter 3 : Enzymatic polymerisation of 1,10-Phenanthroline-5,6-dione as a redox mediator for lactate sensing

3.1 Introduction

Lactic acid detection and quantitation is important in various areas of healthcare and sports nutrition.[1] It is normally measured in serum samples for diagnosis and medical management of a wide range of different medical issues including hyperlactatemia, sepsis, lactic acidosis and hypoxia-induced cancer.[2] Many lactic acid biosensors have been previously designed for serum sample analysis to enable rapid diagnosis of medical issues. Use of enzymatic biosensors for clinical diagnosis are favourable due to their low cost, specificity and sensitivity. Generally, they are based on lactate oxidase (LOx) or lactate dehydrogenase (LDH) immobilisation on a transducer surface.[3] [4] The focus of this work is based on lactic acid sensing in the dairy industry where the measurement of lactic acid is important for quality testing of different products including milk, yoghurt, cheese, low-lactose products and whey products. Other areas of lactic acid analysis include monitoring of fermentation processes used for the production of polylactic acid (PLA).[5] Usually, sample analysis relies on time-consuming HPLC techniques. However, the use of lactic acid biosensors could solve this issue by promoting rapid analysis of samples with on-site testing.

3.1.1 Mediated approaches to lactate sensing

A bienzyme amperometric graphite-Teflon composite biosensor was used for lactic acid quantitation in cow milk, goat milk and whey protein concentrates (WPC).[6] This 2nd generation sensor combined the use of ferrocene as a mediator with enzymes horse-radish peroxidase (HRP) and L-lactate oxidase (L-LOD). Results were compared with colorimetric enzymatic assays in which the sensor demonstrated the ability to distinguish between WPC supplemented and non-supplemented yoghurt, which was not possible with the colorimetric assay. Therefore, the sensor was advantageous relative to alternative approaches used in lactic acid monitoring. The majority of biosensors used in dairy monitoring tend to be mediated systems due to the benefits when working with samples that contain a complex matrix e.g. fermentation samples.

Electron transfer mediators include ortho-quinoidal compounds which have been of interest in electrochemical biosensors due to their chemical stability, electrochemical reversibility, ideal equilibrium potential and their high reactivity towards redox-active enzymes.[7] In the case of GOx sensors, quinones are reduced by a two-electron (hydride) transfer reaction involving an electron transfer mechanism that is governed by electron-accepting forces of the compounds without hindering their chemical

properties.[7] Ortho-quinoidal compounds are favourable for GOx mediated systems due to the high self-exchange rate constants of quinones combined with their high rate of cross reaction with the reduced form of GOx and the electrode surface.[7] [8]

3.1.2 The use of Phenanthrolines as mediators in enzyme electrodes

1,10-Phenanthroline is the primary compound of a class of chelating agents which together form a large number of chemical compounds with different metal complexes. These complexes have previously been studied for their ability to act as redox indicators for quantitative analysis given their high redox potential.[14] Studies have shown how these PD compounds can be used as redox mediators for oxidases and can enable fabrication of reagent-less biosensors when electrodeposited or polymerised onto a transducer surface.[14]

This work focuses on 1,10-Phenanthroline-5,6-dione (PD) and its ability to act as a redox mediator in lactate biosensing. PD (*Figure 3.1*) is a versatile ortho-quinoidal compound that contains two diiminic nitrogen atoms that allow metal ion binding and the *o*-quinoid part of the molecule that is responsible for redox activity. [9] [10]

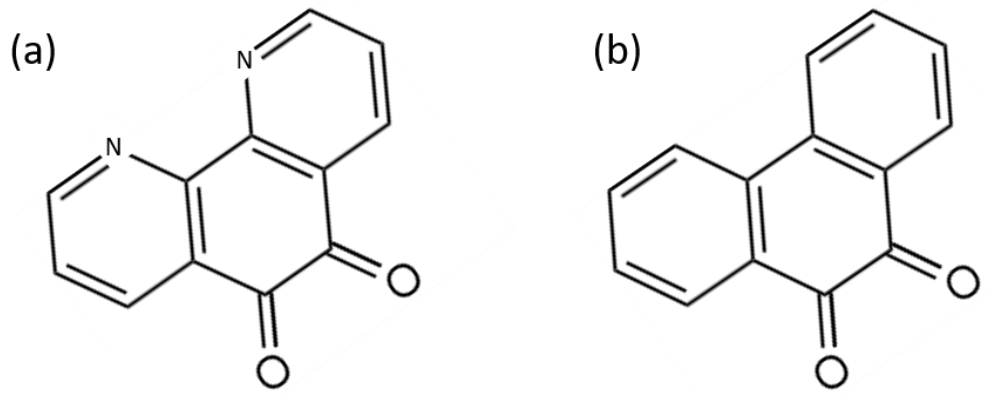

Figure 3.1 Chemical structures of (a) 1,10-Phenanthroline-5,6-dione and (b) 9,10-Phenanthrenequinone

PD along with another ortho-quinoidal compound 9,10-Phenanthrenequinone (PQ) were used in a study to investigate their use as mediators in amperometric graphite rod electrodes modified with GOx.[7] The two electrodes were prepared by depositing 3 µL of either PD or PQ onto the surface of a graphite rod electrode three times before enzyme modification with GOx. The enzyme mediated catalytic reaction for glucose

can be described in *equations 3.1-3.3* below.[7 8] During the reaction, quinone is reduced to hydroquinone in the presence of the reduced enzyme GOx and is reoxidised by the heterogeneous electrode reaction (*Scheme 3.1*). This results in an electrochemical signal which is proportional to the concentration of the analyte and in the case of the work by Zor *et al.* 2014, glucose in the sample. [7]

$$\text{Glucose} + GOx_{(FAD)} \rightarrow \text{Gluconolactone} + GOx_{(FADH_2)} \quad \text{.....(3.1)}$$

$$GOx_{(FADH_2)} + PD_{(OX)} \rightarrow GOx_{(FAD)} + H_2PD_{(RED)} \quad \text{.....(3.2)}$$

$$H_2PD_{(RED)} \rightarrow PD_{(OX)} + 2e^- + 2H^+ \quad \text{.....(3.3)}$$

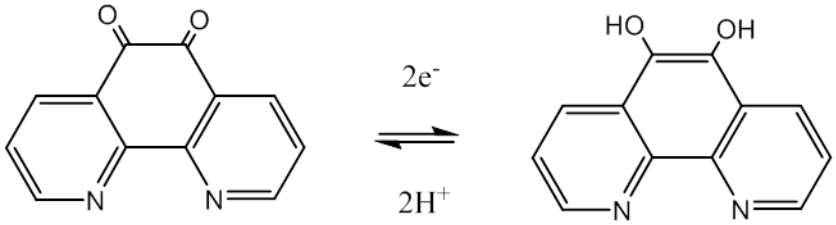

Scheme 3.1 Redox states of 1,10-Phenanthroline,5,6-dione.

Results of the two mediated sensors showed that PD is a more efficient mediator for use in biosensors compared to PQ with current response seven times higher than that of the PQ-modified sensor. It is suggested this may be due to the presence of azomethane moieties on the PD structure which can enable higher electron (hydride)-accepting potency and therefore faster electron transfer rate.[7]

The reactivity of both mediators was also assessed using a model "single electron transfer FAD-dependant enzyme", $NADP^+$ ferredoxin reductase, which showed that PD had a higher reactivity than PQ. [7] Investigations have also been performed that involve the use of Osmium Phenanthroline compounds such as Os (4,4'-dimethyl, 2,2'-bipyridine)$_2$(1,10-Phenanthroline-5,6-dione) in the development of reagentless dehydrogenase carbon paste amperometric electrodes for glucose detection, where the alternative enzyme GDH was used. [11]

3.1.3 Enzymatic polymerisation of redox active species for mediated sensing

Recent studies have shown how PD can be used for the development of thin-film glucose biosensors [8 7 12], via enzymatically synthesised poly(1,10-Phenanthroline-5,6-dione) (pPD) in the presence of the enzyme, GOx. [12] This technique allowed the

encapsulation of the GOx enzyme within a polymer film that was formed during the production of H_2O_2 (*Scheme 3.2*). Here, the ability of GOx to form H_2O_2 was exploited in order to form the pPD film, as depicted in *Scheme 3.3*. [12] The pPD/GOx/GR was prepared by submerging a GOx-modified graphite rod electrode in a buffer solution containing both the enzyme substrate, glucose (25 mM), and the mediator, PD (5 mM) for 24 hrs at 4 °C.

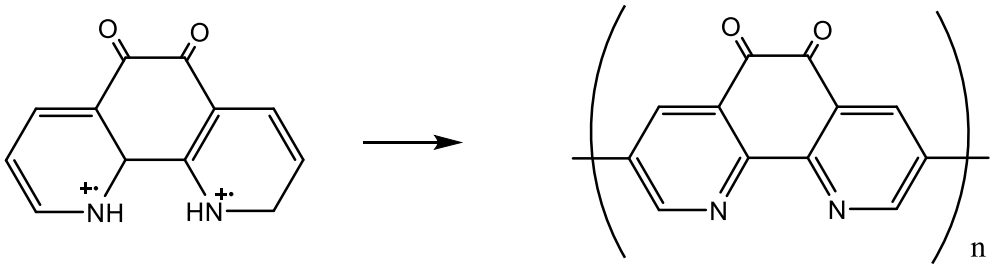

Scheme 3.2: Proposed polymerisation of poly(1,10-Phenanthroline-5,6-dione) in presence of oxidant H_2O_2.

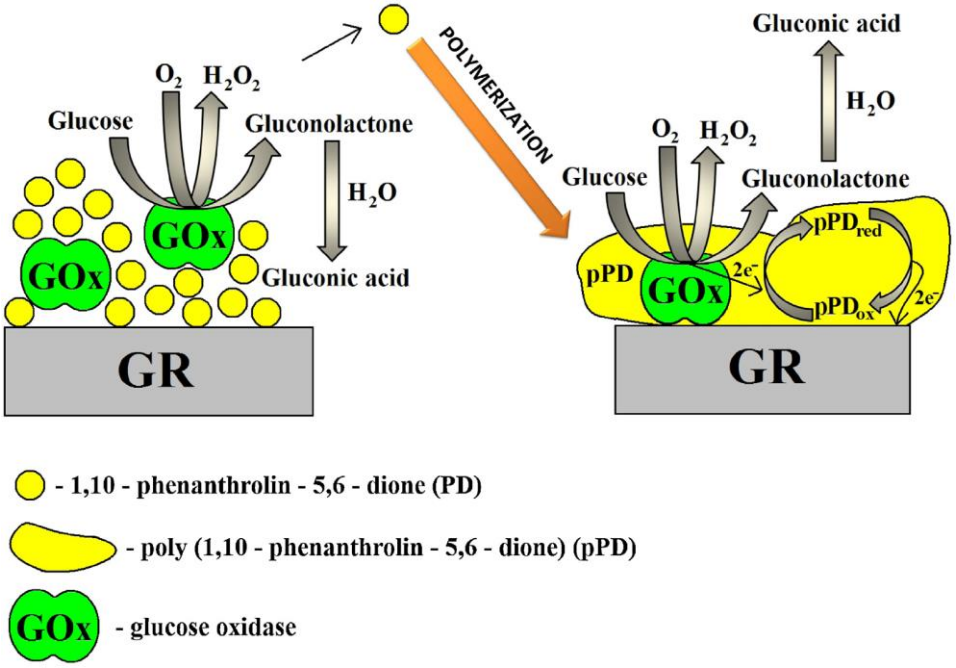

Scheme 3.3 Formation of enzymatically synthesised poly(1,10-Phenanthroline-5,6-dione)[12]

The advantages in the use of redox polymers for second generation sensing include their ease of preparation, chemical stability and their biocompatibility with proteins e.g. enzymes. GOx and LOx, which was used in this study, has the ability to generate H_2O_2 during catalysis of its substrate. This initiates polymer synthesis which causes a biocompatible "shell" to form over the now embedded enzyme which in turn, decreases the diffusion rate of the enzyme reaction. [12]

3.1.4 Use of graphite ink modifiers as underlying layers in sensor design

Previous studies involving biocompatible enzymatic-inks were used for direct detection of glucose [13], and exploited graphite inks to enable "on-demand" and "on-site" fabrication of enzymatic sensors that could cater to specific needs of the user. Using the graphite ink, enzymatic roller pens were designed which demonstrated good reproducibility and the ability to draw bio-catalytic conducting traces on a wide range of surfaces. Therefore, it can be introduced into new alternative biosensor applications.

3.2 Chapter aims

The research presented in this chapter involves a combination of conducting biocompatible ink layers coupled with PD electrodeposition, enhanced by enzymatic polymerisation. The advantages of this approach are the incorporation of both the desired enzyme (LOx) and mediator (pPD) onto the electrode which avoids the use of solution mediated approaches. To date, there has been no evidence of the use of PD in lactate sensor development or for use in fermentation monitoring. Therefore, we propose enzymatic synthesis of pPD as a redox active film for development of a lactate biosensor with quantitation of lactic acid in a dairy fermentation process. The main objectives are outlined below.

- Development of direct and solution mediated lactate sensors based on LOx detection using 5 mM $K_3Fe(CN)_6$;
- Design and optimisation of a mediated lactate biosensor based on 1,10-Phenanthroline-5,6-dione film formation;
- Comparison studies of poly(1,10-Phenanthroline-5,6-dione) films with and without an underlying graphite ink layer;
- Detection and determination of lactate concentration in a diluted fermentation sample.

3.3 Experimental

3.3.1 Materials

Poly (ethylene glycol), Chitosan, Xylitol, 1,10-Phenanthroline 5,6-dione, potassium phosphate dibasic anhydrous, potassium dihydrogen phosphate, Lactate Oxidase from Aerococcus viridans, Poly (ethylene glycol) diglycidyl ether, Bovine serum albumin, graphite powder and Sodium L-lactate standard were all purchased from Sigma Aldrich. Acetic acid was purchased from AppliChem Panreac, an ITW company.

3.3.2 Instrumentation

All electrochemical techniques were carried out on a Solartron 1285 potentiostat with electrochemical software CorrWare and CorrView for data analysis. A three-electrode cell utilised Pt wire as counter electrode, a Ag/AgCl reference electrode (stored in 3 M KCl) and either platinum, glassy carbon or screen printed carbon electrode as working electrode. Macro electrodes were polished using 1 μm MetaDi Monocrystalline Diamond suspension followed by rinsing in deionised water and sonication to remove any residual polishing agent. A reflectance microscope with digital CCD Olympus software was used for surface imaging at modified carbon screen printed electrodes and Scanning Electron Microscopy with Energy Dispersive X Ray spectroscopy was performed on a Hitachi with Au/Pd sputter coater.

3.4 Procedures

3.4.1 Preparation of graphite ink

The preparation of graphite ink solution (GInk) was adapted from that described by Bandodkar *et al*.[13] The binders PEG (60 % in dH_2O) and chitosan (1 % in 0.1 M acetic acid) were mixed in a 2:1 ratio in the presence of the stabiliser xylitol (2 M in dH_2O), followed by addition of graphite powder to give 40 % w/v. The so-prepared ink was stirred for 10 minutes before sonication for 30 minutes (to ensure dispersion) and stored at 4 ^{o}C. The ink underwent both surface (reflectance microscopy and SEM/EDX) and electrochemical characterisation.

3.4.2 Preparation of LOx electrode at Pt and GC electrodes

Electrodes were prepared based on the method described in Chapter 2 (see *section 2.4.1*). A four-layer reagent system consisting of (a) 5 μL of a 0.5 % chitosan in 0.8 % acetic acid (b) 5 μL of enzyme mixture (4 U LOx for lactate detection in the presence

of 0.5 mg/mL BSA in 0.02 M PB (pH 6.0)) (c) Repeat step (a) (d) 5 µL of 0.05 % GA (in the case of direct and solution mediated electrodes) or 1.5 % PEGDE (in the case of GC or SPE for PD modification). Each layer was allowed to dry at room temperature between modification steps. Electrodes used in are labelled Pt/Chit/LOx/Chit/GA and GC/Chit/LOx/Chit/GA.

GInk modified electrodes involved drop casting 1 µL of GInk onto the GCE surface which was allowed to dry at room temperature for 10 minutes. This was followed by LOx immobilisation by additions as described above with step (d) 1.5 % PEGDE. Electrodes are referred to as GCE/LOx or GCE/GInk/LOx.

3.4.3 Lactate response at modified Pt and GC electrodes using direct and solution phase mediation

Response of lactate (0.99 and 1.96 mM) at a modified Pt electrode (Pt/Chit/LOx/Chit/GA) was measured via CV over potential range -0.3 V to 1.0 V vs. Ag/AgCl at 100 mVs^{-1}. CC was performed with E_{app} = 0.8 V vs. Ag/AgCl for 5 s.

Solution phase mediated sensing was performed via CV at modified GC electrodes (GC/Chit/LOx/Chit/GA) with Lactate (0-7 mM) in the presence of 5 mM $K_3Fe(CN)_6$ over the potential range -0.5 V to 0.7 V vs. Ag/AgCl at 20 mVs^{-1}. Lactate calibration (0-12 mM) was carried out via chronocoulometric analysis with E_{app} = 0.38 V vs. Ag/AgCl for 5 s.

3.4.4 Poly(1,10-Phenanthroline-5,6-dione) film formation at LOx modified GCE

Four methods described below, are employed as part of the optimisation process for effective deposition of PD film on enzyme modified electrodes.

<u>Method A:</u> Electrodeposition by cycling

CV was performed in a solution of PD (5 mM) at a GCE/LOx over the potential range -0.8 V to 0.8 V vs. Ag/AgCl at 100 mVs^{-1} for 30 cycles. The electrode was rinsed with deionised H_2O and allowed to air dry at room temperature. Stability cycling was performed by cycling 0.1 M PB (pH 6.0) at GCE/LOx/pPD for 20 cycles with potential range -0.8 V to 0.8 V vs. Ag/AgCl at 100 mVs^{-1}.

Method B: Enzymatic polymerisation

(**B1**) GCE/LOx electrode was incubated in a solution of PD (5 mM) and 20 mM lactate overnight (18 hrs) at 4 ºC. (Stabilisation of the film followed as per method A).

(**B2**) CV was performed in PD (5 mM) in the presence of lactate (10 mM) at GCE/LOx electrode for 20 cycles. Potential range -0.8 V to 0.8 V vs. Ag/AgCl at 100 mVs^{-1}. (Stabilisation followed as per method A).

(**B3**) Polymerisation of PD involved sequential additions of lactate during potential cycling in the presence of PD (5 mM) and lactate additions (1-4 mM) at GCE/LOx electrode over the potential range -0.8 V to 0.8 V vs. Ag/AgCl at 20 mVs^{-1}. Stabilisation of the film was performed by cycling the electrode in 0.1 M PB (pH 4.0) and (pH 6.0) over the potential range -0.8 V to 0.8 V vs. Ag/AgCl at 100 mVs^{-1}.

All electrodes modified with pPD film (*see Scheme 3.4*) will be labelled GCE/LOx/pPD or GCE/GInk/LOx/pPD.

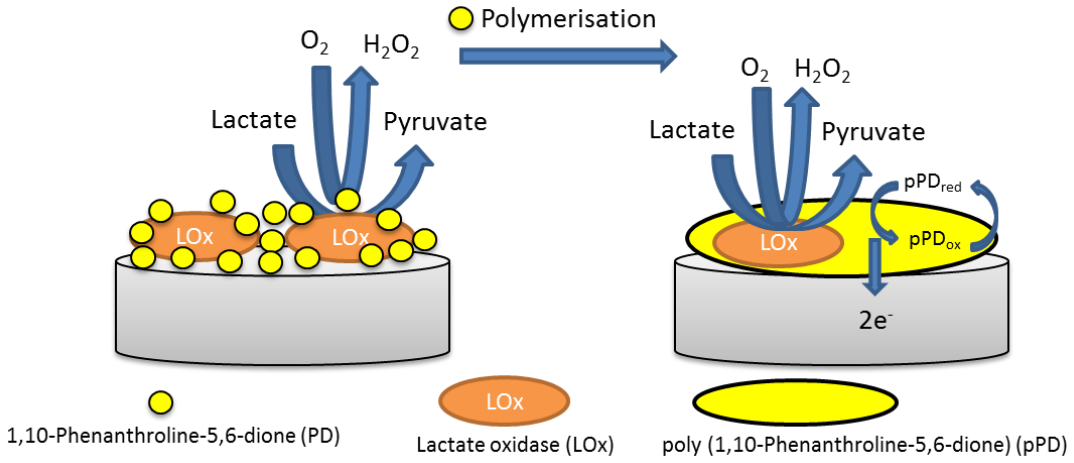

Scheme 3.4: Enzymatic polymerisation of pPD on surface of LOx modified electrode in the presence of substrate.

3.4.5 Optimum method for preparation of poly (1,10-Phenanthroline-5,6-dione) films on enzyme modified GC electrodes

Method B3 resulted in films with greatest stability and highest surface coverage. The details of the optimal procedure is shown below in the presence and absence of a graphite ink underlying layer.

A background CV of the GCE/GInk/LOx or GCE/LOx electrodes in 0.1 M PB (pH

6.0) was performed over the potential range -0.7 V to 0.7 V vs. Ag/AgCl at 100 mVs^{-1}. 5 mM PD (in 0.1 M PB (pH 6.0)) was prepared by sonication (5 minutes). PD deposition via enzymatic polymerisation was performed at modified electrodes (GCE/GInk/LOx or GCE/LOx) at 20 mVs^{-1} over the potential range -0.7 V to 0.7 V vs. Ag/AgCl. Lactate additions followed (0 – 4.76 mM) with CV recorded (under the same conditions) between each addition until a final concentration of 4.76 mM lactate. The electrode was rinsed with 0.1 M PB and returned to blank electrolyte for electrochemical analysis and film studies. Electrodes are labelled as either GCE/GInk/LOx/pPD or GCE/LOx/pPD.

3.4.6 Electrochemical film studies of poly(1,10-Phenanthroline-5,6-dione)

Film stability studies involved cycling 0.1 M PB (pH 6.0) at modified electrodes (bare and GInk) for 20 cycles at 100 mVs^{-1}. Scan rate studies were performed over the relevant ranges in the same electrolyte.

3.4.7 Detection of L-lactate at poly(1,10-Phenanthroline-5,6-dione) modified graphite ink electrodes and fermentation sample analysis

The response to lactate (1.96 mM) at GCE/GInk/LOx/pPD electrode was examined using CV at 100 mVs^{-1} over the range -0.7 V to 0.7 V vs. Ag/AgCl. CC analysis was performed at (E_{app} = -0.12 V or 0.12 V vs. Ag/AgCl) to enable monitoring of the lactate response at cathodic/anodic pPD redox couple signals respectively.

Lactate quantitation was performed in a fermentation sample (1 % v/v in 0.1 M PB (pH 6.0)) by CV at the GCE/GInk/LOx/pPD electrodes followed by spiking with 1.96 mM L-lactate.

CC analysis of the sample was performed using the standard addition method. A background charge vs. time plot was firstly recorded in 0.1 M PB (pH 6.0) followed by measurement in diluted fermentation media (1 % v/v) after which the sample was spiked with lactate over the range 0.24 – 1.23 mM with stirring (10 s) following each addition with a total measurement interval of 40 s.

3.5 Results and Discussion

3.5.1 Electrochemical analysis of Lactate Biosensor

Two lactate biosensors were fabricated using the four-layer sandwich method (see *Section 3.4.2*) for direct and solution mediated sensing. The lactate biosensor was analysed for its ability to detect and quantify lactate via H_2O_2 detection (1st generation = Pt/Chit/LOx/Chit/GA) and in the presence of a mediator (5 mM $K_3Fe(CN)_6$) (2nd generation = GCE/Chit/LOx/Chit/GA). Electrochemical analysis was carried out via CV and CC.

3.5.1.1 Direct lactate response at modified Pt electrode

Figure 3.2 shows a CV of 0.1 M PB and sodium L-lactate standard (0.99 and 1.98 mM) at Pt/Chit/LOx/Chit/GA (LOx = 1 U). An increase in the oxidation peak current at ~ 0.6 V, indicates the production of H_2O_2 from the catalytic breakdown of lactate. The optimum enzyme activity unit was investigated by modifying a series of Pt electrodes with LOx (2-10 U) and performing CC analysis with E_{app} = 0.8 V vs. Ag/AgCl for 5 s. *Figure 3.3* shows the data plot of charge at 0.8 V vs. lactate concentration, with 4 U showing the greatest response to lactate at the modified electrode.

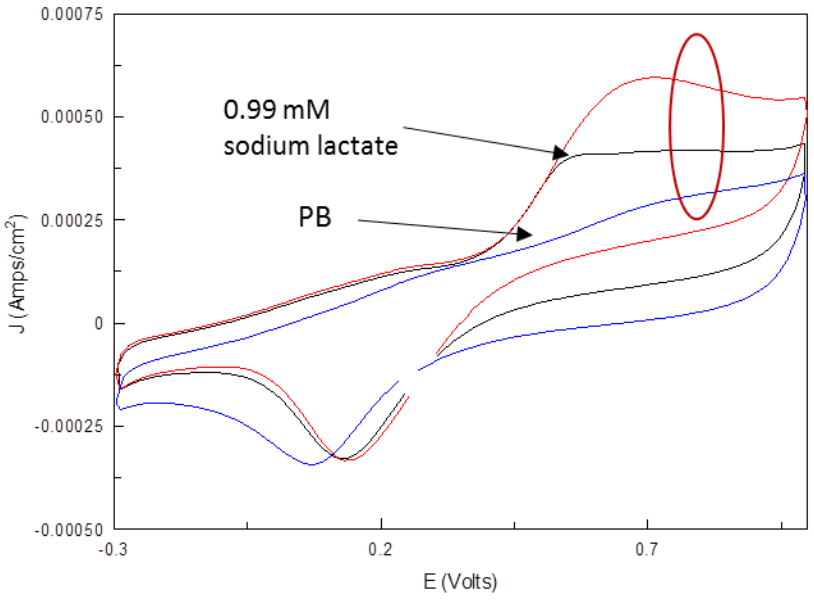

Figure 3.2: CV of background electrolyte (0.1 M PB (pH 6.0)) and lactate (0.99 mM and 1.98 mM) at Pt/Chit/LOx/Chit/GA with potential range -0.3 V to 1.0 V vs. Ag/AgCl at 100 mVs^{-1}.

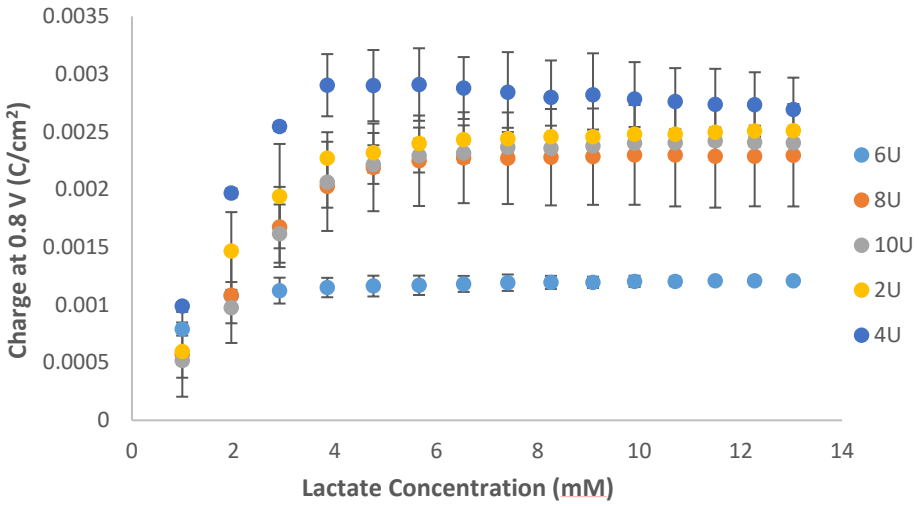

Figure 3.3: CC data of Charge (C/cm^2) vs. lactate concentration (mM) at Pt/Chit/LOx/Chit/GA for (2-10) Units LOx optimisation study (n=3).

Following this, a 4 U LOx electrode (Pt/Chit/LOx/Chit/GA) was calibrated using CC with E_{app} = 0.8 V vs. Ag/AgCl for 5 s. *Figure 3.4* shows the CC response to lactate (0-4 mM) at the modified Pt electrode with an increase in charge as the concentration of the substrate increased, confirming the direct relationship between substrate concentration and charge during the production of H_2O_2.

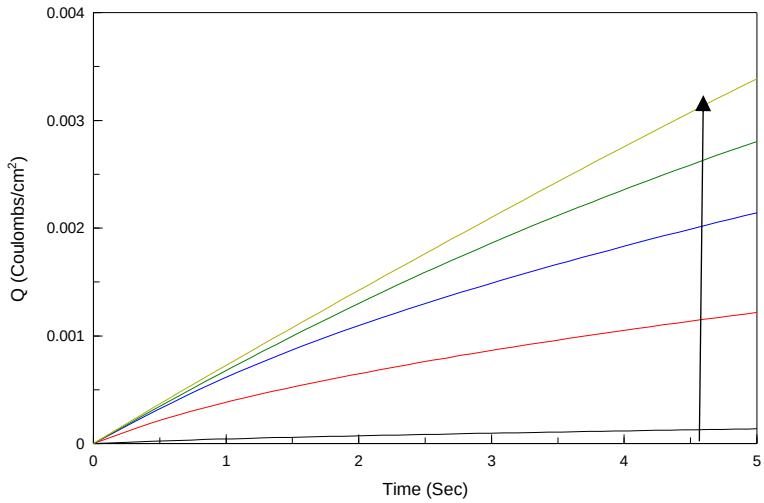

Figure 3.4: Charge vs. Time data for 0-4 mM lactate response at a Pt/Chit/LOx/Chit/GA electrode. The optimum (4 U) LOx activity was utilised.

Results obtained from CC analysis were used to evaluate the analytical data resulting in a linear range of 9.9 x 10^{-4} to 3.96 x 10^{-3} M, sensitivity of 6.64 x 10^{-4} C cm^{-2}mM^{-1}, LOD of 0.43 mM and LOQ of 1.44 mM, as shown in *Table 3.1*. These results can be

compared to a LOx biosensor developed by Cunha-Silva *et al.* where LOx (0.25 U) was immobilised on a Pt electrode with a linear range of 0.75 µM – 1 mM, sensitivity of 14.65 μAmM^{-1} and LOD of 0.75 µM.[1] Here, the difference in analytical data may be due to their enzyme activity unit difference, with Cunha-Silva *et al.* reporting the use of a lower amount of enzyme, 0.25 U, which would result in lower linear range values and sensitivity of the biosensor. The application of this work requires a broader linear range and therefore, higher enzyme activities are required.

Table 3.1: Analytical data for 1st generation lactate biosensor.

Analytical Data for 1st generation Lactate Biosensor (4 U)			
Linear Range (M)	**Sensitivity (C $cm^{-2}mM^{-1}$)**	**LOD (mM)**	**LOQ (mM)**
$9.9 \times 10^{-4} - 3.96 \times 10^{-3}$	6.64×10^{-4}	0.43	1.44

3.5.1.2 Lactate response at LOx modified GCE electrodes solution mediated approach

A 2nd generation lactate biosensor was developed (see *Section 2.4.1.*) with GCE/Chit/LOx/Chit/GA in the presence of 5 mM $K_3Fe(CN)_6$. *Figure 3.5* shows a CV of lactate (0-7 mM), resulting in a linear increase in response evident at 0.3 V vs. Ag/AgCl. Further electrochemical analysis was carried out via CC with E_{app} = 0.3 V vs. Ag/AgCl for 5 s.

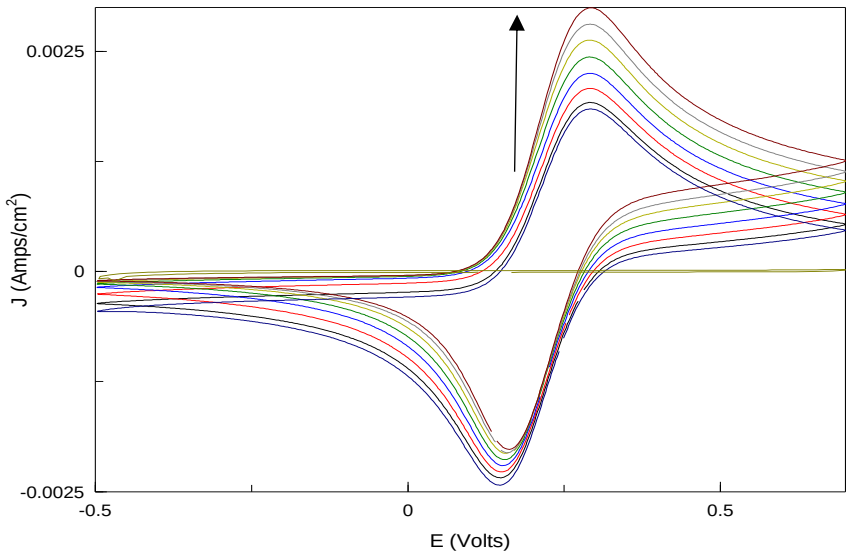

Figure 3.5: CV of 0-7 mM Lactate concentrations at a GC/Chit/LOx/Chit/GA electrode in the presence of 5 mM $K_3Fe(CN)_6$ with potential range -0.5 V - 0.7 V vs. Ag/AgCl at 20 mVs^{-1}.

Figure 3.6(a) shows CC data of increasing charge at a GCE/Chit/LOx/Chit/GA with increasing lactate (0-12 mM). *Figure 3.6(b)* shows corresponding calibration curve of the chronocoulometric analysis giving a linear range of 0.99 - 6 mM, a sensitivity of 1.44 x 10^{-3} C $cm^{-2}mM^{-1}$, LOD of 1.19 mM and LOQ of 3.97 mM as depicted in *Table 3.2* below. As previously described in Chapter 2, there is an initial lag in sensor response to lactate additions which may be due to oxygen interference.

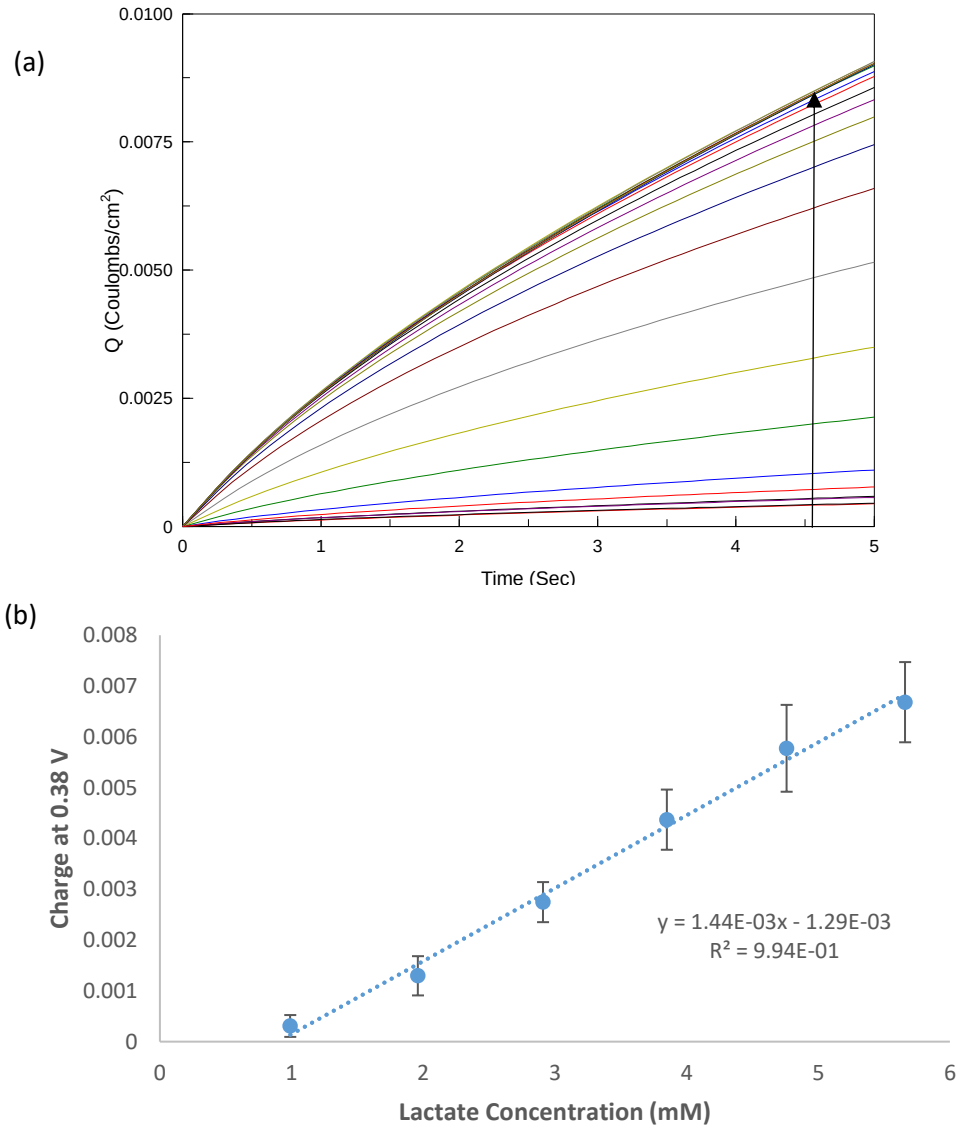

Figure 3.6: (a) Overlay of CC data 0-12 mM Lactate concentrations at a GC/Chit/LOx/Chit/GA electrode in the presence of 5 mM $K_3Fe(CN)_6$ (E_{app} = 0.38 V vs. Ag/AgCl for 5 s). (b) Corresponding data plot of charge vs. concentration (0.99 - 6 mM Lactate) in 5 mM $K_3Fe(CN)_6$ (n=3).

Table 3.2: Analytical data for 2nd generation Lactate biosensor.

Analytical Data for 2nd generation Lactate Biosensor			
Linear Range (M)	**Sensitivity (C $cm^{-2}mM^{-1}$)**	**LOD (mM)**	**LOQ (mM)**
$9.9 \times 10^{-4} - 5.66 \times 10^{-3}$	1.44×10^{-3}	0.54	1.81

3.5.2 Electrochemical growth and characterisation of 1,10-Phenanthroline-5,6-dione film on GCE/LOx

The use of PD was investigated for its use as an electron transfer mediator in lactate biosensing. Electrodes were prepared using a layer by layer system of chitosan/LOx/chitosan/PEGDE (as per *Section 2.4.1*) and will be referred to as GCE/LOx or GCE/LOx/pPD after electrochemical polymerisation of the mediator on the surface of the modified electrode. Electrodeposition of PD was performed using four different methods labelled A, B, C and D, described in *Table 3.3* below.

Table 3.3: Methods of electrode modification with PD:

A	Electrodeposition	Growth by potential cycling in 5 mM PD at GCE/LOx at 100 mVs^{-1}
B1	Enzymatic polymerisation	Overnight incubation of GCE/LOx in 5 mM PD and 20 mM lactate (aerobic and anaerobic)
B2		CV in 5 mM PD in the presence of 10 mM lactate at GCE/LOx (20 cycles)
B3		Growth by sequential lactate additions (0-4 mM) via CV at 20 mVs^{-1} at GCE/LOx

This was carried out to determine the optimum procedure for polymerisation of PD onto the surface of the enzymatic electrode. Following this process, various aspects of the pPD film were studied including the stability, surface coverage and the ability of the pPD to act as a mediator in lactate sensing.

3.5.2.1 Method A

Figure 3.7 shows the first and last (30^{th} cycle) of 5 mM PD at the modified electrode, where a large reduction peak for *Cycle 1* was evident which decreased after further cycling of the compound at the electrode. Film stability studies were performed by

cycling the electrode in PB for 20 cycles, as shown in *Figure 3.8*. Minimal reduction in peak size between cycle 1 and 20 was evident with 0.99 % reduction in the oxidation peak and 0.08 % decrease in the reduction peak *(Table 3.4)* confirming that a stable film had formed.

Figure 3.9 shows a scan rate study performed over the range -0.7 V to 0.7 V vs. Ag/AgCl at scan rates (2-500 mVs^{-1}). *Figure 3.10(a)* shows the corresponding relationship between I_p and scan rate with linearity evident up to 75 mVs^{-1}. The linearity of the I_p vs. $\sqrt{v}$ plot *(Figure 3.10(b))* indicating that the film exhibited semi-infinite diffusion behaviour with diffusion of charge compensating ions controlling the current.[16] The surface coverage was calculated to be $1.28x10^{-9}$ mol/cm^3, as shown in *Table 3.4*. However, this method of deposition was not used for further analysis as other techniques resulted in a higher surface coverage of the pPD film.

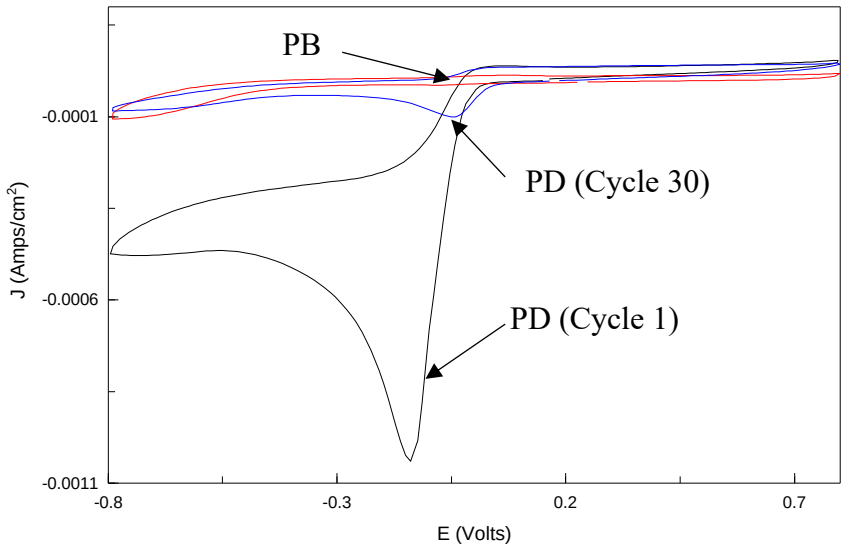

Figure 3.7: Electrodeposition of PD (in 0.1 M PB (pH 6.0) (Cycle 1 and Cycle 30) at a GCE/LOx/PEGDE electrode. Potential range -0.8 V vs. 0.8 V vs. Ag/AgCl at 100 mVs^{-1}.

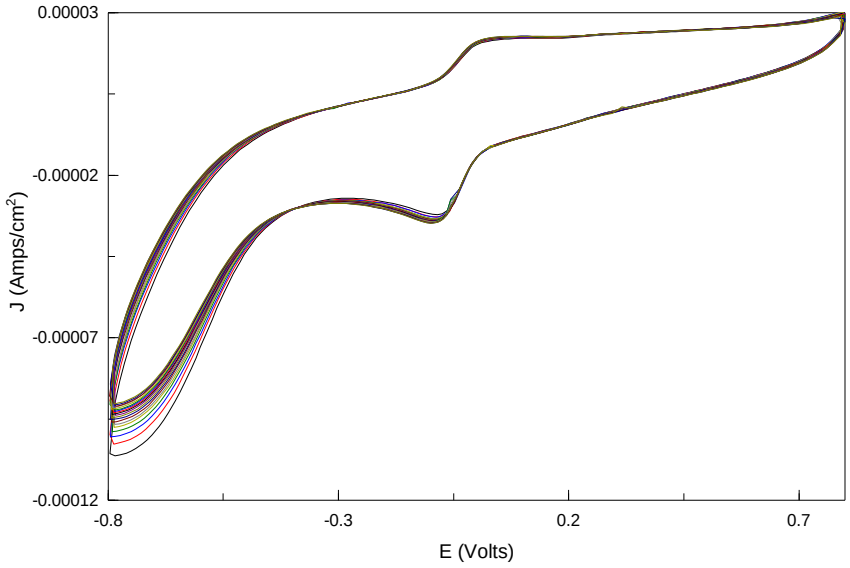

Figure 3.8: Film stability showing background electrolyte at a GCE/LOx electrode after PD electrodeposition. Potential range -0.8 V to 0.8 V vs. Ag/AgCl at 100 mVs^{-1}.

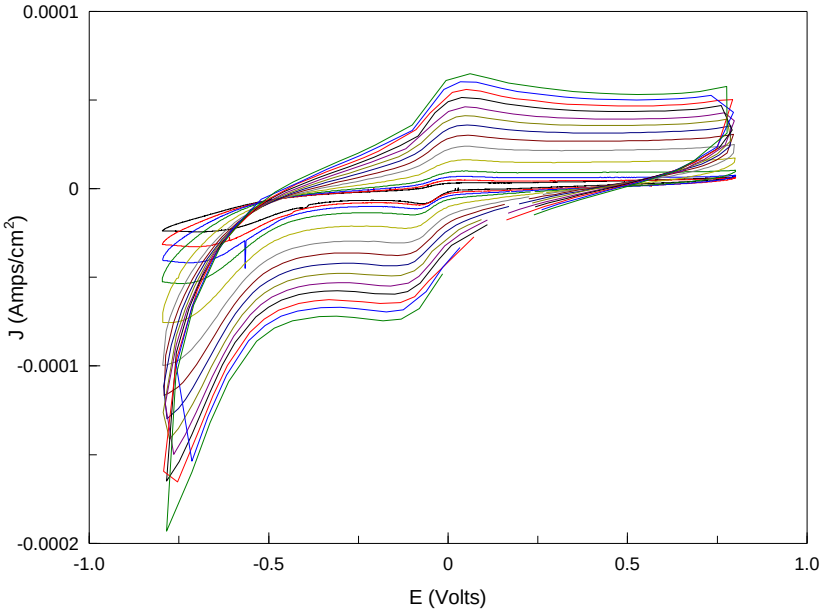

Figure 3.9: Scan rate study of PD film following deposition using Method A. Potential range -0.7 to 0.7 V vs. Ag/AgCl with scan rate of (2- 500 mVs^{-1}).

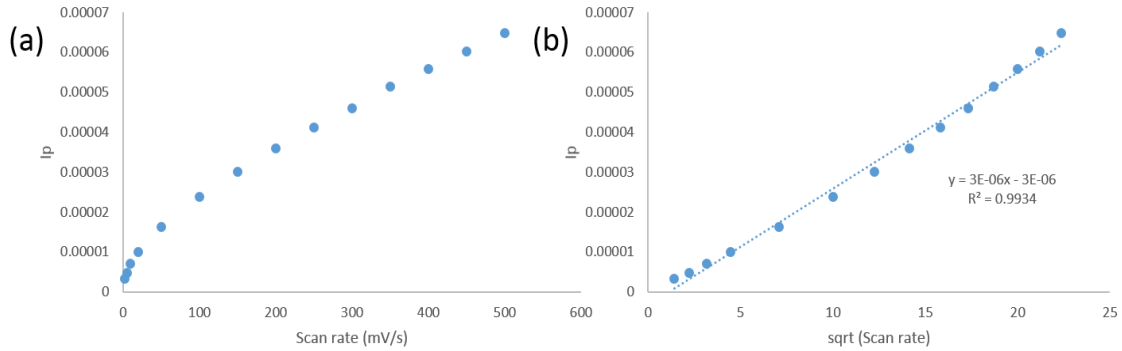

Figure 3.10: Scan rate studies (a) I_p vs. ν (b) I_p vs. $\sqrt{\nu}$

3.5.2.2 Method B1

A study carried out by Hakan *et al.* 2014 showed how PD may be enzymatically polymerised on the surface of an enzyme modified electrode. It involved immersing a GOx modified electrode in a mixture of PD and glucose, in which the presence of the substrate initiates the enzymatic reactions to form H_2O_2, thus polymer synthesis, forming a "shell" over the enzyme. Our approach involved the use of enzymatic polymerisation by incubating the GCE/LOx electrode in 5 mM PD and 20 mM lactate overnight (18 hrs) at 4 ºC. *Figure 3.11* shows a CV of the electrode following film formation, in 0.1 M PB after 18 hrs incubation in PD. CV was carried out for 20 cycles over the potential range of -0.6 V to 0.6 V vs. Ag/AgCl at 100 mVs^{-1}. The overlay of each cycle shows a reduction in peak current, with 18.85 % reduction in oxidation peak and 5.68 % decrease in the reduction peak. The surface coverage of the PD film was calculated to be 6.87 x 10^{-9} mol/cm^3.

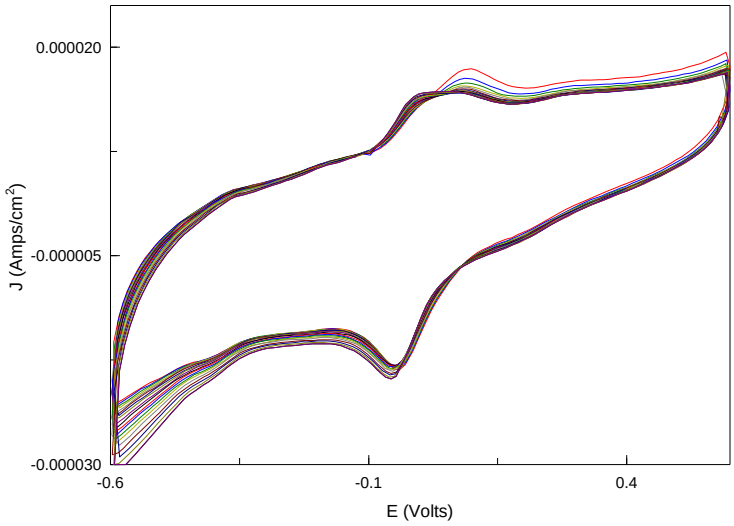

Figure 3.11: Film stability showing (Cycles 1-20) for film formed via Method B1; potential range -0.6 V to 0.6 V vs. Ag/AgCl at 100 mVs^{-1}.

Figure 3.12 shows the response of the so formed GCE/LOx/pPD to the presence of lactate (4.76 and 9.90 mM). The reduction peak responded to the presence of the substrate, indicating that LOx and PD were successful in the detection of Lactate in the presence and absence of the natural mediator oxygen.

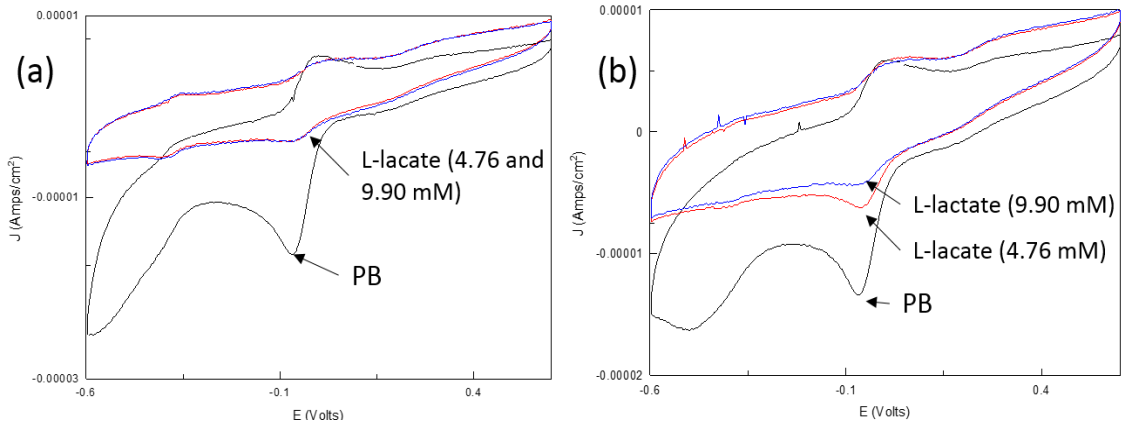

Figure 3.12: CV of background electrolyte followed by response to lactate additions (4.76 and 9.90 mM) at GCE/LOx/pPD under (a) anaerobic conditions (b) aerobic conditions. Potential range -0.6 V to 0.6 V vs. Ag/AgCl at 20 mVs^{-1}

3.5.2.3 Method B2

Method B2 involved voltammetry in 5 mM PD and 10 mM lactate at the GCE/LOx electrode (20 cycles). *Figure 3.13* shows a CV of PB and 5 mM PD with L-lactate (10 mM) (Cycle 1 and Cycle 20 at GCE/LOx. Cycle 1 of the PD and substrate mixture shows a large reduction peak while Cycle 20 was significantly reduced as the polymer

forms a film on the surface of the electrode. The electrode was then rinsed and placed back into 0.1 M PB and cycled for 20 cycles. *Figure 3.14* shows the film formed on the electrode via Method B2 with 3.52 % reduction in the oxidation peak and 2.85 % decrease in the reduction peak after 20 cycles (*Table 3.4*). Method B2 was found to result in a more stable film relative to Method B1 where both methods involve enzymatic polymerisation of the PD film on a LOx modified electrode.

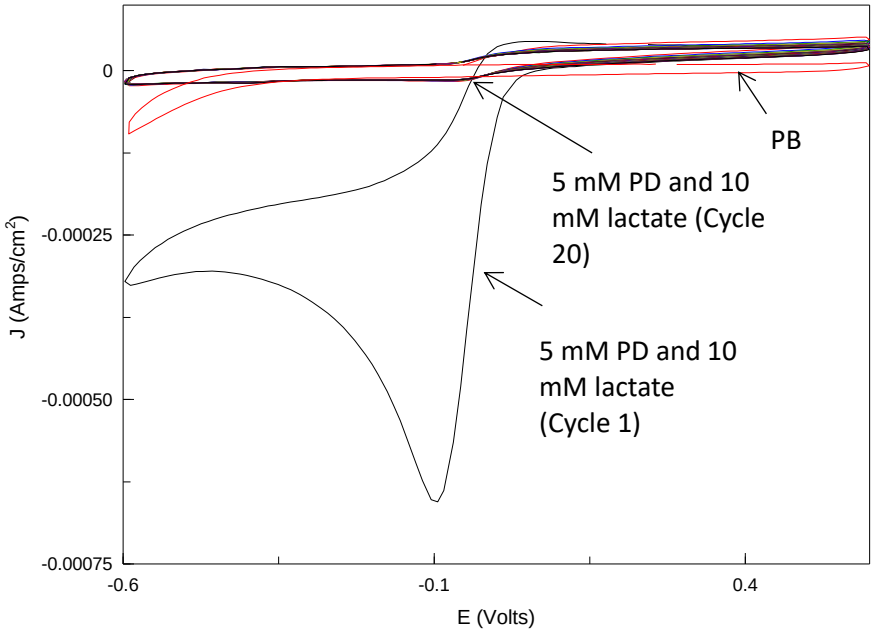

Figure 3.13: Enzymatic polymerisation of 5 mM PD at GCE/LOx in the presence of 10 mM lactate. CV (20 cycles) with potential range -0.8 V to 0.8 V vs. Ag/AgCl at 100 mVs^{-1}.

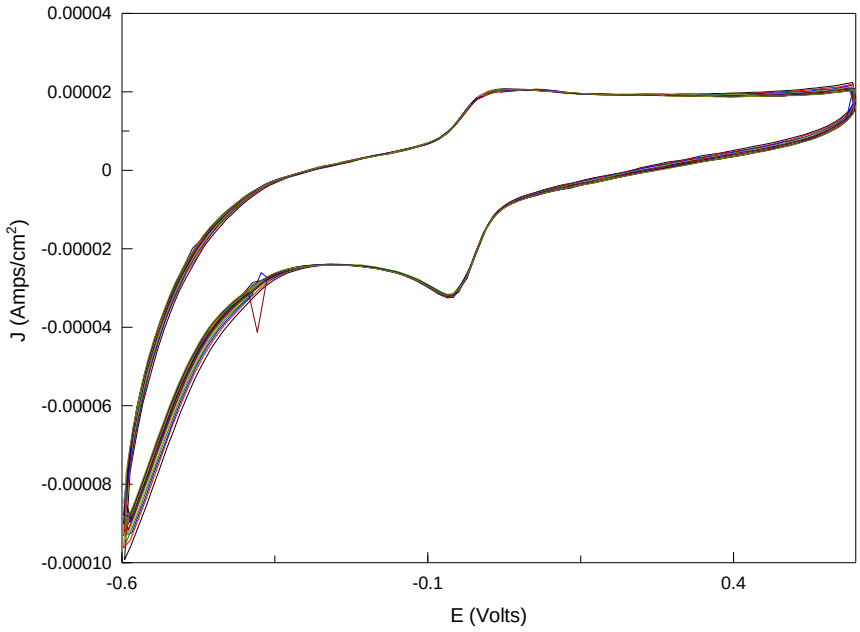

Figure 3.14: Film stability showing background electrolyte (0.1 M PB (pH 6.0)) of PD film formed via method B2, potential range -0.8 V to 0.8 V vs. Ag/AgCl at 100 mVs^{-1}.

Figure 3.15 shows a scan rate study carried out on GCE/LOx/pPD in 0.1 M PB. Two data plots showing the relationship between I_p vs. ν and I_p vs. $\sqrt{\nu}$, are depicted in *Figure 3.16(a)* and *(b)*. The linear relationship between peak current and $\sqrt{\nu}$ indicates the diffusion of charge compensating ions controlling the current, while peak current vs. ν response was linear up to 50 mVs^{-1} . Surface coverage was calculated to be $1.07x10^{-8}$ mol/cm^3.

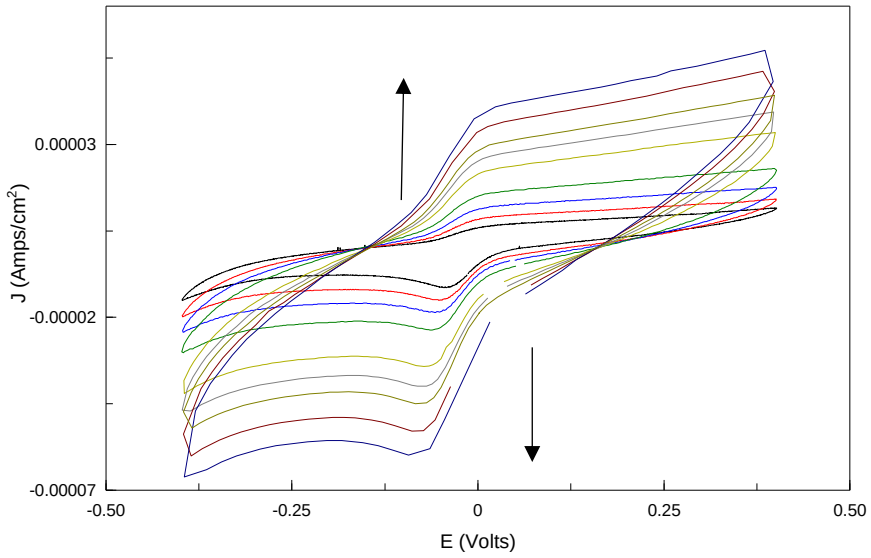

Figure 3.15: Scan rate study showing CV of 0.1 M PB at a GCE/LOx/pPD; potential range -0.4 V to 0.4 V vs. Ag/AgCl over the range (2- 400 mVs^{-1}).

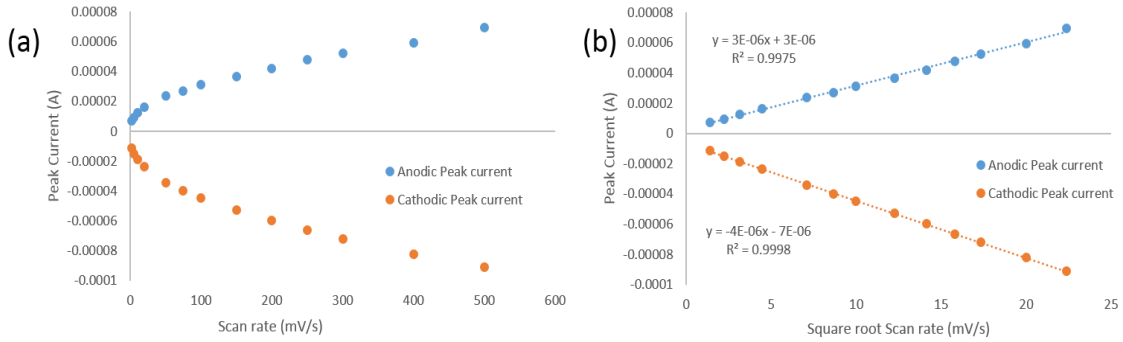

Figure 3.16: Corresponding data plots (a) I_{pa} and I_{pc} vs. ν (b) I_{pa} and I_{pc} vs. $\sqrt{\nu}$

3.5.2.4 Method B3

This approach of enzymatic polymerisation involved increasing lactate concentration (0 – 4.76 mM) at slow scan rates of 20 mVs^{-1}. *Figure 3.17* shows the decrease in reduction peak as the concentration of lactate increased in the cell. There was a slight increase in the oxidation peak during growth. After PD growth was performed, a bright thin yellow film was evident on the electrode surface.

Stability studies of the pPD film were performed at two different pHs (4 and 6). Both films are shown *Figure 3.18*. The films appeared stable as the oxidation and reduction peak currents resulted in minimal reduction after 20 cycles at 100 mVs^{-1}, with 6.64 % reduction in the oxidation peak and 2 % decrease in the reduction peak. A shift in peak potential was also evident, with the redox film demonstrating $E_{1/2}$ = 0.0284 V for the pH 6 environment and $E_{1/2}$ = 0.0854 V in a pH 4 environment, confirming the pH dependant process. Literature has found that the electrochemistry of PD can be influenced by the pH environment with a Nernstian shift in peak potential.[15]An additional redox process was evident at -0.3 V in pH 4 buffer, indicating that the polymer may undergo further reduction processes at this pH.

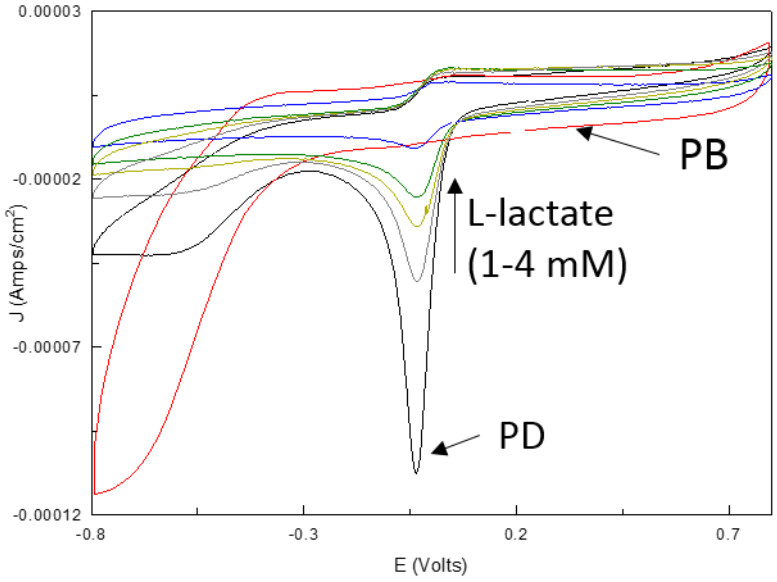

Figure 3.17: CV of 0.1 M PB (pH 6.0), 5 mM PD and lactate additions (1-4.76 mM) at a GCE/LOx. Potential range -0.8 V to 0.8 V vs. Ag/AgCl at 20 mVs^{-1}.

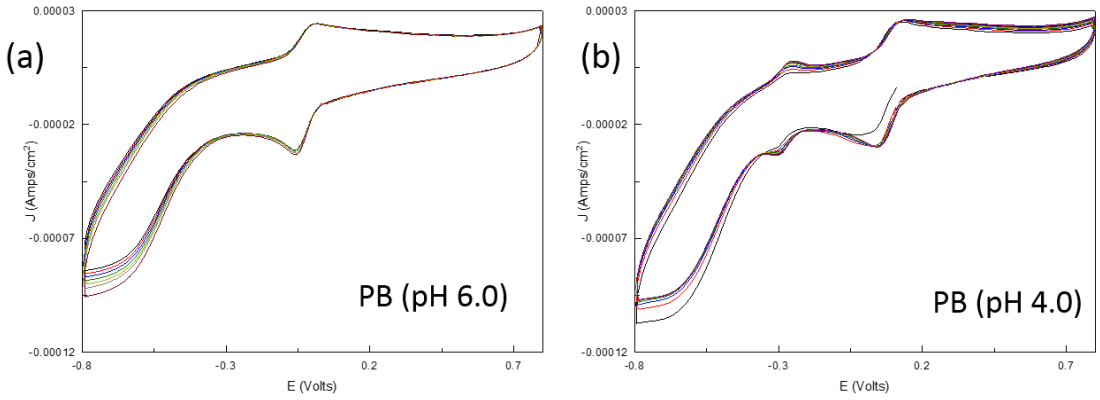

Figure 3.18: pPD film stability at (a) pH 6.0 (b) pH 4.0 via Method B3 with potential range of -0.8 V to 0.8 V vs. Ag/AgCl at 100 mVs^{-1}.

Figure 3.19 shows a CV of the GCE/LOx/pPD in 0.1 M PB at different scan rates (2-300 mVs^{-1}). At slower scan rates (2 mVs^{-1}), the oxidation and reduction peaks appeared to superimpose over each other and are symmetric, characteristic of an ideal reversible surface voltammogram.

Figure 3.20 shows two data plots of (a) I_{pa} and I_{pc} vs. ν and (b) $\sqrt{\nu}$. The linear trend observed in *(a)* indicates a thin film behaviour redox process. This can help to understand the electron transfer kinetics involved in the redox process of the PD polymer film.

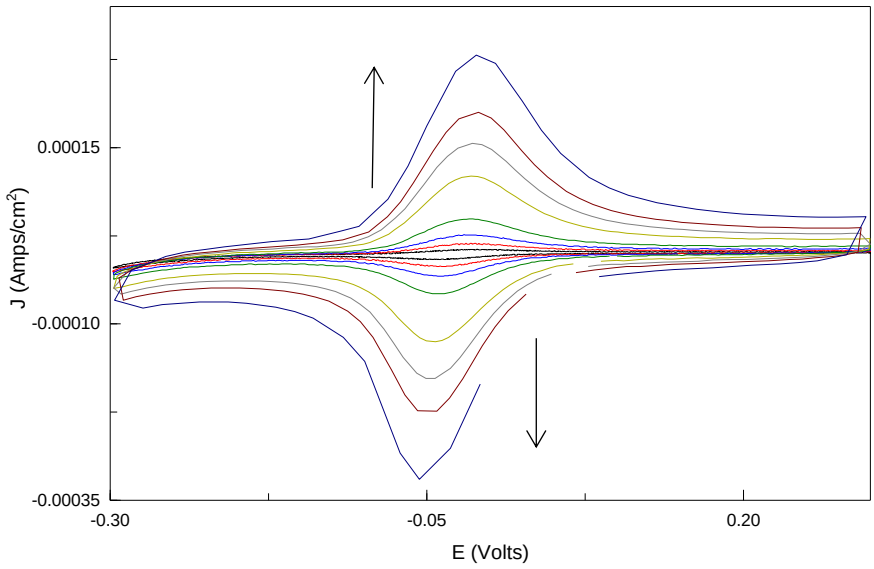

Figure 3.19: Scan rate study showing CV of 0.1 M PB (pH 6.0) at GCE/LOx/pPD; potential range -0.3 V to 0.3 V vs. Ag/AgCl with scan rate (2- 300 mVs^{-1}).

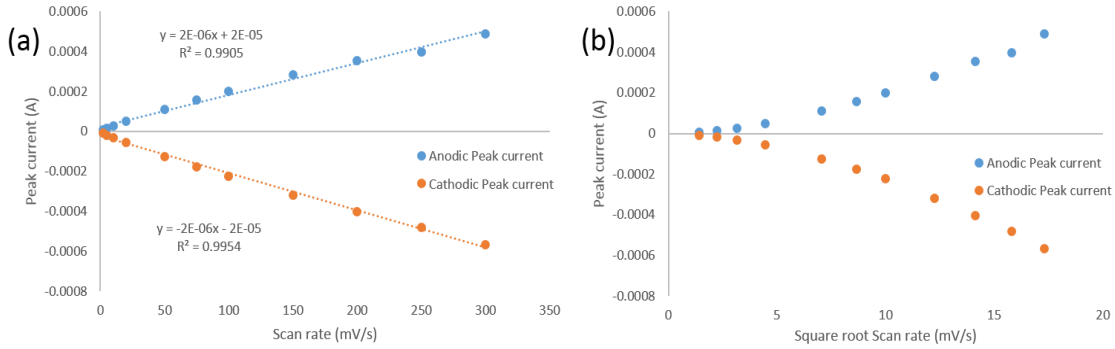

Figure 3.20: Corresponding data plot of (a) I_{pa} and I_{pc} vs. ν (b) I_{pa} and I_{pc} vs. $\sqrt{\nu}$.

The results of Method B3 indicate that it is the most suitable method of polymerisation of PD on the enzymatic sensor. The surface coverage for this technique was calculated to be 2.76 x 10^{-8} mol/cm^3, which was the highest surface coverage of all four methods as shown in *Table 3.4*.

Table 3.4: Electrochemical data of GCE/LOx/pPD via Method A, B1, B2 and B3.

Method	**A**	**B1**	**B2**	**B3**
ΔE_p (V)	0.1109	0.089	0.0965	0.0687
$E_{1/2}$ (V)	0.0410	0.0125	0.021981	0.020233
$\Gamma_{(Ox)}$ (mol/cm^3)	1.28×10^{-9}	6.87×10^{-9}	1.07×10^{-8}	2.76×10^{-8}
$\Gamma_{(Red)}$ (mol/cm^3)	8.93×10^{-9}	7.60×10^{-9}	1.59×10^{-8}	1.86×10^{-8}
Stability*				
Ox	0.99%	18.85%	3.52%	6.64%
Red	0.08%	5.68%	2.85%	2.00%
$FWHPM_{(Ox)}$ (V)	0.146	0.164	0.115	0.141
$FWHPM_{(Red)}$ (V)	0.169	0.110	0.099	0.098

*% Decrease in electroactivity for anodic and cathodic currents

3.5.3 Use of graphite ink in Lactate biosensor fabrication

CV and CA were carried out on a graphite ink modified GCE (described in *Section 3.4.2*) prior to enzyme immobilisation in order to determine the surface area of the electrode and to calculate the capacitance of the ink layer using the Cottrell equation. *Figure 3.21* shows a CV of 0.1 M PB solution, pH 6.0, at a GCE/GInk at scan rate (20–500 mVs^{-1}) showing how scan rate is directly proportional to peak current. Peak current at 0.25 V vs. scan rate was plotted which showed a slope value of 9.22×10^{-6} and ($R^2 = 0.99$) with capacitance of the ink calculated to be 9.22 µFarad cm^{-2} using the following equation.

$$i = C.A.\nu$$

Where,

i = Peak current

C = Capacitance

A = Area of electrode

ν = scan rate

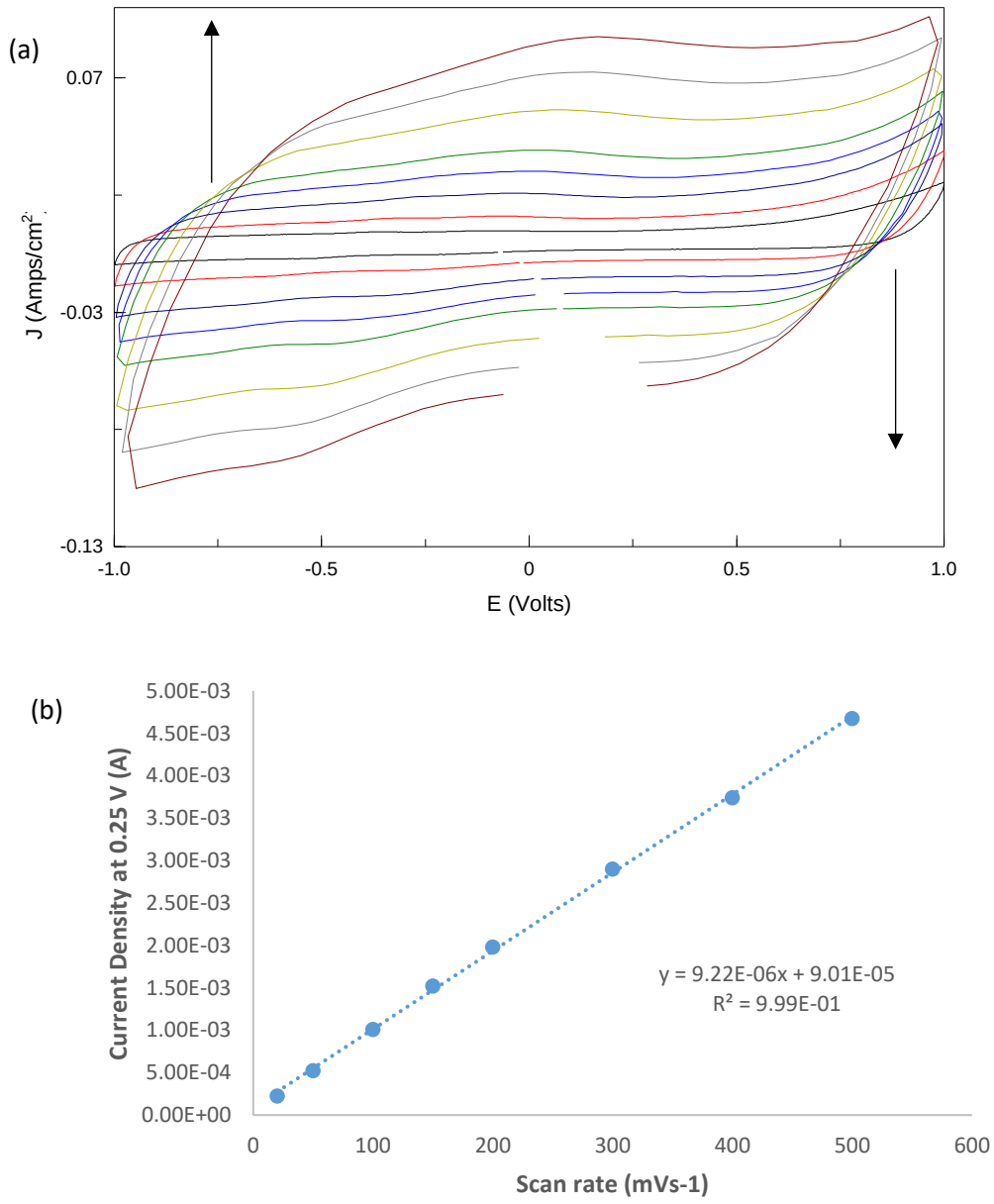

Figure 3.21: (a) Scan rate study showing CV in 0.1 M PB (pH 6.0) at GInk modified GC electrode over the range -1.0 V to 1.0 vs. Ag/AgCl at various scan rate (20- 500 mVs^{-1}) (b) Current density vs. ν for GInk modified GCE with slope equivalent to capacitance.

The electroactive surface area of GCE/GInk was determined by CV and CA analysis. 0.1 M PB and 5 mM $K_3Fe(CN)_6$ were analysed at a GCE/GInk *via* CV with a potential range of -0.5 V to 0.5 V vs. Ag/AgCl and scan rate of 100 mVs^{-1}. As shown in *Figure 3.22*, oxidation occurred at 0.2 V.

Following this, CA at E_{app} = 0.3 V vs. Ag/AgCl was performed in the presence of 5 mM $K_3Fe(CN)_6$ at GCE/GInk electrode (*Figure 3.23).*An increase in current density

was observed with 5 mM $K_3Fe(CN)_6$ which was used to construct a Cottrell plot of current density vs. $1/\sqrt{time}$. The Cottrell equation was used to determine the surface area of the GCE/GInk to be 0.2277 cm^2, which was three times greater than that of the geometric area (0.0707 cm^2).

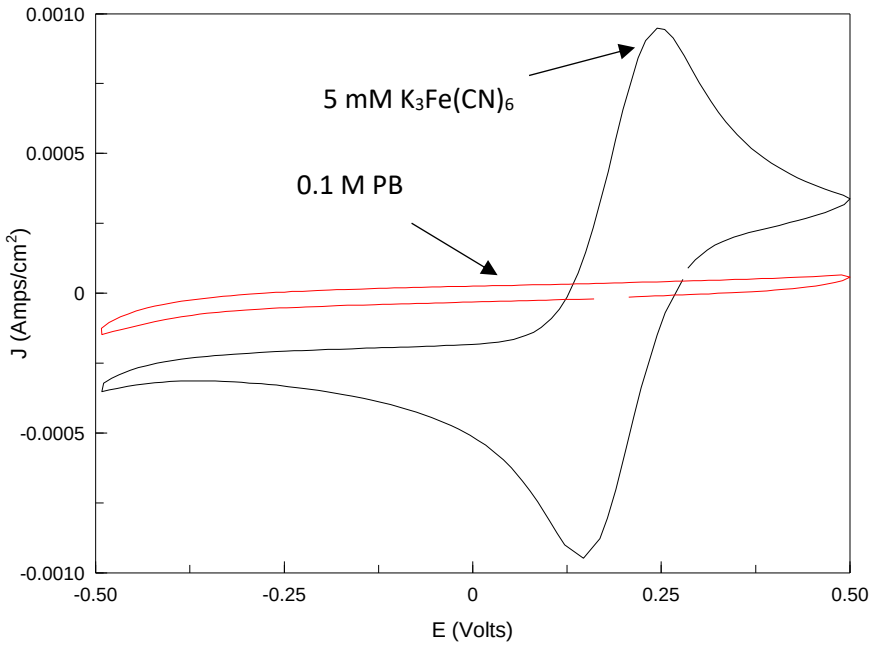

Figure 3.22: CV of 0.1 M PB and 5 mM $K_3Fe(CN)_6$ at GCE/GInk. Potential range of -0.5 V to 0.5 V vs. Ag/AgCl at 100 mVs^{-1}.

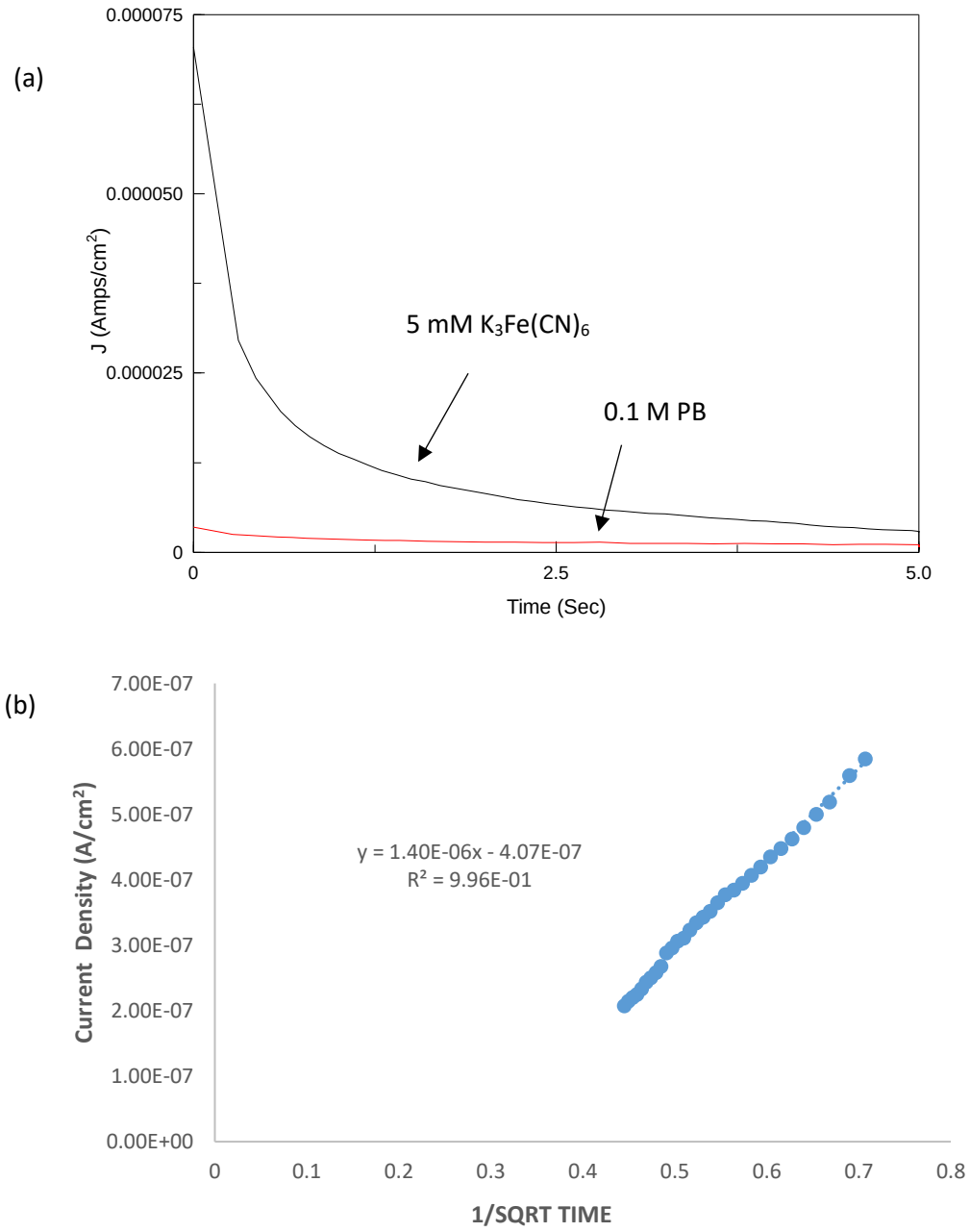

Figure 3.23: (a) CA response to 0.1 M PB and 5 mM $K_3Fe(CN)_6$ at a GCE/GInk (E_{app} = 0.3 V vs. Ag/AgCl for 5 s). (b)Cottrell plot of 5 mM $K_3Fe(CN)_6$ at GCE/GInk.

3.5.3.1 Electrochemical studies of graphite ink LOx modified electrode with pPD film

The optimum method for the preparation of a pPD film on a GC electrode was determined to be Method B3 (see *Section 3.4.5* for optimum film preparation method). Therefore, the following experiments involving pPD film formation were carried out using this procedure at a GCE/GInk/LOx electrode.

Figure 3.24 shows a CV during the film formation of pPD onto a GCE/GInk/LOx electrode. A decrease in the reduction peak at 0.1 V was evident as the concentration of sodium lactate standard increased in the electrochemical cell. After film formation, the working electrode was rinsed with deionised water. The appearance of the GCE/GInk/LOx/pPD showed a thin bright yellow film, indicating the polymerisation of pPD on the surface of the modified electrode. It can be suggested that the polymerisation was initiated by the presence of the LOx enzyme and its substrate, sodium lactate, in the electrochemical cell, as per enzymatic polymerisation method. As discussed previously, literature shows that H_2O_2 production, formed in the catalytic breakdown of the substrate, can initiate polymer formation. [12]

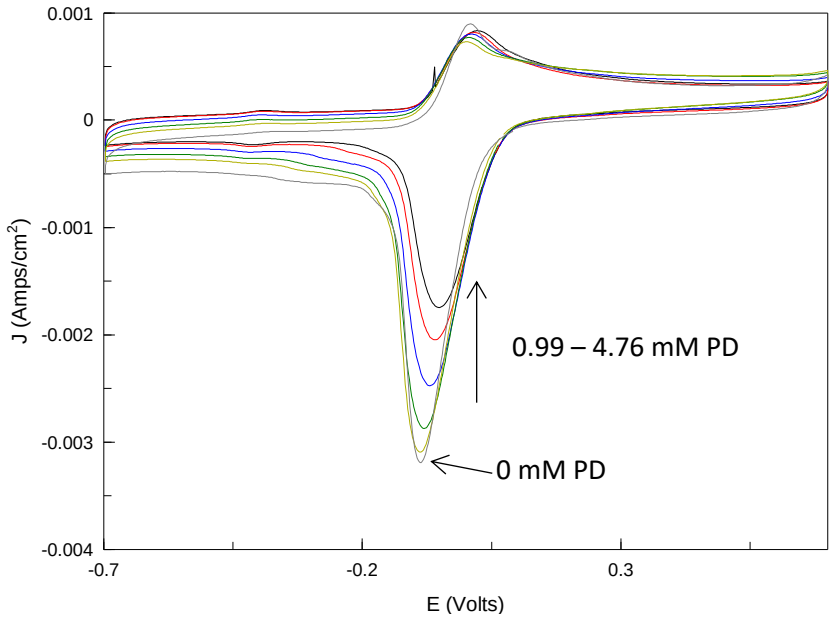

Figure 3.24: CV of 5 mM PD with lactate additions (0-4.76 mM) at a GCE/GInk/LOx electrode with potential range -0.7 V to 0.7 V vs. Ag/AgCl at 20 mVs^{-1} (Method B3 utilised).

Figure 3.25 shows a CV of the redox film at the GCE/GInk/LOx/pPD modified electrode at 20 mVs^{-1}. In order to determine the stability of the pPD film upon cycling, CV was carried out for 20 cycles at 100 mVs^{-1} (*Figure 3.26)*. Minimal reduction in the peak current values of the oxidation and reduction peaks was found after 20 cycles. The last cycle (Cycle 20) showed large sharp peaks present after the continued cycling which indicates that the pPD film modified on the electrode surface has high stability and held high current density levels. The appearance of the electrode surface showed no evidence of leaching after 20 cycles. Results show that using the graphite ink in the

initial layer of the GCE, prior to PD polymerisation, allows a better quality thin film to be achieved. Advantages of the Graphite ink inner layer include its ability to increase the stability of the film, giving more defined oxidation and reduction peaks in *Figure 3.26* relative to *Figure 3.18* without the GInk. It also showed it improved the electrochemical reversibility of the polymer, which may be due to interactions between the conducting ink layer and the PD film.

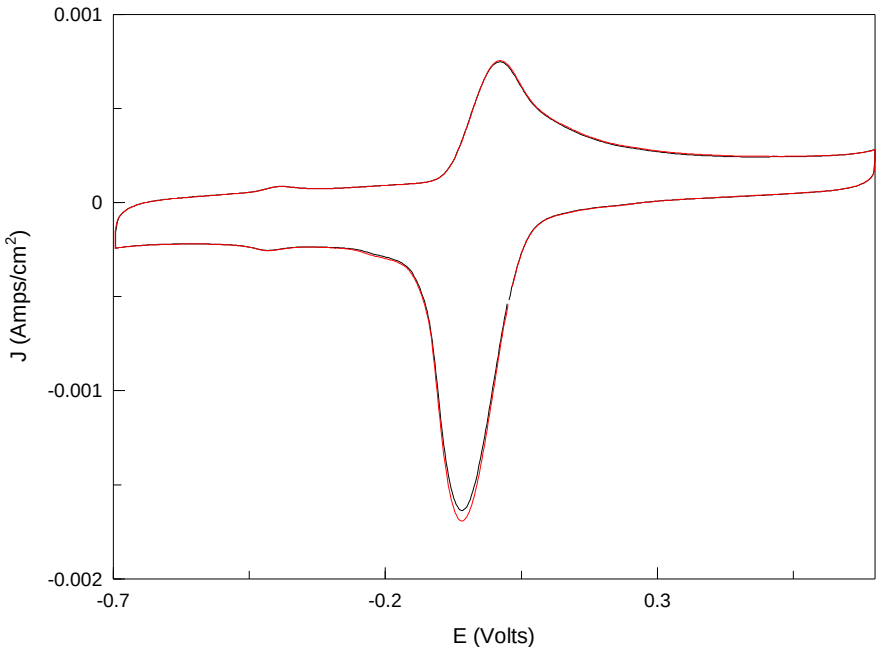

Figure 3.25: CV of 0.1 M PB at the GCE/GInk/LOx/pPD. Potential range -0.7 V to 0.7 V vs. Ag/AgCl at 20 mVs^{-1} (3 cycles).

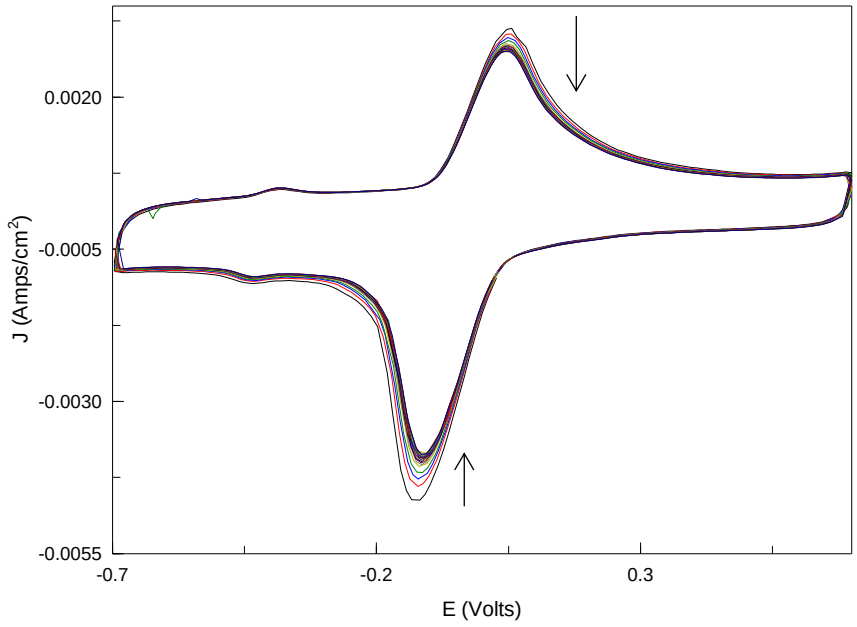

Figure 3.26: Film stability showing background electrolyte of pPD film formed at a GCE/GInk/LOx; potential range -0.7 V to 0.7 V vs. Ag/ AgCl at 100 mVs^{-1} (20 cycles).

3.5.4 Response of pPD to lactate at graphite ink LOx modified electrode with pPD film

After characterisation of the pPD film and electrochemical studies of the electrode surface, the electrode was studied for its response to lactate using CV and CC.

Figure 3.27 shows a CV in background electrolyte and 0.99 mM sodium lactate with response to lactate evident at 0.1 V indicating oxidation of pPD as I_{pa} increases and I_{pc} decreases at -0.1 V following reduction of the mediator *(Equations 3.4 – 3.6)*.

$$Lactate + LOx_{(FAD)} \rightarrow Pyruvate + LOx_{(FADH2)} \quad (3.4)$$

$$LOx_{(FADH2)} + PD_{(OX)} \rightarrow LOx_{(FAD)} + H_2PD_{(RED)} \quad (3.5)$$

$$H_2PD_{(RED)} \rightarrow PD_{(OX)} + 2e^- + 2H^+ \quad (3.6)$$

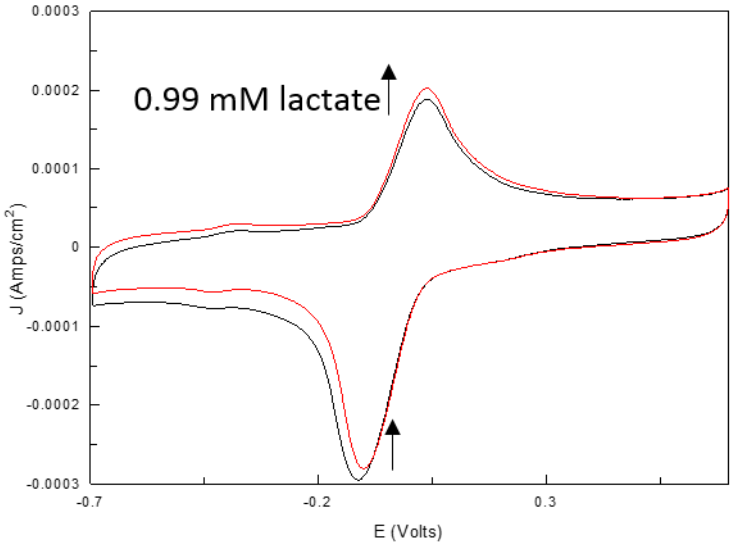

Figure 3.27: CV of 0.1 M PB (pH 6.0) and 0.99 mM lactate at a GCE/GInk/LOx/pPD. Potential range -0.7 to 0.7 V vs. Ag/AgCl at 100 mVs^{-1}.

Therefore, CC can be carried out with E_{app} of 0.12 V or -0.12 V vs. Ag/AgCl. The first potential used for analysis was -0.12 V which studied the change in charge at the reduction peak potential. *Figure 3.28(a)* shows the chronocoulometric response to 0.1 M PB (pH 6.0) and lactate concentrations ranging from 0.25 mM to 3.85 mM at GCE/GInk/LOx/pPD with (E_{app} = -0.12 V vs. Ag/AgCl) for 5 s. Results showed an increase in charge in the presence of lactate at GCE/GInk/LOx/pPD. *Figure 3.28*(b) showed the corresponding charge vs. lactate concentration (0.25 – 3.85 mM) plot, showing a linear relationship (c) between 0.25 – 0.99 mM sodium lactate. The results showed that after 0.99 mM, the charge no longer increased. We can suggest that the enzyme has reached its maximum substrate concentration and the enzyme is now saturated i.e. V_{max}. The sensitivity of the biosensor was 2.49 x 10^{-4} C $cm^{-2}mM^{-1}$.

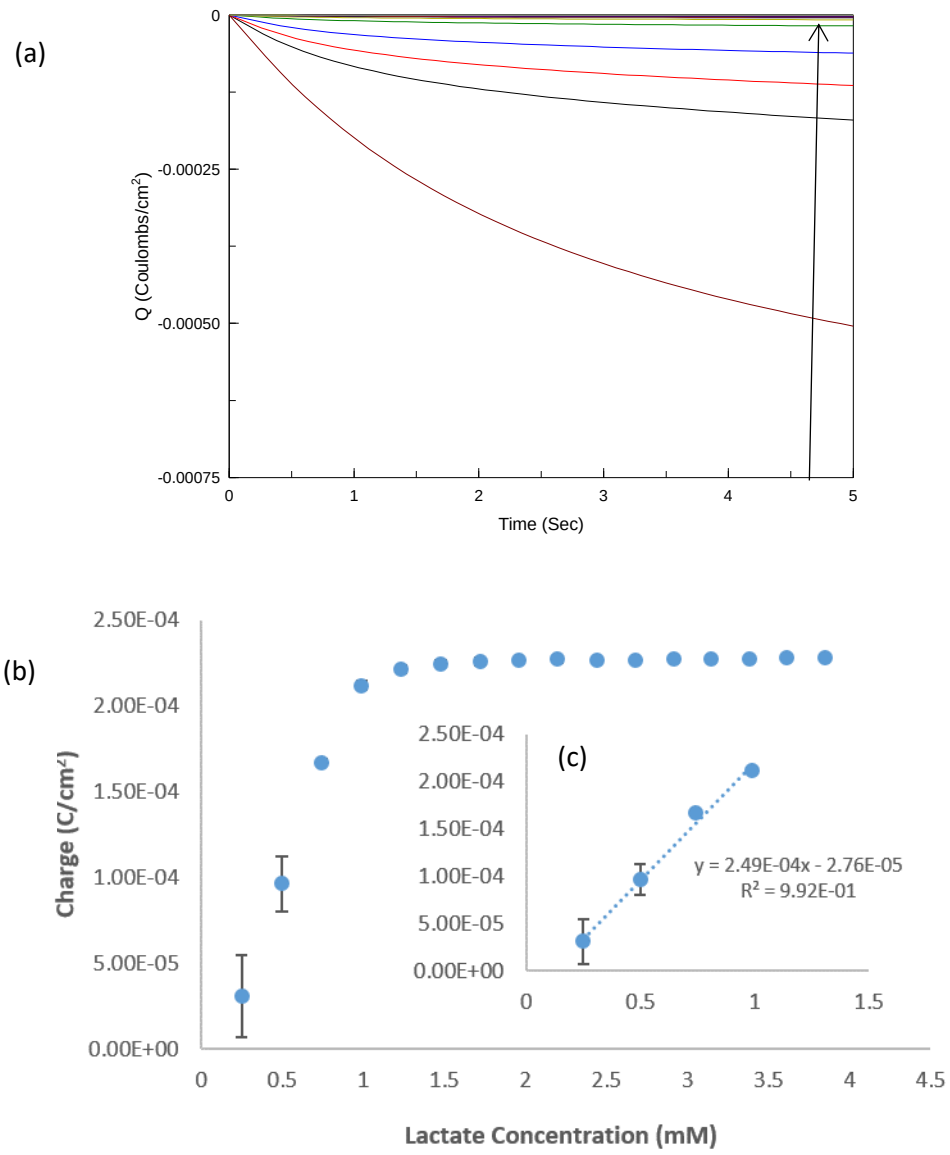

Figure 3.28: (a) CC data of 0.1 M PB (pH 6.0) and lactate additions (0-3.85 mM) at a GCE/GInk/LOx/pPD (E_{app} = -0.12 V vs. Ag/AgCl for 5 s). (b) Corresponding data plot of charge (E_{app} = -0.12 V vs. Ag/AgCl) vs. lactate concentration (0 – 3.85 mM). (c) Calibration plot of charge (E_{app} = -0.12 V vs. Ag/AgCl) vs. lactate concentration (0 -0.99 mM) (n=3).

CC was performed again to study the relationship between charge and concentration at the oxidation peak (E_{app} = 0.12 V vs. Ag/AgCl). *Figure 3.29(a)* shows the CC response to 0.1 M PB (pH 6.0) and lactate concentrations (0.74 mM to 2.44 mM) at the GCE/GInk/LOx/pPD. *Figure 3.29(b)* shows an increase in charge at the electrode in the presence of lactate with linear range 0.74 – 2.44 x 10^{-3} M, sensitivity of 4.11 x 10^{-4} C $cm^{-2}mM^{-1}$, LOD of 0.06 mM and LOQ of 0.19 mM (*Table 3.5)*. The results of the calibration of GCE/GInk/LOx/pPD *via* CC analysis showed that (E_{app} = 0.12 V vs.

Ag/AgCl) which operates at the oxidation potential of the pPD film, gave a greater linear range in lactate concentration relative to (E_{app} = -0.12 V vs. Ag/AgCl).

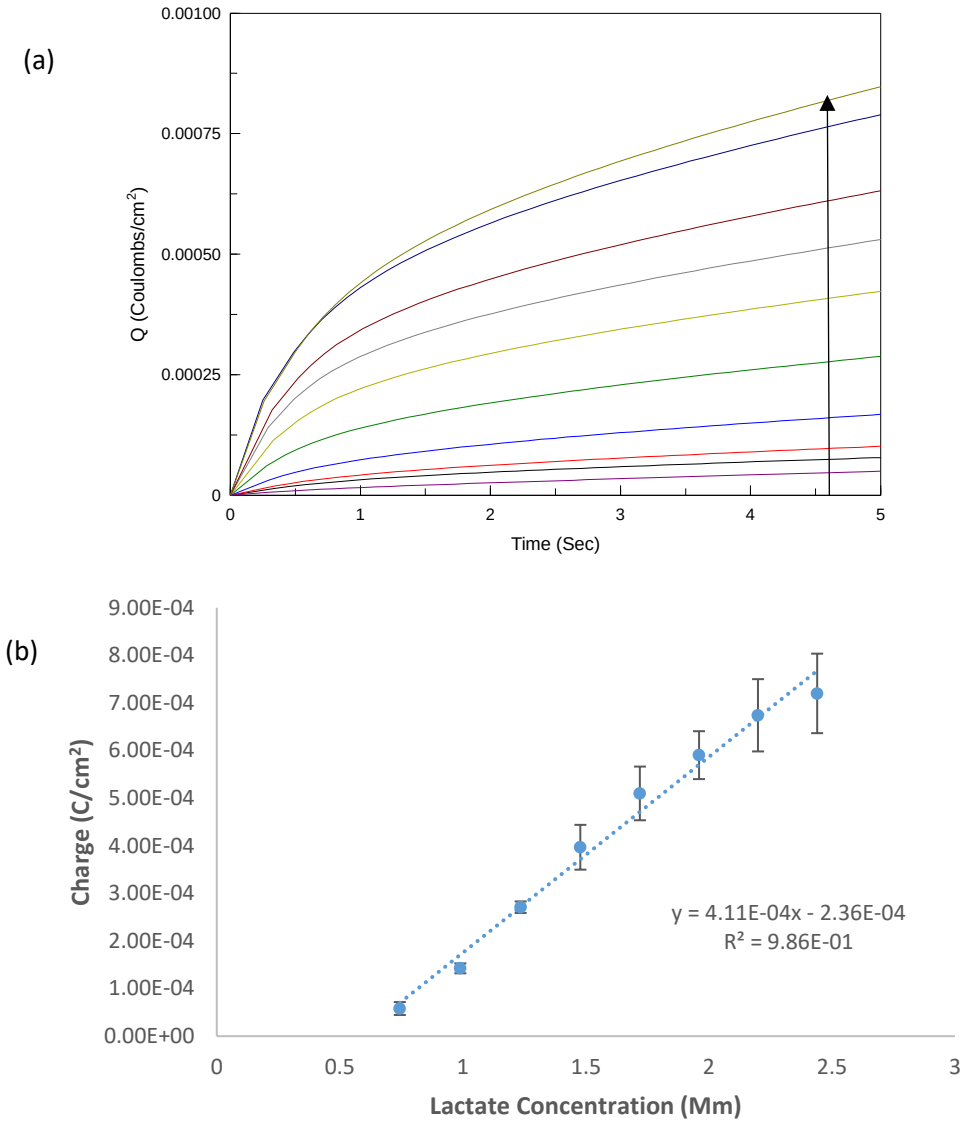

Figure 3.29: (a) CC response of 0.1 M PB (pH 6.0) and lactate additions (0.74-2.44 mM) at a GCE/GInk//LOx/pPD electrode (E_{app} = 0.12 V vs. Ag/AgCl for 5 s). (b) Corresponding calibration plot of charge vs. lactate concentration (0 – 2.44 mM) (n=3).

Table 3.5: Analytical data for GCE/GInk/LOx/pPD.

Analytical Data for Lactate Biosensor			
Linear Range (M)	**Sensitivity (C $cm^{-2}mM^{-1}$)**	**LOD (mM)**	**LOQ (mM)**
0.74 – 2.44 x 10^{-3}	4.11 x 10^{-4}	0.06	0.19

3.5.5 Determination of lactate concentration in Fermentation sample (t = 0)

The focus of this work was to develop biosensors for rapid quantitative measurements in dairy samples. This is explored in great detail in *Chapter 4* using biosensors described in *Chapter 2*. Here, we investigated the use of the biosensor (GCE/GInk/LOx/pPD) modified with a conducting graphite ink layer, LOx and enzymatically polymerised pPD for quantitative analysis of a fermentation sample (diluted 1 % v/v in 0.1 M PB (pH 6.0). The GCE/GInk/LOx/pPD was deployed in the determination of lactate in a real industry fermentation sample (t = 0), meaning a sample taken at the start point of a lactic acid fermentation process. Therefore, low lactic acid levels will be presented in this sample type. Results from the biosensor were correlated with HPLC-RI results which were performed by the industry partner on-site within a couple of hours after the sample was retrieved from the fermentation vessel. Here, we investigate the use of this biosensor (GCE for accurate measurement of lactate concentration in a diluted fermentation sample (t = 0) using CV and CC techniques. *Figure 3.30* shows a CV of 0.1 M PB, pH 6.0, the fermentation sample (t = 0) and the sample spiked with 1.96 mM lactate. The response to lactate can be seen at ~ 0.1 V.

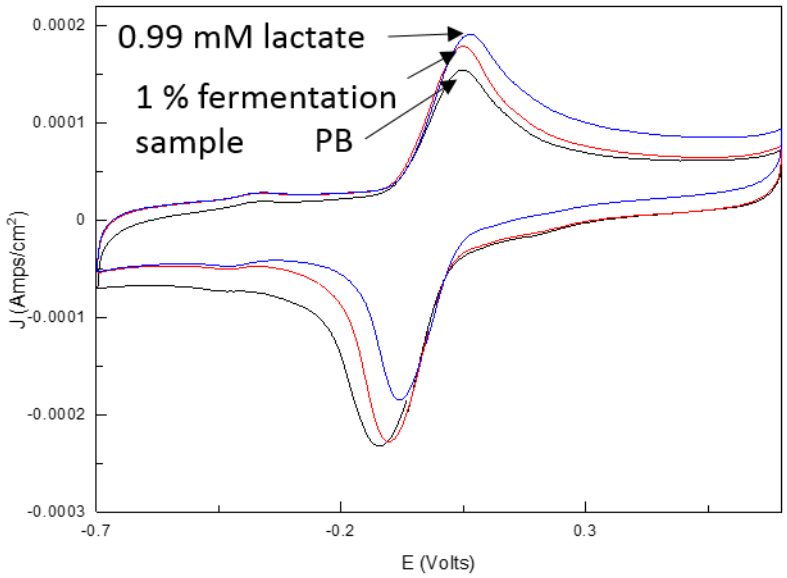

Figure 3.30: CV of 0.1 M PB (pH 6.0), fermentation sample (1 % v/v in 0.1 M PB (pH 6.0)) and 1.96 mM lactate at a GCE/GInk/LOx/pPD electrode. Potential range -0.7 to 0.7 V vs. Ag/AgCl at 100 mVs^{-1}.

CC followed using E_{app} = 0.12 V vs. Ag/AgCl, Figure 3.31 shows charge vs. concentration plot of spiked lactate (0 – 1.23 mM) in diluted fermentation sample (t = 0) corrected for the contributing lactate signal from the fermentation sample. The corresponding calibration curve was then used to calculate the lactate content in the sample. The biosensor measured 48.81 mM lactate (5582 ppm) for an undiluted sample, in comparison to HPLC-RI data which measured lactate concentration of 69.39 mM (7776 ppm) in the same sample, showing 71.78 % agreement. Deviations of the lactate biosensor result may be due to very low levels of lactate present in the sample as it was taken at the start of the fermentation process. Therefore, less dilution of the sample prior to analysis could solve quantitation issues of (t = 0) samples.

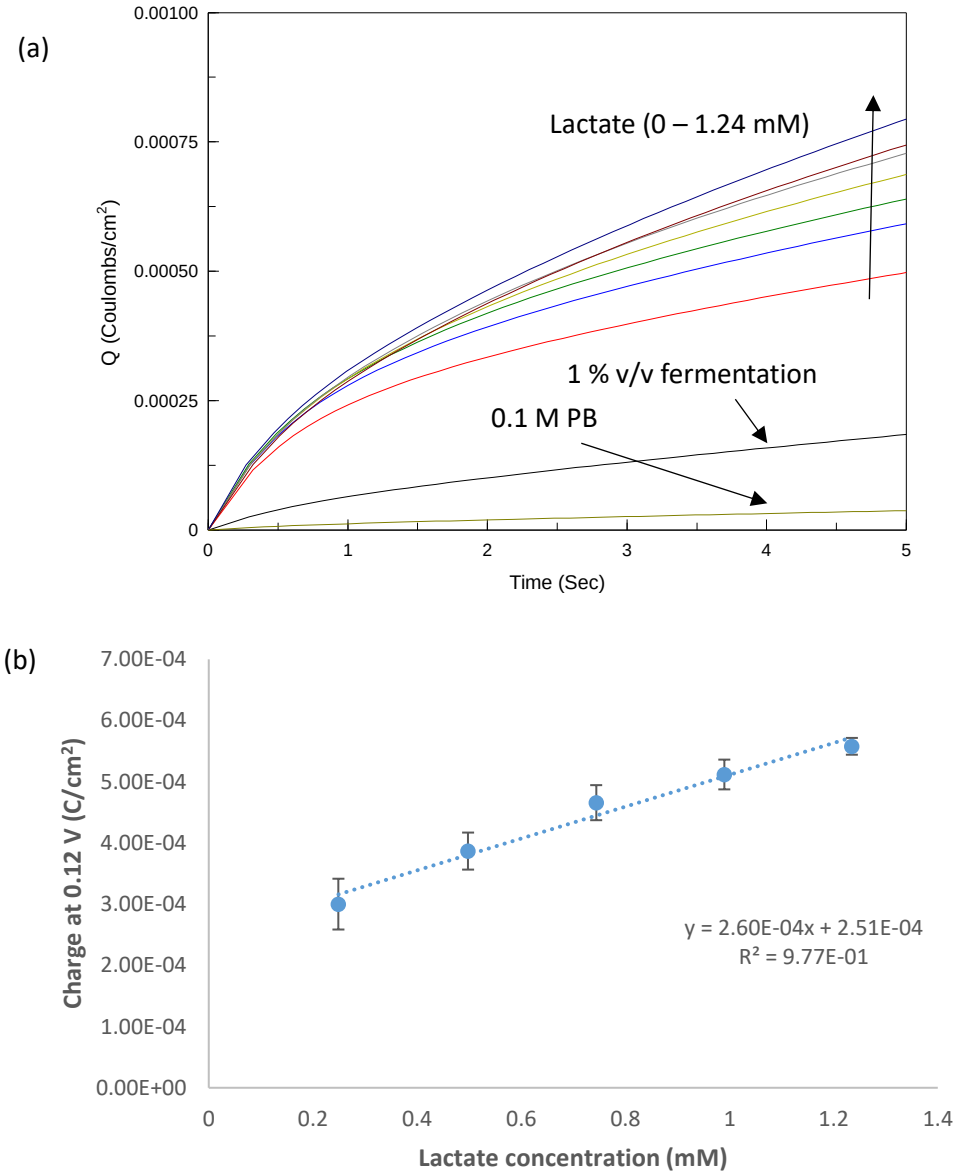

Figure 3.31: (a) CC data response to 0.1 M PB (pH 6.0), fermentation sample (t = 0) (1 % v/v in 0.1 M PB) and lactate additions (0-1.24 mM) at a GCE/GInk/LOx/pPD electrode (E_{app} = 0.12 V vs. Ag/AgCl) for 5 s. (b) Corresponding calibration plot of charge vs. lactate concentration (mM) in fermentation sample (t = 0) (1 % v/v in 0.1 M PB) (n=3).

3.5.6 Surface characterisation of LOx electrode

3.5.6.1 Optical light microscope

Surface analysis was carried out at each stage of modification of a commercial carbon screen-printed electrode. *Table 3.6* shows a description of each stage of surface modification. It should be noted that at stage C, the enzyme immobilisation layer, a four-layer system was used that consisted of chitosan/LOx/chitosan/PEGDE (see *Section 3.4.2*).

Table 3.6: Electrode configuration of electrodes for Light microscope analysis.

A	SPE
B	SPE/GInk
C	SPE/GInk/LOx
D	SPE/GInk/LOx/pPD

Figure 3.32(a) shows a bare SPE at 100 x magnification with no surface modification. *Figure 3.32(b)* shows the same SPE following a 1 µL deposition of GInk at 100 x magnification. Although *(a)* and *(b)* are very similar, the SPE/GInk appears to have an increased surface area compared to the bare SPE. Both images are carbon surfaces so should not be too different in appearance. *Figure 3.32 (c)* shows the SPE after modification of the LOx enzyme layer. Here, we can see a slight change in the surface of the working area of the electrode due to the presence of protein structures. The greatest change can be seen in *Figure 3.32(d)* and *Figure 3.33* due to the presence of the polymer, pPD on the surface of the electrode where clusters of rod-shaped structures were evident with further examination via SEM.

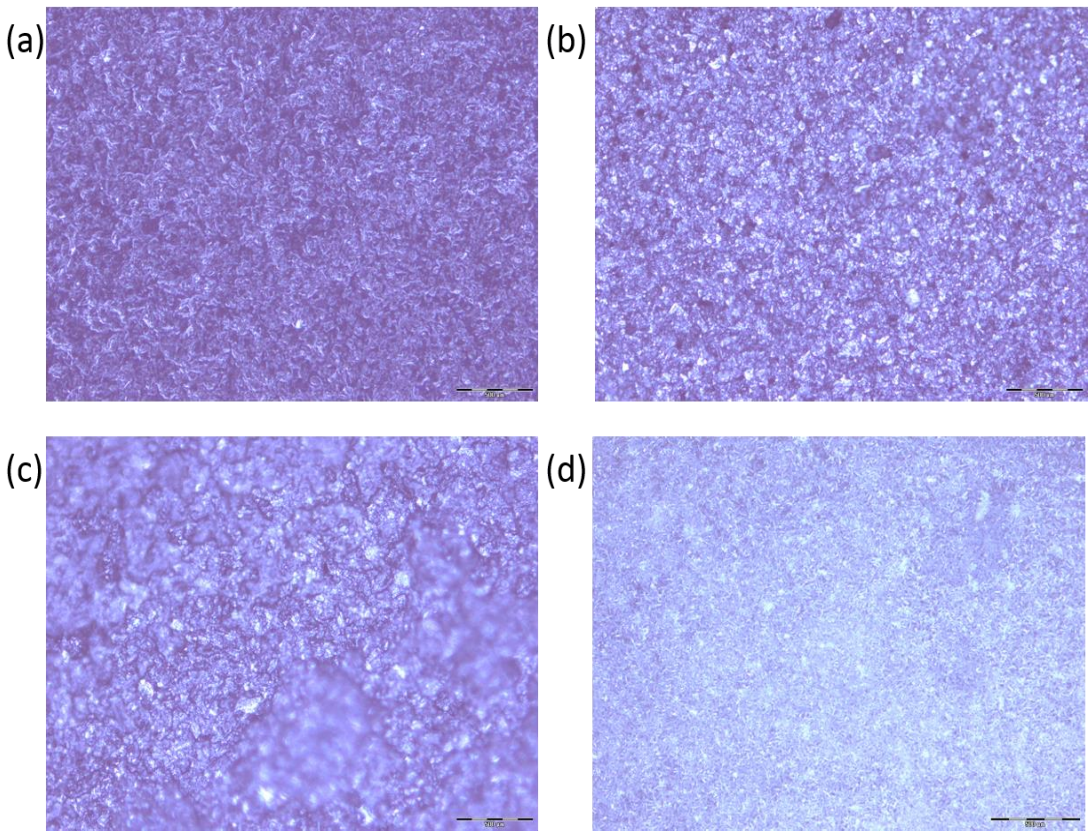

Figure 3.32: Light microscopic images of (a) Bare SPE (b) SPE/GInk (c) SPE/GInk/LOx (d) SPE/GInk/LOx/pPD at 100 x magnification.

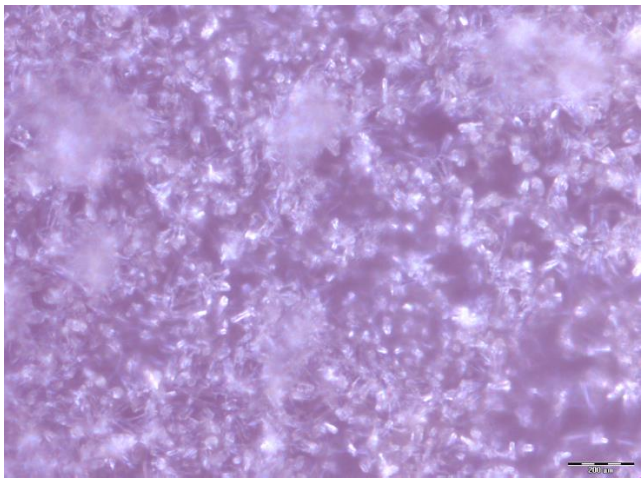

Figure 3.33: Microscopic images of SPE/GInk/LOx/pPD film (enzymatically polymerised via Method B3) at 500 x magnification.

3.5.6.2 Scanning Electron Microscopy

Scanning electron microscopy (SEM) images were taken of both a commercial bare carbon SPE and a modified SPE/GInk/LOx/pPD. *Figure 3.34* and *Figure 3.35* shows SEM images of a bare SPE *(a)* and a modified SPE (SPE/GInk/LOx/pPD) *(b)*. The images show the difference of the surface area after the SPE was modified with enzyme immobilisation and polymerisation of the mediator PD. *Figure 3.35* shows the contrast of both surfaces at the µM scale, with rod-like structures appearing on the surface of SPE/GInk/LOx/pPD. The structures varied greatly in width and length with average measuring at 6.47 µM (*Figure 3.36)*.

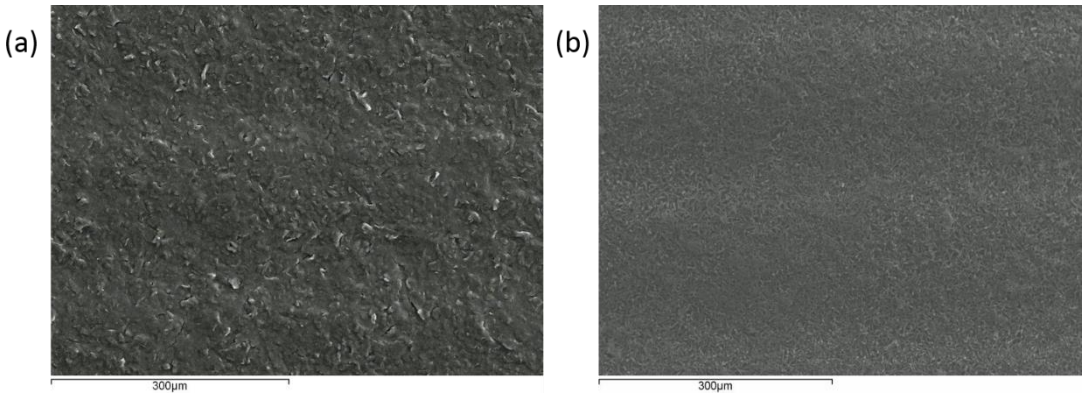

Figure 3.34: SEM image of (a) Bare SPE (b) SPE/GInk/LOx/pPD.

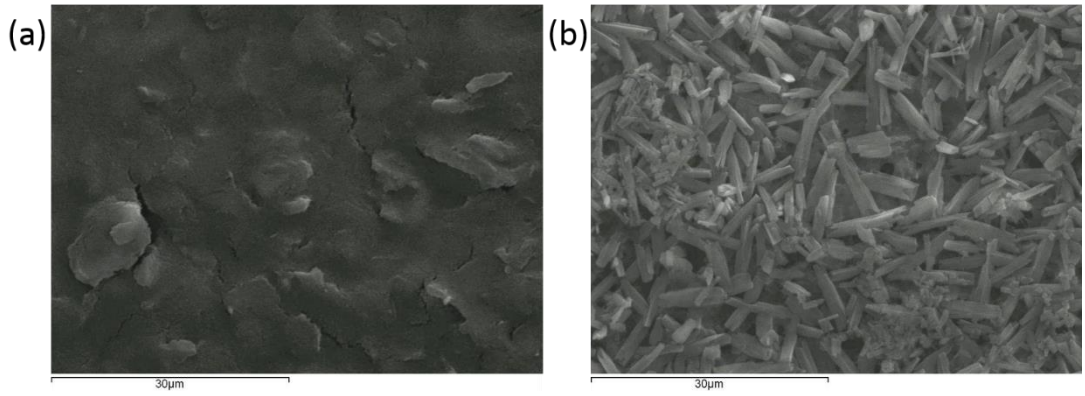

Figure 3.35: SEM image of (a) Bare SPE (b) SPE/GInk/LOx/pPD.

Figure 3.36: SEM image of SPE/GInk/LOx/pPD.

3.5.6.3 Energy Dispersive X-ray analysis

Energy Dispersive X-ray (EDX) Analysis was also carried out on the surface of a bare SPE and modified SPE (SPE/GInk/LOx/pPD) in order to identify if there was a difference in the elemental composition. *Figure 3.37* and *Figure 3.38* show EDX spectrums of a bare SPE and a modified SPE/GInk/LOx/pPD. The bare SPE identified the presence of carbon as expected and presence of chloride from possible residual electrolyte. EDX analysis shows the modified SPE/GInk/LOx/pPD contained a presence of carbon, potassium and chloride which may be due to residual electrolyte on the electrode surface. Phosphorus and aluminium were also detected by EDX which were not found to be present on the bare SPE.

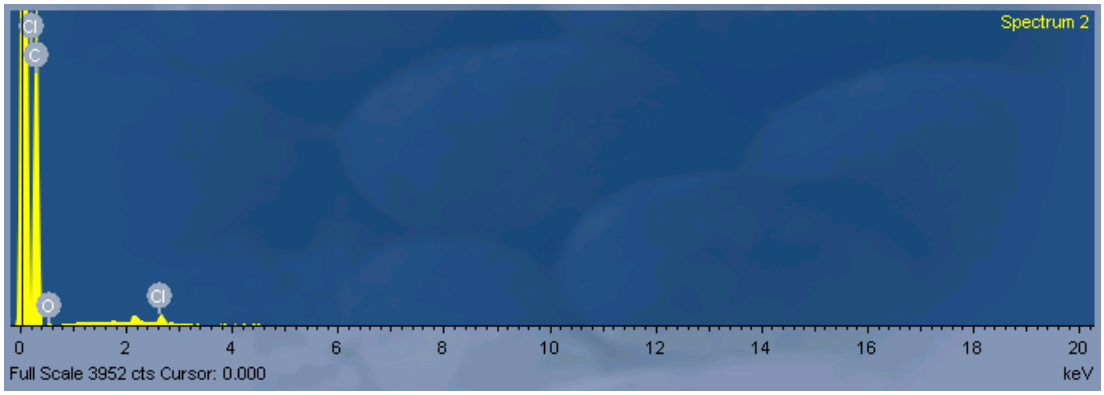

Figure 3.37: EDX Spectrum of Bare SPE.

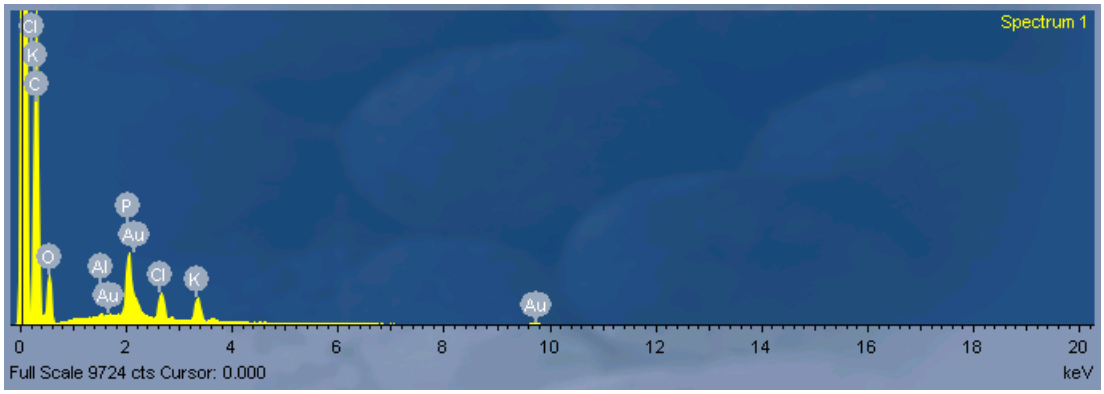

Figure 3.38: EDX spectrum of SPE/GInk/LOx/pPD.

3.5.6.4 Scanning electrochemical microscopy of LOx electrodes

Scanning electrochemical microscopy was performed on the lactate biosensor GCE/Chit/LOx/Chit/GA for further surface imaging. Area scans were carried out on the enzyme modified electrode using 5 mM $K_3Fe(CN)_6$ as an electron transfer mediator where the tip potential was held constant (E_T = -0.4 V vs. Ag/AgCl) which causes reduction of Fe^{3+} to Fe^{2+}. An approach curve was performed at the GCE/Chit/LOx/Chit/GA in order to determine the appropriate position of the tip over the substrate (modified electrode) in the electroactive region.

Figure 3.39 shows an approach curve towards the enzymatic LOx biosensor substrates (E_T = -0.4 V vs. Ag/AgCl). As the tip approached the LOx modified surface, the current decreased causing a negative feedback response. A sharp decrease in current was evident on approach to the modified electrode and the experiment was stopped at this point. As described in *Chapter 2*, Redox competition mode was used where both the tip and modified substrate electrode competed for the oxidised form Fe^{3+}. High local electroactivity was detected as low current was measured at the SECM tip on approach to the enzyme modified surface.

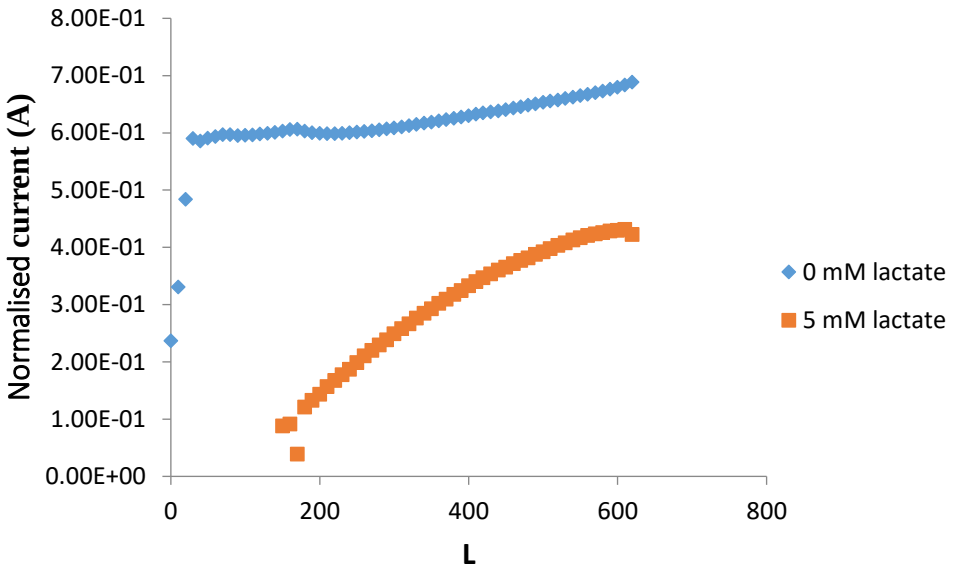

Figure 3.39: Normalised current (I_{TIP}/I_{Inf}) vs. distance (L) where L = d/a and d = distance from tip Pt ultramicroelectrode (UME) to substrate, a = tip radius 10 mm, RG = 23.8. Curves recorded above the Chit/GA-LOx film, by translating the UME vertically (z approach curve). E_T = -0.4 V vs. Ag/AgCl, E_{sub} = OFF, 5 mM $K_3Fe(CN)_6$ in PB pH 6.0.

A series of approach curves were performed at the LOx electrode with varying concentrations of $K_3Fe(CN)_6$. *Figure 3.40* shows approach curves to the LOx electrode in 0.1 – 2 mM $K_3Fe(CN)_6$ where current was measured at E_T = 0.4 V vs. Ag/AgCl showing the relationship between tip current and the concentration of $K_3Fe(CN)_6$. Here, an increase in $K_3Fe(CN)_6$ concentration caused greater reduction in current due to a negative feedback response.

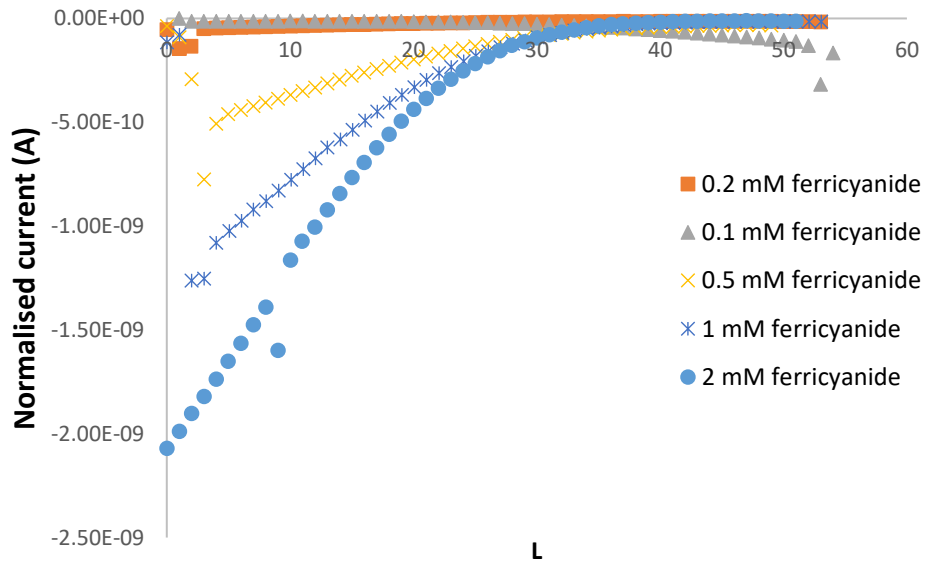

Figure 3.40: Approach curves to LOx sensor in various mediator concentrations in the presence of 15 mM lactate (E_T = 0.4 V) SGTC mode

Figure 3.41 shows area scan experiments at a GCE/Chit/LOx/Chit/GA with 5 mM $K_3Fe(CN)_6$ in the absence (0 mM) and presence of lactate (20 mM). Resulted showed that in the presence of substrate (20 mM), current signal decreased at the enzyme modified region of the electrode surface. Therefore, the active region of the LOx modified surface can be visualised. The UME tip was held at the reduction potential (E_{app} = -0.4 V vs. Ag/AgCl) for reduction of Fe^{3+} to Fe^{2+}. The presence of LOx causes regeneration of Fe^{2+} as the UME tip competes for Fe^{2+} reduction.

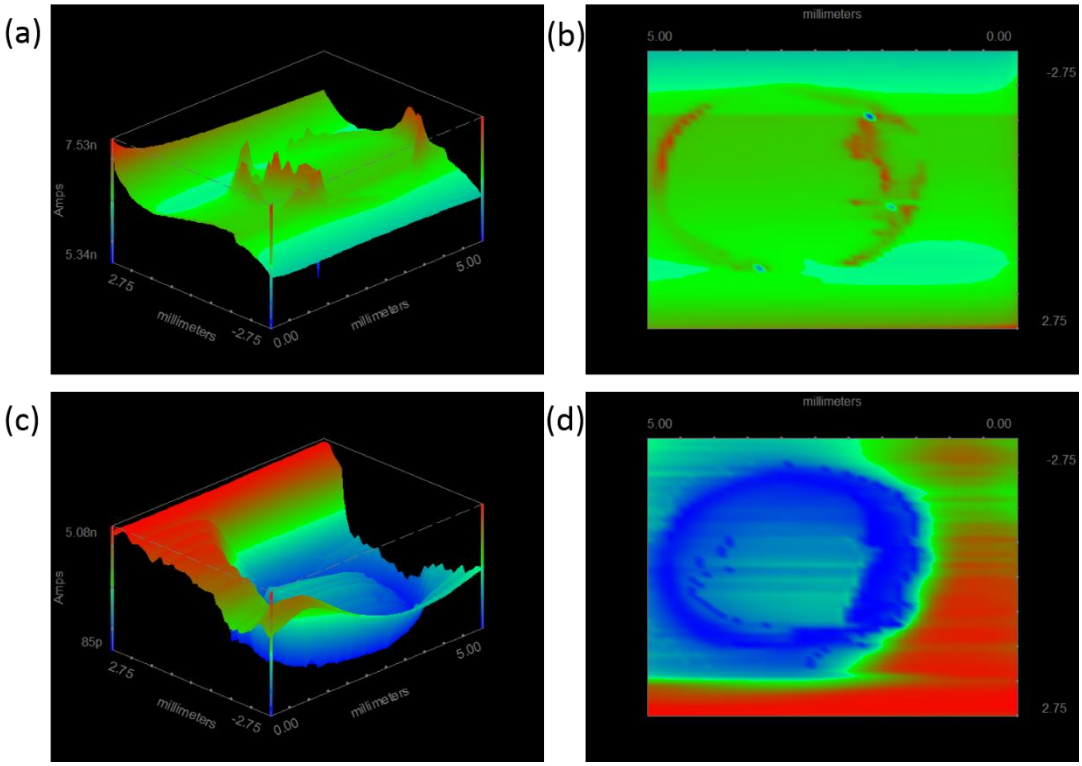

Figure 3.41: Area scan SECM experiment at E_T = -0.4 V vs. Ag/AgCl E_{sub} = OFF, (20 mm Pt, RG = 23.8) 5000 x 5000 mm^2 100 mm per point at LOx modified GCE substrate in 0 mM (a and b) 20 mM (c and d) lactate in the presence of 5 mM $K_3Fe(CN)_6$.

3.6 Conclusion

1st and 2nd generation lactate biosensors were designed and electrochemically analysed using CV and CC analysis. LOx modified Pt electrodes were used for direct detection of lactate while LOx modified GC electrode were analysed for their response to lactate via solution phase mediation in the presence of 5 mM $K_3Fe(CN)_6$. Analytical performance of the 2nd generation biosensor (GCE/Chit/LOx/Chit/GA) resulted in linear range of 9.9 x 10^{-4} to 5.66 x 10^{-3} M, sensitivity of 1.44 x 10^{-3} C $cm^{-2}mM^{-1}$, LOD of 0.54 mM and LOQ of 1.81 mM.

1,10-Phenanthroline-5,6-dione was studied for its potential use as a redox mediator in lactate sensing via thin film voltammetry. Film formation involved potential cycling of a GCE/LOx in 5 mM PD with series of lactate additions (0-4 mM) was determined to be the most effective method for polymerisation of PD onto the surface of a modified GC electrode, resulting in a rod like structures formed on the surface. Graphite ink was formulated as a conducting layer prior to enzyme immobilisation with LOx and enzymatic polymerisation of PD on the surface of a GC electrode. Comparison studies showed the GInk improved the reversibility of the PD film when polymerised on the electrode and provided a greater surface area for layer-by-layer modification. The lactate biosensor gave a linear range of 0.74 – 2.44 x 10^{-3} M, a sensitivity of 4.11 x 10^{-4} C $cm^{-2}mM^{-1}$, LOD of 0.06 mM and LOQ of 0.19 mM. The GCE/GInk/LOx/pPD allowed for determination of lactate concentration in a fermentation sample (t = 0 diluted 1 % v/v in 0.1 M PB (pH 6.0)). Results showed the biosensor measured lactate concentration of 5582 ppm relative to the standard HPLC-RI method result of 7776 ppm. The lower estimation of lactate content could be due to a low concentration of lactate in a (t = 0) sample. Further studies could establishe whether a lower dilution factor could improve the accuracy of the result. Overall this novel lactate biosensor has shown its potential use as an analytical method for rapid lactate concentration in fermentations samples prior to HPLC-RI analysis.

The use of SEM and scanning electrochemical microscopy (SECM redox competition mode) provided surface topographical and imaging/enzyme reactivity information respectively. Experiments included approach curves and line scans to confirm the enzymatic catalytic response of the LOx modified electrode in the absence and present of lactate using $K_3Fe(CN)_6$. Area scans were used to identify the LOx enzyme active region on the electrode in the absence and presence of substrate.

3.7 Bibliography

1. Cunha-Silva H, Arcos-Martinez MJ. Dual range lactate oxidase-based screen printed amperometric biosensor for analysis of lactate in diversified samples. *Talanta*. 2018;188 779-787. doi:10.1016/j.talanta.2018.06.054
2. Pundir CS, Narwal V, Batra B. Determination of lactic acid with special emphasis on biosensing methods: A review. *Biosens Bioelectron*. 2016;86:777-790. doi:10.1016/j.bios.2016.07.076
3. Taurino I, Reiss R, Richter M, Fairhead M, Thony-Meyer L, De Micheli G, Carrara S. Comparative study of three lactate oxidases from Aerococcus viridans for biosensing applications. *Electrochima Acta*. 2013;93:72-79. doi:10.1016/j.electacta.2013.01.080
4. Di J, Cheng J, Xu Q, Zheng H, Zhuang J, Sun Y, Wang K, Mo X, Bi S. Direct electrochemistry of lactate dehydrogenase immobilized on silica sol-gel modified gold electrode and its application. *Biosens Bioelectron*. 2007;23(5):682-687. doi:10.1016/j.bios.2007.08.002
5. Pescuma M, de Valdez GF, Mozzi F. Whey-derived valuable products obtained by microbial fermentation. *Appl Microbiol Biotechnol*. 2015;99(15):6183-6196. doi:10.1007/s00253-015-6766-z
6. Herrero AM, Requena T, Reviejo AJ, Pingarrón JM. Determination of L-lactic acid in yoghurt by a bienzyme amperometric graphite-Teflon composite biosensor. *Eur Food Res Technol*. 2004;219(5):556-559. doi:10.1007/s00217-004-0973-7
7. Zor E, Oztekin Y, Mikoliunaite L, Voronovic J, Ramanviciene A, Anusevicius Z, Bingol H, Ramanavicius A. 1,10-Phenanthroline-5,6-dione and 9,10-phenanthrenequinone as redox mediators for amperometric glucose biosensors. *J Solid State Electrochem*. 2014;18(6):1529-1536. doi:10.1007/s10008-013-2368-9
8. Zor E, Oztekin Y, Ramanaviciene A, Anusevicius Z, Bingol H, Barkauskas J, Ersoz M, Ramanaviciene A. Amperometric Glucose Biosensor Based on Glucose Oxidase, 1,10-Phenanthroline-5,6-dione and Carbon Nanotubes. *J Electrochem Soc*. 2014;161(13):H3064-H3069. doi:10.1149/2.0061413je
9. Hadadzadeh H, Olmstead MM, Rezvani AR, Safari N, Saravani H. Synthesis, structure, spectroscopic, magnetic and electrochemical studies of NiII phen-

dione complex. *Inorganica Chim Acta*. 2006;359(7):2154-2158. doi:10.1016/j.ica.2006.02.015

10. Yokoyama K, Wakabayashi A, Noguchi K, Nakamura N, Ohno H. Structure and spectroelectrochemical property of a ruthenium complex containing phenanthroline-quinone, and assembly of the complexes on a gold electrode. *Inorganica Chim Acta*. 2006;359(3):807-814. doi:10.1016/j.ica.2005.05.038
11. Hedenmo M, Narváez A, Domínguez E, Katakis I. Reagentless amperometric glucose dehydrogenase biosensor based on electrocatalytic oxidation of NADH by osmium phenanthrolinedione mediator. *Analyst*. 1996;121(12):1891-1895. doi:10.1039/an9962101891
12. Ciftci H, Oztekin Y, Tamer U, Ramanaviciene A, Ramanavicius A. Electrochemical biosensor based on glucose oxidase encapsulated within enzymatically synthesized poly(1,10-phenanthroline-5,6-dione). *Colloids Surfaces B Biointerfaces*. 2014;123:685-691. doi:10.1016/j.colsurfb.2014.10.032
13. Bandodkar AJ, Jia W, Ramírez J, Wang J. Biocompatible Enzymatic Roller Pens for Direct Writing of Biocatalytic Materials: “Do-it-Yourself” Electrochemical Biosensors. *Adv Healthc Mater*. 2015;4(8):1215-1224. doi:10.1002/adhm.201400808
14. Oztekin Y, Krikstolaityte V, Ramanaviciene A, Yazicigil Z, Ramanavicius A. 1,10-Phenanthroline derivatives as mediators for glucose oxidase. *Biosens Bioelectron*. 2010;26(1):267-270. doi:10.1016/j.bios.2010.05.005
15. Wu M, Mao X, Li X, Yang X, Zhu L. 1,10-phenanthroline-5,6-dione adsorbed on carbon nanotubes: The electrochemistry and catalytic oxidation of ascorbic acid. *J Electroanal Chem*. 2012;682:1-6. doi:10.1016/j.jelechem.2012.06.007
16. Evans DH, O’Connell KM, Petersen RA, Kelly MJ. Cyclic voltammetry. *J Chem Educ*. 1983;60(4):290. doi:10.1021/ed060p290

Chapter 4 : Deployment of glucose, lactose and lactic acid biosensors in dairy sample monitoring

4.1 Introduction

The dairy industry is one of the largest food processing sectors in the world. Along with the main processing of milk in dairy manufacturing facilities, another important side stream process includes lactic acid and polylactic acid (PLA) production.[1] Often used for the production of bio-plastics, polylactic acid is made from both (+) and (-) lactic acid isomers. Fermentation processes using lactic acid bacteria (LAB) can be used for the manufacture of lactic acid. Under optimum conditions, the LAB proliferate in whey permeate and promote the production of lactic acid as a result of lactose fermentation.[2] During the fermentation process, the usual conditions are often monitored including temperature, pH, and dissolved O_2 levels. Continuous monitoring of lactose and lactic acid are required for understanding the reaction progress. Samples are generally taken at various time points during the fermentation process and analysed for their lactose and lactic acid content. *Figure 4.1* shows an ideal fermentation process which involves a decrease in lactose content and an increase in lactic acid concentration over time showing a typical inter conversion of the analytes.

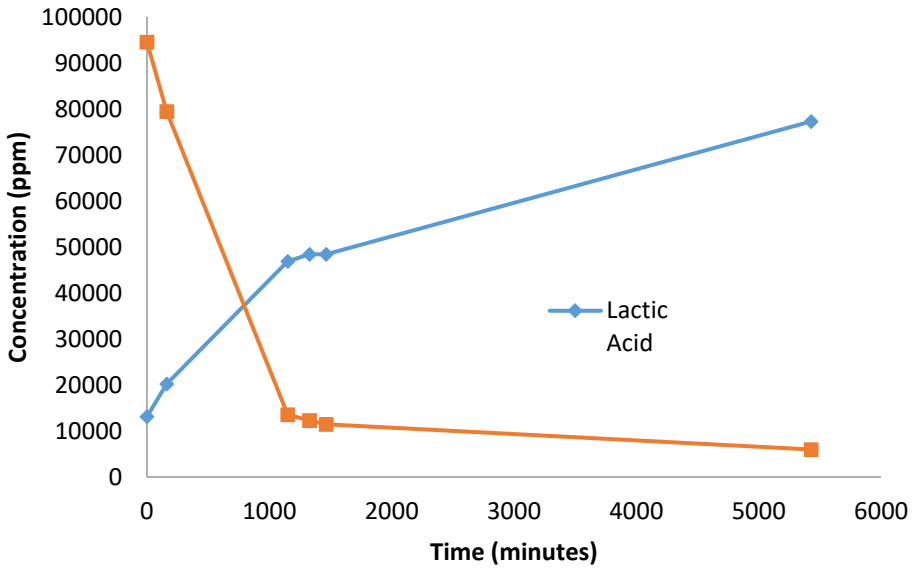

Figure 4.1: Typical lactose fermentation process for lactic acid production.

Currently, the industry sector relies on analytical methods such as High Pressure Liquid Chromatography (HPLC) for the quantitation of key analytes in each sample taken. A common method for lactose and lactic acid detection includes HPLC-RI which is a highly accurate method.[3] However, it requires the use of highly trained

personnel to perform and obtain data. It is also a very time-consuming, laborious procedure with many industrial companies choosing to send their samples to external labs for testing. This can lead to severe delays and causes halts in production. Such methods can be utilised to assess the quality of final products but are unsuitable for use in the monitoring of the process which requires faster turnaround time to result.[4] Biosensors form an alternative detection method for on-site testing of key analytes in a dairy fermentation bioprocess, being rapid detection methods that have been developed for use in various different medical and pharmaceutical fields.[5] The development of biosensors for use in lactic acid production could assist in overcoming issues with sample testing and lead towards cost effective, rapid and easy to use portable biosensors. Such sensors would eliminate the use of external laboratories and would the requirement for highly skilled personnel to perform sample testing on site. With the use of specific enzymes, biosensors can be developed to detect and quantify glucose, lactose and lactic acid in dairy samples including whey permeate, milk protein isolates (MPI) and fermentation samples.[4]

Kamanin *et al.* reported the development of a biosensor with potential use in the fabrication of a prototype for use in fermentation process monitoring.[4] Screen-printed sensors were modified with glucose oxidase, alcohol oxidase and lactate oxidase and immobilised using BSA and GA. The crosslinking of these compounds ensures a suitable pore size for enzyme immobilisation and good diffusion between substrates and other metabolites. The biosensor was used for testing of fermentation samples (0 – 72 hours) and results were compared with HPLC, GC and CE methods. Good correlation was observed between the biosensor relative to reference method with a 48 h fermentation sample showing glucose concentration determined via the biosensor of 0.19 ± 0.01 M and reference method 0.214 ± 0.002 M. Similar results were observed for lactate concentration with 0.15 ± 0.02 M obtained from the biosensor and 0.15 ± 0.01 M for reference method. The correlation indicates the potential for the biosensor to undergo further optimisation and expand its use in biosensor fabrication.

Further optimisation of such biosensors could lead the way to at-line biosensors for continuous monitoring of processes in the dairy industry. The use of at-line measurement systems to monitor lactose in industry has been of interest due to the ability to continuously measure product stream. Glithero *et al.* describe the development and trialling of an “at-line” lactose third generation biosensor connected

to an injection analyser. The prototype was installed in Fonterra, a dairy factory in New Zealand between 2011-2012. Comparison of results from grab-sample analysis and the prototype was executed to ensure the efficiency of the installed sensor. The sensor was used to monitor wastewater streams which will aid in the efficiency of the manufacturing plant, increase sales in product and decrease effluent waste from the plant.[6] Samples were taken by the sensor every 2-3 minutes to semi-continually monitor the concentration of lactose of the wastewater over a 3 month period, which can see 100-300,000 litres of wastewater produced each hour. Results obtained from the sensor showed lactose content range between 0-8 % w/v (0-0.23 M) during testing. By using such a sensor, analysts were able to determine the total loss of lactose from the plant which counted for lost sales and loss of useful product. This demonstrates the successful use of biosensors in industry and shows the potential use of sensors for on-site analysis or continuous monitoring of processes.

4.2 Chapter aims

The main aim of this work was to detect and determine the concentrations of glucose, lactose and lactic acid in real industrial samples using the sensors developed in *Chapter 2*. Direct detection of glucose and lactose in whey permeate samples was performed using modified Pt electrodes. A solution mediated approach using $K_3Fe(CN)_6$ was carried out for the determination of lactose and lactic acid in milk protein isolates (MPI) and fermentation samples provided by the industry partner, using enzymatic biosensors fabricated at carbon SPE or GCE via CV, CC and CA techniques. The results obtained from electrochemical analysis were correlated with other established approaches including HPLC and other commercial sensor methods (Lactosens) (https://www.chr-hansen.com/en/food-cultures-and-enzymes/test-and-equipment/cards/product-cards/lactosens). Each biosensor was used to quantify glucose, lactose and/or lactic acid content in the following dairy sample matrices;

A. Whey permeate
B. Milk Protein Isolates
    I. MPI 1 (low-lactose sample)
    II. MPI 10 (standard sample)
C. Fermentation samples

4.3 Experimental

4.3.1 Materials

MetaDi Monocrystalline Diamond suspension (1 μm) was purchased from Akasel. Glucose Oxidase from *Aspergillus niger* (Type VII, lyophilized powder 10KU), β-galactosidase from *Aspergillus oryzae* (25KU), Chitosan (from Shrimp shells, practical grade), D-(+)-Glucose (≥99.5% (GC)), Bovine Serum Albumin (lyophilized powder, ≥ 96 % (agarose gel electrophoresis)), Poly(ethylene glycol) diglycidyl ether (average Mn 500), and Potassium phosphate dibasic trihydrate (ReagentPlus ≥99.0%) were all obtained from Sigma Aldrich. D (+)-Lactose 1-hydrate BioChemica, Glutaraldehyde solution 25 % for synthesis, Acetic acid (100%) and Potassium di-Hydrogen Phosphate for Analysis, ACS were purchased from ITW reagents.

4.3.2 Instrumentation

Experiments were carried out on two different electrochemical systems. The majority of experiments were performed on a Solartron 1285 Potentiostat connected to a computer with general purpose electrochemical software CorrWare and electrochemical data analyser CView. A three electrochemical cell set up was used that contained a platinum wire for the counter electrode, Ag/AgCl reference (in 3 M KCl) along with the modified electrodes.

The determination of lactose in fermentation samples was performed on a DropSens portable potentiostat (model = μSTAT200) (see *Figure 4.2*) to demonstrate the potential for on-site analysis of samples. Modified commercial screen-printed electrodes were used for analysis with data analysis software DropView200.

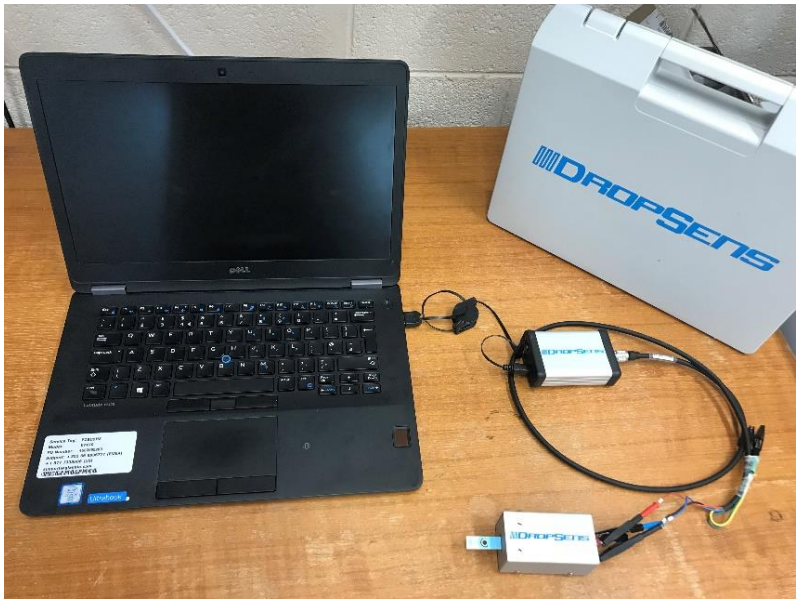

Figure 4.2: DropSens portable potentiostat for on-site analysis

4.4 Procedures

4.4.1 Sample preparation

Whey permeate samples were prepared by dilution in 0.1 M PB (pH 6.0) to 1 % w/v for direct detection and quantitation of glucose and lactose. Samples subsequently underwent sonication for 10 minutes.

MPI samples were prepared by diluting to 1 % w/v in 5 mM $K_3Fe(CN)_6$ (in 0.1 M PB (pH 6.0)) followed by sonication for 10 minutes.

Fermentation samples were stored as frozen aliquots and defrosted at room temperature prior to analysis. Each sample (different time point in the process) was then heated to 40 ^oC for 1 hour to ensure homogenisation before dilution to in 5 mM $K_3Fe(CN)_6$ (0.1 M PB (pH 6.0)) to 1 % v/v. Due to high levels of lactate in fermentation sample taken at (t = 1076), it was diluted to 0.25 % v/v.

4.4.2 Direct detection of glucose and lactose in whey permeate samples using modified Pt electrodes

CV was performed at a Pt/Chit/GOx/Chit/GA electrode using whey permeate samples which were diluted in 0.1 M PB (pH 6.0) (1 % w/v) and then spiked with 1.98 mM glucose; potential range -0.2 V to 1.0 V at 100 mVs^{-1}. CC was carried out E_{app} = 0.8 V vs. Ag/AgCl to determine background glucose content in the sample via the standard

addition method with additions of 0 – 9.09 mM glucose.

CV was carried out at a Pt/Chit/GOxβ-gal/Chit/GA using whey permeate samples diluted in 0.1 M PB (pH 6.0) (1 % w/v) and then spiked with 1.98 mM lactose; potential range -0.1 V to 1.0 V vs. at 100 mVs^{-1}. CC was performed E_{app} = 0.65 V vs. Ag/AgCl was then utilised to detect and quantify lactose in the whey permeate sample via standard addition method of 0 – 9.09 mM lactose.

Extrapolation of data for charge vs. concentration plots was carried out to determine concentration of glucose or lactose in the relevant sample (1 % w/v). Glucose contributing signals were subtracted from the lactose signal in order to correct for background glucose present in the whey permeate sample.

4.4.3 Determination of lactose in Milk Protein Isolate samples using solution mediated approach

CV analysis was performed at GC/Chit/GOxβ-gal/Chit/GA electrode using MPI sample (MPI 1 and MPI 10) diluted in 5 mM $K_3Fe(CN)_6$ (in 0.1 M PB (pH 6.0)) (1 % w/v), followed by additions of lactose (0 – 9.09 mM); potential range -0.3 V to 0.5 V vs. Ag/AgCl at 100 mVs^{-1}. CC analysis for the same samples involved E_{app} = 0.35 V vs. Ag/AgCl followed by lactose additions (0.09 – 9.09 mM)

Data values for charge vs. concentration were plotted and extrapolation of the data performed in order to determine lactose concentration in diluted sample (1 % w/v).

4.4.4 Lactose quantitation in fermentation samples using a solution mediated system at modified SPE

Determination of lactose content in fermentation samples taken at time intervals (t = 0, t = 880, t = 1206 minutes) over the period 0 - 1206 minutes was performed. This measurement involved modified screen printed electrodes and the use of a portable potentiostat for on-site industry testing. Samples were diluted in 5 mM $K_3Fe(CN)_6$ in 0.1 M PB (pH 6.0) (1 % v/v).

CA analysis at E_{app} = 0.25 V vs. Ag/AgCl was performed for the above samples, spiked over the range (0 - 9.09 mM for t = 0, 0 – 2.43 mM for t = 880 and 0 – 1.23 mM for t = 1206) with quantitation via the standard addition method. The t = 0 sample point involved a higher lactose level and hence the concentration range was extended.

4.4.5 Determination of Lactic acid content in fermentation samples using a solution mediated approach at modified GCE

Determination of lactic acid was performed in fermentations samples taken at time intervals (t = 0, t = 887 and t = 1076) over the period 0 – 1076 minutes. Measurements involved using GC/Chit/LOx/Chit/GA electrodes. Samples were diluted in 5 mM $K_3Fe(CN)_6$ in 0.1 M PB (pH 6.0) (1 % v/v).

CC was performed with (E_{app} = 0.38 V) vs. Ag/AgCl for the above samples spiked over the range (0 – 2.91 mM) with quantitation via the standard addition method.

4.5 Results and Discussion

Here, we examine the use of biosensors, developed as described in Chapter 2, as analytical tools in the determination of glucose, lactose and lactate in a range of real samples obtained from a dairy industry partner. Direct detection and concentration content of glucose and lactose was performed for diluted whey permeate samples. A solution mediated approach was taken for the analysis of lactose in the case of MPI samples. Lactose and lactic acid determination for fermentation samples (at various time points) involved the use of redox mediator $K_3Fe(CN)_6$ at modified SPE or GC electrodes.

4.5.1 Whey permeate sample analysis

The concentration of glucose and lactose in whey permeate was determined by CV and CC analysis. Due to the presence of GOx in the lactose dual-enzyme biosensor and catalytic reactions involved, results obtained for lactose concentration may be overestimated due to the presence of free glucose in the sample. Therefore, a glucose biosensor was utilised to obtain free glucose concentration which was subtracted from the value obtained for lactose.

Figure 4.3 shows a CV of 0.1 M PB (pH 6.0), whey permeate sample (1 % w/v) and the sample spiked with 1.98 mM glucose at a Pt/Chit/GOx/Chit/GA electrode. A small difference in current value resulted in the case of the diluted whey permeate sample relative to the electrolyte, while additions of 1.98 mM glucose showed an increase in current between 0.5 V – 1.0 V, indicating H_2O_2 production, as a result of the glucose turnover.

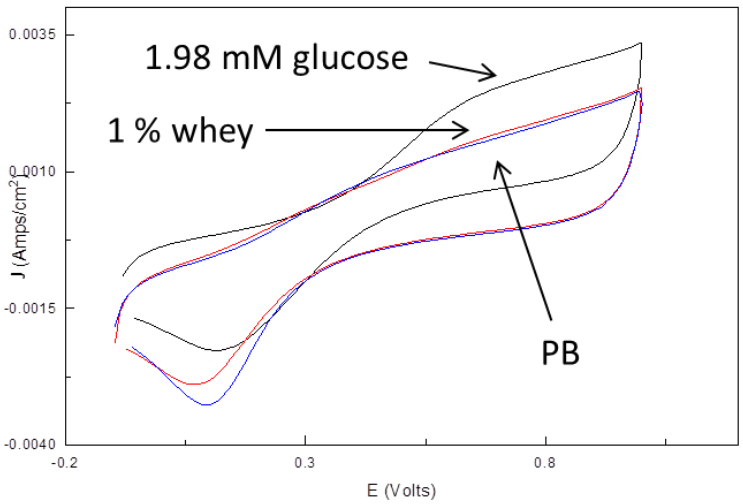

Figure 4.3: CV of 0.1 M PB (pH 6.0), whey permeate (1 % w/v) followed by addition of glucose (1.98 mM) at Pt/Chit/GOx/Chit/Pt. Potential range -0.2 V to 1.0 V and a scan rate of 100 mVs^{-1}.

CC was performed at a Pt/Chit/GOx/Chit/GA, E_{app} = 0.8 V vs. Ag/AgCl for 0.1 M PB, whey permeate sample (1 % w/v) followed by glucose additions (0.99 – 9.09 mM) *(Figure 4.4(a))*. Extrapolation of data *(Figure 4.4(b))* resulted in a glucose concentration of 1.3 mM in the whey permeate sample (1 % w/v), corresponding to 130 mM in the undiluted sample.

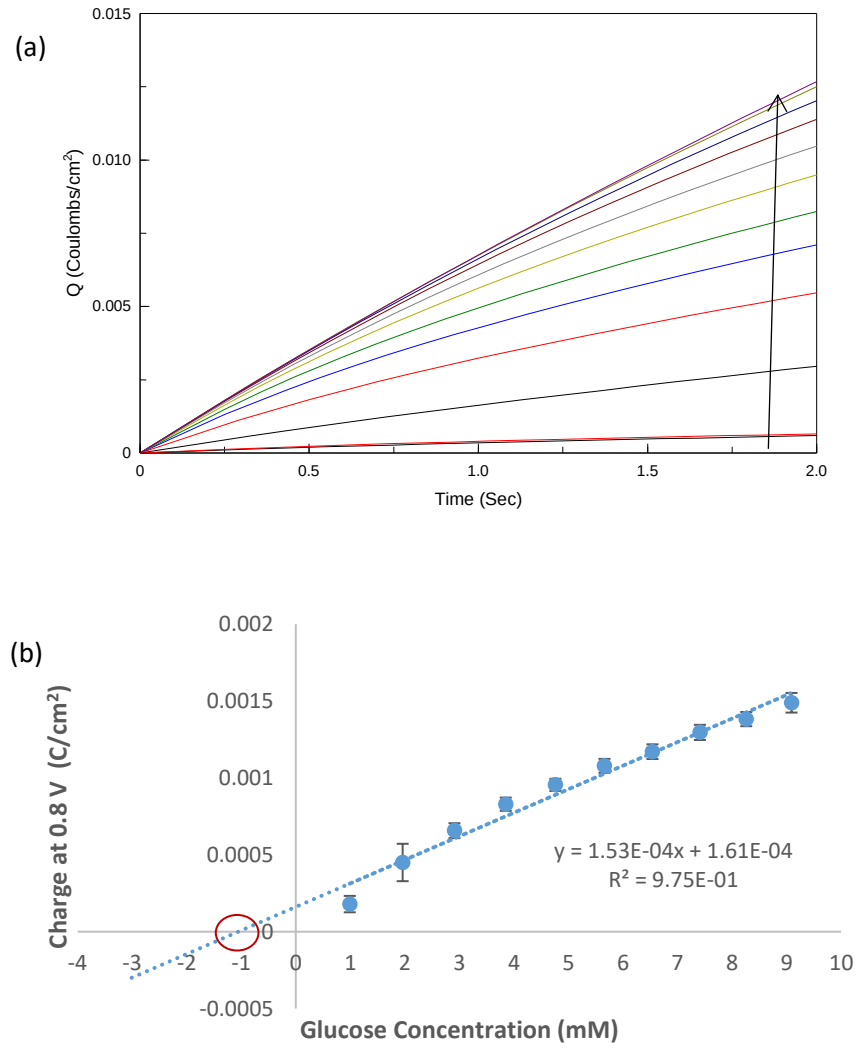

Figure 4.4: (a) Chronocoulometric data showing response to 0.99 – 9.09 mM glucose concentrations at Pt/Chit/GOx/Chit/GA in a whey permeate sample (1 % w/v diluted in 0.1 M PB) E_{app} = 0.8 V vs. Ag/AgCl. (b) Calibration curve of charge (C/cm^2) vs. glucose concentration (mM) in whey permeate sample (1 % w/v) (R^2 = 0.9755) (n = 3).

The quantitation of lactose in whey permeate was carried out using CV at a Pt/Chit/GOxβ-gal/Chit/GA electrode. *Figure 4.5* shows a CV of 0.1 M PB (pH 6.0), whey permeate sample (1 % w/v) and sample spiked with 1.98 mM lactose. An increase in current was observed at 0.65 V vs. Ag/AgCl corresponding to H_2O_2 production for the 1 % whey permeate sample relative to the background electrolyte (PB, pH 6.0) and a further increase in current after spiking the sample with 1.98 mM lactose. Background signals were evident over the range 0.65 -0.9 V and a 100-fold sample dilution was required (in PB pH 6.0).

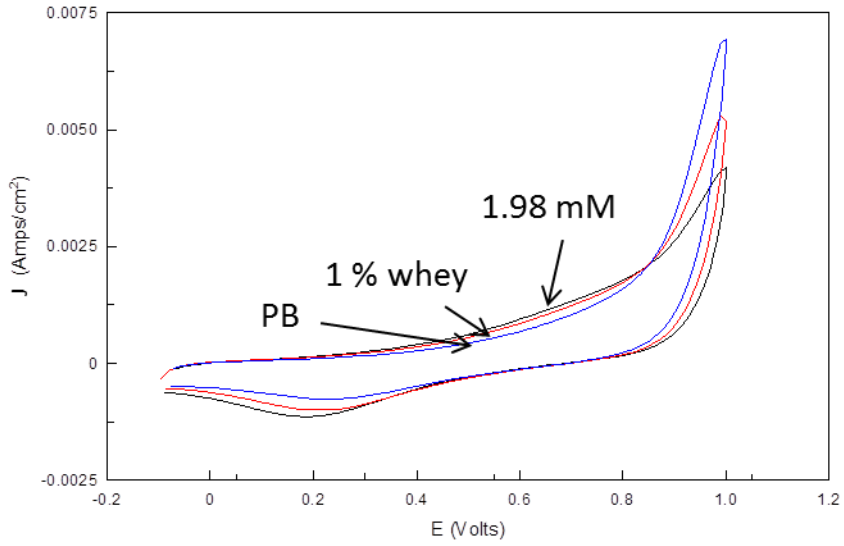

Figure 4.5: CV of 0.1 M PB (pH 6.0), whey permeate sample (1 % w/v) and spiked lactose (1.98 mM) at Pt/Chit/GOxβ-gal/Chit/GA. Potential range -0.1 V to 1.0 V vs. Ag/AgCl at 100 mVs^{-1}.

CC analysis followed at E_{app} = 0.65 V vs. Ag/AgCl for 2 s (*Figure 4.6*). Results showed a linear relationship between charge and lactose concentration for direct detection at a Pt/Chit/GOxβ-gal/Chit/GA electrode. Extrapolation of data (*Figure 4.6(b)*) was carried out for charge vs. concentration plots to determine lactose concentration in the diluted sample. The lactose biosensor measured 25 mM lactose in the whey permeate sample (1 % w/v). To account for free glucose in the sample, the glucose signal was subtracted from the lactose signal which resulted in 23.7 mM determined lactose levels. Results were compared with the Certificate of Analysis (COA) (provided by the industry partner) for the whey permeate sample data which showed 25.7 mM lactose, resulting in 92.2 % correlation between the biosensor and the standard analytical approach for lactose measurement (HPLC-RI) in whey permeate samples.

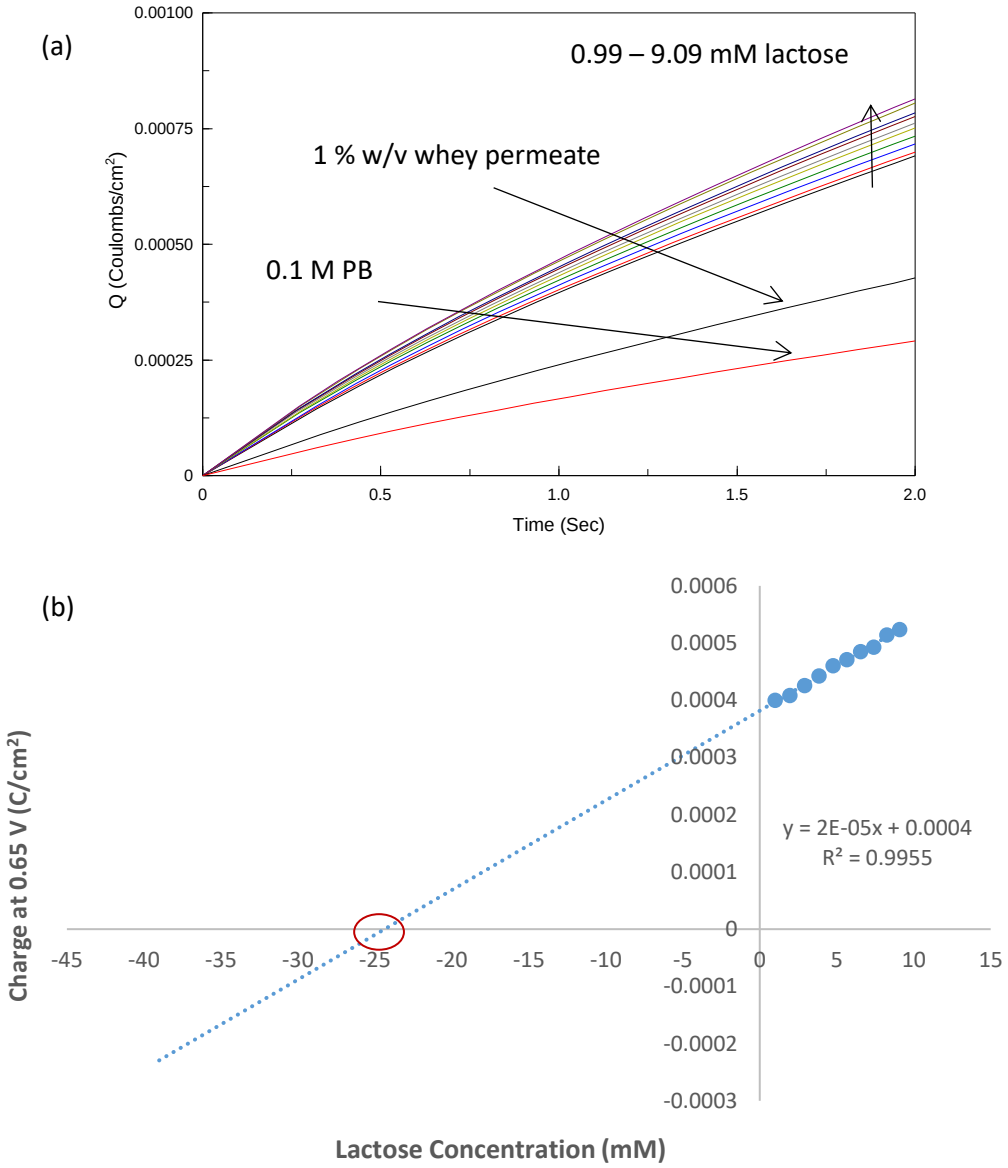

Figure 4.6: (a) Chronocoulometric data of 0.99 – 9.09 mM lactose concentrations in whey permeate sample diluted in 0.1 M PB (pH 6.0) (1 % w/v) E_{app} = 0.65 V vs. Ag/AgCl for 2 s (b) Calibration curve of lactose concentration (0.99 – 9.09 mM) vs. charge at 0.65 V vs. Ag/AgCl in a diluted whey permeate sample (1 % w/v) (R^2 = 0.99).

4.5.2 Milk Protein Isolate sample analysis by solution phase mediation

A 2nd generation biosensor was utilised for the determination of lactose concentration in two MPI samples, labelled MPI 1 and MPI 10. MPI 10 is a standard lactose sample whereas the MPI 1 sample has low-lactose content. The samples were diluted in 5 mM $K_3Fe(CN)_6$ (in 0.1 M PB (pH 6.0)) (1 % w/v) prior to analysis at GC/Chit/GOxβ-gal/Chit/GA electrodes via solution phase mediation of lactose. *Figure 4.7* shows a CV background electrolyte, solution mediation 5 mM $K_3Fe(CN)_6$ followed by MPI 10 sample (1 % w/v) spiked with 0 - 9.09 mM lactose added via standard addition. Here,

an increase in current is evident at the oxidation peak between 0.2 – 0.4 V. As discussed previously in *Chapter 2*, increased Fe^{2+} reoxidation signals resulted in enhanced current as Fe^{3+} is required to oxidise the $FADH_2$ enzyme prosthetic group FAD, as described in *Equations 2.2-2.4*.

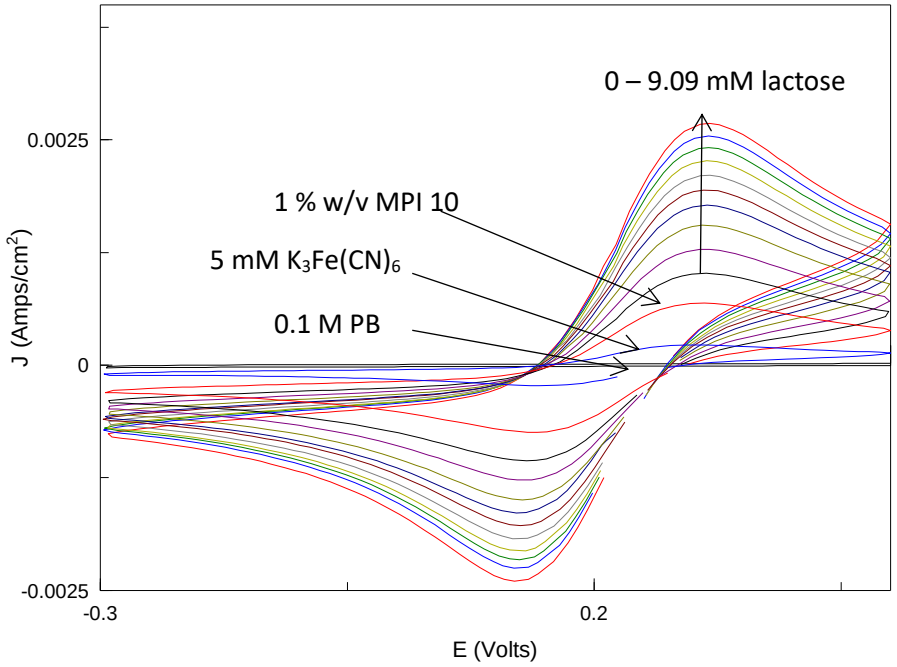

Figure 4.7: Overlay of CV data for 0 - 9.09 mM Lactose concentrations in MPI 10 diluted in 5 mM $K_3Fe(CN)_6$ (1 % w/v); potential range -0.3 V to 0.5 V vs. Ag/AgCl and a scan rate of 100 mVs^{-1}.

CC analysis was performed (E_{app} = 0.35 V vs. Ag/AgCl) for both MPI 1 and MPI 10 samples to determine the concentration of lactose via standard addition. *Figure 4.8* shows background electrolyte, 5 mM $K_3Fe(CN)_6$, MPI 10 sample (1 % w/v) followed by spiked lactose additions (0.09 – 0.9 mM). Extrapolation of the corresponding data shows the biosensor measured 0.45 mM lactose in the diluted MPI 10 sample (1 % w/v).

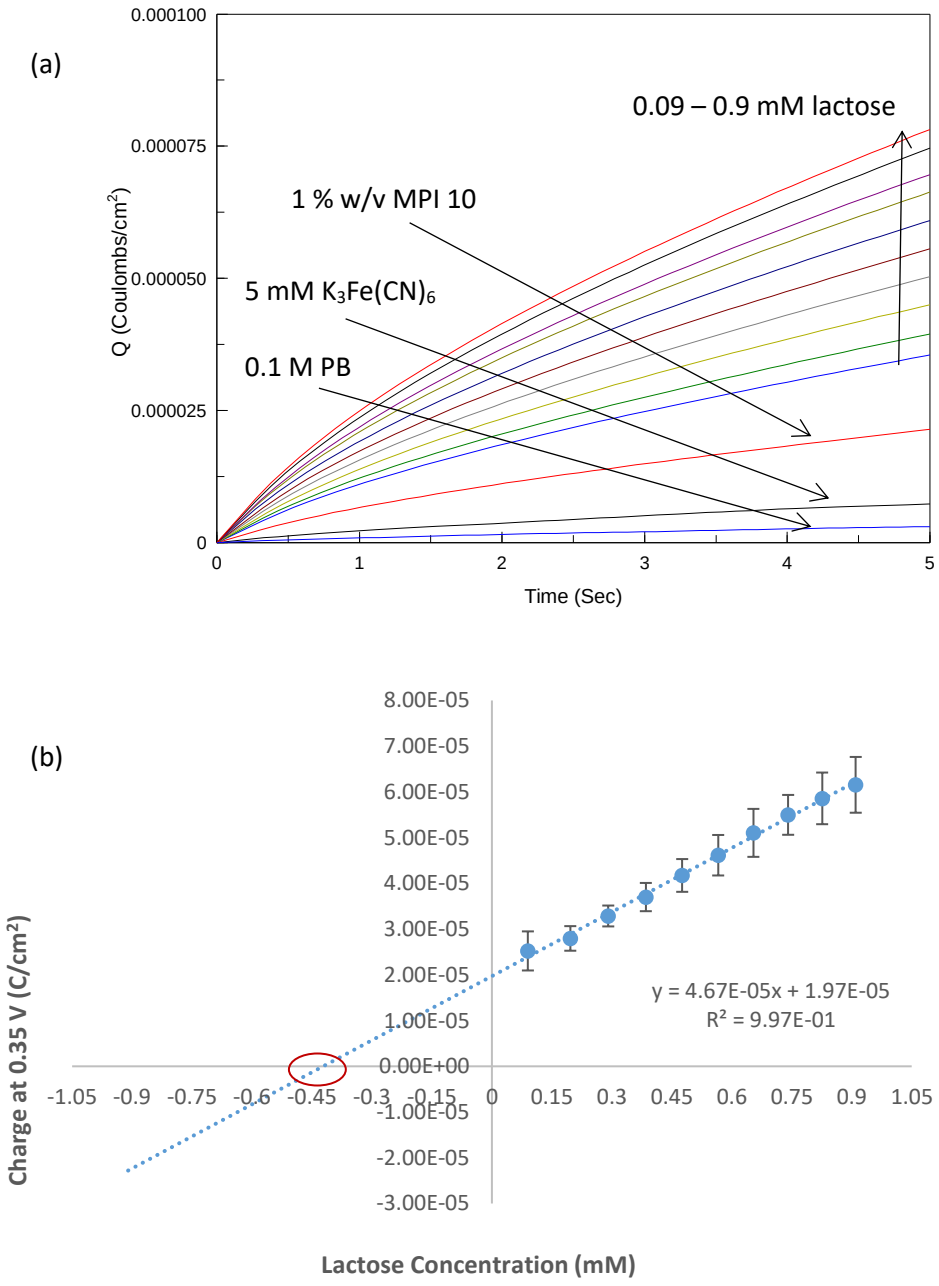

Figure 4.8: (a) Overlay of CC data of 0.1 M PB, 5 mM $K_3Fe(CN)_6$, MPI 10 (diluted to 1 % w/v) and lactose additions (0.09 - 0.9 mM). Charge measured at 0.35 V vs. Ag/AgCl at 5 s. (b) Extrapolation of data for charge vs. lactose concentration (0.09 - 0.9 mM) in a diluted MPI 10 sample (1 % w/v) (n=3).

Lactose determination was performed for the MPI 1 sample (1 % w/v) by chronocoulometric analysis with E_{app} = 0.35 V vs. Ag/AgCl (*Figure 4.9*) showing an increase in charge for lactose. Extrapolation of the corresponding CC data resulted in 0.34 mM lactose in the diluted MPI 1 sample (1 % w/v) measured at the GC/Chit/GOxβ-gal/Chit/GA electrode.

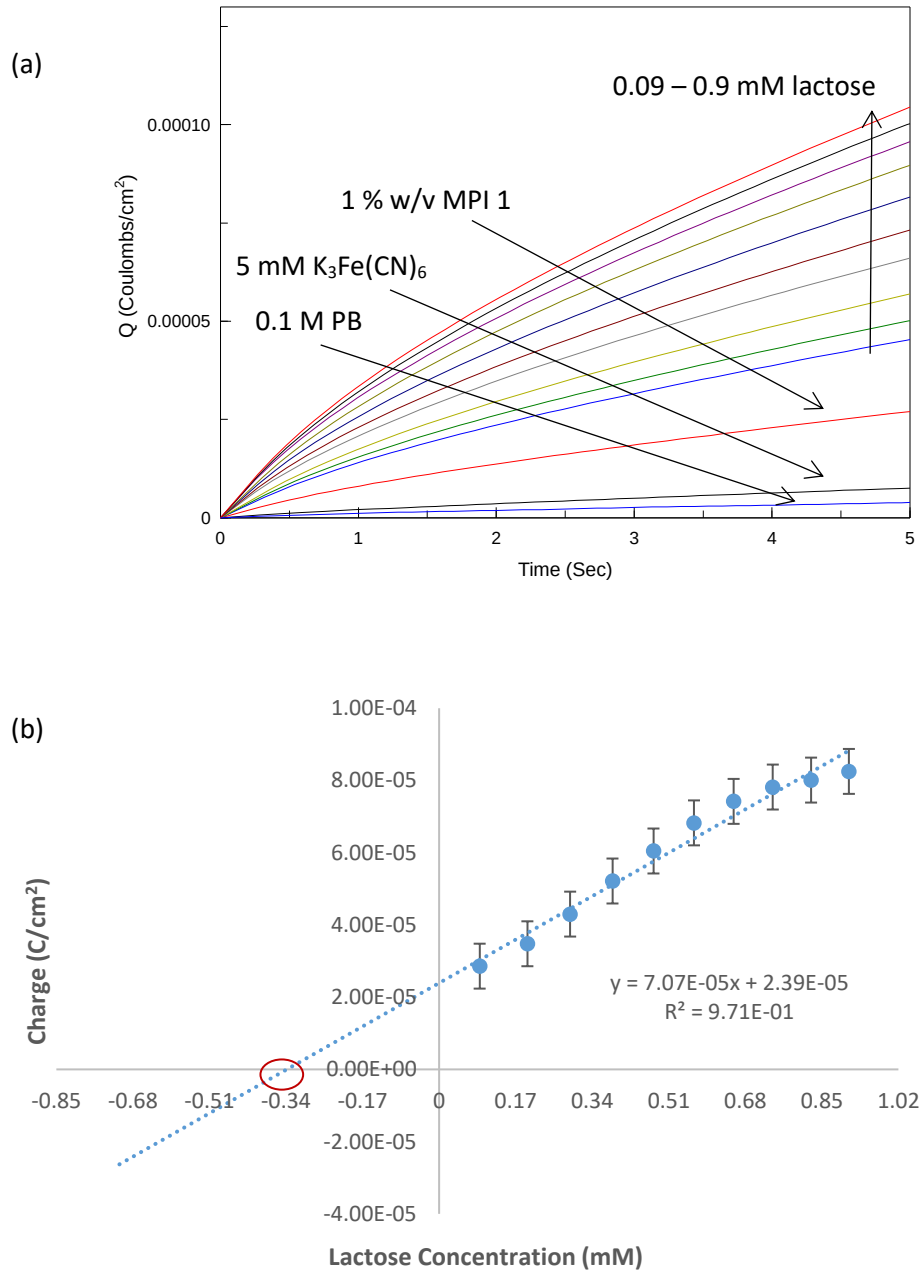

Figure 4.9: (a) Overlay of data of 0.1 M PB (pH 6.0), 5 mM $K_3Fe(CN)_6$ and MPI 1 sample (1 % w/v) spiked with 0.09 – 0.9 mM lactose concentrations. CC with E_{app} = 0.35 V vs. Ag/AgCl. (b) Extrapolation of corresponding data for charge at 0.35 V vs. Ag/AgCl and lactose concentration (mM) in a diluted MPI sample (1 % w/v) (n=3).

Results from the GC/Chit/GOxβ-gal/Chit/GA electrode (labelled Biosensor in *Table 4.1*) was compared with three other methods for lactose quantitation in MPI samples. Lactosens is a commercially available sensor for measurement of low lactose content in milk or other dairy products.[7]

Table 4.1 shows the values obtained by the other analytical techniques including HPLC methods with two different detection methods (RI and IC-PAD). HPLC was

carried out by external labs with the HPLC-IC-PAD method being the most reliable analytical technique for lactose quantitation in this sample type. The results of the biosensor developed in this work showed a 67 % correlation for the MPI 1 sample with the HPLC-IC-PAD method and 95 % correlation for the MPI 10 sample. The underestimation of lactose in the MPI 1 sample may be due to a very low concentration of lactose present in the sample. In this case a higher dilution factor may help to determine a more accurate level of lactose.

Table 4.1: Comparison of data obtained from Lactosens, Biosensor, HPLC-RI and HPLC-IC-PAD in g/100g, mM and ppm values.

Sample Description	**Lactosens (g/100g)**	**Biosensor (g/100g)**	**HPLC-RI (g/100g)**	**HPLC–IC-PAD (g/100g)**	**% error***
MPI 1	0.53	1.16	0.6	0.87	
MPI 10	1.375	1.54	1.7	1.61	
	(mM)	**(mM)**	**(mM)**	**(mM)**	
MPI 1	15.5	34	17.5	25	
MPI 10	40.2	45	49.6	47	
	(ppm)	**(ppm)**	**(ppm)**	**(ppm)**	
MPI 1	5300	11638.2	5990.25	8557.5	36 %
MPI 10	13750	15403.5	16978.08	16088.1	4.26 %

***** % error of biosensor relative to HPLC-IC-PAD method

4.5.3 Fermentation sample analysis

4.5.3.1 Determination of lactose in fermentation sample using enzyme modified screen-printed electrodes

Lactose detection in fermentation samples at various time points was carried out at the industry partner location using SPE/Chit/GOxβ-gal/Chit/GA electrodes with the aid of a portable Dropsens potentiostat. Initial studies were performed to demonstrate the expected decreasing trend in lactose concentration over the time period of the fermentation process. *Figure 4.10* shows a CV of 0.1 M PB (pH 6.0), 5 mM $K_3Fe(CN)_6$ and fermentation samples (Time 0 – 1347 minutes) at a SPE/Chit/GOxβ-gal/Chit/GA electrode. Results were as expected as the initial sample (t = 0) showed the highest current response at the modified SPE while (t = 1347) gave the lowest current response, indicated lower levels of lactose in the sample.

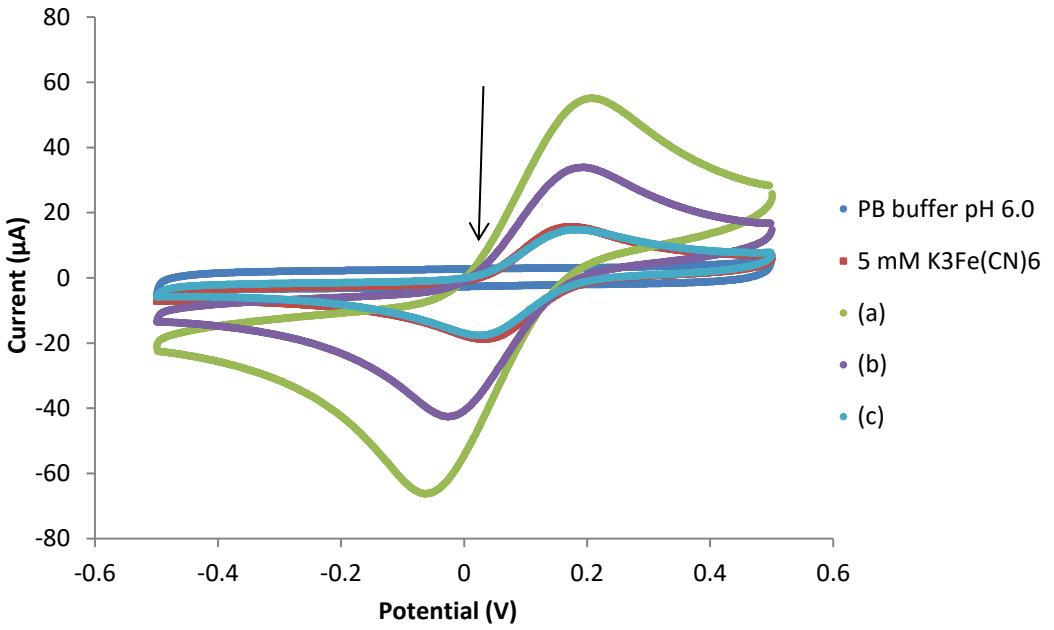

Figure 4.10: CV of 0.1 M PB (pH 6.0), 5 mM $K_3Fe(CN)_6$ and fermentation samples ((a) t = 0, (b) t = 1093 and (c) t = 1347) diluted in 5 mM $K_3Fe(CN)_6$ (1 % v/v) at a SPE/Chit/GOxβ-gal/Chit/GA electrode. Potential range -0.5 V to 0.5 V vs. Ag/AgCl at 100 mVs^{-1}.

Following this, CA analysis was carried out for quantitative analysis of lactose in a fermentation sample taken at (t = 0) (E_{app} = 0.25 V vs. Ag/AgCl). Measured current was obtained for background electrolyte, fermentation sample (t = 0) (1 % v/v) followed by spiking with (0 – 9.09 mM) lactose at the modified SPE. The calibration curve generated (*Figure 4.11*) has been corrected for the signal contribution of the diluted fermentation sample. This was used to calculate lactose content in the sample which was determined to be 306 mM for the undiluted sample or 110,440 ppm. Results were compared to HPLC-RI which measured 110,318 ppm indicating a 99.86 % correlation between the values.

This curve enabled further quantitation for subsequent samples including a (t = 0) sample (diluted in 5 mM $K_3Fe(CN)_6$ to 1 % v/v). Inter-correlation results were obtained by using three modified SPE to measure current in the same (t = 0) fermentation sample. *Table 4.2* shows the results for lactose quantitation using three different lactose biosensors measuring between 279 – 284 mM (95418 – 97213 ppm) for the undiluted sample. HPLC data obtained measured 223 mM (80596 ppm), meaning the % agreement between the average result of the biosensor and HPLC data was 80.23 %.

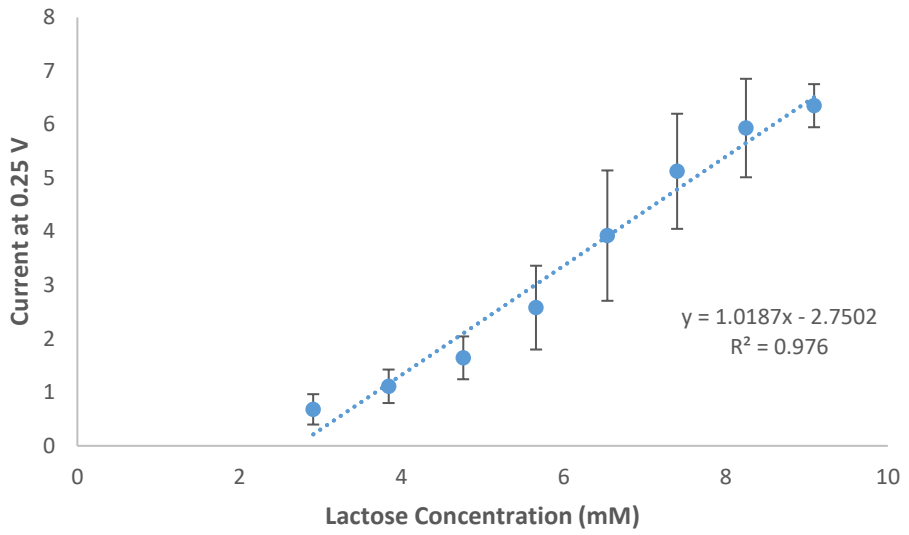

Figure 4.11: Data plot for CA analysis showing calibration of lactose biosensor at (t = 0) sample (diluted in 5 mM $K_3Fe(CN)_6$ to 1 % v/v). Additions of lactose prior to each measurement resulted in range of 0 – 9.09 mM (n=2).

Table 4.2: Inter-correlated results of fermentation sample taken at (t = 0) for lactose determination using calibration curve *(Figure 4.11)*.

	Sensor 1 Current* (µA)	**Sensor 2 Current* (µA)**	**Sensor 3 Current* (µA)**
5 mM $K_3Fe(CN)_6$	0.1452	0.1000	0.1202
t = 0 sample (1 % v/v)	0.2967	0.2353	0.2219
t = 0 sample (1 % v/v) – 5 mM $K_3Fe(CN)_6$	0.1514	0.1353	0.1016
Lactose concentration in ORIGINAL sample (100%)			
SENSOR (mM) / (ppm)	284 mM / 97213 ppm	283 mM / 96871 ppm	279 mM / 95418 ppm
HPLC (mM) / (ppm)	223 mM / 80596 ppm	223 mM / 80596 ppm	223 mM / 80596 ppm

*Current taken at E_{app} = 0.25 V vs. Ag/AgCl.

Lactose quantitation was performed in the case of middle (t = 880) and end (t = 1206) point fermentation samples using SPE/Chit/GOxβ-gal/Chit/GA electrodes. Samples were diluted 1/100 in 5 mM $K_3Fe(CN)_6$ as required for accurate measurement due to the sample matrix (*Figure 4.12*). CA (E_{app} = 0.25 V vs. Ag/AgCl) was performed.

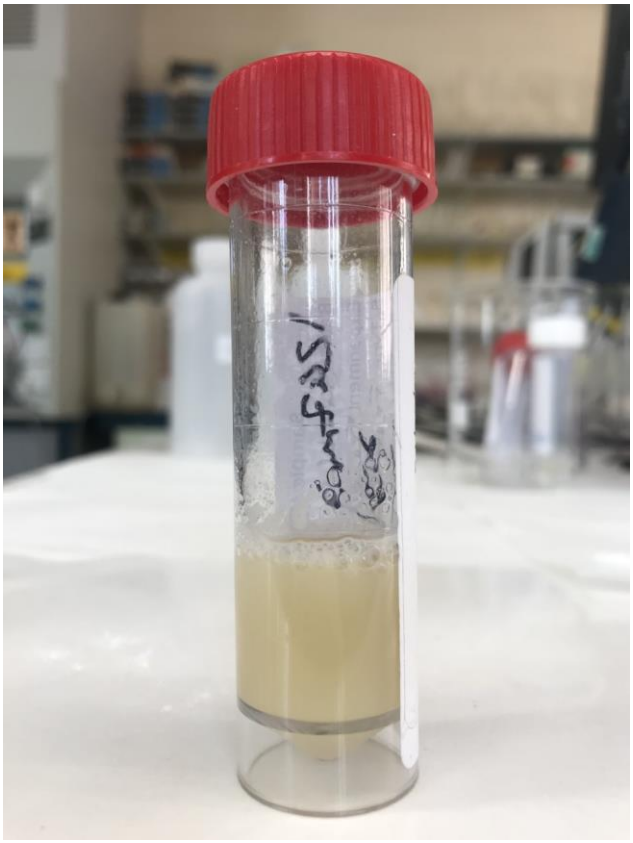

Figure 4.12: Fermentation sample provided by Industry partner.

Figure 4.13(a) shows current vs. concentration plot for spiked lactose (0 - 2.43 mM) in (t = 880) fermentation sample (1 % v/v) corrected for the contributing lactose signal from the fermentation sample. The calibration curve was then used to calculate the lactose content in the sample which was determined to be 175 mM or 63056 ppm in an undiluted sample. HPLC data measured 181 mM or 65,303 ppm showing 96.81 % agreement between the two analytical methods.

Following this, an end point sample (t = 1206) was analysed under the same conditions with spiked lactose in the range (0 – 1.23 mM) (*Figure 4.13(b)*). This was then used to calculate lactose concentration of 4.4 mM or 16112 ppm. Comparison with HPLC analysis which measured 4.3 mM or 15830 ppm with 92.86 % agreement.

(a)

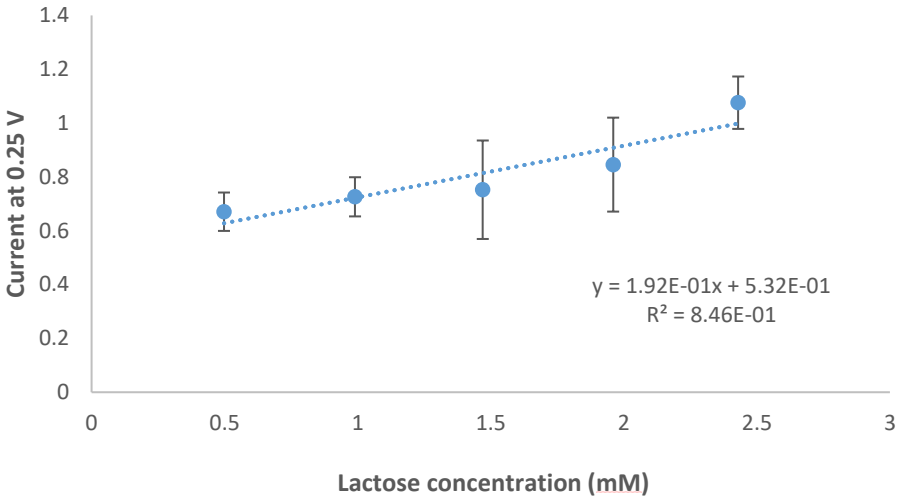

(b)

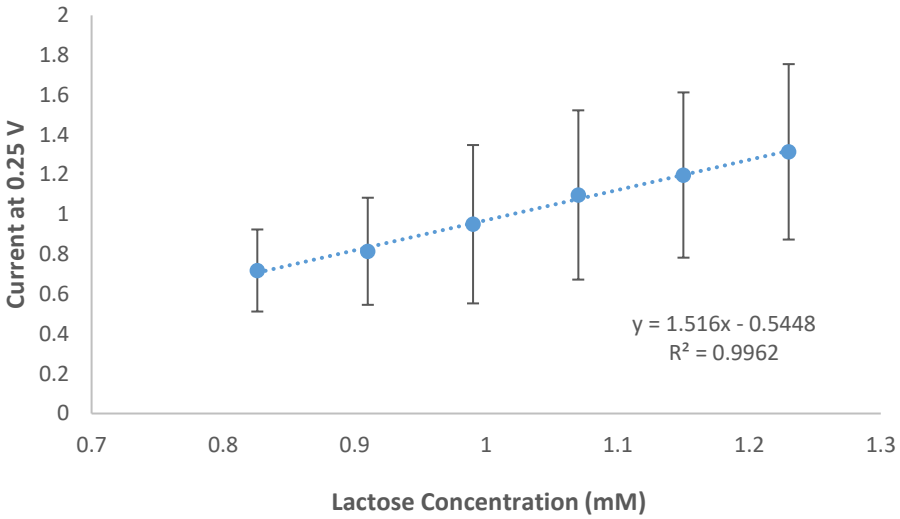

Figure 4.13: (a) Data plot showing calibration of Lactose biosensor at (t = 880) sample (diluted in 5 mM $K_3Fe(CN)_6$ to 1 % v/v). Additions of lactose prior to each measurement resulted in range 0 – 2.43 mM (n=2). (b) Data plot showing calibration of Lactose biosensor at (t = 1206) sample (diluted in 5 mM $K_3Fe(CN)_6$ to 1 % v/v). Additions of lactose prior to each measurement resulting in range 0 – 1.23 mM (n=2).

Table 4.3 shows a summary of the data obtained from the SPE/Chit/GOxβ-gal/Chit/GA electrode and the HPLC-RI method for fermentation sample analysis. Results show the correlation between the biosensor and the HPLC-RI data, indicating the potential of the biosensor to be used in fermentation analysis for lactose concentration. The ability of the biosensor to perform on-site testing with time to result of 5 s, along with excellent correlation with respect to chromatographic and similar sensing instrumentation highlight the success and potential of the developed sensor for use in lactose quantitation

Table 4.3: Lactose determination for (t = 0 - 1247) minutes for Biosensor vs HPLC-RI

Time (min.)	Lactose HPLC-RI		Lactose Biosensor (ppm)		% error
	ppm	mM	ppm	mM	
0	110318	306.6	110470	306.2	0.14%
880	65303	181.2	63056	175.4	3.19%
1206	15830	4.4	16112	4.7	7.14%

4.5.3.2 Solution mediated lactic acid measurement in fermentation samples using modified GCE

The determination of lactic acid in fermentation samples was performed using modified GC electrodes labelled GC/Chit/LOx/Chit/GA (see electrode preparation section *2.4.1*) in the presence of 5 mM $K_3Fe(CN)_6$ utilised in sample dilution.

Chronocoulometric analysis was carried out with E_{app} = 0.38 V vs. Ag/AgCl on each of the samples. Start (t = 0), Middle (t = 887) and End (t = 1076) point fermentation samples were analysed for lactic acid content using the LOx modified GC electrode. Extrapolation of the data obtained for concentration vs. charge was carried out to determine lactic acid content in the sample (1 % v/v) of each time point (*Figure 4.14*).

The biosensor measured 5603 ppm lactate in the (t = 0) sample relative to HPLC-RI analysis which measured 7776 ppm, resulting in 72.05 % agreement between the two analytical systems.

The (t = 887) fermentation sample was analysed under the same conditions with the biosensor measuring 70598 ppm in the undiluted sample compared to HPLC-RI data of 74852 ppm, 94.32 % agreement.

Following this, the end point sample (t = 1076) resulted in 94130 ppm for the biosensor and 90,175 ppm obtained from HPLC-RI analysis, 95.61 % agreement.

The underestimated measure of lactic acid in the (t = 0) sample may be due to the sample having a lower concentration of the analyte compared to samples taken at other time points where the concentration of lactic acid has increased during fermentation.

(a)

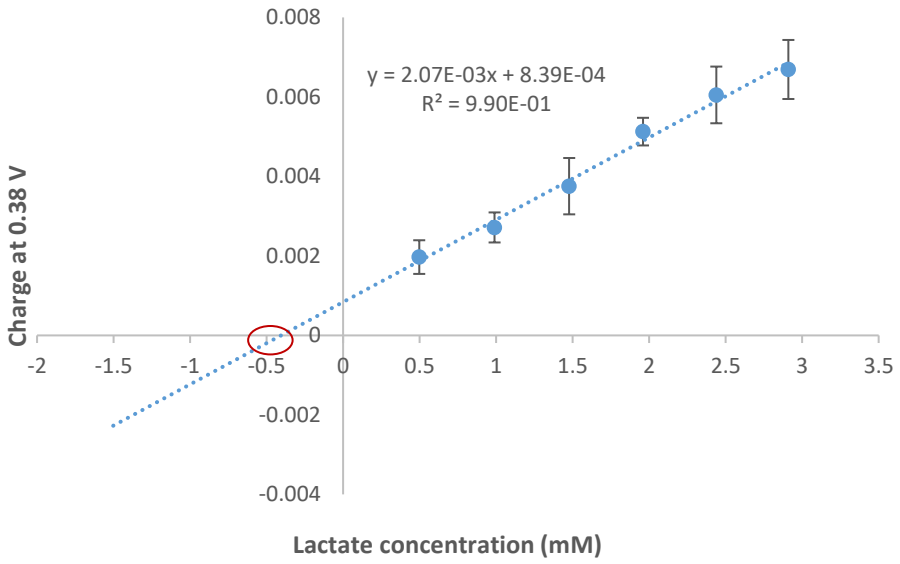
y = 2.07E-03x + 8.39E-04
R² = 9.90E-01
Charge at 0.38 V
Lactate concentration (mM)
0.008
0.006
0.004
0.002
0
-0.002
-0.004
-2
-1.5
-1
-0.5
0
0.5
1
1.5
2
2.5
3
3.5

(b)

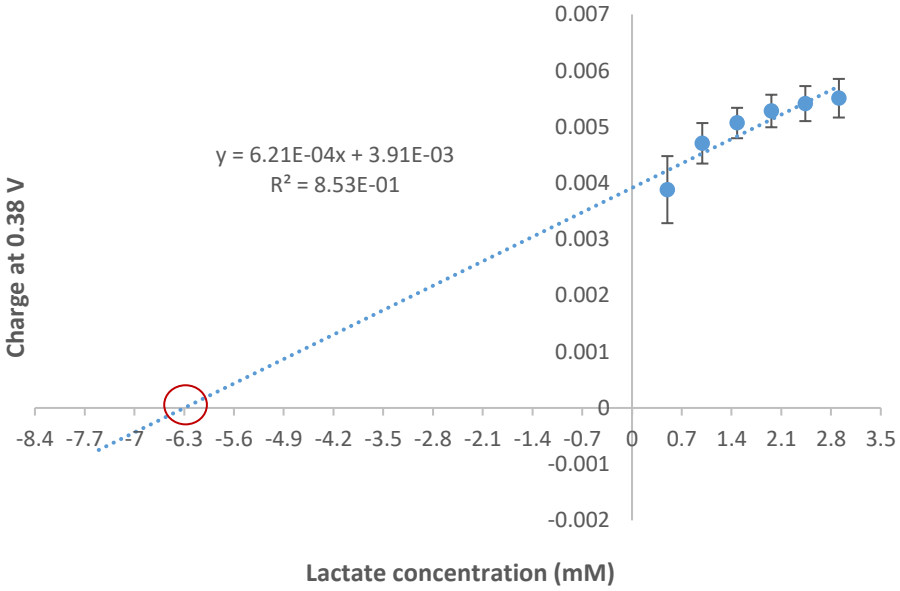
y = 6.21E-04x + 3.91E-03
R² = 8.53E-01
Charge at 0.38 V
Lactate concentration (mM)
0.007
0.006
0.005
0.004
0.003
0.002
0.001
0
-0.001
-0.002
-8.4
-7.7
-7
-6.3
-5.6
-4.9
-4.2
-3.5
-2.8
-2.1
-1.4
-0.7
0
0.7
1.4
2.1
2.8
3.5

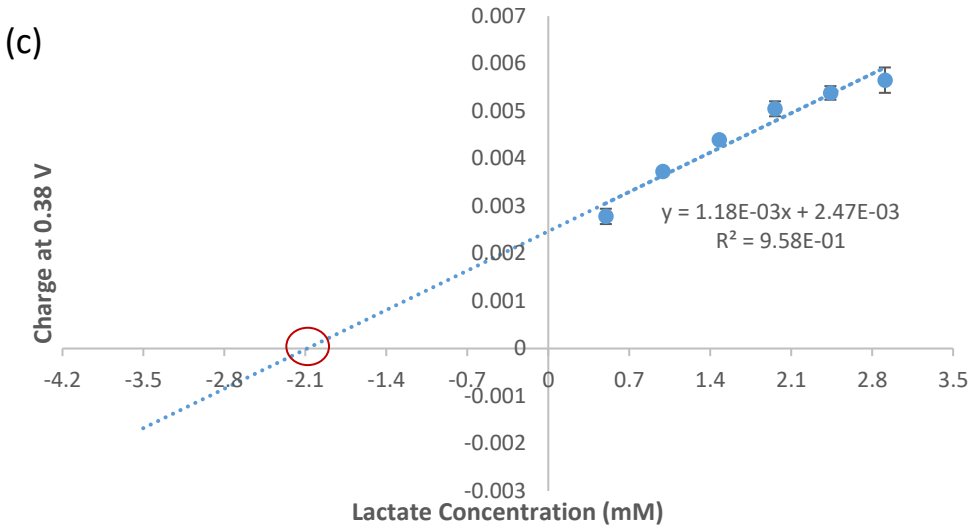

Figure 4.14: (a) Extrapolation of data from calibration of lactic acid at (t = 0) sample (diluted in 5 mM $K_3Fe(CN)_6$ to 1 % v/v). Additions of lactate prior to each measurement (n=3). (b) Extrapolation of data from calibration of lactic acid at (t = 887) sample (diluted in 5 mM $K_3Fe(CN)_6$ to 1 % v/v). Additions of lactate prior to each measurement (n=3). (c) Extrapolation of data from calibration of lactic acid in (t = 1076) sample (diluted in 5 mM $K_3Fe(CN)_6$ to 0.25 % v/v). Additions of lactate prior to each measurement (n=3).

Table 4.4 shows a summary of the results obtained from the biosensor and HPLC-RI data, including the % error of the biosensor relative to HPLC-RI data.

Table 4.4: Results of lactic acid determination for biosensor vs. HPLC-RI

Time (min)	Lactate HPLC-RI		Biosensor		% error
	ppm	mM	ppm	mM	
0	7776	69	5603	50	27.95%
887	74852	668	70598	630	5.68%
1076	90175	805	94130	840	4.39%

Capability for process monitoring is demonstrated by the data shown in *Figure 4.15* showing concentration (ppm) vs. time (minutes) for lactose and lactic acid determination in fermentation samples (t = 0 - 1247) using the biosensor developed in this work. The results obtained from the biosensor and the standard method used by the industry partner, HPLC-RI, is shown for each sample tested. Here, results were as expected showing a trend of inter-conversion between lactose and lactic acid. Results obtained using the two analytical techniques show the correlation between results for the lactose and lactic acid content determined for each sample. It is evident that the biosensor has the ability to detect and quantify both lactose and lactic acid over the course of the fermentation process. This graph represents the success of the biosensor and shows its potential use for fermentation process monitoring in the future.

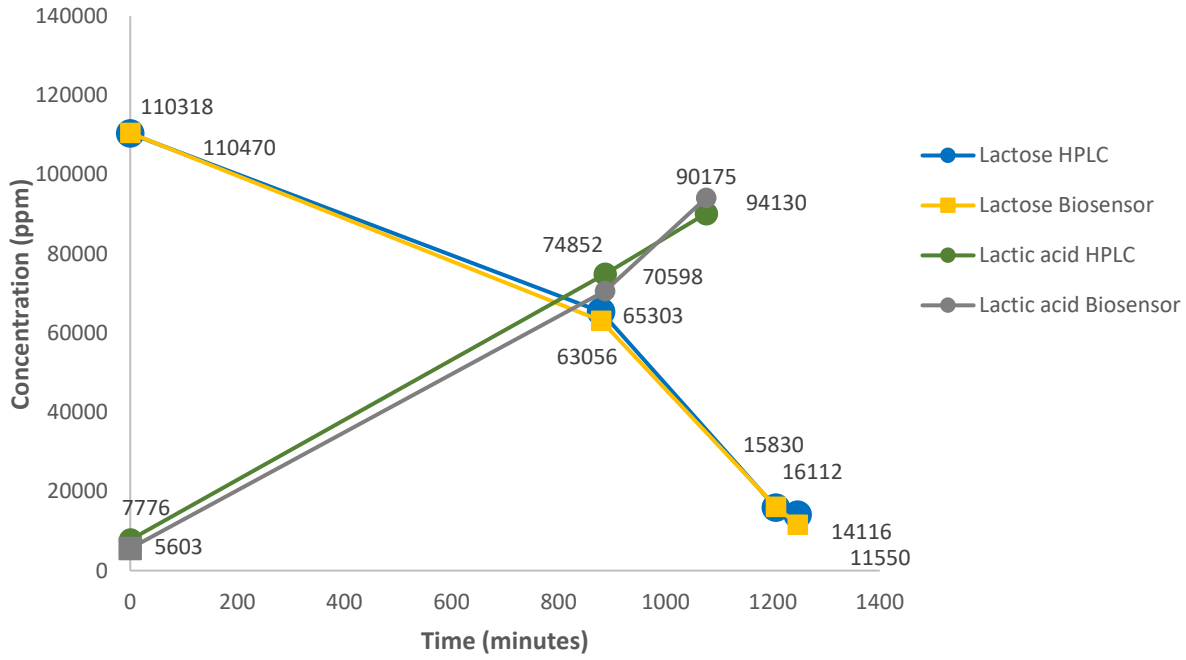

Figure 4.15: Concentration (ppm) vs. Time (minutes) plot for lactose and lactic acid analysis determined by HPLC-RI and Biosensors showing a decrease in lactose concentration as time increases during lactic acid fermentation.

4.6 Conclusion

Glucose, lactose and lactic acid sensors, described in *Chapters 2 and 3*, were used for the analysis of dairy samples including whey permeate, milk protein isolates and different time points of a fermentation process. Glucose and lactose sensors were deployed for direct sensing using modified Pt electrodes in whey permeate analysis. Samples were prepared by diluting 1/100 prior to analysis for glucose background testing and lactose quantitation. The biosensors measured 23.7 mM lactose in the whey permeate sample, correcting for free-glucose contributing signals, with 92.2 % correlation with results obtained from the sample COA.

Modified GC electrodes were used for lactose quantitation in milk protein isolates using a solution mediated approach. Samples were diluted 1/100 with 5 mM $K_3Fe(CN)_6$ to act as the redox mediator. The lactose biosensor measured 1.16 mM for the MPI 1 and 1.54 mM for the MPI 10 sample. Results were compared with HPLC analysis and a commercial Lactosens sensor. Results show the biosensor developed in this work to be closer to the HPLC-IC-PAD result relative to the Lactosens result.

Lactose quantitation in fermentation samples was carried out using the modified SPE and a DropSens potentiostat. Results were compared to HPLC-RI analysis, resulting in 93 - 100 % correlation between results. Lactate was also measured in different time points of the fermentation process using solution mediated approach with modified GC electrodes. Results showed 72 - 96 % correlation with HPLC data. It is suggested that the greater difference in values between the biosensor and HPLC results could be due to a lower concentration of lactic acid in (t = 0) samples.

This work shows the enormous potential use of the developed biosensors for successful determination of glucose, lactose and lactic acid content in a range of complex dairy samples. To date, there has been few reports of sensors for high lactose quantitation with many commercially available sensors, including Lactosens, limiting their use in low lactose or lactose-free products. Here, we have developed sensors for high and low lactose and lactic acid quantitation in whey permeate, milk protein isolates and various time points of a fermentation process.

4.7 Bibliography

1. Pescuma M, de Valdez GF, Mozzi F. Whey-derived valuable products obtained by microbial fermentation. *Appl Microbiol Biotechnol*. 2015;99(15):6183-6196. doi:10.1007/s00253-015-6766-z
2. Abdel-Rahman MA, Tashiro Y, Sonomoto K. Recent advances in lactic acid production by microbial fermentation processes. *Biotechnol Adv*. 2013;31(6):877-902. doi:10.1016/j.biotechadv.2013.04.002
3. Costa MP Da, Frasao BDS, Lima BRCDC, Rodrigues BL, Junior CAC. Simultaneous analysis of carbohydrates and organic acids by HPLC-DAD-RI for monitoring goat's milk yogurts fermentation. *Talanta*. 2016;152:162-170. doi:10.1016/j.talanta.2016.01.061
4. Kamanin SS, Arlyapov VA, Machulin A V., Alferov VA, Reshetilov AN. Biosensors based on modified screen-printed enzyme electrodes for monitoring of fermentation processes. *Russ J Appl Chem*. 2015;88(3):463-472. doi:10.1134/S1070427215030167
5. Rocchitta G, Spanu A, Babudieri S, Latte G, Madeddu G, Galleri G, Nuvoli S, Bagella P, Demartis M, Fiore V, Manetti R, Serra PA. Enzyme biosensors for biomedical applications: Strategies for safeguarding analytical performances in biological fluids. *Sensors (Switzerland)*. 2016;16(6). doi:10.3390/s16060780
6. Glithero N, Gorton L, Schuhmann W, Pasco N, Clark C. At-line measurement of lactose in dairy-processing plants. *Anal Bioanal Chem*. 2012;405(11):3791-3799. doi:10.1007/s00216-012-6598-y
7. https://www.chr-hansen.com/en/food-cultures-and-enzymes/test-and-equipment/cards/product-cards/lactosens

Chapter 5 : Conclusion and Future Work

5.1 Conclusion

As discussed in *Chapter 1*, there is a need to develop rapid sensing technologies for quantitative monitoring of glucose, lactose and lactic acid in the dairy industry. This work examined the development of biosensors for use in a wide range of dairy samples including whey permeate, milk protein concentrates and fermentation samples at various time points across a bioplastic production process.

Glucose, lactose and lactic acid biosensors were developed using a four layer system of Chitosan/Enzyme(s)/Chitosan/GA or PEGDE using direct and solution mediated approaches. Initially, direct detection of analytes was performed to examine the analytical performance of the biosensor under industry required conditions i.e. room temperature at pH 6.0 via CV, CA and/or CC electrochemical techniques. A solution based mediator, $K_3Fe(CN)_6$, was then used to improve sensitivity and lower the operating potential (E_{app} = 0.3 V vs. Ag/AgCl) of the biosensor, eliminating issues with background electroactive species present in dairy samples. The effect of different cross-linking agents (GA and PEGDE) on analytical performance was investigated using the glucose biosensor in the presence of the mediator, $K_3Fe(CN)_6$. Although studies showed PEGDE increased the linear range of the biosensor, it was not employed for use in on-site sample analysis as it was found to be unsuitable for SPE modification.

Further studies with the lactate biosensor investigated the use of phenanthroline derivative, 1,10-Phenanthroline-5,6-dione, as a novel mediator for lactate sensing. Four different methods involving electrodeposition and enzymatic polymerisation techniques were studied to determine the optimum method for poly(1,10-Phenanthroline-5,6-dione) film formation on an enzyme modified electrode. Electrodeposition with CV proved to be the least effective method with lower surface coverage, while enzymatic polymerisation via CV at a slow scan rate with lactate additions resulted in the highest surface coverage and most suitable film behaviour. Graphite powder was utilised to formulate an ink for use as a conducting inner layer to study whether or not it could enhance the analytical performance of the redox active film. The addition of the conducting ink improved the reversibility of the pPD film and provided greater surface area for layer by layer modification. Final studies demonstrated the ability of the ink modified enzymatic (pPD) biosensor to successfully detect and quantify lactate levels in a diluted fermentation sample with

71.78 % correlation with HPLC-RI analysis.

The final chapter of this study examined the use of the developed biosensors for accurate measure of glucose, lactose and/or lactic acid in three different dairy samples including whey permeate, milk protein concentrate and fermentation samples taken at different time points over a bioplastic production process. A direct detection approach was taken when quantifying glucose and lactose in a diluted whey permeate sample using the enzyme modified Pt electrodes. The biosensor showed a 92.2 % correlation when compared with results obtained by HPLC-RI. Other samples, milk protein isolates and a range of fermentation samples, were analysed for their lactose and lactic acid levels using a solution mediated approach with modified SPE or GC electrodes. The biosensor results for the MPI samples were compared with HPLC and a commercially available sensor, Lactosens. The biosensor developed in this work showed a greater correlation with HPLC results relative to the Lactosens. The fermentation samples were diluted with $K_3Fe(CN)_6$ and results were compared with HPLC data carried out by the industry partner. Lactose quantitation was performed using modified SPE and a portable Dropsens potentiostat for on-site testing of the samples via chronoamperometry analysis. The results obtained by the biosensor developed here resulted in 93-100 % correlation with HPLC. Lactate quantitation of the fermentation samples was carried out on LOx modified GC electrodes using chronocoulometric analysis, where results obtained showed a 72-96 % correlation with HPLC lactate analysis. This work shows the enormous potential of the developed biosensors for successful determination of glucose, lactose and lactic acid content in a range of complex dairy samples. To date, there has been few reports of sensors for high lactose quantitation with many commercially available sensors, including Lactosens, limiting their use in low lactose or lactose-free products. Here, we have developed sensors for high and low lactose and lactic acid quantitation in whey permeate, milk protein isolates and various time points of a fermentation process.

The use of scanning electrochemical microscopy (SECM redox competition mode) provided surface topographical and imaging/enzyme reactivity information respectively. Approach curves and line scans confirmed the enzymatic catalytic response in the presence and absence of substrates glucose, lactose and lactate using $K_3Fe(CN)_6$. Area scans were used to identify the enzyme active region of glucose, lactose and lactic acid biosensors in the absence and presence of substrate.

5.2 Future Work

Challenges in fermentation sample analysis and process monitoring require analytical devices for rapid on site testing, which could include optimisation of second generation sensing methodologies at solid electrodes with transfer to thick film transducers. Enzyme kinetic evaluation would generate insights into fundamental properties of the biolayer and alternative mediator loading/type/mechanisms via electrochemical investigations. The base conducting ink formulation examined here in Chapter 3 could be further modified with optimal materials and performance tested with respect to biocompatibility, chemical and physical stability, redox behaviour and film properties, operating voltage and functionality (lactose levels <0.2 % lactose could be targeted as an industry need).

New ink formulation studies could be extended to encapsulate the bienzyme system with suitable inorganic mediators (e.g. nanoporous polymeric materials, PEDOT conducting polymers, carbon nanocomposites, metallic nanomaterials, phenanthroline 1, 2 diones, ferrocene derivatives) for signal selectivity and sensitivity.

Sensor prototype fabrication and capability for multiplexed mode would be a key advance which will involve transfer of optimised enzyme/mediator/ink formulation onto screen printed electrodes in 4 x working electrode format to include (a) control (b) lactate (c) glucose and (d) lactose simultaneous sensing capability in one sample.

Overall, there is tremendous potential for suitable biosensing devices in the dairy sector where the need for quality control requires on-site robust analysis with rapid time to result.

5.3 Modules completed and credits gained

Table 5.1: Modules completed and credits awarded

Code	Modules	Credits
CH801	Core Skills and Research Techniques in Chemistry	5
GST8	Grant management and Compliance	5
GST2	Finding information for your thesis	5
	Total Credits = 15	

5.4 Poster presentations and Conferences attended

- Agilent Technologies Analytical Arena, 29-30th November 2017.
- "Development of lactose biosensor for fermentation monitoring" Conference for Analytical Sciences in Ireland, Maynooth University, 16-17th May 2018.
- "Towards Rapid Electronic Sensor Technologies in Dairy Processing – Glucose and Lactose Biosensor Development" Rapid Methods Europe, Amsterdam, The Netherlands, 5-7th November 2018.
- "Towards Rapid Electronic Sensor Technologies in Dairy Processing - Mediated Lactose and Lactate Biosensing in Fermentation Media" – Chemistry Research Colloquium, TU Dublin and RCSI, 20-21st June 2019.